

**A STUDY OF PYRITE REACTIVITY AND
THE CHEMICAL STABILITY OF CEMENTED PASTE BACKFILL**

by

VALÉRIE J. BERTRAND

B.Sc., University of Ottawa, 1991

A THESIS SUBMITTED IN PARTIAL FULFILLMENT OF
THE REQUIREMENTS FOR THE DEGREE OF
MASTER OF APPLIED SCIENCE

in

THE FACULTY OF GRADUATE STUDIES
(Department of Mining and Mineral Process Engineering)

We accept this thesis as conforming
to the required standard

THE UNIVERSITY OF BRITISH COLUMBIA

December 1998

© Valérie J. Bertrand, 1998

In presenting this thesis in partial fulfilment of the requirements for an advanced degree at the University of British Columbia, I agree that the Library shall make it freely available for reference and study. I further agree that permission for extensive copying of this thesis for scholarly purposes may be granted by the head of my department or by his or her representatives. It is understood that copying or publication of this thesis for financial gain shall not be allowed without my written permission.

Department of Mining & Mineral Process Engineering

The University of British Columbia
Vancouver, Canada

Date 15-12-98

ABSTRACT

A two-fold study was carried out to 1) characterize the evolution of the reactivity of pyrite in the early cycles of kinetic test leaching, using cyclic voltamperometry, and 2) document the weathering characteristics of various paste backfill mixtures that contain pyritic tailings, when exposed to leaching environments similar to those encountered in mine settings.

Pyrite leaching experiments were carried out on 6 different pyrite samples from existing mines. Cyclic voltamperometry was performed on carbon paste electrodes (CPE) containing fine grained pyrite samples on the unleached samples and after leaching periods of 4, 10 and 20 weeks. Pyrite reactivity profiles, supported by scanning electron microscope (SEM) observations and leachate chemistry data showed that minor phases of sphalerite and galena present in the pyrite samples were the most important parameters affecting pyrite reactivity in the initial leaching cycles. Sphalerite and galena were found to effectively retard the oxidation of pyrite in the early leaching cycles. As sphalerite and galena were leached out, an increase in the reactivity of pyrite was observed, followed by a gradual loss of reactivity from precipitate coatings. At a fundamental level, mineral surface characterization by cyclic voltamperometry was found useful in the interpretation of kinetic test data for the prediction of acid rock drainage (ARD) generation.

For the backfill weathering study, paste backfill samples of 4 different mines were leached in deionized water (pH 5.5) in flooded and alternating air-flooded environments

and in a simulated ARD solution ($\text{Fe}=500 \text{ mg/l}$, $\text{SO}_4=1.5 \text{ g/l}$ and $\text{pH } 2.5$) for 20 weeks. SEM, solid phase chemistry, paste pH, acid-base accounting measurements and leachate chemistry were also used to document the weathering characteristics of cemented paste backfill (CPB). This study revealed that hydrated portland cement minerals are pH sensitive and highly soluble. Short-term exposures of portland-CPB to circum-neutral water or to ARD solution promoted the dissolution of the binder material, increasing the porosity of the backfill and further infiltration of aqueous solution. Long-term exposure or flooding of CPB was found to promote the precipitation of secondary, expansive minerals such as gypsum in addition to solubilizing primary cement minerals. Detailed chemical analyses and acid-base accounting indicated that the neutralizing potential added to the material by the cement phase is short-lived and the small volumes added are insufficient to neutralize the acid generating potential of the mixture. All ARD solution-leached CPB samples formed an increasingly thick crust of precipitates that, with time, reduced the ability of the CPB to neutralize the ARD solution

TABLE OF CONTENTS

ABSTRACT	II
TABLE OF CONTENTS	IV
LIST OF TABLES.....	IX
LIST OF FIGURES.....	XI
LIST OF PLATES.....	XVII
ACKNOWLEDGEMENT	XXIII
1 INTRODUCTION.....	1
1.1 PROBLEM DEFINITION AND OBJECTIVES	1
1.1.1 <i>Pyrite Reactivity Study</i>	1
1.1.2 <i>Chemical Stability of Cement Paste Backfill</i>	3
1.2 BACKGROUND.....	7
1.2.1 <i>Pyrite Reactivity Study</i>	7
1.2.1.1 Pyrite Oxidation Controls.....	9
1.2.1.2 Electrochemistry Applied to the Study of Pyrite Reactivity.....	11
1.2.2 <i>Cemented Paste Backfill in the Mining Industry</i>	12
1.2.2.1 Cement Chemistry, Hydration and Chemical Stability	14
1.2.2.2 CPB in the Mine Environment	17
2 MINE SITE DESCRIPTIONS.....	26
2.1 COMPARISON OF MINE SITE AND EXPERIMENTAL CONDITIONS	28
3 EXPERIMENTAL METHODOLOGY	29

3.1	PYRITE EXPERIMENTS.....	29
3.1.1	<i>Sample Preparation and Analyses</i>	29
3.1.2	<i>Leaching Apparatus</i>	30
3.1.3	<i>Chemical analyses</i>	32
3.1.4	<i>Mineralogical and Electrochemical Characterisation of Pyrite</i>	33
3.2	PASTE EXPERIMENT.....	36
3.2.1	<i>Paste Sample Preparation</i>	36
3.2.1.1	Paste Components.....	36
3.2.1.2	Paste Mixing.....	37
3.2.1.3	Pre-Leaching Sample Preparation.....	42
3.2.2	<i>Leaching Apparatus and Leaching Cycles</i>	43
3.2.3	<i>Post-Leaching Sample Preparation</i>	44
3.2.4	<i>Chemical Analyses of the Paste Experiment</i>	46
3.2.4.1	Paste pH and Acid-Base Accounting Measurements.....	48
4	RESULTS – PYRITE REACTIVITY STUDY.....	49
4.1	MINERALOGY, CHEMISTRY AND STOICHIOMETRY OF UNLEACHED PYRITES.....	49
4.2	ELECTROCHEMISTRY OF THE UNLEACHED PYRITE SAMPLES.....	56
4.3	EVOLUTION OF LEACHATE CHEMISTRY.....	62
4.4	EVOLUTION OF PRECIPITATE COATINGS DURING LEACHING.....	67
4.4.1	<i>Huckleberry pyrite</i>	67
4.4.2	<i>Louvicourt Pyrites</i>	68
4.4.3	<i>Tizapa Pyrite</i>	68
4.4.4	<i>Zimapan Pyrite</i>	69
4.4.5	<i>Brunswick Pyrite</i>	70
4.5	EVOLUTION OF PYRITE REACTIVITY.....	77
4.5.1	<i>Huckleberry pyrites</i>	77
4.5.2	<i>Louvicourt Pyrites</i>	78

4.5.3	<i>Tizapa pyrite</i>	79
4.5.4	<i>Zimapan pyrite</i>	79
4.5.5	<i>Brunswick</i>	80
4.5.6	<i>Evolution of Pyrite Reactivity</i>	88
5	RESULTS – CEMENTED PASTE BACKFILL STUDY	88
5.1	CHEMICAL ANALYSES OF TAILINGS, BINDER AND PASTE.....	88
5.2	ASPECT OF CURED PASTE SAMPLES.....	91
5.3	WATER ABSORPTION BY THE PASTE	92
5.4	CHEMISTRY OF PASTE LEACHATES	95
5.4.1	<i>Flooded and Cycled Water-Leached Environments</i>	95
5.4.2	<i>Fe₂(SO₄)₃ Solution-Leached Environment</i>	108
5.4.3	<i>Summary of Observations from Leachate Chemistry</i>	117
5.5	SOLID PHASE CHEMISTRY OF LEACHED PASTE.....	120
5.5.1	<i>Tizapa</i>	120
5.5.2	<i>Brunswick</i>	122
5.5.3	<i>Louvicourt</i>	123
5.5.4	<i>Francisco I. Madero</i>	124
5.5.5	<i>Summary of Observations from the Solid Phase Chemistry</i>	129
5.6	BUFFERING CAPACITY AND ACID-BASE ACCOUNTING	131
5.6.1	<i>Evolution of Acid Producing and Acid Neutralizing Potentials:</i>	131
5.7	SCANNING ELECTRON MICROSCOPE (SEM) OBSERVATIONS.....	137
5.7.1	<i>Tizapa</i>	137
5.7.2	<i>Brunswick</i>	141
5.7.3	<i>Louvicourt</i>	143
5.7.4	<i>Francisco I. Madero</i>	146
5.7.5	<i>Summary of Observations from Scanning Electron Microscopy</i>	164
5.8	COMPRESSIVE STRENGTH MEASUREMENTS.....	167

6	DISCUSSION	172
6.1	PYRITE REACTIVITY STUDY	172
6.1.1	<i>Effect of Precipitate Coatings on the Passivation of Pyrite: Huckleberry and Louvicourt-1 Samples 172</i>	
6.1.2	<i>Effect of Stoichiometry on Pyrite Reactivity: Louvicourt-1 and Louvicourt-2 Samples</i>	175
6.1.3	<i>Effect of Mineral Impurities on Pyrite Reactivity</i>	176
6.1.3.1	Galvanic Protection by Sphalerite: Louvicourt-2 and Tizapa Samples	176
6.1.3.2	Effect of the Presence of Galena: Zimapan and Brunswick Samples	178
6.1.4	<i>The Huckleberry Problem.....</i>	179
6.2	CHEMICAL STABILITY OF PASTE MIXTURES	180
6.2.1	<i>Effect of Cementing Tailings Waste.....</i>	180
6.2.2	<i>Cemented Backfill Alteration with Leaching</i>	182
6.2.2.1	Water-Leached Environments.....	182
6.2.3	<i>Ferric Sulfate or Artificial ARD Environments</i>	189
7	CONCLUSIONS	193
7.1	PYRITE REACTIVITY STUDY	193
7.1.1	<i>Huckleberry Pyrite.....</i>	195
7.1.2	<i>Application of this Study to Field Investigations</i>	195
7.2	CEMENTED PASTE BACKFILL LEACHING STUDY	197
8	RECOMMENDATIONS.....	202
8.1	PYRITE REACTIVITY STUDY	202
8.2	PASTE BACKFILL STUDY	203
	REFERENCES	206
	APPENDIX I - ANALYTICAL RESULTS: PYRITE LEACHATE	214
	APPENDIX II - ANALYTICAL RESULTS: PASTE BACKFILL LEACHATE	219

LIST OF TABLES

Table 1.1: Chemical Composition of Normal Portland Cement (Canada type 10 or Mexico no. 1).....	15
Table 1.2 Concrete Subjected to Sulfate Attack	20
Table 1.3: Replacement Components of Portland Cement to Improve Sulfate Resistance of Concrete.....	23
Table 2.1: Summary of Sample Geological Setting and Mineralogy	26
Table 2.2 Hydrogeologic Conditions at Mine Sites where Backfill is or will be Used...	28
Table 3.1 Leachate Analyses Carried Out at UASLP.....	32
Table 3.2 Leachate and Solids Analyses Carried Out at CIDT	33
Table 3.3 Paste Sample Preparation.....	40
Table 3.4 Paste Leaching Scenarios.....	43
Table 3.5 Solids Phase Analyses for the Paste Experiments	48
Table 4.1 Solid Phase chemistry of Pyrite Samples	51
Table 4.2 Normative Mineralogy of Pyrite Samples	52
Table 4.3 Average Stoichiometry of Pyrites.....	53

Table 4.4 Open Current Potentials of Pyrite Samples (Volts, SHE)	56
Table 4.5 Relative Reactivities of Pyrites.....	90
Table 5.1 Chemical Analyses of Tailings and Binders Used in Paste Mixtures.....	90
Table 5.2 Final Composition of Paste Samples	90
Table 5.3a, b Paste Water Content: 5 weeks and 20 weeks	93
Table 5.4 Tizapa - Description of Leached Paste Sections.....	125
Table 5.5 Brunswick - Description of Leached Paste Sections	125
Table 5.6 Louvicourt - Description of Leached Paste Sections.....	126
Table 5.7 Francisco I. Madero - Description of Leached Paste Sections	127
Table 5.8 a, b, c, d Paste pH and Acid-Base Accounting Test Results.....	133
Table 5.9 Unconfined Compressive Strength of Paste Samples.....	169
Table 6.1 Dissociation Constants for Secondary Minerals of Zn and Pb	179
Table 6.2 Solubility Products and Dissociation Constants of Secondary Minerals Derived from Hydrated Portland Cement and Other Reference Minerals.....	185

LIST OF FIGURES

Figure 1.1 Paste Backfill Leaching Environments	20
Figure 2.1 Sites Location of Huckleberry, Louvicourt and Brunswick mines, Canada ...	27
Figure 2.2 Site Location of Tizapa, Zimapan and Francisco I. Madero (FIM) mines, Mexico	27
Figure 3.1 Pyrite Leaching Apparatus	32
Figure 3.2 Preparation of Carbon Paste Electrode (CPE).....	35
Figure 3.3 Electrochemical Cell (front clip attached to CPE)	35
Figure 3.4: a. Mixing Paste Sample b. Standard Slump Test	42
Figure 3.5 Rodding Paste into Mould	
Figure 3.6 Curing of Paste Samples.....	42
Figure 3.7 Leaching Cells	
Figure 3.8 Lab Set up, Paste Leaching Study	44
Figures 3.9 a, b, c: Paste Sample Preparation Steps for Mineralogical Observations	45
Figure 4.1 All unleached pyrite samples	
Figure 4.2 Close up view	60

Figure 4.3 Galena	
Figure 4.4 Sphalerite.....	61
Figure 4.5 Pyrite Leachate pH.....	63
Figure 4.6 Pyrite Leachate Redox Conditions.....	64
Figure 4.7 Pyrite Leachate Conductivities.....	64
Figure 4.8 Pyrite Leachate Sulfate Concentrations.....	65
Figure 4.9 Pyrite Leachate Total Iron Concentrations.....	65
Figure 4.10 Pyrite Leachate Zinc Concentrations.....	65
Figure 4.11 Pyrite Leachate Lead Concentrations.....	66
Figure 4.12 Pyrite Leachate Copper Concentrations.....	66
Figure 4.13 Pyrite Leachate Arsenic Concentration.....	66
Figure 4.14 Huckleberry Water-Leached Pyrites	
Figure 4.15 Huckleberry Solution-Leached Pyrites.....	82
Figure 4.16 Louvicourt-1 Pyrite	
Figure 4.17 Louvicourt-2 Pyrite.....	83
Figure 4.18 Tizapa Pyrite	
Figure 4.19 Zimapan Pyrite.....	85

Figure 4.20 Zoom on Initialization points, Zimapan Pyrites	86
Figure 4.21 Brunswick pyrites	
Figure 4.22 Zoom of Initialization Points.....	87
Figure 4.23 All Pyrites, 4-week Leached.....	88
Figure 4.24 All Pyrites, 10-week Leached	
Figure 4.25 All Pyrites, 20-week Leached.....	89
Figure 5.1 Superficial Oxidation of Freshly Cured Tizapa Paste Samples.....	91
Figure 5.2 Water Absorption in Cyclic-Leaching (water) Environment	94
Figure 5.3 Water Absorption in Flooded-Leaching (water) Environment	94
Figure 5.4 Water Absorption in $\text{Fe}_2(\text{SO}_4)_3$ Solution.....	94
Figure 5.5 Flooded Cells – Leachate pH	
Figure 5.6 Cycled Cells - Leachate pH.....	100
Figure 5.7 Flooded Cells – Conductivity	
Figure 5.8 Cycled Cells - Conductivity	100
Figure 5.9 Flooded Cells - Redox Potential	
Figure 5.10 Cycled Cells - Redox Potential.....	101
Figure 5.11 Flooded Cells - Dissolved Iron	
Figure 5.12 Cycled Cells - Dissolved Iron.....	102

Figure 5.13 Flooded Cells – Dissolved Zinc	
Figure 5.14 Cycled Cells - Dissolved Zinc	102
Figure 5.15 Flooded Cells - Dissolved Lead	
Figure 5.16 Cycled Cells - Dissolved Lead	103
Figure 5.17 Flooded Cells - Sulfate Concentration	
Figure 5.18 Cycled Cells - Sulfate Concentration	103
Figure 5.19 Flooded Cells – Calcium Concentration	
Figure 5.20 Cycled Cells - Calcium Concentration	104
Figure 5.21 Flooded Cells - Calcium depletion rate	
Figure 5.22 Cycled Cells – Calcium depletion rate	104
Figure 5.23 Flooded Cells - Magnesium Concentration	
Figure 5.24 Cycled Cells - Magnesium Concentration.....	105
Figure 5.25 Flooded Cells - Magnesium depletion rate	
Figure 5.26 Cycled Cells – Magnesium depletion rate.....	105
Figure 5.27 Flooded Cells - Potassium Concentration	
Figure 5.28 Cycled Cells - Potassium Concentration	106
Figure 5.29 Flooded Cells – Potassium Depletion Rate	
Figure 5.30 Cycled Cells – Potassium Depletion Rate	106

Figure 5.31 Flooded Cells - Silicon Concentration	
Figure 5.32 Cycled Cells - Silicon Concentration	107
Figure 5.33 $\text{Fe}_2(\text{SO}_4)_3$ Cells - pH.....	112
Figure 5.34 $\text{Fe}_2(\text{SO}_4)_3$ Cells - Conductivity	112
Figure 5.35 $\text{Fe}_2(\text{SO}_4)_3$ Cells – Redox Potential	112
Figure 5.36 Ferric Hydroxide Coating on Paste Sample	113
Figure 5.37 $\text{Fe}_2(\text{SO}_4)_3$ Cells – Dissolved Iron	113
Figure 5.38 $\text{Fe}_2(\text{SO}_4)_3$ Cells – Dissolved Zinc.....	113
Figure 5.39 $\text{Fe}_2(\text{SO}_4)_3$ Cells – Dissolved Lead	114
Figure 5.40 $\text{Fe}_2(\text{SO}_4)_3$ Cells – Sulfate Concentration	114
Figure 5.41 $\text{Fe}_2(\text{SO}_4)_3$ Cells – Calcium Concentration.....	114
Figure 5.42 $\text{Fe}_2(\text{SO}_4)_3$ Cells – Calcium Depletion Rate	115
Figure 5.43 $\text{Fe}_2(\text{SO}_4)_3$ Cells – Magnesium Concentration.....	115
Figure 5.44 $\text{Fe}_2(\text{SO}_4)_3$ Cells – Magnesium Depletion Rate	115
Figure 5.45 $\text{Fe}_2(\text{SO}_4)_3$ Leach Cells – Potassium Concentration	116
Figure 5.46 $\text{Fe}_2(\text{SO}_4)_3$ Leach Cells – Potassium Depletion Rate.....	116

Figure 5.47 $\text{Fe}_2(\text{SO}_4)_3$ Leach Cells – Silicon Concentration	116
Figure 5.48 Tizapa Paste - UCS with Leaching Time	170
Figure 5.49 Brunswick Paste - UCS with Leaching Time.....	170
Figure 5.50 Louvicourt Paste - UCS with Leaching Time	170
Figure 5.51 Francisco I. Madero Paste - UCS with Leaching Time.....	171

LIST OF PLATES

Plate 4.1 Zimapan Pyrite	
Plate 4.2 Brunswick Pyrite	
Plate 4.3 Louvicourt-2 Pyrite	
Plate 4.4 Tizapa Pyrite	
Plate 4.5 Huckleberry Pyrite	
Plate 4.6 Louvicourt-1 Pyrite.....	54

HUCKLEBERRY PYRITES

Plate 4.7 Water-Leached, 20 weeks	
Plate 4.8 Water-Leached, 20 weeks	
Plate 4.9 Solution-Leached, 20 weeks	
Plate 4.10 Solution-Leached, 20 weeks.....	69

LOUVICOURT-1 PYRITES

Plate 4.11 4-week leached	
Plate 4.12 20-week leached	
Plate 4.13 20-week leached.....	70

LOUVICOURT-2 PYRITES

Plate 4.14 Pyrite surface at 10 weeks	
Plate 4.15 Pyrite surface at 20 weeks	
Plate 4.16 Pyrite at 10 weeks	
Plate 4.17 20-week leached.....	71

TIZAPA PYRITES

Plate 4.18 Pyrite surface at 20 weeks
Plate 4.19 Oxidized sphalerite, 20 weeks
Plate 4.20 Precipitate cover, 20 weeks
Plate 4.21 Oxidized galena, 20 weeks.....72

Zimapan Pyrites

Plate 4.22 Pyrite surface at 20 weeks
Plate 4.23 Corrosion pits at 4 weeks
Plate 4.24 Anglesite precipitates, 20 weeks.....73

BRUNSWICK PYRITES

Plate 4.25 Pyrite surface at 20 weeks
Plate 4.26 Pyrite corrosion pits, 20 weeks
Plate 4.27 Anglesite and galena, 4 weeks.....74

PASTE BACKFILL PLATES

Plate 5.1 Portlandite crystals
Plate 5.2 Typical EDX of portlandite
Plate 5.3 Secondary gypsum crystals
Plate 5.4 Typical EDX of gypsum.....149

Plate 5.5 Acicular ettringite
Plate 5.6 Typical EDX of ettringite..... 150

Plate 5.7 Amorphous tobermorite	
Plate 5.8 Typical EDX of amorphous tobermorite.....	150

TIZAPA BACKFILL

Plate 5.9 Portlandite cover on sample surface	
Plate 5.10 Bottom of layer 1	
Plate 5.11 Bottom of layer 1	
Plate 5.12 Poorly developed Tobermorite, below layer 1	
Plate 5.13 Core of sample	
Plate 5.14 Primary ettringite on incompletely hydrated cement grain.....	151
Plate 5.15 Poorly developed Tb, layer 1	
Plate 5.16 Ettringite, upper layer 1	
Plate 5.17 Secondary gypsum, upper layer 1	
Plate 5.18 General paste aspect, layer 1	
Plate 5.19 Ettringite in core of sample	
Plate 5.20 Good tobermorite development at core of sample.....	152
Plate 5.21 Porous layer 1	
Plate 5.22 Depleted tobermorite, layer 1	
Plate 5.23 Area of good tobermorite, layer 1	
Plate 5.24 Layer 1, iron sulfate precipitate	
Plate 5.25 EDX of iron sulfate precipitate.....	153
Plate 5.26 Good tobermorite cover, layer 2.....	154

BRUNSWICK BACKFILL

Plate 5.27 Layer 1

Plate 5.28 Layer 1

Plate 5.29 Less resistant tobermorite, layer 1

Plate 5.30 Abundant tobermorite, layer 2..... 154

Plate 5.31 Good tobermorite cover, layer 1

Plate 5.32 General aspect of paste, layer 1

Plate 5.33 Paste surface

Plate 5.34 General aspect of paste, layer 1

Plate 5.35 Poor tobermorite cover, layer 1

Plate 5.36 Possible 2ry ettringite, layer 1..... 155

Plate 5.37 General aspect of paste, layer 2

Plate 5.38 Fe-sulfate precipitate, layer 2

Plate 5.39 Inside large pore, layer 2

Plate 5.40 General aspect of paste, layer 3

Plate 5.41 Layer 3..... 156

LOUVICOURT BACKFILL

Plate 5.42 Massive tobermorite

Plate 5.43 Dendritic tobermorite

Plate 5.44 EDX of tobermorite developed from slag

Plate 5.45 General aspect of paste mixture..... 157

Plate 5.46 Less tobermorite in upper layer 1	
Plate 5.47 More abundant tobermorite in lower layer 1.....	158
Plate 5.48 Poorly developed Tb, upper layer 1	
Plate 5.49 Upper layer 1	
Plate 5.50 More developed Tb, lower layer 1	
Plate 5.51 Secondary gypsum, lower layer 1	
Plate 5.52 Tobermorite-lined fracture in paste	
Plate 5.53 Close-up view of tobermorite.....	159
Plate 5.54 Depleted tobermorite, layer 1	
Plate 5.55 Masses of tobermorite at upper layer 1	
Plate 5.56 Increased Tb content, below layer 1	
Plate 5.57 Fracture developed possibly along existing plane of weakness.....	160
Plate 5.58 Botryoidal mass of iron sulfate precipitate	
Plate 5.59 EDX of iron sulfate precipitate (type of jarosite?)	
Plate 5.60 Possibly ettringite, layer 2	
Plate 5.61 Well developed tobermorite, lower layer 2.....	161
 FRANCISCO I. MADERO BACKFILL	
Plate 5.62 Layer 1, flooded sample	
Plate 5.63 Core of flooded sample	
Plate 5.64 Layer 1, hydrated cement phase.....	162

Plate 5.65 General aspect of paste

Plate 5.66 Good development of tobermorite, layer 1

Plate 5.67 Layer 1

Plate 5.68 Monosulfoaluminate (?), below layer 1

Plate 5.69 Core of sample.....163

ACKNOWLEDGEMENT

This project was the first of an international collaboration and technology exchange between the University of British Columbia and the Universidad Autónoma de San Luis Potosí. Although the logistics for this project were sometimes challenging, the project was carried out with great success thanks to the efforts of many determined people. In particular I would like to sincerely thank my supervisor and project co-ordinator Dr Richard Lawrence for his time and attention, Dr Marcos Monroy, Dr George Poling and Dr Ignacio Gonzalez for their supervision, valuable comments and discussions throughout the study and for their support and friendship. I would also like to thank Dr Marcello Veiga, and Dr Ralph Hackle for their comments and revisions.

Funding of this research was provided by a grant from the National Science and Engineering Research Council of Canada (NSERC), by Noranda Technology Centre (NTC), Centro de Investigación y Desarrollo Tecnológico (CIDT) of Peñoles, the University of British Columbia, the Universidad Autónoma de San Luis Potosí, Universidad Autónoma Metropolitana-Ixtapalapa of Mexico City. In particular, I would like to thank Luc St-Arnaud and Michael Li of NTC, Louis Racine of Louvicourt mine and Arie Moerman of Brunswick mining division, Noranda. Thanks also goes out to Benjamin Ruiz and Carlos Lara of CIDT, and Peter Campbell formerly of Huckleberry mines. I thank Sally, Frank, Marina, Terry, Shannon, Pary, Dr. Dunbar and Dr. Scoble at the department of Mining and Mineral Process Engineering of UBC for their support.

Me gustaria agradecer a Irene Chavira y Roel Cruz-Gaona por su invaluable ayuda con los experimentos que lleve a cabo en México, y tambien por su paciencia y amistad. Tambien agradezco a Ulices, Pancho, Israel, Lorena, Teresita y Eliceo por sus atenciones y, claro, su amistad.

Finalement, j'aimerais remercier du fond du coeur Stéphane D'Aoust et Thérèse Bertrand ainsi que Kathy et Tracy pour leur soutien moral, encouragement et amitié.

1 INTRODUCTION

1.1 PROBLEM DEFINITION AND OBJECTIVES

The oxidation of sulfide-rich mining wastes produces drainage water of poor quality, contaminated by dissolved heavy metals and which is often of low pH. This contaminated drainage is termed acid rock drainage (ARD) and is the most costly environmental problem facing the mining industry today. In many cases, the only solution is long term treatment once the process of oxidation is under way. A key mineral in ARD generation is pyrite (FeS_2) which, although not the most reactive sulfide mineral, is by far the most common, frequently present in large quantities in mining wastes. This study has been carried out to observe the electrochemical behaviour of pyrite oxidation to determine if such fundamental observations might be used to refine the prediction of the behaviour of pyritic mine wastes. Building on the knowledge of pyrite reactivity, experiments have been carried out to observe the chemical stability of paste backfill containing pyritic tailings, exposed to various leaching conditions encountered in mine settings.

1.1.1 Pyrite Reactivity Study

A considerable amount of research has been carried out in the last two decades to improve the understanding of mineral waste oxidation and provide methods to control the generation of ARD. Fundamental studies of pyrite oxidation such as the processes involved, oxidation rates and reaction products, abound in the literature (Singer and

Stumm, 1970; Lawson, 1982; Moses *et al.*, 1987; Brown and Jurinak, 1989; Nicholson *et al.*, 1989; Moses and Herman, 1991; Nicholson, 1994; Blowes *et al.*, 1995; Eidså *et al.*, 1997). The application of this fundamental knowledge to field conditions, to predict drainage water quality, remains difficult because of the heterogeneous nature of mineral waste piles and the multitude of chemical reactions and physical factors that can affect the generation of ARD and subsequent water quality.

The mining industry has typically relied on the use of simple and often short-term laboratory weathering tests such as humidity cells to attempt to predict the behaviour of mining wastes exposed to the environment and quality of the drainage water. An increasing number of government agencies require that specific static and kinetic tests be carried out on mineral wastes, prior to permitting a new mining operation to determine the potential of waste to generate acid. Mineral waste characterization programs required by the government of British Columbia, Canada, are presented in the BCAMD Draft Acid Rock Drainage Technical Guide (Steffen, Robertson and Kirsten Ltd., 1989), with revisions by Price and others (1997). The limitation to kinetic tests is that only products are measured without detailed information on sulfide oxidation kinetics or the possible change in oxidation rate, for example, with the evolution of precipitation products. In addition, the data generated by some of these tests has been shown to vary depending on the procedures followed for a given tests (Lawrence and Wang, 1997), and to be difficult to extrapolate to predict the future chemical behaviour of mine wastes and the quality of the leachates derived from them (Bethune *et al.*, 1997; Otwinowski, 1997). Inaccurate predictions on ARD generation can have costly consequences such as over-design of treatment facility or worse yet, unplanned environmental restoration costs due to design

failures. Reduction in risks and costs associated with the management of mining wastes is the objective of the great amount of research actively being carried out to improve prediction techniques.

In the first part of this thesis, cyclic voltamperometry was used to study the effects of oxidative leaching on the reactivity of pyrite. Cyclic voltamperometry is an established investigative tool used in electrochemical studies to characterize surface and/or semiconducting properties of metals and minerals. Electrochemical techniques of various kinds have been used extensively in the mineral processing industry (review by Peters, 1984). Cyclic voltamperometry was used in conjunction with mineralogical investigation techniques to characterize the relative reactivity of various pyrite samples, and the evolution of reactivities as leaching progressed. The study was carried out with the aim to document the influence of intrinsic and extrinsic factors on the reactivity of pyrite. The objectives of this first part of the study are:

- 1) Investigate the usefulness of this relatively rapid and simple technique as an acid rock drainage predictive tool,
- 2) Measure the initial effects of leaching on pyrite to attempt to improve the understanding and subsequent interpretation of humidity cell data in the early stages of leaching.

1.1.2 Chemical Stability of Cement Paste Backfill

Due to the uncertainty associated with oxidation of mining wastes and the lack of fail-proof, effective protection against ARD, especially for sulfide-rich wastes, the mining

industry is increasingly pushing to minimize the surface disposal of waste to try to avoid the possible environmental problems associated with that practice. An option that is gaining popularity in the mining industry is the use of total tailings, including sulfide-rich tailings, as backfill material within the mine. Backfill is commonly used in mining operations to provide underground support and improve ore recovery, and as a method to dispose of some of the waste generated. Recent technological developments allow the use of total tailings, including the fine portion, which has traditionally been avoided because of excessive water retention and associated backfill stability problems. Cement can be added in small proportion to the mixture to increase the short and/or long term strength of the backfill (Landriault et al., 1998). This material is referred to as cemented paste backfill (CPB).

Advantages to using cemented, total tailings backfill include the decrease in volume of waste to be disposed of on the surface, thereby reducing the liability associated with the long-term care of a tailings disposal facility and the possible environmental problems associated with the oxidation of that waste in the case of reactive tailings. Another reported advantage is the added neutralization capacity provided by the cement to reactive tailings. The neutralized tailings could potentially serve a dual purpose: preventing the oxidation of the waste and the subsequent generation of ARD, as well as neutralizing existing ARD actively produced within the mine when coming in contact with the backfill material.

Backfill stability studies generally focus on the rheological or geotechnical properties of the backfill material. Many investigations are carried out to evaluate lower cost mineral additives to replace portions of Ordinary Portland Cement (OPC) while preserving the

strength of the cured material and into improvements in the short and/or long term strength of the mixtures (Hopkins and Beaudry, 1989; Lord and Liu, 1998; Gay and Constantiner, 1998; Noranda Technology Centre, 1998a,b,c,d; Archibald and Chew, 1998). Very few studies have been carried out on the reactivity or chemical stability of cured paste mixtures exposed to various environmental conditions. It is well known in the concrete industry that fine, sulfidic aggregate has deleterious effects on the setting ability of hydrated cement and its long-term durability. Furthermore, high concentrations of sulfate such as those commonly present in the tailings water used to make the mixtures or present in the mine waters (or ARD) coming in contact with the backfill are recognized in the concrete industry as aggressive solutions. Sulfates react with the hydrated cement to produce expansive minerals that cause the material to crack and lose its strength. The resulting physical weakening of the backfill concrete is highly undesirable, especially when the backfill is used to provide physical support of the underground structures. The physical breakdown of the backfill can also result in the exposure of reactive sulfide particles to the environment, thereby increasing the risk of oxidation.

In the second part of this study, the chemical stability of cemented paste mixtures that contain reactive waste was studied following 20-week leaching periods in environments similar to those encountered in a mine setting. The principal objective of the paste backfill stability study was to document the changes in properties occurring within various pastes when exposed to these leaching environments.

The objectives of this second part of the study were to provide insights on questions and actual problems reported by mines currently using or planning to use CPB, namely:

- 1) Decreasing backfill strength with time resulting in higher than expected dilution of ore when blasting next to backfilled areas,
- 2) Effectiveness of CPB to neutralize reactive tailings used in the backfill mixture and to buffer ARD produced within the mine.
- 3) The feasibility of using reactive tailings in above-ground applications of CPB

In the first part of the study, 6 samples of pyrite from mines in Canada and Mexico (Huckleberry, Louvicourt samples 1 and 2, Brunswick and Zimapan, Tizapa respectively) were studied using cyclic voltamperometry, scanning electron microscope (SEM), energy dispersive x-ray analysis (EDX), chemical analyses of solids and of the leachate to obtain information on the reactivity of each pyrite in the early cycles of leaching. In the second part, 4 paste backfill samples were prepared using the formulation specified by each mine (Louvicourt, Brunswick, Tizapa and Francisco I. Madero) to study their weathering characteristics when subjected to various leaching environments. SEM, EDX, acid-base accounting analyses as well as of solid phase and leachate chemistry was used for this investigation.

In the remaining section of this chapter, the reactivity of pyrite will be discussed followed by a detailed review of the use of paste backfill in the mining industry and the potential problems associated with exposure to environments encountered in a mine setting. Chapter 3 presents the methodology and sample preparation procedures developed for both the pyrite and backfill studies. Chapter 4 presents the results, analyses of data,

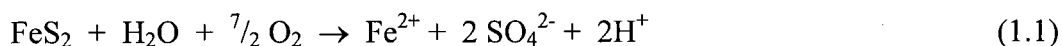
together with brief summaries of observations. A discussion of the results is presented in Chapter 5. Chapter 6 presents the conclusions of the study together with recommendations for further investigations and which could benefit similar studies.

1.2 BACKGROUND

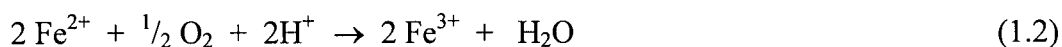
1.2.1 Pyrite Reactivity Study

Pyrite oxidation reactions and their mechanisms are generally well understood. The overall reactions can be summarized as follows:

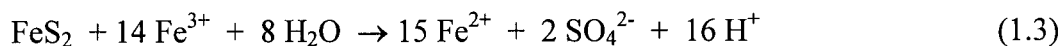
Initial circum-neutral oxidation of pyrite:



Slow, rate limiting Fe^{2+} oxidation (more rapid, bacterially mediated at $\text{pH} \leq 3.5$):



Ferric iron oxidation of pyrite at $\text{pH} \leq 3.5$:



Although pyrite may not be the most reactive sulfide mineral, the complete oxidation of one mole of pyrite in a bacterially mediated environment $\text{pH} \leq 3.5$ can liberate 16 protons and a considerable amount of dissolved metals. By comparison, the oxidation of one mole of a monosulfide mineral such as sphalerite (ZnS), galena (PbS) and covellite (CuS) will liberate one mole of dissolved metal (Me^{2+}), one mole of sulfate but no protons:



Under circum-neutral pH conditions, dissolved metal will combine with hydroxide to precipitate sparingly soluble metal hydroxide according to equation 5, slowly decreasing the activity of OH⁻ in solution.



Reactions (1.1) to (1.5) show that, once started, the oxidation of sulfide minerals becomes difficult to stop or slow down without costly control measures. For this reason, the key to successful management of potentially acid-generating waste is to prevent the initiation of oxidation reactions.

Static and kinetic tests have been devised to provide information on the potential of mineral wastes to oxidize, the time of initiation of acid generation and the expected loading of metals and low pH water to the receiving environment. This information is obtained from the interpretation of the leachate chemistry data, from the comparison of sulfide oxidation rates and carbonate mineral depletion rates measured during leaching. Extrapolation of the calculated rates and ion loading suggests a time frame for acid generation: onset, duration and metal loading to receiving waters.

In many cases, however, leachate data yields data that can be difficult to interpret and, therefore, make predictions with any degree of certainty. Such is the case for the low-grade ore waste of the new Huckleberry mine in British Columbia, one of the pyrites studied in this project. Kinetic test results for Huckleberry low-grade ore was inconclusive as to the onset of oxidation of sulfide minerals contained in the rock. Static

tests carried out on this material showed a neutralization potential ratio (NPR) of 0.78, characterizing it as *likely acid generating* according to current British Columbia Guidelines (Price et al., 1997). During 3 years of kinetic (column leach) tests, however, pH, sulfate and calcium levels remained elevated (Lawrence, 1997). The high sulfate and calcium concentrations were attributed to the dissolution of the high gypsum content of the material. Consequently, no sulfide oxidation rates or neutralization depletion rates were extractable from the leachate data, such that no predictions were possible as to the onset of ARD or expected metal loading. As a result, the mine had to assume the material to be reactive and dispose of the material into the tailings pond rather than use it as construction material of the inner pond wall where it would become flooded within 8 years.

In light of the costly disposal alternative for this material of uncertain ARD potential, the first part of this thesis studied the reactivity of pyrite (the principal sulfide mineral in the waste) in both gypsum-saturated and gypsum-free environments, to document the evolution of the reactivity of pyrite as leaching progressed. The results were expected to help evaluate the probability of the waste to oxidize within the time frame of 8 years exposed to air and water. Five other pyrites were studied along with Huckleberry to evaluate the effects of mineralogical characteristics on the reactivity of pyrite in general.

1.2.1.1 Pyrite Oxidation Controls

Sulfide mineral oxidation reactions are documented as surface controlled, based on the availability of reactive sites to participate in the exchange of charges with an oxidizing agent such as oxygen or ferric iron in the case of pyrite (Lowsen, 1982; Moses et al.,

1987; Brown and Jurinak, 1989; Nicholson et al., 1988; Moses and Herman, 1991; Nicholson, 1994). Bacterial oxidation of pyrite, for example by *T. ferrooxidans*, is also documented to be surface controlled. The oxidation of ferrous iron and/or sulfide was found to be facilitated by the attachment of the bacteria to the mineral surface (Herrera et al., 1989; Free et al., 1993). When pyrite is exposed to air and water, the oxidation products of pyrite produce coatings that decrease the surface area of the grain available for oxidation, effectively decreasing the rate of pyrite oxidation. The occurrence of precipitate coatings on pyrite and its effect of decreasing reaction rates are documented by Nicholson and others (1990). Thick precipitate coatings of iron hydroxide, iron oxyhydroxides and jarosite on oxidized pyrite grains are also documented by Jambor (1994), Bigham (1994) and Alpers and others (1994).

Oxidation being a surface controlled reaction, the rate of oxidation of a pyrite is documented to be influenced by the mineralogy, stoichiometry, crystal morphology and defects of pyrite crystals. McKibben and Barnes (1986), Kwong (1993) and Kwong and Lawrence (1994) have indicated that the relative abundance of physical or chemical defects and the occurrence of mineralogical impurities associated with pyrite, influence the distribution of surface free energy on pyrite grains. Locations of higher energy created by defects are more likely to oxidize than grains or parts of grains having lower surface energy. These researchers conclude that oxidation rate of pyrite depends heavily on the mineralogical characteristics of the mineral. Little is known, however, on how these parameters interact to influence the reactivity of pyrite. Kwong (1994) suggested a theoretical order of importance of mineralogical factors influencing the rate of sulfide oxidation based on laboratory weathering tests. Measurements of local redox potentials

gave indications of local reactivity but did not provide a bulk measurement of the reactivity of a pyrite sample, which could be compared to that of another sample. Bulk reactivity measurements on a bulk sample of pyrite (averaging all defects) would provide information on the acid generation potential of pyrite that may be closer to field conditions.

1.2.1.2 Electrochemistry Applied to the Study of Pyrite Reactivity

Electrochemical oxidation of pyrite combined with surface spectroscopy studies has identified kinetic processes of oxidation in various ionic solutions and pH environments. The application of cyclic voltamperometry to hydrometallurgical studies is reviewed by Li and others (1992). Buckley and others (1988), Wadsworth and others (1993), and Li and Wadsworth (1993) used cyclic voltamperometry to document the formation of sulfur, or polysulfide layers on the surface of pyrite following electrode oxidation in slightly acidic or neutral pH solutions. These coatings were found to effectively decrease the leachability or reactivity of the underlying pyrite.

Doyle and Mirza (1996) used cyclic voltamperometry to characterize pyrites from different sources to evaluate the effects of pyrite composition and electric properties (rest potential, resistivity, net concentration of donors and charge carrier concentration) on the oxidation behaviour of pyrite. They found poor correlation between chemical or electric characteristics and pyrite reactivity using their methodology. Their working electrodes consisted of polished pyrite grain, documented in later studies to be largely affected by polishing of the grain, with responses often dominated by fractures or irregularities in the surface of the grain-electrode. Lázaro and others (1995) indicated that electrochemical

responses obtained from carbon paste electrodes (CPE) - a mixture of pyrite, graphite and non-conducting silicon oil – are average responses of the many grains exposed at the electrode surface, including those given by grain-surface impurities and crystal defects. The averaging effect of CPE was found to produce highly repeatable results.

Cyclic voltamperometry using CPE was used in this study to document the reactivity of six different pyrite samples and try to correlate the mineralogical characteristics of each sample with its measured reactivity. The evolution of pyrite reactivity with increasing leaching time was also studied by that method.

1.2.2 Cemented Paste Backfill in the Mining Industry

Backfill can consist of any mining residue depending on the purpose of the backfill; from large waste rock blocks to the coarser portion of mineral processing residues (tailings) or a mixture of all rock sizes. The very fine size portion of tailings has traditionally been avoided as the water it contains drains out more slowly, resulting in backfill stability problems. Mineral processing fines are typically discarded to the tailings containment areas. Decreasing grades of mineral deposits now being exploited has resulted, however, in increasing volumes of mineral processing waste to be disposed of. Shortage of land or resources to build additional tailings impoundments is forcing the mining industry to evaluate ways to reuse the additional waste being generated. Recent technological advancements in tailings dewatering have permitted the inclusion of larger proportions of fines in backfill without the problem of excessive bleeding (drainage of excess water from the mixture) (Cincilla *et al*, 1997; Dahlstrom, 1997; Williams, 1997). Backfill containing a high proportion of fines is a popular solution to the problem of increasing

mineral processing wastes. Paste backfill refers to the thick yet fluid consistency of the fresh mixture, which is specially designed for pipe flow and easy emplacement in stopes of various sizes and shapes. Contrary to plain backfill, paste fill can contain total tailings, which include a considerable proportion of fines. To facilitate pumping and placement of the mixture and minimize erosion of the pipe used for the transport of the paste, it is recommended that the backfill mixture contain a minimum of 15 to 20 % solids finer than 20 μm (Landriault et al., 1998).

Cement can be added to paste mixtures to decrease bleeding of the backfill once in place and/or to increase the strength of the backfill upon curing (Landriault et al., 1998). One of the first uses of cemented backfill in the mining industry occurred at the BHP Mount Isa mine in Australia where, since the early 1930's, large blocks of waste rock were thrown into a vertical shaft along with hydrolysed cement to fill open stopes and accommodate their particular mining sequence. An overview of the Canadian experience with the various types of backfill is given by Udd (1989).

Another advantage of adding cement to paste backfill is the highly alkaline composition of cement material, which provides additional neutralizing capacity to tailings that are potentially acid generating, such as pyritic tailings (Levens and Boldt, 1994). Ideally, this waste management practice could alleviate the need to dispose of reactive waste in an engineered impoundment where, apart from the construction, maintenance and land costs, the reactive waste could oxidize and become an expensive environmental liability.

1.2.2.1 Cement Chemistry, Hydration and Chemical Stability

Cement is one of the most commonly used materials in the construction industry and much is already known about its chemistry, its strengths and weaknesses and its interaction with a variety of aggregates (Taylor, 1997). Under normal circumstances, the inherent chemical stability, physical strength and workability of concrete allows its use in a variety of settings. Table 1.1 describes the various elements that make up Ordinary Portland Cement (OPC) used in CPB, along with the principal hydration reactions involved in the curing of cement mixtures. The cement industry uses abbreviated nomenclature for the unhydrated cement components such that the oxide in the mineral phases is referred to by one letter: C=CaO, S=SiO₂, A=Al₂O₃, F=Fe₂O₃, S=SO₄, H=H₂O. In the cement literature, the alite phase of cement is written C₃S, referring to the composition: 3CaO·SiO₂, or, in analytical chemistry, Ca₃SiO₅. This terminology is used in parts of Table 1.1 and in subsequent text to permit the correlation with the cement literature.

Some agents are known to interact destructively with the components of the concrete, undermining its integrity. Of these, reactive mineral aggregates (i.e. sulfidic aggregates), high concentrations of sulfate in the mixing water or excess atmospheric CO₂ upon drying make up the principal destabilizing agents of concrete (Kosmatka *et al.* 1995). These processes are briefly described as:

Table 1.1: Chemical Composition of Normal Portland Cement (Canada type 10 or Mexico no. 1)

Principal components of dry cement	Typical portion	Principal hydration products	Function
tricalcium silicate: C ₃ S Ca ₃ SiO ₅ (alite) Rapid hardening, early strength development	~50 %	1) $2 C_3S + 6 H_2O \rightarrow Ca_3Si_2O_7 \cdot 3H_2O^{(a)} + 3Ca(OH)_2^{(b)}$ 70% reacted in 28 days	^{a)} Tobermorite gel: principal binding agent of cement ^{b)} Portlandite: no cementing properties
dicalcium silicate: C ₂ S Ca ₂ SiO ₄ (belite) Slow hardening, later stage strength development (after 1 week)	~25 %	2) $2 C_2S + 4 H_2O \rightarrow Ca_3Si_2O_7 \cdot 3H_2O^{(a)} + Ca(OH)_2^{(b)}$ 30% reacted in 28 days, 90% in 1 year	Same as above
tricalcium aluminate: C ₃ A Ca ₃ Al ₂ O ₆ Consumes Ca(OH) ₂ , produces a high heat of hydration	~10 %	3) $C_3A + 12 H_2O + Ca(OH)_2 \rightarrow Ca_4Al_2O_6(OH)_2 \cdot 12H_2O^{(c)}$ 4) $C_3A + 10 H_2O + CaSO_4 \cdot 2H_2O \rightarrow Ca_4Al_2(SO_4) \cdot 12H_2O^{(d)}$ 5) $C_3A + 26H_2O + 3 CaSO_4 \cdot 2H_2O \rightarrow Ca_6Al_2(SO_4)_3(OH)_{12} \cdot 26H_2O^{(e)}$	^{c)} Tetracalcium aluminate hydrate: some early strength development. ^{d)} Monosulfoaluminate and ^{e)} Ettringite: expansive minerals produced from the reaction of dissolved gypsum with C ₃ A.
tetracalcium aluminoferrite: C ₄ AF Ca ₄ Al ₂ Fe ₂ O ₁₀ Manufacturing purpose to reduces clinkering T°, responsible for colour effects in cement	~8 %	6) $C_4AF + 10 H_2O + 2 Ca(OH)_2 \rightarrow Ca_6Al_2Fe_2O_{14} \cdot 12H_2O^{(f)}$ 7) $C_4AF + 50 H_2O + 6 CaSO_4 \cdot 2H_2O + Ca(OH)_2 \rightarrow 2 Ca_6Al_2(SO_4)_3(OH)_{12} \cdot 26H_2O^{(e)}$	^{f)} Calcium aluminoferrite hydrate: rapid hydration but little strength contribution. Slow hydration reaction to produce ettringite
Gypsum: C _S H ₂ CaSO ₄ ·2H ₂ O Very rapid dissolution, slows the rate of C ₃ A hydration to avoid flash setting	~5 %	Dissolved gypsum may participate in reactions (4), (5), (6) and (7), depending on the local pore water chemistry.	Too much gypsum may favour the formation of ettringite over portlandite.
Fe, K, Mg Present in clays used to make Portland cement.	Few %		May be included in any cement phase in solid solution.

Notes: This table adapted from Kosmatka 1995 and Taylor 1997

⁽¹⁾ tricalcium silicate hydrate or “tobermorite gel”: composition may vary and may include trace concentrations of Fe, Mg, K.

Carbonation:

Carbonation refers to the excessive shrinkage of concrete upon drying caused by the penetration of atmospheric CO₂, transforming hydroxides to carbonates. These reactions lower the alkalinity of concrete, destabilizing the curing process. High water:cement ratios, low cement content and/or short curing period enhance the potential for carbonation to occur. This phenomenon is normally restricted to shallow depth or at the surface of the concrete.

Alkali-aggregate reactions:

The reaction between reactive mineral aggregates used in the concrete mixture and the sodium and potassium alkalis present in the cement cause expansive secondary mineral growth. Growths of the secondary minerals create internal stresses within the concrete causing it to crack and lose its strength.

Sulfate attack:

The interaction of the sulfate ion present in the pore water with the hydrated compounds of the cement also results in expansive secondary mineral growth (gypsum and/or ettringite) combined with disintegration of the primary binding material (tobermorite gel).

Water dissolution:

Another deleterious agent of particular importance in the backfill environment is the interaction of neutral pH water with concrete, dissolving and leaching out some of the pH sensitive or water-soluble components of hydrated cement such as portlandite (Ca(OH)₂)

or tobermorite gel ($\text{Ca}_3\text{Si}_2\text{O}_7 \cdot 3\text{H}_2\text{O}$). This can be particularly deleterious when contact occurs during the curing period of the freshly mixed cement (Adenot and Buil 1992; Carde and Francois 1997).

1.2.2.2 CPB in the Mine Environment

The utilization of cement in the mining industry as a binder of tailings in paste backfill is a unique application as a very small proportion of cement is normally used to bind tailings, commonly less than 10 or even 5 % of dry weight, when common concentrations of cement in concrete range from 30 to 40%. In addition, water to cement (w/c) ratios, important in the hydration and subsequent curing of cement, are also considerably higher in CPB applications compared to normal concrete. This ratio is expressed as the mass of water divided by the mass of cementing materials. Kosmatka and others (1995) explain that lower w/c ratios provide the greatest unconfined compressive strength (ucs) in normal concrete. Lamos and Clark (1989) come to the same conclusion with respect to tailings backfill. Normal concrete w/c ratios, typically around 0.5, yield 28-day ucs values ranging between 25 and 35 MPa. Typical CPB applications, such as the four mines studied in this work, have w/c ratios ranging from 5 to 10. CPB mixtures can, therefore, be expected to develop poorer ucs values upon curing than concrete containing the same amount of cement.

In addition, the tailings or aggregate mixed with the cement to form paste backfill is regarded in the cement industry as undesirable aggregate because of its very fine grain size and most importantly, because of its composition, in the case of high sulfide tailings. The Canadian Standards Association (Standard A23.1) specifies the lower and upper

limits of grain size that should make up the fine size portion of aggregate. Standard A23.1 specifies a lower limit of 5 to 10% passing 160 μ m and upper limit of 80 to 100% passing 2.5 mm. Furthermore, the Canadian Portland Cement Association (CPCA) (Kosmatka et al., 1995) indicates that the fine aggregate content should be no larger than 45% by mass or volume of the total aggregate content, above which the cement cannot efficiently coat all aggregate particles. When a large proportion of small size particles are used as aggregate, the mixture will require a larger cement content to effectively coat all the particles and meet specified strength requirements. In the case of CPB, the tailings used as aggregate are often finer than 150 μ m. Consequently, the cement added to the paste mixture can be expected to underperform in terms of strength development upon curing compared to a similar cement proportion used in conjunction with standard aggregate.

Pyritic aggregate is normally avoided in cement mixtures because of its reactivity and the consequent production of sulfates. Sulfate is a documented aggressive agent that participates in expansive secondary mineral growths within the concrete (Shayan, 1988; DeCeukelaire, 1991; Idorn, 1992; Casanova et al., 1996). These reactions create internal stresses that lead to cracking and disintegration of the cured concrete. The details of these reactions are discussed in the later paragraphs.

In summary, the constituents of paste backfill are far from ideal to provide a mixture of optimum compressive strength. The strength requirement for paste backfill is, however, commonly much lower than for a building material. In the four cases studied, the UCS requirement range between 0.5 and 3.5 MPa, depending on the purpose of the backfill. Indeed, backfill used to fill empty voids surrounded by rock mass requires minimal

strength, enough to prevent liquefaction when blasting other areas of the mine or in the event of seismic activity.

Higher backfill strengths are required when the material is used to hold rock faces against which active mining is planned. In these cases, the strength of the backfill material must not be decreased by cement-altering reactions. In a mine setting, the backfill is unfortunately exposed to various conditions that can be detrimental to the chemical stability of cemented tailings backfill such as sulfate attack from sulfate rich ARD generated within the mine or present in the tailings water used to make up the backfill mixture and water dilution of the cement phase of incompletely cured backfill. Figure 1.1 shows different leaching environments to which backfill can be exposed. All stopes are backfilled in this figure, the red colour backfill indicates exposure to ARD generated within the host rock whereas the grey colour indicates exposure to neutral pH, infiltrating water. The cyclic-leached environment (top) represents cases where backfill is temporarily exposed to either infiltrating rain water underground but above the water table or exposed to meteoritic water in above ground applications. Flooded-leached environment (bottom left) represents backfill submerged in circum-neutral pH groundwater, and the ARD environment (bottom right) represents backfill submerged in low pH ARD water containing high concentrations of sulfate and metals. These three potential leaching environments were studied in this project.

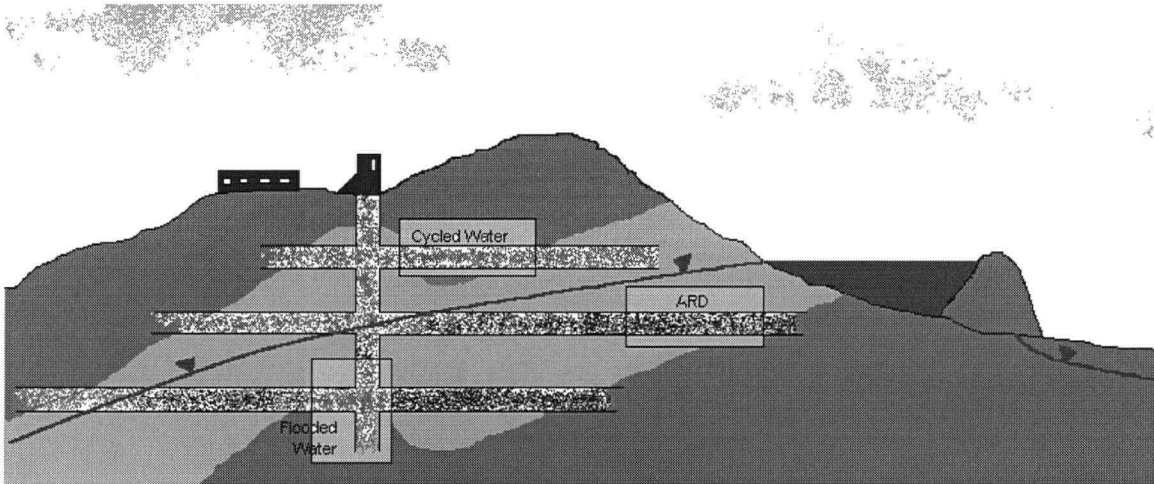


Figure 1.1 Paste Backfill Leaching Environments

1.2.2.2.1 Sulfate attack:

Sulfate is omnipresent in most metal mines, either in the groundwater in contact with the deposit or in the wastewater generated by ore processing. Sulfate concentrations in mineral processing water are often greater than 1.5 g/l, classified as aggressive water in the cement industry (Table 1.2).

Table 1.2 Concrete Subjected to Sulfate Attack

Degree of exposure	Water soluble sulfate in soil sample (%)	Dissolved sulfate in contact with concrete (g/l)	Portland cement type to be used
Very severe	> 2.0	> 10.0	50
Severe	0.2 – 2.0	1.5 – 10.0	50
Moderate	0.1 – 0.2	0.15 – 1.5	20, 40 or 50

Adapted from Kosmatka *et al.*, 1995

Cemented backfill paste is normally made from tailings piped directly from the processing plant to which cement is added in a secondary mixing step. The hydration

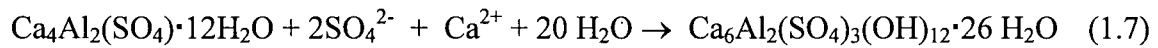
water of the mixture consists in large part of this sulfate-rich residue water. The only method of reducing the sulfate concentration from the tailings water would be to thoroughly wash the tailings or precipitate out the sulfate as a stable mineral phase, both uneconomical and inefficient (Noranda Technology Centre, 1998a). A second source of sulfate is acid rock drainage (ARD) which may not necessarily be acidic but may contain high (aggressive) concentrations of sulfate generated by the oxidation of sulfide minerals. In the first case, where sulfate is found within the tailings water, the chemical stress is generated within the paste. In the case of ARD, the chemical stress or aggressivity is external.

The chemical process of sulfate attack on hydrated concrete can be summarised as follows:

Free sulfate ions present in solution (from ARD or from sulfate present in the pore solution of the backfill) can combine with calcium of dissolved portlandite ($\text{Ca}(\text{OH})_2$) to form gypsum according to reactions 1.6:



Gypsum growth in pore spaces creates pressure that, when occurring at a large scale, can induce cracking of the backfill. Crystallisation pressures can reach 70 to 2000 MPa (Ouellet et al., 1998). Another expansive reaction is the formation of ettringite ($\text{Ca}_6\text{Al}_2(\text{SO}_4)_3(\text{OH})_{12} \cdot 26 \text{H}_2\text{O}$) from the reaction of aqueous sulfate and calcium, (from dissolved portlandite and free sulfate or from dissolved gypsum) and the monosulfate phase of cement ($\text{Ca}_4\text{Al}_2(\text{SO}_4) \cdot 12\text{H}_2\text{O}$) according to reaction 1.7:



The higher molecular weight and larger crystal lattice of ettringite compared to monosulfate phase will also induce expansive forces or crystallisation pressures within the backfill that can result in cracking and disintegration (Fu et *al.*, 1995; Taylor, 1997).

Mineral additives such as ground blast furnace slag, silica fumes or fly ash can be added or partially replace OPC to modify fill mixture properties, such as workability of the mixture, to increase the strength of the fill at a particular stage of curing or resistance to chemical attack (Mangat and Khatib, 1995; Gifford and Gillott, 1997; Taylor, 1997). Mineral additives such as those presented in Table 1.3 are used to reduce the cost of the binding agent without decreasing the strength of the fill. In order to improve the sulfate resistance of concrete, the amount of calcium hydroxide and calcium aluminate hydrate must be minimized.

Table 1.3: Replacement Components of Portland Cement to Improve Sulfate Resistance of Concrete

Additive	Effect
Fly ash: coal combustion residue; low calcium (Torii <i>et al.</i> 1995) (Djuric <i>et al.</i> 1996)	Lower air and pore volume, reduced permeability, increased resistance to sulfate absorption into concrete.
Silica fumes: Silicon, silicon alloy smelting ash residue; minimum 75% silicon, very low calcium and aluminium oxides (Akoz <i>et al.</i> 1995)	Lower air and pore volume, very reduced permeability, decreases gypsum and ettringite formation, increased electrical resistivity (corrosion protection)
Blast furnace slag: glassy iron smelting residue; calcium silicates and aluminosilicates may be high (13-15%) Al ₂ O ₃ slag or low (3-5%) Al ₂ O ₃ slag (Irassar <i>et al.</i> 1996)	Lower air and pore volume, reduced permeability, may increase mixture strength in the end.

1.2.2.2 Dissolution of the Cement Phase of Backfill

The dissolution of cement phases in contact with meteoritic and groundwater has been studied by the French Commission on Atomic Energy with respect to degradation of cemented containers of nuclear waste. Carde and Francois (1997) who used ammonium nitrate leaching solution previously determined to leach cements in a similar but more rapid way than water, point out that a zone of lesser strength is formed in the leached area and that the decreased strength is due to increased porosity resulting from the complete leaching of the portlandite phase of cement (Ca(OH)₂). The increase in porosity was calculated to be equal to the proportion of portlandite in their concrete mixtures. A

progressive decalcification of the tobermorite phase was also observed. Leaching of these phases were the only deterioration found to occur in concrete samples kept immersed in the leaching solution. In wet-dry cycled experiments, an increase in pore solution ion concentration was found to promote the precipitation of secondary expansive minerals such as ettringite causing internal stresses and microcracking of the concrete. Adenot and Buil (1992) used deionized water in similar leaching experiments and observed similar alteration: thin leached zones characterized by partial or complete dissolution of portlandite but preceded by the dissolution of ettringite and monosulfoaluminate phases. Calcium to silicon ratios of the tobermorite phase were also found to decrease from the core of the specimens towards the surfaces, reflecting a decreasing calcium concentration in the pore solution of the edges of the samples. Advancement of the dissolution front was calculated to be proportional to the diffusion rate of deionized water in the concrete. The cores of their flooded samples were observed to possess a similar composition to the cores of the unleached samples. In similar experiments to those of Adenot and Buil, Revertégat and co-workers (1992) determined that dissolution of portlandite started to occur at pH 12.5 and became more severe as the pH of the pore solution dropped. Using additional samples made of cement and fly ash, they documented the increased resistance of this binder mixture to leaching. They determined that this binder mixture uses portlandite in its hydration process, effectively decreasing the amount of portlandite available to be leached, resulting in a lower loss of porosity.

That research indicates that deionized water is indeed an effective leaching agent of concrete, dissolving away portlandite thereby increasing the porosity of the material, as well as decalcifying or degrading tobermorite gel, the principal binding agent of cement. The considerably higher porosity of backfill material compared to concrete suggests that leaching solution will more effectively penetrate the backfill and alter the pore solution chemistry, creating disequilibrium conditions between the solution and the solid phase and accelerating the dissolution of the cement phases of the backfill.

2 MINE SITE DESCRIPTIONS

Figure 2.1 shows the location of the Canadian mines sites and Figure 2.2, the location of Mexican mine sites studied in this project. Table 2.1 below identifies the mine sites from which samples were obtained for both the pyrite reactivity and cemented paste chemical stability studies. A summary description of the geological setting, deposit type and mode of pyrite occurrence is also presented.

Table 2.1: Summary of Sample Geological Setting and Mineralogy

Mine	Location	Deposit type	Pyrite occurrence ¹
Huckleberry 1997 - present	British Columbia, Canada	Skarn deposit Cu, Mo	Vein fill, coarse granular pyritohedrons
Louvicourt 1992 - present	Québec, Canada	Volcanogenic massive sulfide in felsic tuff, chert and mudstone host rock ² . Cu, Zn, Ag, Au	Fine-grained massive pyrite, cubic Some chalcopyrite and sphalerite
Brunswick 1950's - present	New Brunswick, Canada	Volcanogenic massive sulfide in felsic volcanic and volcanoclastic host rock ³ Pb, Zn, Cu, Au	Fine-grained massive pyrite, cubic
Tizapa 1994 - present	Mexico state, Mexico	Stratiform volcanogenic massive sulfide in andesitic metamorphised volcanoclastic host rock Zn, Pb, Cu, Au, Ag	Fine-grained massive pyrite, cubic
Francisco I. Madero (FIM) Project	Zacatecas, Mexico	Stratiform volcanogenic sulfides in metamorphised andesitic volcanoclastic host rock Pb-Zn, Cu (Ag)	Fine-grained massive pyrite, cubic
Zimapan 1920's (?) - present	Hidalgo, Mexico	Skarn Pb-Zn deposit Pb, Zn, Ag, Cu, (Au)	Medium to large grained cubic pyrite crystals

(1) Pyrite mode of occurrence in samples used for tests

(2) Tourigny *et al.*, 1994; (3) Luff *et al.*, 1992

Mine Site Locations

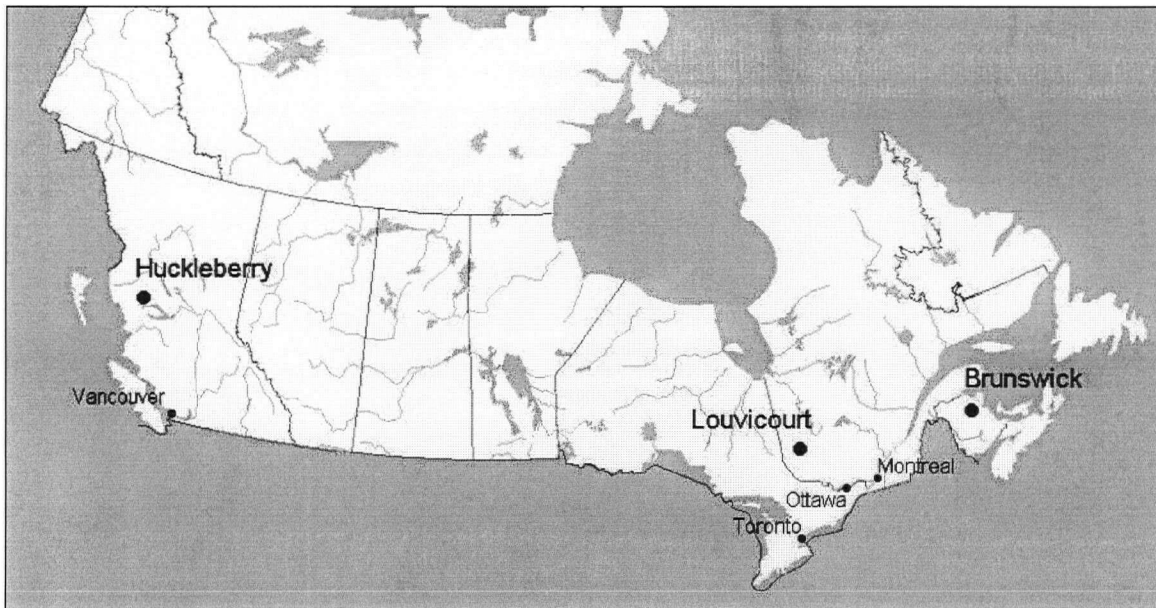


Figure 2.1 Sites Location of Huckleberry, Louvicourt and Brunswick mines, Canada



Figure 2.2 Site Location of Tizapa, Zimapan and Francisco I. Madero (FIM) mines, Mexico

2.1 COMPARISON OF MINE SITE AND EXPERIMENTAL CONDITIONS

Table 2.2 Describes the site conditions encountered at the different mine sites where paste backfill will be used. These conditions can be compared to the experimental conditions carried out in this study, presented in Chapter 3, Section 3.2.2, Table 3.4.

Table 2.2 Hydrogeologic Conditions at Mine Sites where Backfill is or will be Used

Site	Mine Site Water Quality	Backfill Mix Water Quality	Use of Backfill (or projected use)
Louvicourt	pH: 8.3 SO ₄ : 620 mg/l Fe _{tot} : 0.05 mg/l Cu: 0.03 mg/l Zn: 0.10 mg/l	pH: 7.55 SO ₄ : 700 mg/l Fe _{tot} : 0.64 mg/l Cu: 0.03 mg/l Zn: 0.40 mg/l	Pyritic tailings, Underground use, (since 1992), future surficial use possible.
Tizapa	SO ₄ ²⁻ : 2.4 mg/l	n.a.	Planned underground use.
Brunswick	pH: 2.9 ⁽¹⁾ SO ₄ : 6900 mg/l Fe _{tot} : 1100 mg/l Cu: 8.4 mg/l Pb: 2.7 mg/l Zn: 1650 mg/l	n.a.	Underground use. June 1998 startup of backfill plant.
Francisco I. Madero	Early development stage, no data available.		Planned underground use.

(1) Average water chemistry from 0-mile brook, from January 13, 1989 to July 3, 1997 (Moerman, 1997).
n.a.: not available

3 EXPERIMENTAL METHODOLOGY

All pyrite and paste experiments, as well as parts of the analyses, were carried out in Mexico. The laboratory equipment for both studies was constructed and previously tested at the University of British Columbia (UBC). The laboratory set up was then dismantled and rebuilt at the Universidad Autonoma de San Luis Potosí (UASLP), in Mexico. Pyrite, tailings and slag samples were sent directly from the mines to UASLP where they were prepared and the paste samples were mixed and cured prior to leaching. The 20-week leach cycles for both experiments, as well as most mineralogical analyses, were carried out at UASLP. Mineralogical analyses of the leached paste mixtures were carried out at UBC. X-ray diffraction analyses were carried out at UASLP. Cyclic voltamperometry was carried out at the Universidad Autonoma Metropolitana – Ixtapala (UAMI) in Mexico City. Leachate samples from both the pyrite and the paste experiments were sent for analyses to the Centro de Investigación y Desarrollo Tecnológico (CIDT) of Peñoles in Monterrey, Mexico.

3.1 PYRITE EXPERIMENTS

3.1.1 Sample Preparation and Analyses

Pyrite was obtained from composite hand samples chosen by the geologist of each mine to represent the most common mode of occurrence at the site. The samples containing coarse pyrite crystals (Huckleberry and Zimapan) were put in a double bag of 6 mil polyethylene and fragmented with a steel head hammer to release pyrite crystals.

Individual pyrite crystals containing no visible oxidation coating or inclusions of other minerals were hand-selected for use in the tests.

Hand samples of pyrite from the Louvicourt and Tizapa mines consisted of massive fine grained pyrite (75-90% pyrite content), making the segregation of individual crystals by hand practically impossible. The whole samples were therefore prepared directly without the separation of gangue or minor impurities. Samples were reduced to -6.25 mm using a jaw crusher previously cleaned by repeated passings of clear glass. No pure silica sand was available for this purpose.

Pyrite crystals and crushed particles were soaked in an acid bath of 2N HCl for 1 hour to remove oxidation coatings, followed by six repeated rinsing in deionized water. The pyrite samples were oven dried at 35°C for 24 hours. Dry grinding was performed in two steps, first using a glass-cleaned ring pulverizer to reduce the grain size and obtain a first batch of the required particle size and second, with an agate mortar to grind down the coarse material leftover from the ring pulverizer. The ground pyrite was dry sieved using standard 105 and 150 μm Tyler sieves. The +105 –150 μm fraction was retained for the leaching tests. Sieves were washed in an ultrasound bath and completely dried between the different samples. Pyrite samples were kept in a glass dessicator under vacuum between the various preparation steps and when not in use to avoid oxidation of pyrite surfaces.

3.1.2 Leaching Apparatus

The leaching apparatus was designed to promote the oxidation of the different pyrite samples and facilitate the measurement and comparison of the early effects of leaching on pyrite grains. Mineralogical observations, as well as chemical and electrochemical analyses, were performed on the unleached pyrite and after 4, 10 and 20 weeks of leaching. The leaching apparatus consisted of 5 cm diameter Büchner Funnels™: a polyethylene container with a flat perforated bottom and open top, attached at the bottom to a funnel (Figure 3.1). A 45 µm filter paper was placed at the bottom of the container to retain the pyrite particles. 20 gm of pyrite was placed in each funnel. The leaching solution was devised to simulate rainwater: distilled water with a pH adjusted to 5.5 by the addition of CO₂, prepared immediately before use. 15 ml of leaching solution, enough to cover the sample, was added to each sample twice weekly. The pyrite samples were left inundated for 3 hours, after which the solution was extracted by vacuum suction, re-filtered and analyzed. The pyrite samples were left exposed to ambient air between each leaching cycle. Three (3) samples of each pyrite were prepared and leached simultaneously. One (1) sample was removed at the end of each period for the various analyses.

Additional samples of Huckleberry pyrite were leached with Huckleberry waste rock leach solution. The solution was generated in two leaching columns, each containing 2.5 kg of crushed low-grade ore (-3.33mm +1.68 mm). The crushed ore was previously rinsed with 5 litres of deionized water to wash out all the fines (finer than 1.68 mm). To each column was added 250 ml of deionized water with the pH adjusted to 5.5 with CO₂. The water was retained in the columns for 1 hour after which the bottom valve was

opened to let the solution freely drain out. The leachate was then filtered and used to leach samples of Huckleberry pyrite prepared in the same way as the water-leached pyrite. The remaining solution was acidified and submitted for chemical analyses.

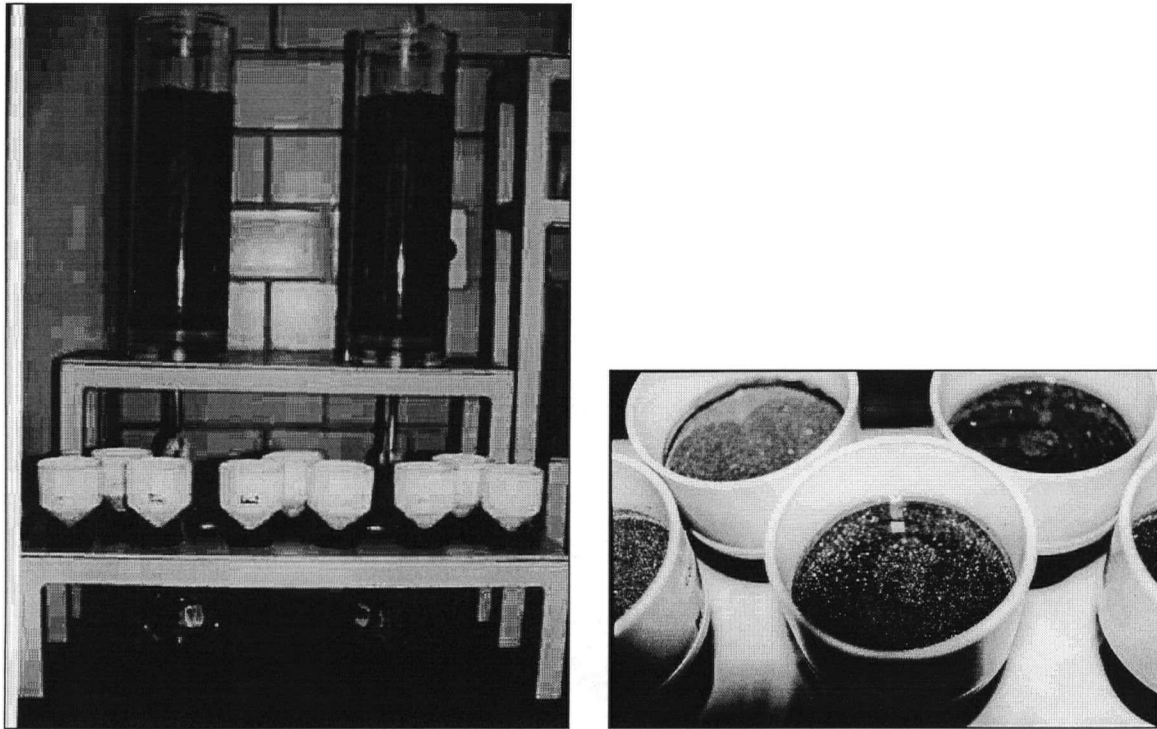


Figure 3.1 Pyrite Leaching Apparatus

3.1.3 Chemical analyses

Routine chemical analyses were performed on leachate solutions obtained by the pyrite experiment and by the Huckleberry waste rock columns for the parameters listed in Tables 3.1 and 3.2. The solution pH, redox potential, conductivity and ferrous iron were analysed upon collection at UASLP, the other leachate parameters, as well as solids analyses of the unleached pyrite samples were analyzed at the chemical laboratory of the Centro de Investigación y Desarrollo Tecnológico (CIDT) of Peñoles in Monterrey,

Mexico. The pyrite leachate solutions were acidified with concentrated HCl to a pH < 2 and stored at 4°C between monthly shipments to Peñoles via courier.

Table 3.1 Leachate Analyses Carried Out at UASLP

Analysis	Instrument
pH, redox potential	Beckman ϕ 320 combined pH and redox meter
Conductivity	Cole Parmer portable conductivity meter Model 19820-00 0.1N KCl (Calomel) probe, all values adjusted to the standard hydrogen electrode (SHE).
Ferrous iron	UV Spectrophotometer Beckman DU 650, using O-phenanthroline indicator

Table 3.2 Leachate and Solids Analyses Carried Out at CIDT

Sample type	Analyses	Methodology and Instrument
Leachate Solutions (both pyrite and paste backfill experiments)	Fe _{total} , Cu, Zn, Pb, As, Al, Sb, S, Si, Ca, Mg, K	Atomic absorption spectrometer (AA) determination (Perkin-Elmer model 5000)
	SO ₄ ²⁻	Gravimetric determination
Solids (unleached pyrite samples)	CO ₃ , SO ₄ , CaO, K ₂ O, MgO, MnO, Na ₂ O, SiO ₂ , Al ₂ O ₃ Ag, As, Bi, C, Cd, Cu, Cr, Fe, Ni, Pb, S, Se, Te, Zn.	Aqua-regia digestion and AA analysis (Perkin-Elmer 5000)

3.1.4 Mineralogical and Electrochemical Characterisation of Pyrite

All pyrite samples were characterized mineralogically and chemically prior to leaching to determine stoichiometric compositions, as well as crystal habit and form. Polished

sections of the hand samples containing the pyrite from each mine were prepared for observation under both optical (reflected light) microscope and scanning electron microscope (SEM). Reflected light microscopy was carried out using a Versamet Union microscope, whereas SEM observations were carried out using a Philips XL30 Scanning Electron Microscope. Quantitative chemical microanalyses were carried out on the polished sections using the energy dispersive x-ray (EDAX) of the SEM. Loose grain mounts of the leached pyrites were prepared after each leaching period (4, 10 and 20 weeks). The grain mounts consisted a dusting of the pyrite grains over double-sided carbon tape fixed to a metal holder. These samples were carbon-coated for SEM observations. Qualitative chemical microanalyses were carried out using EDAX to identify the precipitation products formed after each leaching period.

Electrochemical analyses were carried out on unleached pyrites and after 4, 10 and 20 weeks of leaching to characterise pyrite surfaces and verify the presence of precipitates imperceptible with the SEM. At the end of each leaching cycle, the pyrite samples were oven dried at 35°C and transported to the electrochemistry laboratory of the UAMI in air tight polyethylene containers, for voltamperometric studies. An EG&G PAR M273 Potentiostat coupled to a PC with the M270 software were used to generate a voltage cycle of 20 mV/sec and record the voltamperometric response respectively. A 3-electrode system was used, of which a carbon paste (graphite-pyrite, 50% wt) electrode (CPE) was used as the working electrode. The carbon and pyrite were carefully blended together with laboratory grade silicon oil in an agate mortar (Figure 3.2). The resulting paste was placed in a 0.5 ml plastic syringe into which was inserted a platinum electrode welded with silver to a copper wire end, in turn connected to the current source. The

counter electrode consisted of a graphite rod, the reference electrode a Hg/HgSO₄/K₂SO₄ (sat), SSE (Eh=0.615V, SHE). The electrode system was placed in a Pyrex™ glass cell containing an electrolyte solution of 0.1M NaNO₃ with a pH of 6.5, through which was bubbled purified nitrogen gas for a minimum of 45 minutes before the start of the experiments. Nitrogen was blown on top of the solution throughout the tests to provide an inert atmosphere within the cell. The set-up is shown on Figure 3.3.

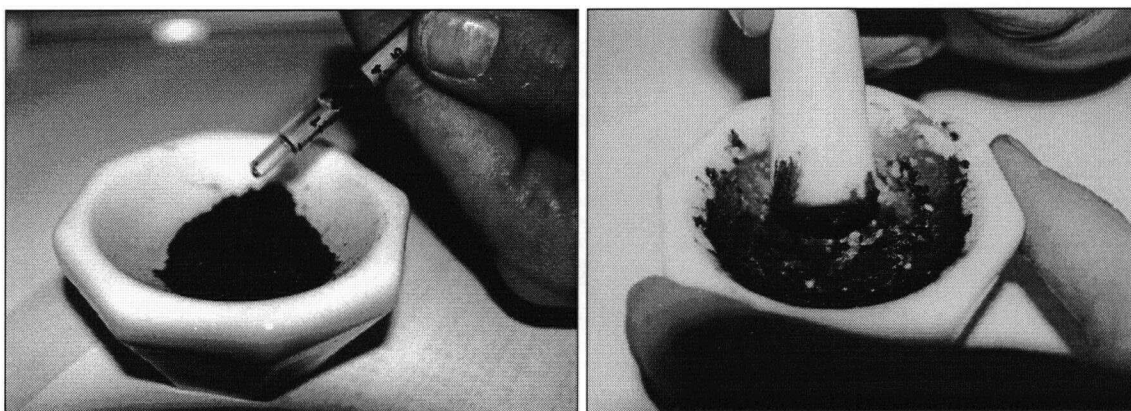


Figure 3.2 Preparation of Carbon Paste Electrode (CPE)

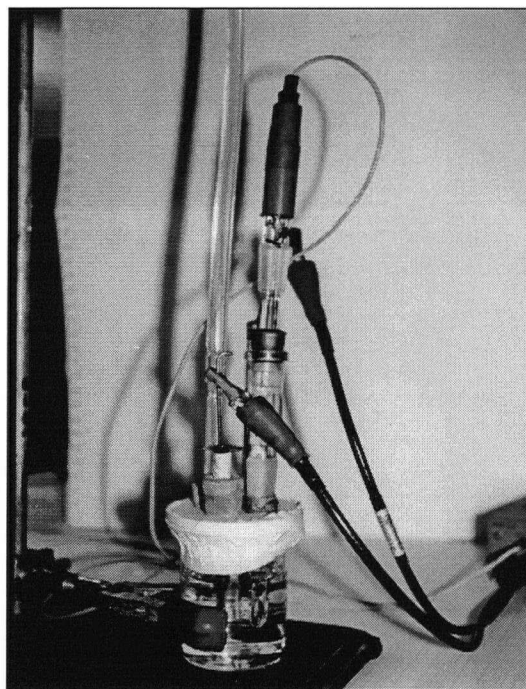


Figure 3.3 Electrochemical Cell (front clip attached to CPE)

The zero current potential (rest potential) of the CPE was established before conducting the potential sweep by letting the electrode system rest for a minimum of 5 minutes until a stable reading was obtained. Single-cycle potential sweeps were initiated in both the anodic and cathodic directions (to induce pyrite surface oxidation and reduction respectively) within the range of -1.0 to $+0.7$ V. This range was established from the “no current response” of a CPE that did not contain pyrite, placed in the 0.1 M NaNO_3 electrolyte solution. A new working electrode (CPE) surface was obtained after each sweep by squeezing out a small amount of paste from the syringe and levelling the CPE tip on a 600 grit silica carbide sand paper. Multiple analyses were carried out of each sweep range in order to obtain a repeatable (representative) response usable for a comparative study.

3.2 PASTE EXPERIMENT

3.2.1 Paste Sample Preparation

3.2.1.1 Paste Components

Tailings were sent by courier from the mine site to UASLP in airtight containers with enough residual water to cover the tailings and prevent oxidation during transport. Wet tailings were oven dried at 40°C for 72 hours or until constant weight. FIM tailings were shipped dry and were used without preliminary treatment.

Dry tailings were used in the paste mixture in order to standardize the mixing procedure and to have control of the water content of each mixture. City tap water was used to make up the paste samples since not enough tailings water was available to make the required volumes of samples, and some tailings' water chemistry (FIM samples) were unavailable. The tailings were not washed prior to drying, therefore the sulfate present in the tailings water and pore water likely precipitated then redissolved upon hydration of the paste mixture. Drying the tailings prior to use is not believed to have caused major changes in the chemistry of the tailings.

Ordinary Portland Cement (OPC) Type 1, the Mexican equivalent of Canadian Portland Cement No.10, was used as binding agent as prescribed in all paste recipes submitted by the mines. The cement was analyzed chemically before forming the paste samples to make sure that it met specifications. The chemical composition of the cement is shown in Table 5.5 of Chapter 5.

3.2.1.2 Paste Mixing

The paste backfill formulation of each mine was followed as closely as possible in the preparation of paste samples. Since the FIM project is still in the feasibility stage, the project consultant's suggested formulation (based on general guidelines) was followed for that mine. The formulation to be used at FIM in the future may differ from that made in this study. Table 3.3 shows the proportions of tailings, water and binder required for each paste recipe (shaded) and actual proportions used to make up the paste for each mine for this investigation (un-shaded). Standard slump tests (CSA test method A23.2-5C) were carried out to determine paste consistency using a standard slump cone. Slump test results are expressed as cm of slump of the material once the cone had been removed. A large slump corresponds to a more liquid, less consistent paste.

Initially, a single tailings sample was used to determine the relative proportions of cement, water and aggregate necessary to achieve the right slump since not enough tailings samples were available to carry out repeated tests. The test indicated that only the site-specific tailings could give the required slump within the given range of component proportions. Consequently paste mixtures were made by using a fixed amount of binder and tailings from each mine to which was added the minimum amount of water suggested in each recipe. The amount of water was then slowly increased if necessary until the mixture reached the specified slump range. In some cases, the maximum water content specified by the recipe would not yield an adequate slump and the mixture would be too stiff. In these instances, a compromise between water content and acceptable slump range was made in order to obtain an adequate mixture.

Paste mixing and moulding was carried out according to ASTM specifications C192-90a and C470 for concrete mixtures. Key elements of these specifications are as follows:

1) Mixing of paste (Figure 3.4 a, b):

- A plastic, non reactive container was used to mix the paste components,
- The batch size of the backfill mixture was larger than the volume of the slump cone,
- All constituents were dry and well mixed prior to water addition,
- The batch was hand mixed for 20 minutes until homogeneous, following which the slump test was carried out,
- The water content was adjusted if necessary and the batch was re-mixed for 10-15 minutes following which a second slump measurement was taken,
- Slump measurements were not repeated more than twice per batch,
- The paste material used for the slump test was put back in the mixing container and used to fill the moulds.

Table 3.3 Paste Sample Preparation

Mine	Total Solids ¹ (% weight of paste)	Binder (% weight of dry solids)		Water Content	Slump	Curing
		Cement ²	Additives ³			
Louvicourt	~78 %	0.9 %	3.6 %	~22 %	15 - 18 cm	Suggested 28 days
	75 %	0.9 %	3.6 %	25 %	14.8 cm	14 days
Brunswick	78-80 %	5 %	none	20 - 22 %	20 cm	--
	78 %	5 %	0	22 %	23.3 cm	14 days
Tizapa	82.5 - 84.5 %	6 - 8 %	none	15.5 - 17.5 %	17.5 - 22.5 cm	Minimum. 7 days
	80 %	6.22 %	0	20 %	17.0 cm	14 days
FIM	76 - 78 %	3 - 4 % (unspecified binder type)		22 - 24 %	14 - 18 cm	--
	76 %	3 %	0	24 %	17.8 cm	14 days

¹ Solids constituted of dry tailings

² Mexican Portland no. 1, equivalent to Canadian Portland type 10

³ Blast furnace slag sent by Louvicourt mine

Recipe

Actual sample compositions

2) Mould material and mould filling (Figure 3.5):

- Non reactive, non-absorptive, watertight, single use cylindrical polyethylene moulds were used having an internal diameter equal to $\frac{1}{2}$ the vertical height (5 cm diameter x 10 cm height),
- The filling sequence was dictated by the size and shape of the mould:
 - filling was carried out in 2 layers of 5 cm each,
 - each layer was given 25 strokes with a rounded end glass rod to evacuate air bubbles,
 - a slight tap on bottom of mould was given after rodding.

3) Curing of samples (Figure 3.6):

- Samples were covered with a plastic sheet to prevent rapid drying of the surface. Wet sponges were kept under the plastic sheet as sources of humidity,
- Curing was carried out in a temperature and humidity monitored environment with minimised air currents. The average curing temperature was $20^{\circ}\text{C} \pm 2^{\circ}\text{C}$ and average humidity was $80\% \pm 10\%$.

Concrete samples, for which the above specifications were designed, possess considerably more binder or cement (commonly around 30 % binder) than paste material made by the mining industry (commonly less than 8% binder). As a consequence, a deviation to specification C192 had to be made where the paste samples were not de-moulded after 24 hours because of the lack of strength of some samples. All samples were de-moulded after a humid cure period of 14 days.



Figure 3.4: a. Mixing Paste Sample



b. Standard Slump Test

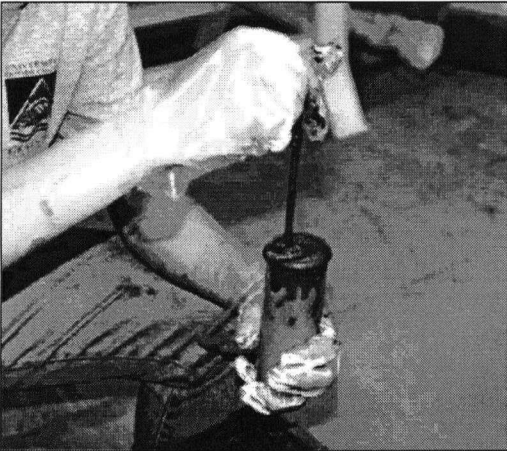


Figure 3.5 Rodding Paste into Mould

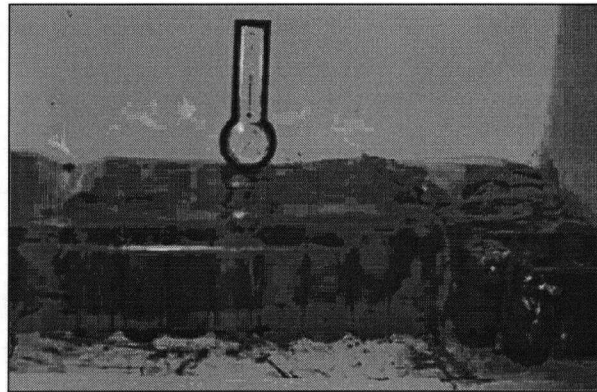


Figure 3.6 Curing of Paste Samples

3.2.1.3 Pre-Leaching Sample Preparation

Cured samples were wet-cut into two pieces using a thoroughly cleaned and degreased circular saw (diamond saw). The pieces consisted of a cylinder of 10 cm length for compressive strength test and a separate piece of 2 to 3 cm thick (termed a puck) polished on one side intended for mineralogical observations. The sample surfaces in contact with the mould were lightly sanded to remove the thin oxidation coating that had started to

form upon curing for some samples. Both pieces of each sample were oven dried at 40°C for 48 hours, weighed and measured before placement in the leaching cells.

3.2.2 Leaching Apparatus and Leaching Cycles

The leach solutions and leach cycles were devised to simulate the different modes of exposure of a cemented paste backfill, as shown in Figure 1.1 of Chapter 1. Table 3.4 explains how these environments were simulated in the laboratory to recreate the various leaching scenarios.

Table 3.4 Paste Leaching Scenarios

Mine Setting	Mode of Leaching	Leaching Solution	Leaching Frequency
Sub-aerial backfill or in underground mine above the water table	Alternating dry (ambient air) and flooded cycles	Simulated rain water: distilled water, pH adjusted to 5.5 with CO ₂	1 week cycle: 24 hours flooded then drained and let open to ambient air for 6 days
Flooded backfill (below the water table), absence of ARD in mine water	Constantly flooded cycles, 2 week water circulation period	Simulated rain water: distilled water, pH adjusted to 5.5 with CO ₂	1 week cycle: ½ cell volume taken out for analyses and replaced with fresh solution
Flooded backfill in contact with acidic groundwater produced in the mine	Constantly flooded cycles, bi-weekly solution replacement	Fe ₂ (SO ₄) ₃ solution, 0.005 M or (1.5g/l SO ₄ ²⁻) pH 2.4 - 2.6	½ week cycle: replacement of entire cell solution

The leaching cells consisted of 8.5 cm diameter, 15 cm tall, clear acrylic cylinders equipped with an evacuation valve at the bottom and removable cap and valve at the top (Figure 3.7). Some additional cells were made at UASLP having slightly different dimensions (5 cm diameter, 20 cm tall) for the lack of similar size material but with an

equal volume as the cells made at UBC. Figure 3.8 shows the laboratory set-up for the cemented paste fill leaching study. Three cells were prepared for each sample and leaching environment so that one sample could be removed after each designated leaching period for destructive analyses. Three (3) samples were prepared and leached simultaneously in a ferric sulfate solution, 3 in a flooded water environment and 3 in the alternating air-water environment for each mine. After every leaching period (5, 10 and 20 weeks) 1 leaching cell was dismantled for analysis of the solid phase. In each of the first five weeks, leachate solutions of the three leach cells characterizing the same environment were combined to form one large sample for analysis. Between the 5th and 10th week, leachate samples were a composite of the two remaining cells of the same environment and leachate samples between the 10th and 20th week originated from a single leaching cell.

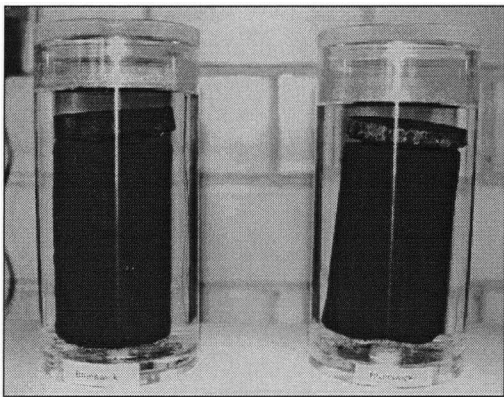


Figure 3.7 Leaching Cells

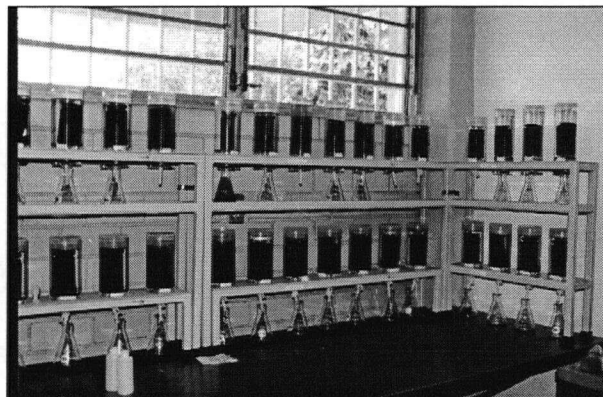


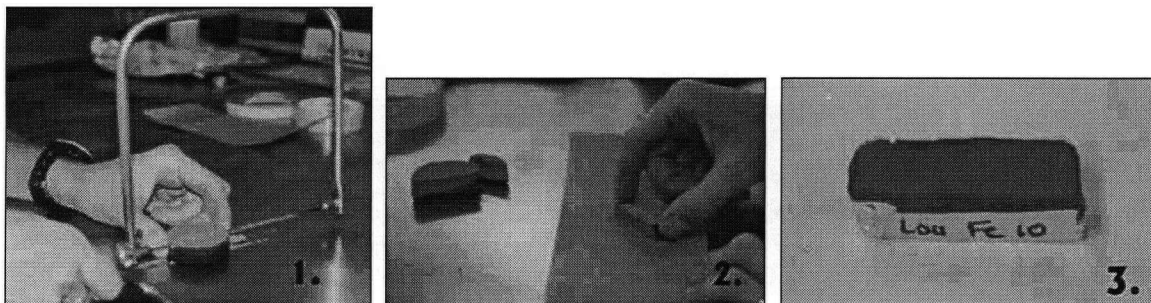
Figure 3.8 Lab Set up, Paste Leaching Study

3.2.3 Post-Leaching Sample Preparation

After each leaching period, the retrieved samples - both cylinder and puck - were measured, weighed and oven dried at 50°C for approximately 72 hours or to a constant weight. The difference between the wet and dry weights was noted for later analysis of

water absorption by the paste sample in the different leaching environments. The dry samples were placed into individual bags of 2-mil polyethylene, properly closed to exclude contact with external moisture. The cylinders were brought to the Soil Mechanics laboratory of the Instituto Politecnico Nacional (IPN) of Mexico City for unconfined compressive strength (ucs) analyses using a Losenheim hydraulic compressor.

The leached paste pucks were very friable and fragile. Consequently, a sample preparation procedure was devised to minimize handling of the sample and maximize the subsequent quality of SEM imaging. The pucks were cut transversally with a fine tooth metal saw and sanded down using 150, 220 then 1500 grit silica sand paper to obtain a flat surface. In the case where pucks were too thin or inappropriate for mineralogical observations, slices of the cylinders were cut out and prepared in the same way. Excess dust and loose particles were lifted from the surface of the cut surface with adhesive tape. The sample was then fixed to aluminium foil with double-sided carbon tape exposing only the flattened, particle-free surface (Figure 3.9 a, b, c). All prepared puck surfaces were photo scanned then carbon coated for SEM observations. Some samples required 2 or 3 coatings of carbon because of their porous nature. Samples were kept in a dessicator between preparation and observation steps.



Figures 3.9 a, b, c: Paste Sample Preparation Steps for Mineralogical Observations

The different oxidation zones of the leached samples were identified by colour and/or textural changes visible on the puck sections and/or cylinders. All the visibly different layers, as well as the core of each sample, were carefully scraped off the 20 week-leached samples (cylinders) and collected for analyses. The 5 and 10 week-leached samples were not used for this purpose, as the oxidation layers were in general too thin to be successfully separated. In cases where no distinct oxidation layers were apparent, a 1mm thick surficial layer was scraped off for analyses.

Mineralogical observations were carried out on the prepared pucks using a Philips XL30 scanning electron microscope (SEM). Chemical microanalyses were performed using an IMIX energy dispersive x-ray (EDX) instrument at UBC. Elemental spectra of the cement phases and precipitates were taken, thereby providing qualitative information about the general composition of these phases. No quantitative information could be extracted from the EDX spectra as the phases of interest were too small and scarce to provide accurate quantitative data with the analytical procedures used.

3.2.4 Chemical Analyses of the Paste Experiment

Routine chemical analyses were performed on leaching solutions (water and simulated ARD or ferric sulfate solutions) and on the leachate produced by the paste backfill leaching cells. Parameters analyzed for the paste backfill study are listed in Tables 3.1 and 3.2 in section 3.1.3. Leachate pH, redox potential, conductivity and ferrous iron were analysed upon collection at UASLP. Other leachate parameters and the hole-rock analyses of tailings, cement and slag were carried out at the analytical laboratory of the Centro de Investigación y Desarrollo Tecnológico (CIDT) of Peñoles in Monterrey, Mexico. The leachate solutions were acidified with concentrated HCl to a pH <2 and stored at 4°C between monthly shipments to Peñoles via courier. Solid phase analyses of the weathered backfill samples were carried out according to the methods listed in Table 3.5. The ferric sulfate-leached Brunswick samples were sent to Chem-Met laboratory of Vancouver for sulfur species analyses. This lab was not equipped to analyse the requested suite of metals and major ions, hence the unused portions of these samples were sent to Chemex laboratory of North Vancouver for analyses of metals and major ions listed in Table 3.5. All the other weathered paste samples were sent directly to Chemex laboratory for sulfur species determination as well as metals and major ions analyses (when sufficient sample mass was available for analyses).

Table 3.5 Solids Phase Analyses for the Paste Experiments

Sample	Analyses	Methodology and Instrument
Unleached solids (tailings, OPC and slag)	FeO, CO ₃ , SO ₄ , CaO, K ₂ O, MgO, MnO, Na ₂ O, SiO ₂ , Al ₂ O ₃ , Ag, As, Bi, C, Cd, Cu, Cr, Fe, Ni, Pb, S, Se, Te, Zn.	Peñoles CIDT: Aqua-regia digestion AA analysis (Perkin-Elmer 5000)
Leached paste	Total Sulfur	Chem Met: Acid leach (oxidation) and gravimetric determination Chemex: Leco 420 combustion furnace with Infra Red detector
	Sulfate	Chem Met and Chemex: Dilute (10%) HCl leach and gravimetric determination
	Al, Ca, Mg, Fe, Cu, Zn	Chemex: HF acid digestion and ICP-AES ¹ analysis (Perkin-Elmer Optima)
	Pb	Chemex: HF acid digestion and AA analysis (Varian 220)

¹ICP-AES: Inductively coupled plasma atomic emission spectroscopy

3.2.4.1 Paste pH and Acid-Base Accounting Measurements

Paste pH measurements were taken on dry tailings and unleached paste backfill for the purpose of comparison and to verify the presence of acidity or available buffering minerals of the samples. Acid-base accounting (ABA) tests were carried out at UASLP to monitor the evolution of the paste buffering capacity as leaching proceeded. The Modified Sobek Method of ABA analysis was followed on all tailings and unleached paste samples as well as on the different oxidation layers of all 20-week leached paste samples.

4 RESULTS – PYRITE REACTIVITY STUDY

4.1 MINERALOGY, CHEMISTRY AND STOICHIOMETRY OF UNLEACHED PYRITES

All pyrite samples studied possessed different chemical compositions, stoichiometries and mineralogical associations. Solid phase chemistry of the pyrite samples, normative mineralogy of the samples and average stoichiometry of pyrite crystals in the samples are summarized in Tables 4.1, 4.2 and 4.3 respectively. SEM micrographs showing sample mineralogy are shown in Plates 4.1 to 4.6.

Mineralogical observations of unleached polished sections showed that the Brunswick and Zimapan samples possessed the greatest amount of sphalerite, galena and arsenopyrite impurities, mainly occurring as small inclusions within pyrite (Plates 4.1 and 4.2). The Brunswick pyrite sample consisted of pyrite concentrate whose particles were ground small enough to expose the separate mineral phases. Louvicourt-2 and Tizapa pyrites contained sphalerite, chalcopyrite, galena as well as some tetrahedrite and arsenopyrite impurities occurring mainly as separate phases in the interstices of pyrite grains (Plates 4.3 and 4.4). Some of these mineral impurities¹ also occurred as inclusions within pyrite crystals. Huckleberry and Louvicourt-1 samples contained the least amount of mineral impurities. Huckleberry pyrite contained no visible inclusions whereas

¹ Mineral impurities refers to the presence of non-pyrite sulfide minerals in the pyrite samples.

Louvicourt-1 contained very few and dispersed inclusions of sphalerite, galena, chalcopyrite and arsenopyrite (Plates 4.5 and 4.6).

Stoichiometric microanalyses of uncrushed pyrite crystals (polished sections) indicated that pyrites in all samples possessed some nickel (Ni), copper (Cu) and arsenic (As) in their crystal lattice. The amount of lattice impurities varied considerably within a single grain and also between the various grains of one sample, as reflected by the high standard deviations of the measurements (Table 4.3). Cross-sectional microanalyses of individual pyrite grains did not reveal any texture differences associated with chemical variations in any of the pyrites.

Table 4.1 Normative Mineralogy of Pyrite Samples

	Huckleberry	Zimapan	Tizapa	Louv. 1	Louv. 2	Brunswick (pyrite concentrate)
crystal habit	Pyritohedrons, large euhedral crystal	Cubic, med. grained euhedral crystal masses	Cubic, fine grained subhedral crystal masses	Cubic, fine grained subhedral crystal masses	Cubic, fine grained subhedral crystal masses	Cubic crystal ground to small fragments
mineralogy	99% Py, some Ma < 1% Sp, Ap, Cp <1% gangue	85% Py 3% Ap 1.5% Ga 1% Sp, < 1% Cp ~ 8% gangue	96% Py 1% Sp 2% Cp < 1% Ga, Ap <1% gangue	86% Py <1% Sp, Ga, Ap, Cp ~13% gangue	81% Py 2% Sp <1% Ca, Ga, Po, Ap ~16% gangue	76% Py 9% Ga 4% Sp <1% Cp ~10% gangue
sample grain size	< 150 um	100-150 um	100-150 um	100-150 um	100-150 um	< 50 um

Notes: Normative mineralogies are calculated from the analytical results of pyrite sample chemistries

Py: pyrite, Ma: marcassite, Sp: sphalerite, Cp: chalcopyrite, Ga: galena, Ap: arsenopyrite, Po: pyrrothoite

Table 4.2 Chemical Analysis of Pyrite Samples

Species	unit	Huckleberry	Zimapan	Tizapa	Louv. 1	Louv. 2	Brunswick (py.concentrate)
S	wt %	47.4	47.3	50.4	40.4	47.4	58.7
S as SO ₄	wt %	0.79	0.41	0.20	0.40	0.20	1.89
S ²⁻	wt %	46.7	46.9	50.2	40.0	47.2	56.8
Fe	wt %	45.2	42.5	45.4	39.4	37.7	38.2
Zn	wt %	0.01	0.70	0.53	0.004	0.98	2.60
Pb	wt %	0.01	1.39	0.12	0.04	0.04	8.00
Cu	wt %	0.02	0.02	0.80	0.04	0.02	0.32
Ni	wt %	<0.005	<0.005	<0.005	<0.005	<0.005	0.006
As	wt %	<0.02	1.18	0.19	0.05	0.06	0.28
Bi	wt %	0.024	0.015	0.031	0.018	0.016	0.030
SiO ₂	wt %	0.50	2.56	0.30	11.2	8.70	0.95
CO ₃	wt %	0.14	0.04	0.01	0.43	0.10	0.74
Al ₂ O ₃	wt %	0.09	0.17	0.11	3.47	6.50	2.12
Na ₂ O	wt %	0.04	0.07	0.07	0.07	0.07	0.01
CaO	wt %	0.45	0.50	0.45	0.55	0.57	0.20
MgO	wt %	0.05	0.01	0.05	0.71	0.31	0.11
MnO	wt %	0.13	0.10	0.15	0.13	0.08	0.02
K ₂ O	wt %	0.02	0.02	0.02	0.02	0.02	0.01
C	wt %	0.06	0.26	0.09	0.09	0.08	0.9
Ag	g/Ton	<2	46	80	10	8	178
Sum		94.13	96.80	98.64	96.60	102.63	113.197

Note: For all samples: Cd <0.005%, Cr <0.02%, Se<0.001%, Te<0.002%
Loss on ignition (LOI) not reported

Table 4.3 Average Stoichiometry of Pyrite Samples

Element (weight %)	Huckleberry sd.dev.	Zimapan sd.dev.	Tizapa sd.dev.	Louv. 1 sd.dev.	Louv. 2 sd.dev.	Brunswick (pyrite concentrate)
S	53.8	50.8	54.1	54.2	53.2	50.3
Fe	45.7	48.6	45.6	45.5	46.3	49.1
Ni	0.09	0.05	0.07	0.08	0.07	0.06
Cu	0.08	0.05	0.06	0.07	0.05	0.05
As	0.36	0.56	0.18	0.16	0.32	0.46
Atomic ratio S:Fe	2.05	1.82	2.07	2.08	2.00	1.78

Note: Average stoichiometry based on EDAX analysis of more than 30 pyrite grains of a polished section

SEM Micrographs of Unleached Pyrites from Polished Sections (Back Scatter view)

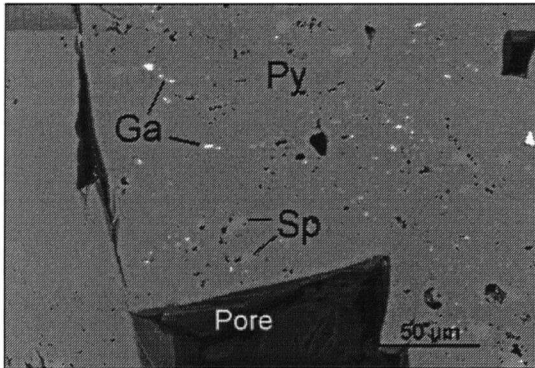


Plate 4.1 Zimapan Pyrite

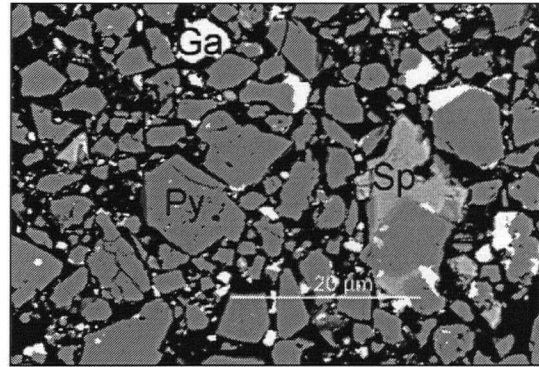


Plate 4.2 Brunswick Pyrite

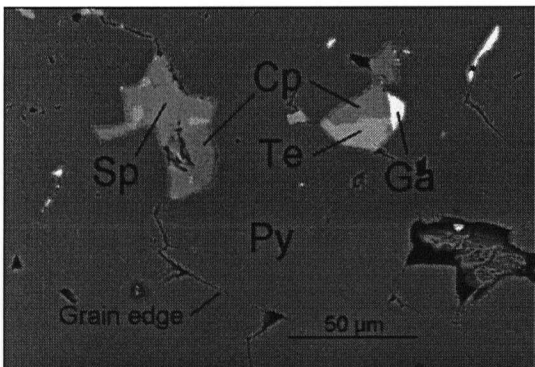


Plate 4.3 Louvicourt-2 Pyrite

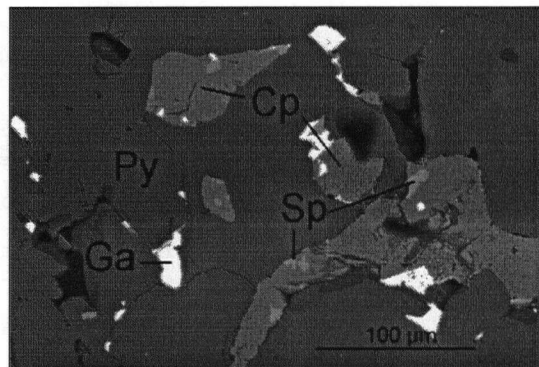


Plate 4.4 Tizapa Pyrite

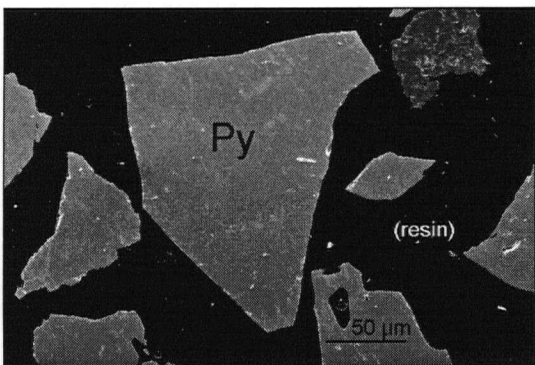


Plate 4.5 Huckleberry Pyrite

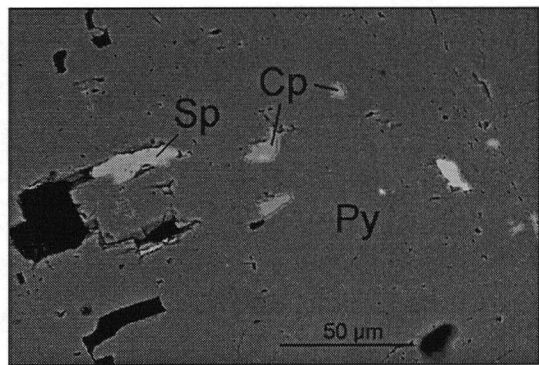


Plate 4.6 Louvicourt-1 Pyrite

Legend:

Py = pyrite; Sp = sphalerite; Ga = galena; Cp = chalcopyrite; Ap = arsenopyrite; Te = tetrahydrite; Gn = gangue

4.2 ELECTROCHEMISTRY OF THE UNLEACHED PYRITE SAMPLES

Stable open current potentials of each pyrite sample were measured before beginning each voltamperometric test. Ocp values are presented in Table 4.4. A correlation was found to exist between ocp values and their content of mineral impurities. Unleached Huckleberry and Louvicourt-1 samples exhibited similar, relatively low ocp values, suggestive of a relatively reactive sample compared to Louvicourt-2, Tizapa and Zimapan. The latter 3 pyrite samples possessed more mineral impurities and were characterized by higher ocp values, indicative of a lower mineral reactivity. The low ocp of the Brunswick sample may be imparted by the high proportions of sphalerite and galena in that sample, which may have overwritten the ocp of the pyrite in the initial leaching cycles. The evolution of Brunswick sample reactivity with leaching time (Section 4.5.5) supports this possibility.

Table 4.4 Open Current Potentials of Pyrite Samples (Volts, SSE)

Sample	Unleached	4 weeks	10 weeks	20 weeks
Huckleberry (water-leached)	-0.27	-0.22	-0.24	-0.22
Huckleberry (column leached)	-0.27	-0.22	-0.22	-0.20
Louvicourt-1	-0.27	-0.21	-0.20	-0.22
Louvicourt-2	-0.19	-0.21	-0.13	-0.22
Tizapa	-0.18	-0.20	-0.15	-0.18
Zimapan	-0.18	-0.18	-0.16	-0.20
Brunswick	-0.29	-0.26	-0.18	-0.13

Figures 4.1 and 4.2 compare the voltamperometric response of pyrites in the unleached samples. The arrows on Figure 4.1 indicate scan directions. For the sake of graph clarity, scan direction arrows have not been added to the other voltamograms. Each sample had a distinct electrochemical response, indicative of the reactivity differences between them. Reactivity was measured by the potential at which oxidation of the sample reached a current of 2.0 μA .

All anodic peaks showed a catalytic behaviour, where for a given potential, a lower current was generated during the forward scan (anodic current) than in the reverse scan (cathodic current). Although the cathodic response of the leached mineral can reveal interesting information on the properties of precipitates covering mineral surfaces, this study focused on the anodic or oxidative behaviour of pyrite to document the reactivity of the pyrite surface after increasing periods of oxidative leaching.

Figures 4.1 and 4.2 indicate that Huckleberry pyrite oxidized at the lowest potential and offered the least resistance as potential was increased. It was concluded to be the most reactive of all unleached samples. Following, in order of decreasing reactivity, were Louvicourt-1, Louvicourt-2 and Tizapa. The close up view of the points of initial current release (Figure 4.2) shows, for Brunswick, and slightly less pronounced for Zimapan, an initial current release prior to the typical curve of pyrite oxidation. An electrochemical study of the oxidation of galena and sphalerite in the same voltametric cell environment (Figures 4.3 and 4.4 respectively) suggested that the lower potential at which the oxidation of the unleached sample appeared to be initiated was more likely attributable to the oxidation of galena. The oxidation of pyrite appeared to resume around 0.420 volts in

both the Brunswick and Zimapan curves as indicated by the sudden increase in current. The relative reactivities of the unleached Zimapan and Brunswick pyrites are not possible to establish because of the presence of galena.

Once pyrite oxidation was initialized however, Figure 4.1 shows that Brunswick pyrite was the most resistant to oxidation. Humidity cell studies of fresh Brunswick tailings and mineralogical studies of old tailings carried out by Noranda Technology Centre (1998f) found Brunswick pyrite to have a relatively low reactivity and to oxidize at a lower rate than what is commonly reported for pyrite.

The varying amount of mineral impurities and distinct chemistry of the pyrite samples, as well as the variable stoichiometric compositions of the pyrites within one sample did not allow for a comparison of pure FeS_2 compounds. The reactivity of the pyrite in each sample could not be directly measured because of these intrinsic differences impossible to eliminate from the sample. It was possible, however, through cyclic voltamperometry, to document the effects of impurities on the reactivity of pyrite as leaching progressed.

Electrochemical Oxidation of Unleached Pyrite Samples

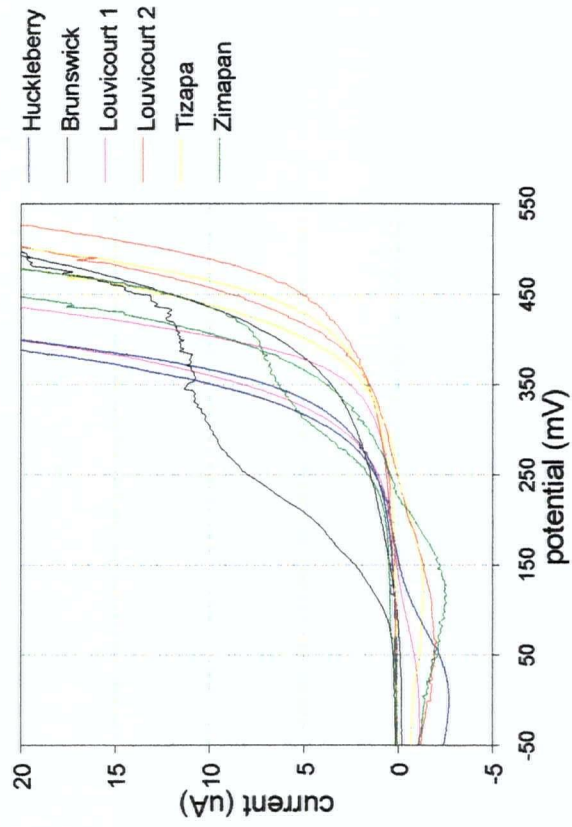
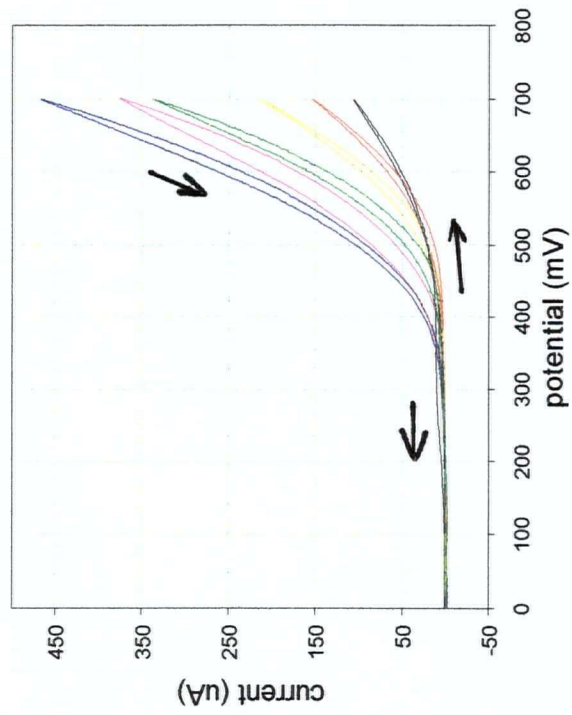


Figure 4.1 All unleached pyrite samples

Figure 4.2 Close up view

**Voltamperometric Responses of Galena and Sphalerite
(CPE in 0.1M NaNO₃ solution)**

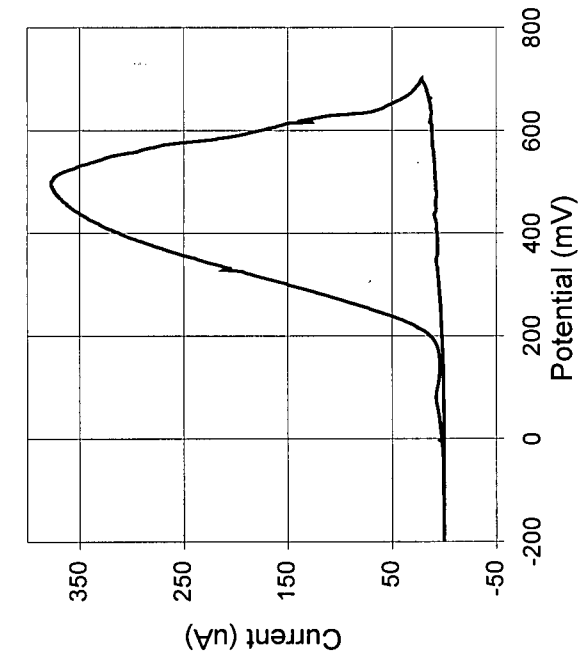


Figure 4.3 Galena

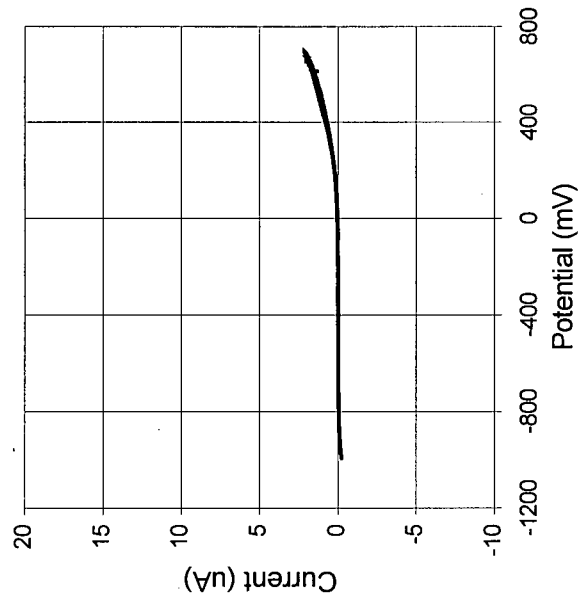


Figure 4.4 Sphalerite

4.3 EVOLUTION OF LEACHATE CHEMISTRY

The chemical analyses of the leachate for all samples are presented in Appendix I (Table I-1). The evolution of leachate composition is plotted as time-series graphs for each of the following elements: pH, conductivity, redox potential, sulfate, total iron, lead, zinc, copper and arsenic (Figures 4.5 to 4.12). The artificial rain water solution (referred to as "Distilled Water") as well as the Huckleberry column solution used to leach a separate Huckleberry pyrite sample (referred to Hk-column) are also plotted as references. The solution-leached and water-leached Huckleberry samples are identified as Hk-l and Hk-w respectively.

After a rapid decline in the first leaching cycles, pH stabilized for all pyrites (Figure 4.3). Redox values (Figure 4.4) remained in the 400-500 mvolt range (SHE) throughout the leaching cycles indicating that oxidizing conditions prevailed, as expected.

Conductivity, sulfate and dissolved iron were markedly higher for both Huckleberry pyrites (water and solution-leached) compared to the other pyrites (Figures 4.5, 4.6 and 4.7) indicating that Huckleberry pyrites were being oxidized at a considerably greater rate than the other pyrites throughout the leaching experiment.

Dissolved metal concentrations varied considerably from one sample to another. Leachate zinc concentrations (Figure 4.8) were directly proportional to the solid phase zinc content of the unleached sample, occurring as sphalerite impurities. Samples with the highest sphalerite content such as Louvicourt-2, Tizapa, Zimapan and especially Brunswick all leached relatively high concentrations of dissolved zinc. Tizapa and

Zimapan leachates showed a decline in dissolved zinc concentration after 12 cycles (6 weeks) of leaching whereas Brunswick and Louvicourt-2 zinc concentrations decreased much more slowly. This indicates that sphalerite in the Brunswick and Louvicourt-2 samples was largely exposed to the leaching solution whereas Tizapa and Zimapan sphalerite was partially locked inside pyrite grains.

Dissolved lead concentrations were also proportional to the initial solid phase lead (galena) content (Figure 4.9). The Brunswick pyrite leached out highest concentrations of lead but only in the first 12 cycles of leaching, after which aqueous lead concentrations reached steady state at approximately 10 mg/l, similar to Zimapan and Tizapa levels. SEM observations indicated that lead tended to precipitate as anglesite ($PbSO_4$).

Copper and arsenic concentrations were relatively low in all leachates (Figures 4.10 and 4.11) reflecting the low chalcopyrite and arsenopyrite content of the samples. Tizapa's aqueous copper concentration corresponds to its slightly higher chalcopyrite content observed in the polished section of the unleached sample.

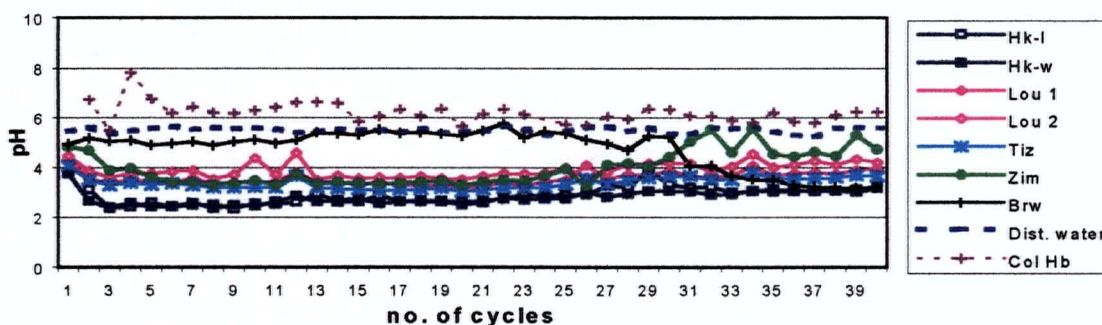


Figure 4.5 Pyrite Leachate pH

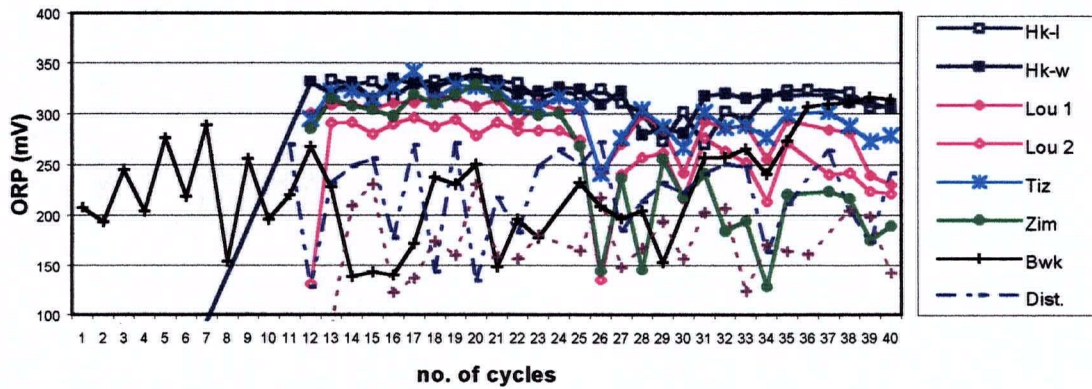


Figure 4.6 Pyrite Leachate Redox Conditions

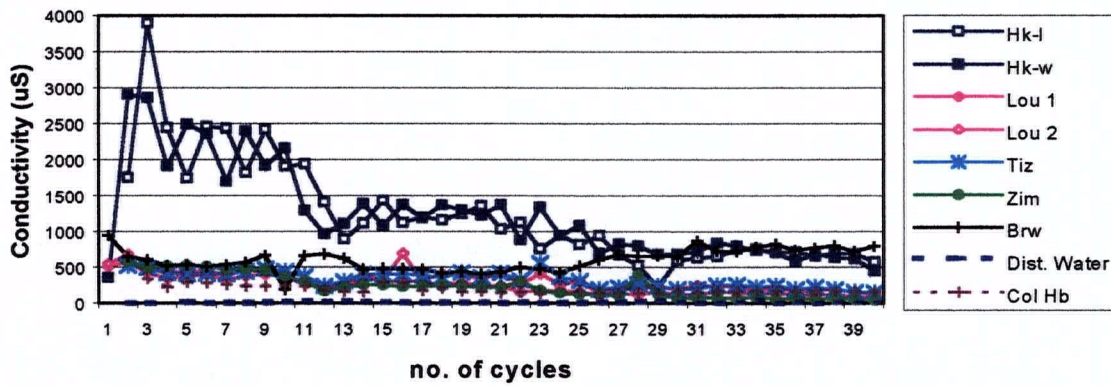


Figure 4.7 Pyrite Leachate Conductivities

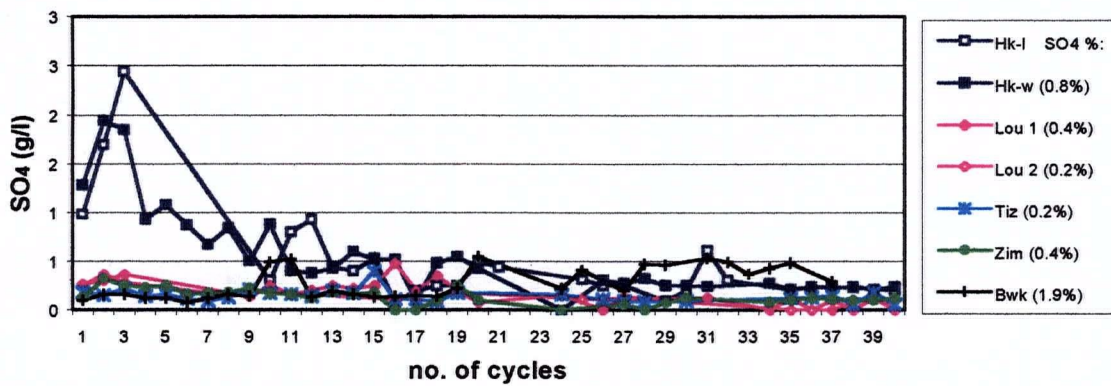


Figure 4.8 Pyrite Leachate Sulfate Concentrations

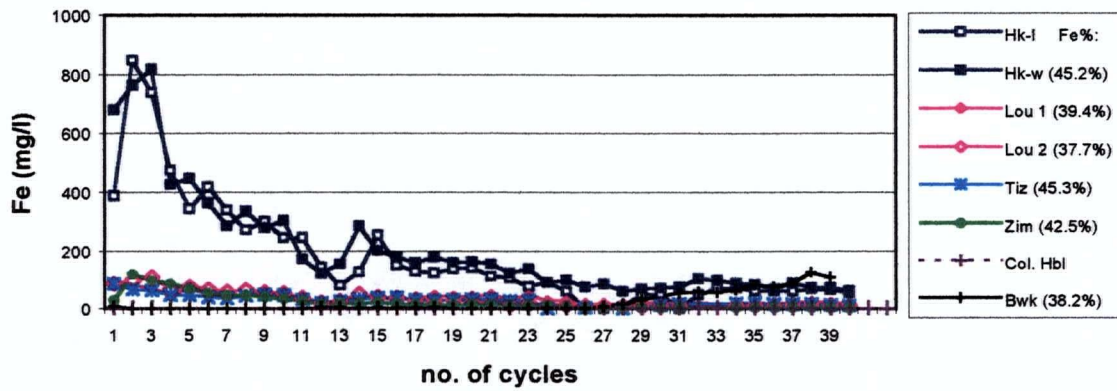


Figure 4.9 Pyrite Leachate Total Iron Concentrations

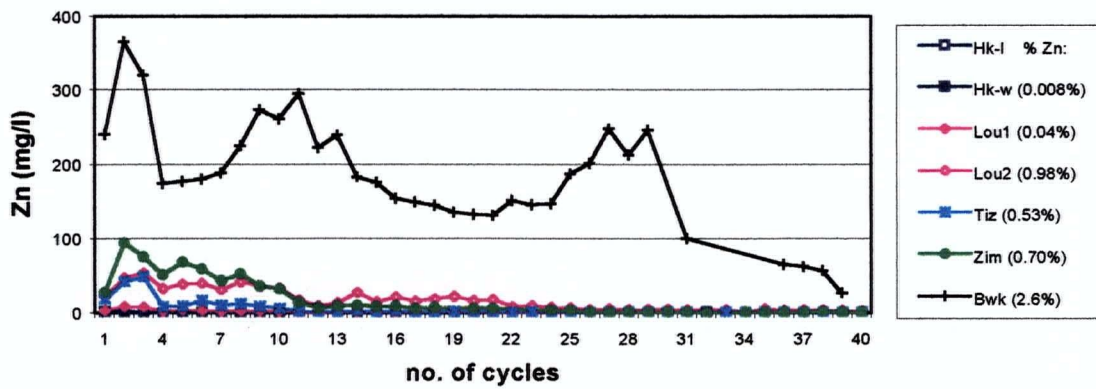


Figure 4.10 Pyrite Leachate Zinc Concentrations

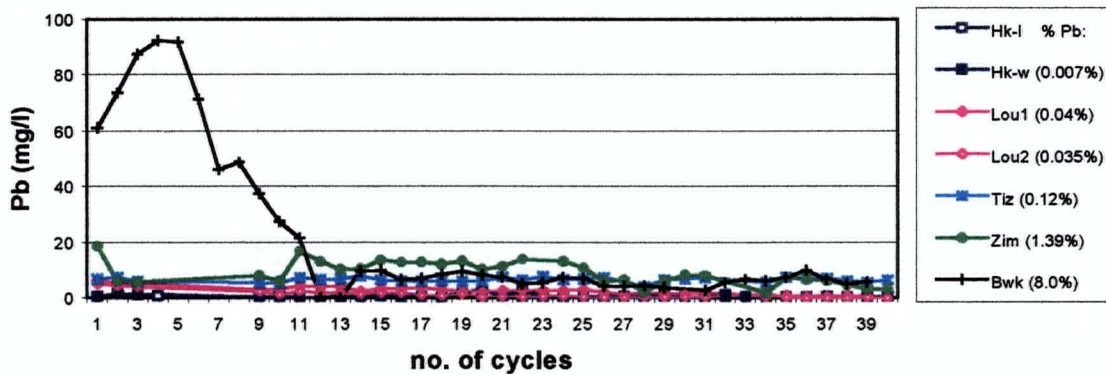


Figure 4.11 Pyrite Leachate Lead Concentrations

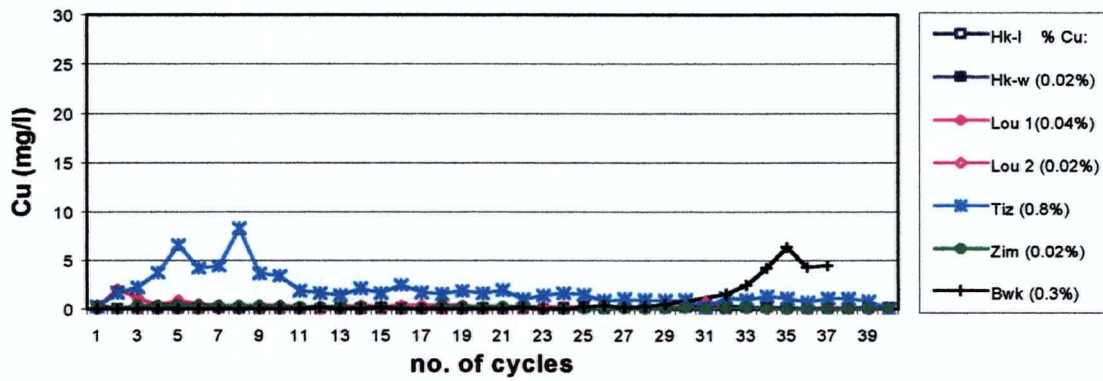


Figure 4.12 Pyrite Leachate Copper Concentrations

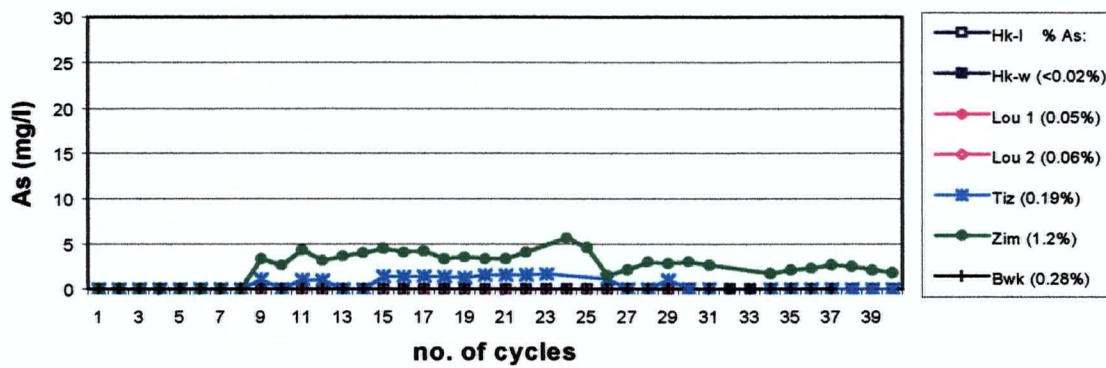


Figure 4.13 Pyrite Leachate Arsenic Concentration

4.4 EVOLUTION OF PRECIPITATE COATINGS DURING LEACHING

4.4.1 Huckleberry pyrite

SEM observations showed differences in precipitation products between the water and waste rock solution-leached Huckleberry samples as early as the 4th week of leaching. The water-leached pyrites conserved relatively sharp grain edges with very few visible coatings (Plate 4.7) or corrosion pits. The solution-leached pyrite surfaces, on the other hand, showed the presence of amorphous precipitates after 4 weeks of leaching, increasing in thickness and extent with advancing leaching cycles (Plate 4.8 and 4.9). Oxidation pits were also more extensive in the solution-leached pyrites (Plate 4.10).

Although precipitates were visible under SEM, infrared spectroscopy did not succeed in identifying the secondary phases, as their amount was insufficient (less than 5%). Consequently, no data are available as to the exact composition of these precipitates. A review of the literature on surface oxidation products formed on pyrites suggests, however, that the precipitates observed under SEM may be amorphous iron oxyhydroxides similar to goethite (α -FeO(OH)) (Jambor, 1994; Bigham, 1994; Kwong, 1993). Amorphous, hydrated iron sulfates can also be present on pyrite surfaces but are less common than iron oxyhydroxides in young mine wastes according to these authors. The thin, amorphous iron precipitates observed in this study will therefore loosely be referred to as iron oxyhydroxides or FeOOH.

4.4.2 Louvicourt Pyrites

Mineralogically similar Huckleberry and Louvicourt-1 pyrite samples yielded similar precipitate coatings upon leaching. Plates 4.11, 4.12 and 4.13 show a precipitate cover similar in form and abundance to Huckleberry solution-leached pyrites. Very few corrosion pits were visible after 20 weeks of leaching.

The Louvicourt-2 pyrites were considerably different from Louvicourt-1 in both the occurrence of precipitates and the aspect of oxidized pyrites. Pyrite surfaces remained relatively free of precipitates until the 20th week, at which point visible amorphous iron precipitates increased in abundance. After 20 weeks of leaching, however, the amount of iron precipitates covering pyrite surfaces remained much lower than the Louvicourt-1 pyrites (Plates 4.14 and 4.15). Corrosion pits were abundant after 20 weeks of leaching, contrary to Louvicourt-1 or Huckleberry pyrites (Plate 4.16). Sphalerite was observed in Louvicourt-2 sample and, where both sphalerite and pyrite were present in the same grain, sphalerite was extensively more riled and pitted than pyrite after 10 and 20 weeks of leaching (Plate 4.17). Sphalerite was being preferentially oxidized over pyrite.

4.4.3 Tizapa Pyrite

Mineralogically similar Tizapa and Louvicourt-2 pyrites also showed similarities in precipitate occurrence and aspect of oxidized mineral phases. The surface of pyrite grains remained relatively free of precipitates throughout the 20 weeks of leaching and, in general, very few corrosion pits were observed (Plate 4.18). Sphalerite was also considerably more corroded than pyrite (Plate 4.19). In addition, sphalerite became more

extensively covered with precipitates than pyrite after 20 weeks of leaching (Plate 4.20).

Galena in the unleached Tizapa sample appeared as mineral impurities within the pyrite grains and exposed to the environment. The exposed galena was readily available to oxidize or dissolve. After 10 and 20 weeks of leaching, no galena was detected but anglesite (PbSO_4) was observed principally on altered galena, suggesting a direct oxidation (replacement) of galena (Plate 4.21). The precipitation of lead sulfate as anglesite explains the absence of lead in the leachate.

4.4.4 Zimapan Pyrite

The Zimapan pyrites showed a similar abundance of amorphous iron precipitates to Louvicourt-1 pyrites. After 20 weeks of leaching, these precipitates covered a considerable portion of most pyrite grains (Plate 4.22). Oxidation pits were also observed as early as the 4th week of leaching, attesting to the highly reactive character of Zimapan pyrite (Plate 4.23). Reactivity may be accentuated, in part, by the occurrence of crystal lattice impurities of As known to act as an electron donor when present in pyrite, thereby promoting pyrite oxidation.

No galena was observed after the 4th week of leaching, replaced by abundant euhedral crystals of anglesite occurring throughout the sample (Plate 4.24). The distribution of anglesite suggests that nucleation formed from the leachate solution rather than by direct replacement of galena phases, implying a previous dissolution or oxidation of galena. The abundance of anglesite appeared to remain constant with advancing leaching cycles.

4.4.5 Brunswick Pyrite

Relatively few iron hydroxide precipitates covered the surfaces of pyrite grains after 20 weeks of leaching (Plate 4.25). Few pyrite corrosion pits were observed in the 4th week of leaching but their occurrence increased with advancing leaching cycles (Plate 4.26). Precipitates of anglesite were observed in the 4th week of leaching throughout the sample along with galena (Plate 4.27). The occurrence of anglesite suggests that, similar to the Zimapan sample, it was precipitated from solution, from previously oxidized galena. Galena was present in the sample after 10 weeks, but absent after 20 weeks of leaching. Sphalerite was not observed in any of the leached samples.

Huckleberry Pyrites

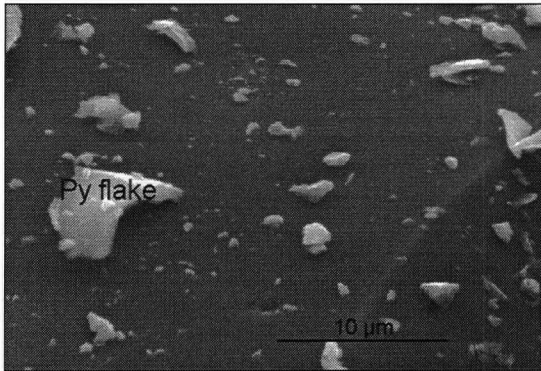


Plate 4.7 Water-Leached, 20 weeks

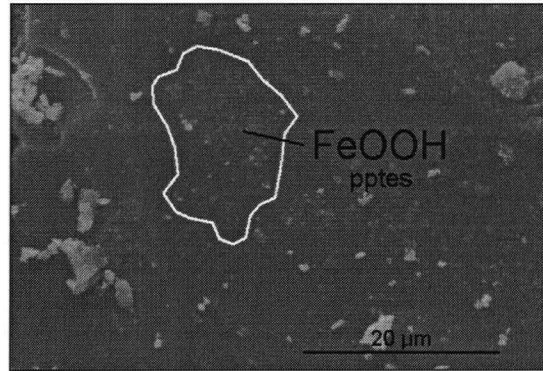


Plate 4.8 Water-Leached, 20 weeks

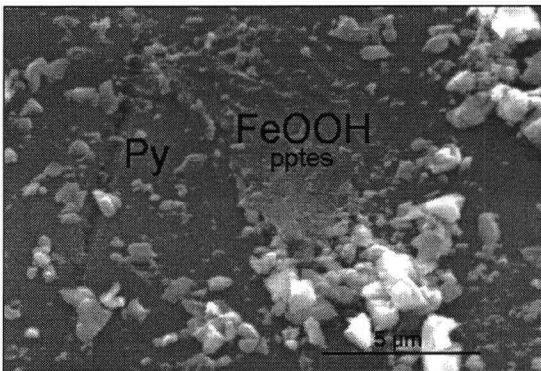


Plate 4.9 Solution-Leached, 20 weeks

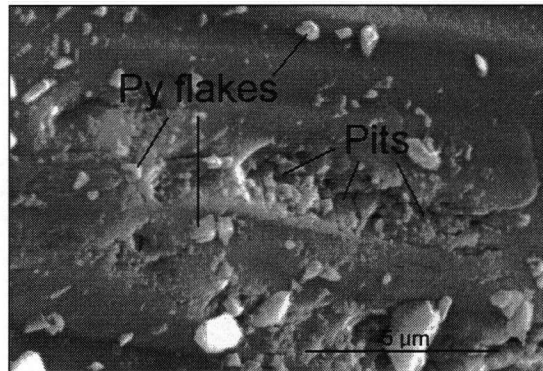


Plate 4.10 Solution-Leached, 20 weeks

Plates 4.7 and 4.8 showing water-leached pyrites possess a smaller amount of amorphous iron hydroxide precipitates of than the solution-leached pyrites shown on Plates 4.9 and 4.10.

Louvicourt-1 Pyrite

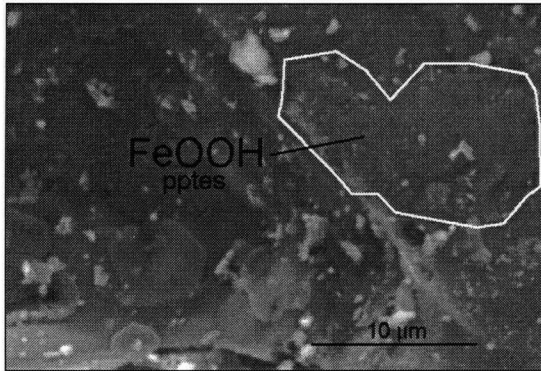


Plate 4.11 4-week leached

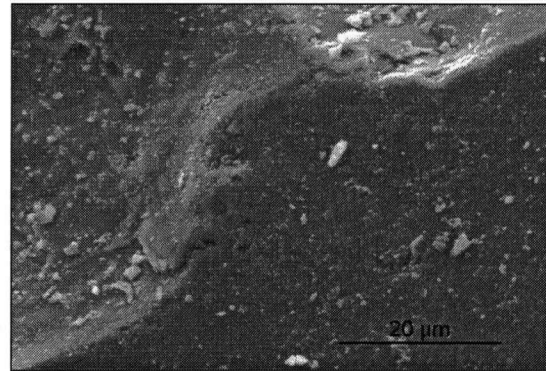


Plate 4.12 20-week leached

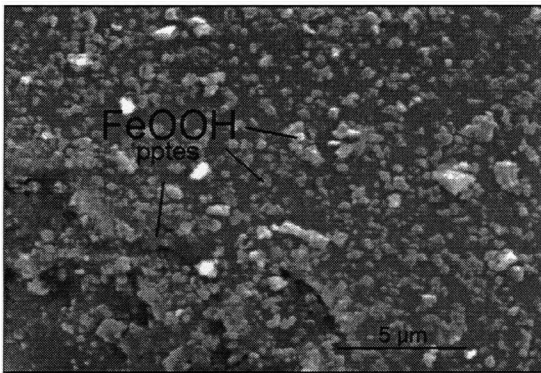


Plate 4.13 20-week leached

Surface-covering iron hydroxide precipitates on Louvicourt-1 pyrites grew more extensive with advancing leaching cycles.

Louvicourt-2 Pyrites

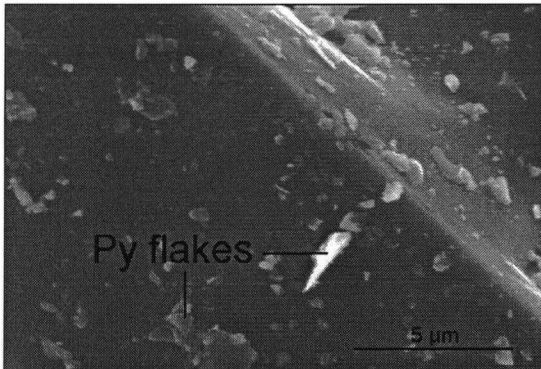


Plate 4.14 Pyrite surface at 10 weeks

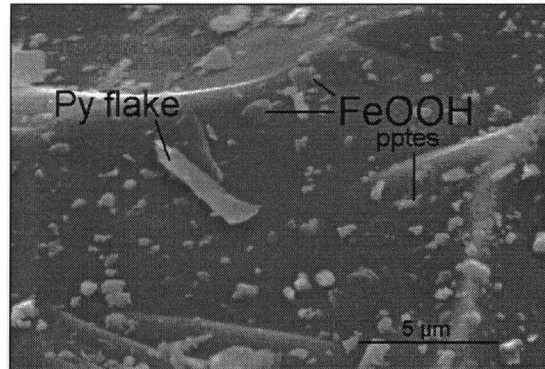


Plate 4.15 Pyrite surface at 20 weeks

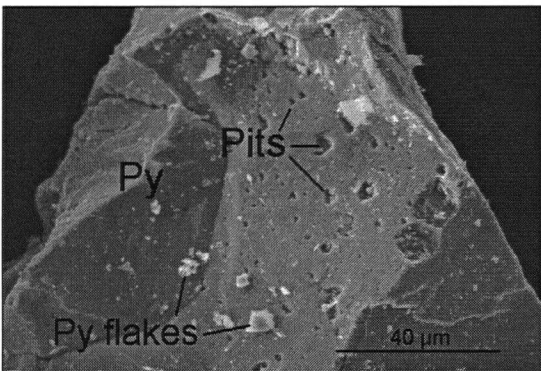


Plate 4.16 Pyrite at 10 weeks

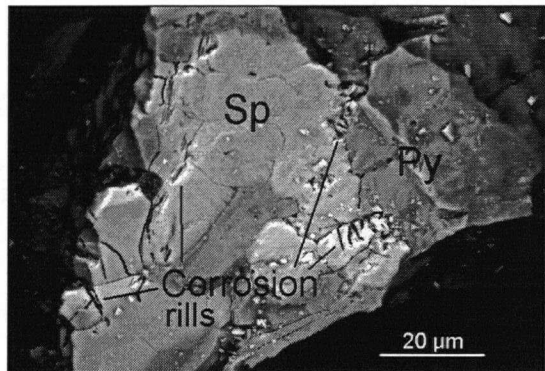


Plate 4.17 20-week leached

Little difference was observed between pyrite surface precipitates after 10 and 20 weeks of leaching (Plates 4.14 and 4.15 respectively). Plate 4.16 shows corrosion pits on pyrite grain free of visible mineral impurities. Plate 4.17 shows preferential sphalearite oxidation over pyrite.

Tizapa Pyrite

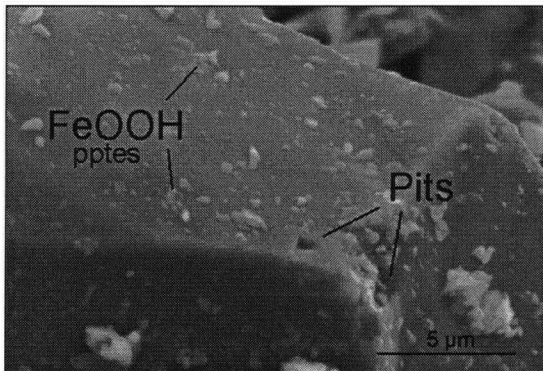


Plate 4.18 Pyrite surface at 20 weeks

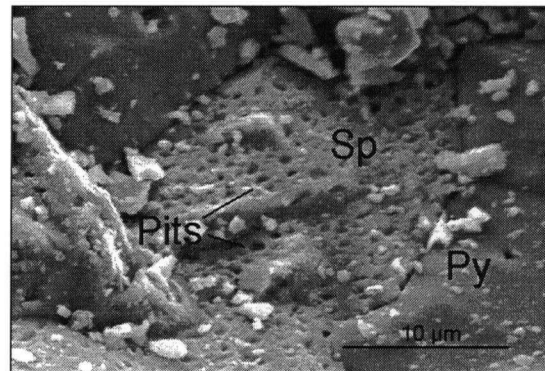


Plate 4.19 Oxidized sphalerite, 20 weeks

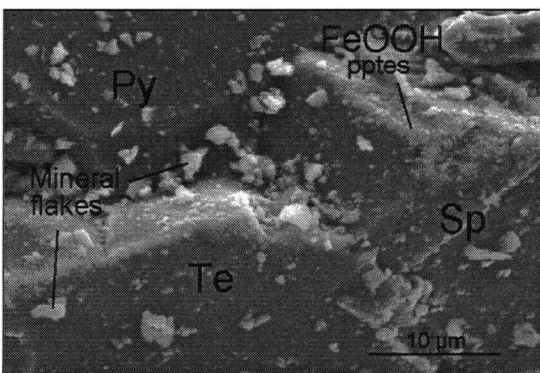


Plate 4.20 Precipitate cover, 20 weeks

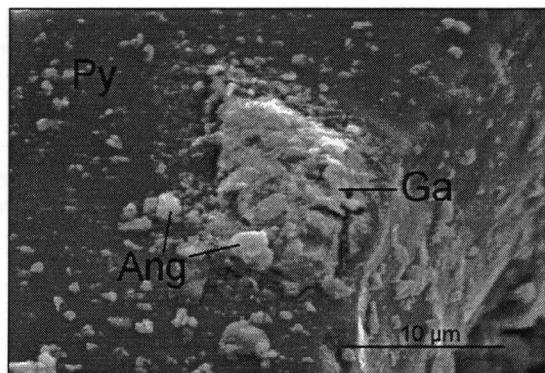


Plate 4.21 Oxidized galena, 20 weeks

After 20 weeks of leaching, pyrite surfaces show very little oxidation and surface precipitates of iron hydroxide (Plate 4.18). Plate 4.19 shows the preferential oxidation of sphalerite over pyrite. Plate 4.20 shows more extensive cover of precipitates over sphalerite and tetrahedrite than pyrite. Plate 4.21 shows the direct oxidation of galena impurity characterized by surface precipitates of anglesite (Ang).

Zimapan Pyrite

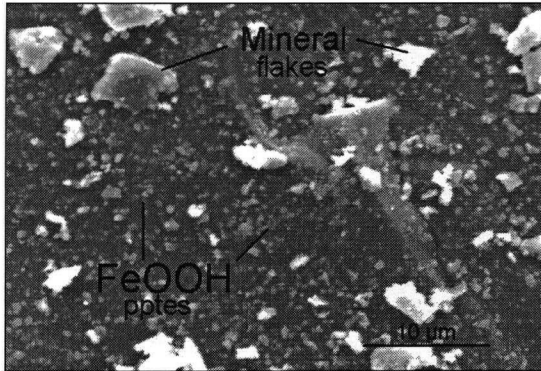


Plate 4.22 Pyrite surface at 20 weeks

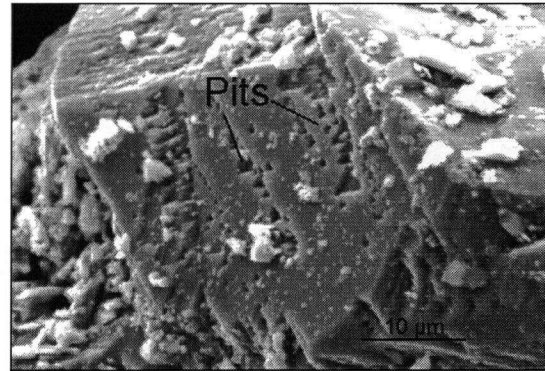


Plate 4.23 Corrosion pits at 4 weeks

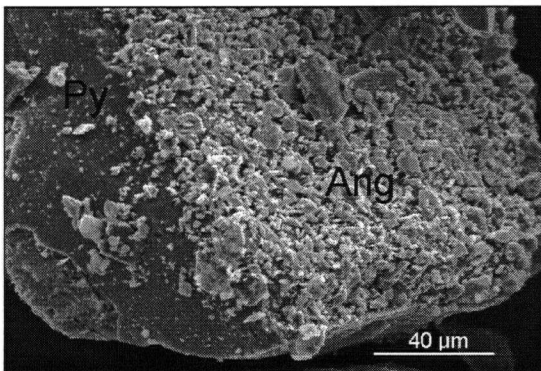


Plate 4.24 Anglesite precipitates, 20 weeks

Plate 4.22 shows the surface of pyrite with extensive cover of amorphous iron hydroxide precipitates. Corrosion pits were abundant on pyrite grains after 4 weeks of leaching (Plate 4.23). Plate 4.24 shows anglesite (Ang) precipitates on the surface of pyrite.

Brunswick Pyrite

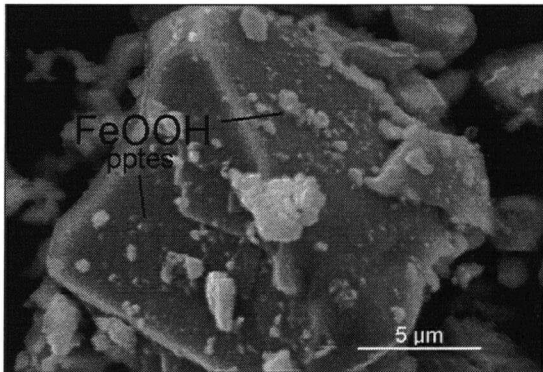


Plate 4.25 Pyrite surface at 20 weeks

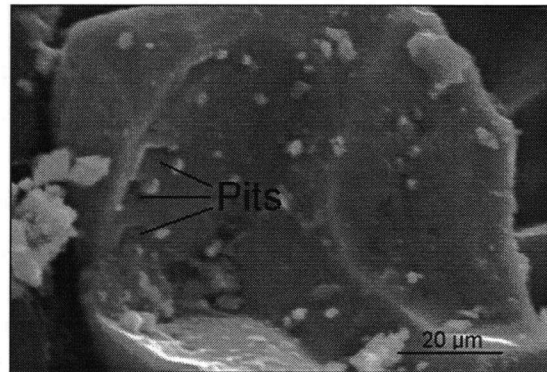


Plate 4.26 Pyrite corrosion pits, 20 weeks

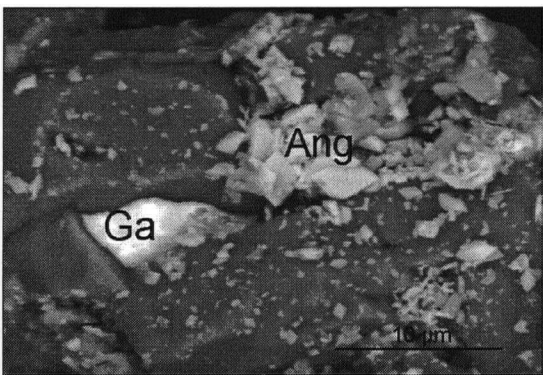


Plate 4.27 Anglesite and galena, 4 weeks

Relatively small amounts of amorphous iron hydroxide precipitates on pyrite surfaces after 20 weeks of leaching (Plate 4.25). Corrosion pits were not commonly observed before 20 weeks of leaching (Plate 4.26). Anglesite (Ang) and galena (Ga) occurred together on pyrite surfaces after 4 weeks of leaching (Plate 4.27). No galena was observed in subsequent cycles.

4.5 EVOLUTION OF PYRITE REACTIVITY

The evolution of the reactivity of pyrite with leaching time is demonstrated in cyclic voltammograms of each sample. In all graphs, each curve represents the voltamperometric response of a particular pyrite sample at a given period (unleached and after 4, 10 and 20 weeks of leaching). The navy blue curve represents the response of the unleached sample and the purple, green and red curves represent the responses of the same pyrite after 4, 10 and 20 weeks of leaching respectively.

4.5.1 Huckleberry pyrites

Figure 4.14 presents the voltamperometric responses of Huckleberry pyrite leached in water. The reactivity of this pyrite decreased over the first 10 weeks, following which a slight gain in reactivity was observed. A net loss of reactivity occurred over the 20 weeks of leaching, characterized by a total positive displacement of the initialization point of 0.03 volts (measured at 2.0 μA). The solution-leached pyrite also showed a decreasing reactivity with leaching time, including a similar gain of reactivity at the 20-week mark (Figure 4.15). A net gain of 0.07 volts occurred over the 20-week leaching period with respect to the unleached pyrite.

The mineralogical observations, leachate chemistry results and electrochemical characterizations suggest that the Huckleberry pyrite is considerably reactive to oxidation

but that a passivation² layer is likely formed on pyrite surfaces, effectively decreasing the reactivity of pyrite after only 4 weeks of leaching. The passivating layer derived from the waste-rock column solution appeared to be more effectively decreasing pyrite reactivity than that derived from water leaching.

4.5.2 Louvicourt Pyrites

As with sample mineralogy and evolution of precipitate coatings, the Louvicourt-1 pyrite showed electrochemical responses after each leaching period, that were very similar to Huckleberry solution-leached pyrites (Figure 4.16). The loss of reactivity was slightly lower in the Louvicourt-1 sample than in the Huckleberry solution-leached sample, with a net positive displacement of only 0.055 volts compared to 0.07 volts for Huckleberry.

Contrary to Louvicourt-1, Louvicourt-2 pyrite became more reactive after 4 weeks of leaching, with a negative displacement of the point of initial oxidation of 0.05 volts (Figure 4.17). In the 10th and 20th week, however, pyrite reactivity decreased, resulting in a net positive advancement of 0.04 volts over the 20 weeks of leaching with respect to the unleached pyrite. The gain of reactivity within the first 4 weeks of leaching coincide with the preferential oxidation and loss of sphalerite over pyrite in the sample observed under SEM and supported by the leachate chemistry data. The subsequent passivation could be attributable to the formation of surficial, amorphous iron precipitates observed

² The terms 'passivation' or 'passivated' in this study refer to a relative decrease in reactivity of the mineral measured as a positive displacement of the point of initialization of mineral oxidation, observed by cyclic voltamperometry. This term is not used to describe the mechanisms or the products responsible for the observed loss of reactivity.

in appreciable quantity in the 20-week leached sample. These precipitates could have effectively passivated pyrite surfaces.

4.5.3 Tizapa pyrite

Tizapa pyrite reactivity evolved in a similar way to that of Louvicourt-2 pyrite, although at a smaller scale. Figure 4.18 shows an initial increase in reactivity in the 4th week of leaching, followed by a reactivity decrease which remained until the 20th week of leaching. A net positive displacement of 0.05 volts occurred after 20 weeks of leaching with respect to the unleached pyrites. The higher resistance to oxidation observed in the 10th week compared to the 20th week, suggests that the precipitate coatings formed at an early stage (10 weeks) were different than those formed after 20 weeks of leaching.

4.5.4 Zimapan pyrite

The Zimapan voltammogram showed an increase in the width of the anodic peak with leaching time (Figure 4.19). With advancing leaching cycles, the reverse scan of the anodic peak released a consistently higher current than the forward scan, measured at a given potential. The forward scan showed a net advancement of the initialization point of pyrite oxidation of 0.1 volts in 20 weeks of leaching. The reverse scan showed an increasing efficiency to oxidize the pyrite surfaces after initialization. A possible explanation for this behaviour is the observed increased abundance of precipitates combined with the increased surface area created by corrosion pits as leaching progressed. The thicker precipitate coating possibly offered increasing resistance to oxidation, but once the potential became sufficiently high to break this barrier, more

current could be generated from the same grains because of the increased surface area created by the corrosion pits. Although pit density remained constant with advancing leaching cycles, pits have a tendency to deepen inside the crystal rather than to enlarge at the surface of the grain (Mustin, 1992). Consequently, the actual surface area of a pitted grain could be increased without a notable increase in the number or width of the pits. The effect of oxidation pits on the reactivity of pyrite was not verified in this study but merits further investigation.

The presence of galena in the unleached sample was observed in Figure 4.2, Section 4.2. A close-up view of the 4, 10 and 20-week anodic scan curves in Figure 4.20 shows that galena was no longer present in the sample after the 4th week of leaching. SEM observations and leachate chemistry indicated that most of the available galena was oxidized in the first 4 weeks of leaching where lead was reprecipitated as anglesite throughout the sample.

4.5.5 Brunswick

The forward scan curves of the Brunswick pyrite voltammograms showed an apparent increase in reactivity with leaching time up to the 10th week of leaching, followed by relative decrease in reactivity in week 20 (Figure 4.21). The presence of galena in the unleached, 4-week and 10-week samples, however, concealed the exact point (or voltage) at which pyrite started to oxidize. It was therefore impossible to calculate the amount of curve displacement. The apparent gain in reactivity observed until week 10 was similar to the Louvicourt-2 response and also most likely attributable to the presence of

sphalerite. Although sphalerite was not visible under SEM in the leached samples, solid phase zinc concentration (corresponding to sphalerite) was the highest in the Brunswick sample. Leachate chemistry indicated that large concentrations of zinc were continually being leached from the Brunswick sample whereas iron was not. Like in the Zimapan and Louvicourt-2 pyrite samples, sphalerite was most likely providing galvanic protection to pyrite at least in the early cycles. With increasing leaching time, the presence of iron hydroxides and anglesite precipitates on pyrite surfaces may have reduced the availability of sphalerite to oxidize in lieu of pyrite. A close-up view of Figure 4.22 indicated that the electrochemical signature of galena was still discernible after 10 weeks of leaching, although very diminished, and was absent from the 20-week voltammogram. Galena along with anglesite was observed under SEM in the 4-week sample, galena was not seen in the 10 and 20-week samples.

The reverse scan of the Brunswick voltammogram showed a pattern similar to the Zimapan pyrites where the anodic peak widened with advancing leaching cycles. Oxidation pits were more abundant after 20 weeks of leaching in the Brunswick sample which, again, could possibly explain the increasing generation of current on the reverse scan.

Cyclic Voltammograms - Huckleberry Pyrites

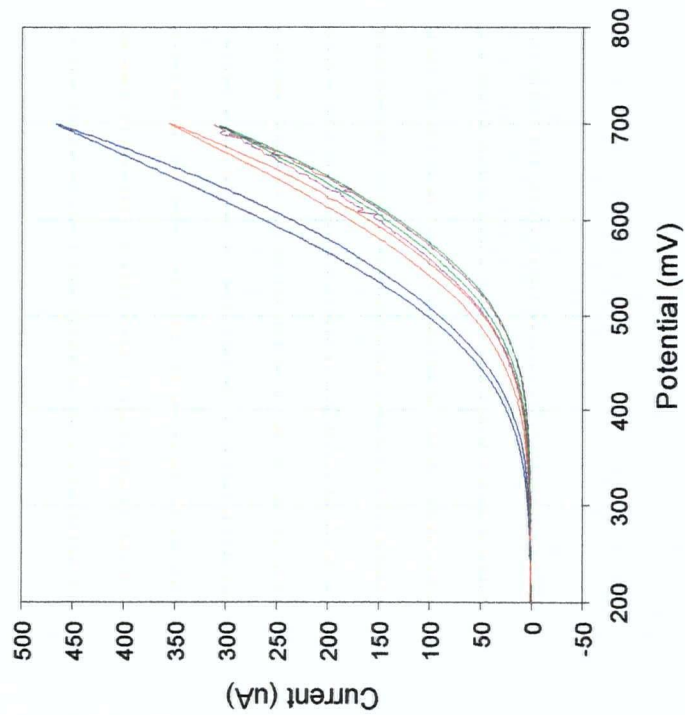
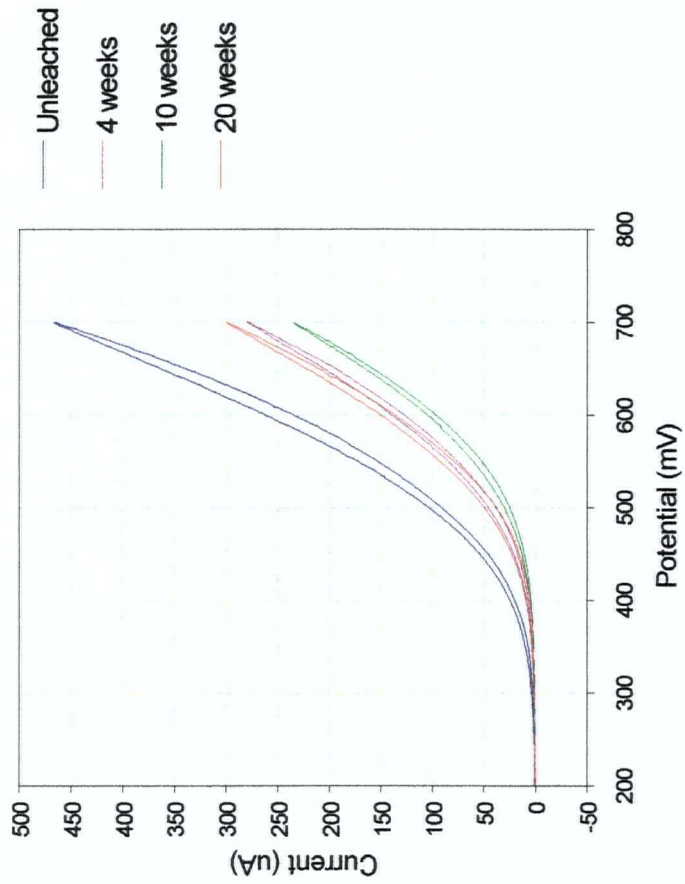


Figure 4.15 Huckleberry Solution-Leached Pyrites

Figure 4.14 Huckleberry Water-Leached Pyrites

Cyclic Voltammograms – Louvicourt Pyrites

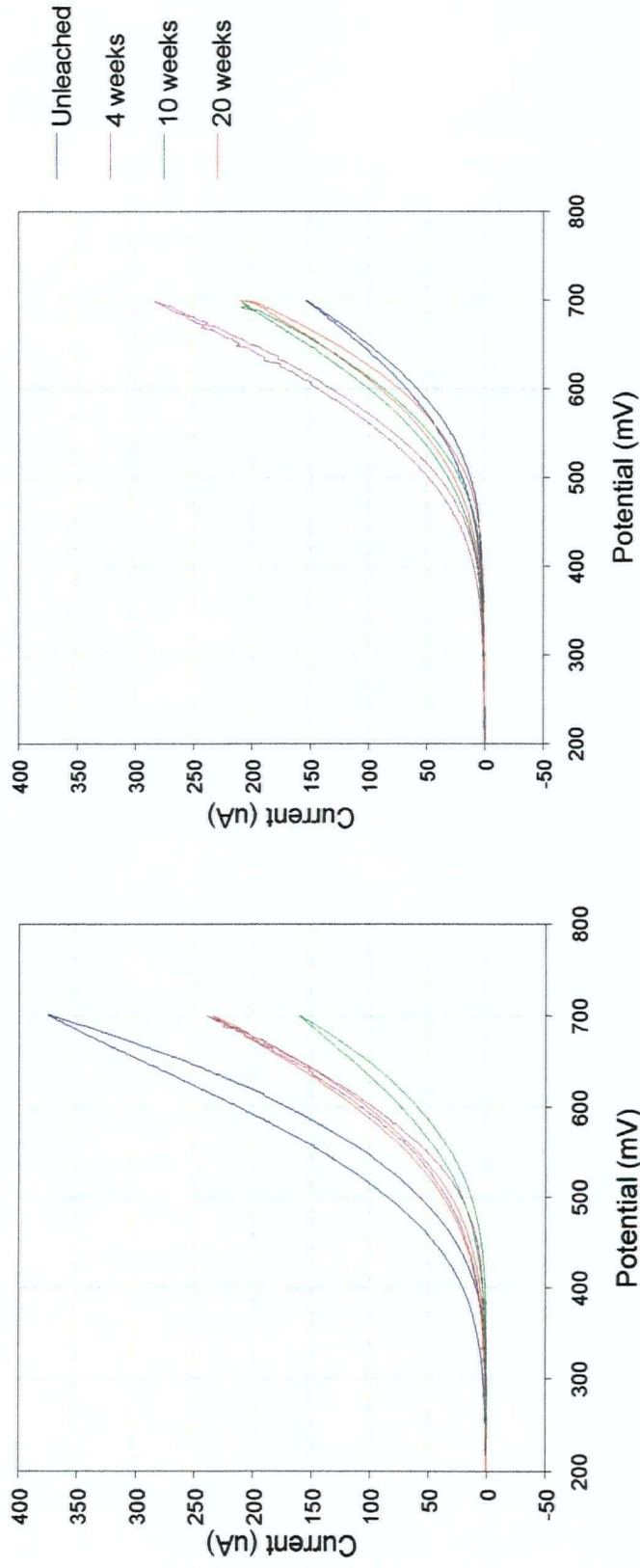


Figure 4.16 Louvicourt-1 Pyrite

Figure 4.17 Louvicourt-2 Pyrite

Cyclic Voltammograms – Tizapa and Zimapan Pyrites

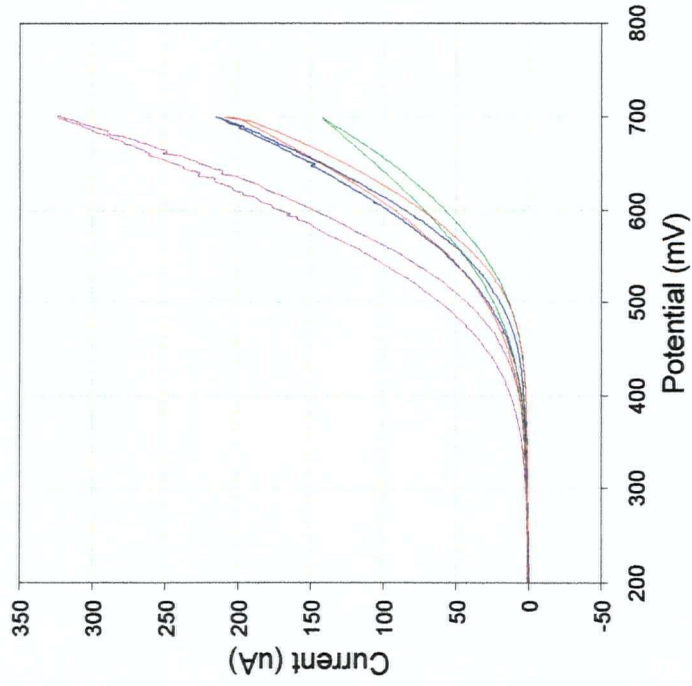


Figure 4.18 Tizapa Pyrite

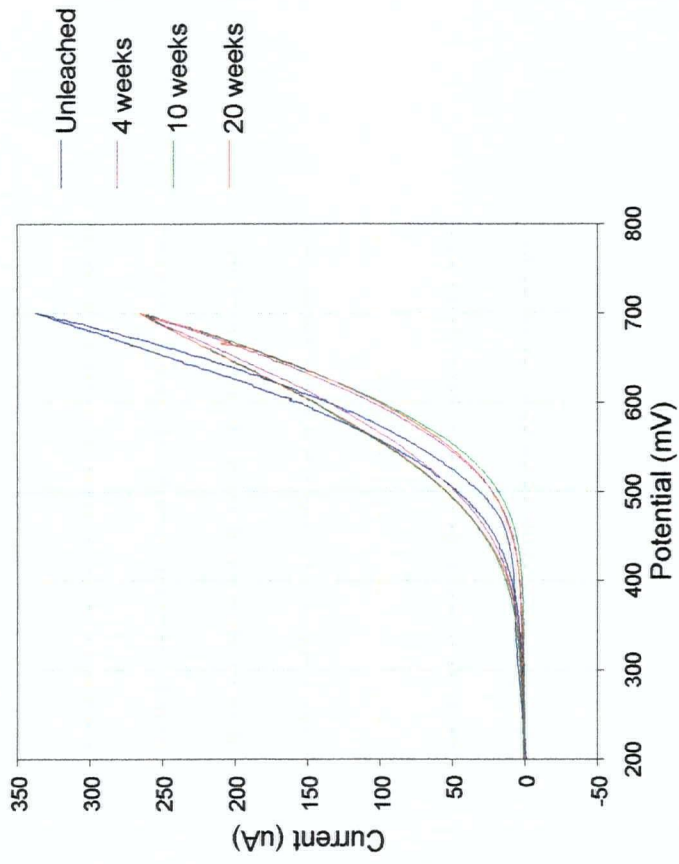


Figure 4.19 Zimapan Pyrite

Cyclic Voltammogram of Zimapan Pyrites (Zoom of initialization points)

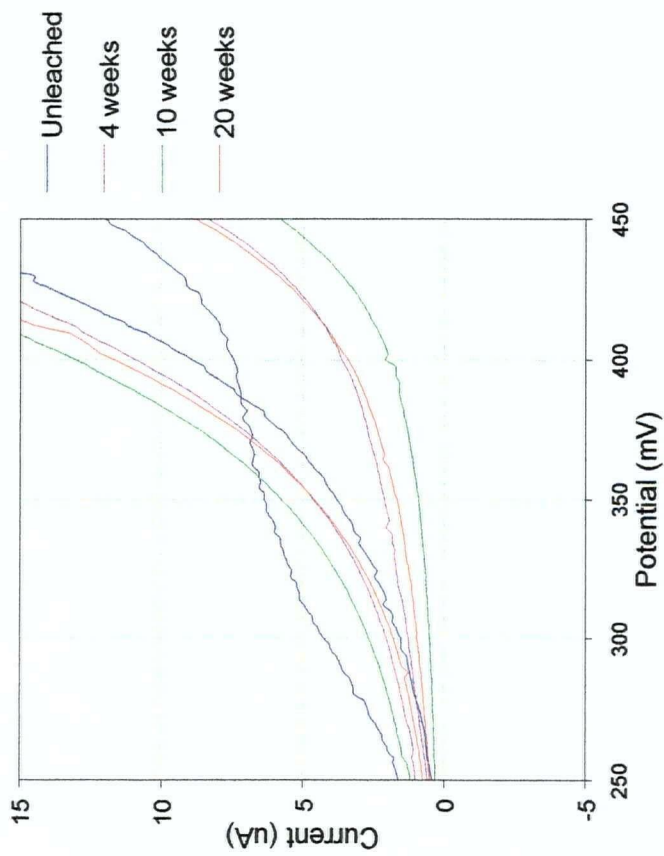


Figure 4.20 Zoom on Initialization points, Zimapan Pyrites

Cyclic Voltammograms – Brunswick pyrite

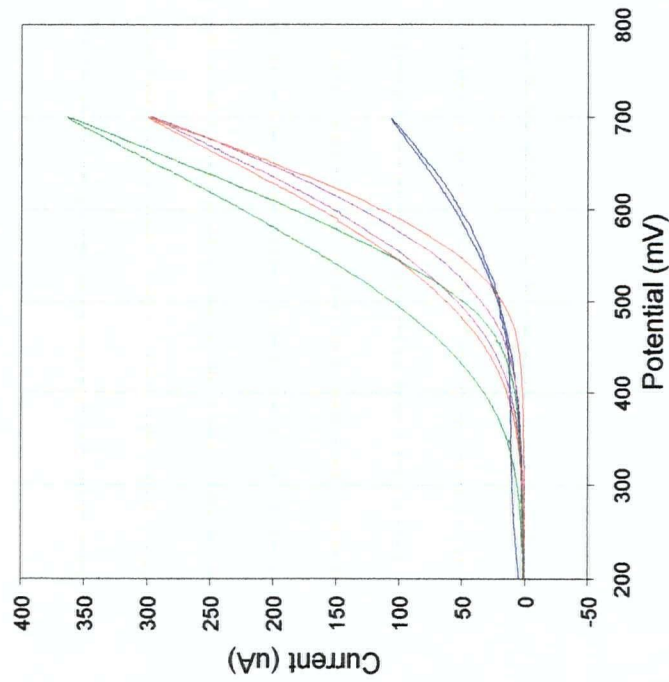


Figure 4.21 Brunswick pyrites

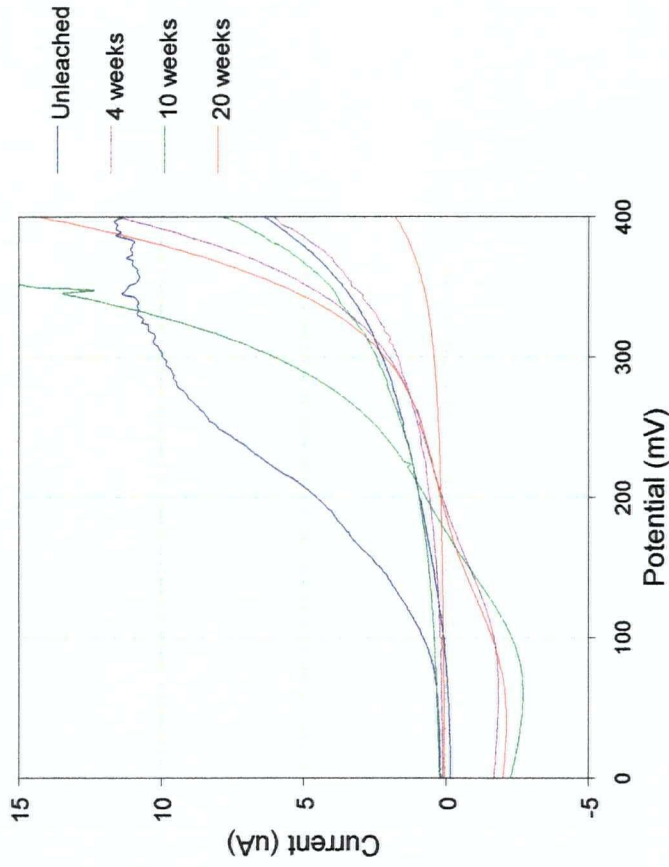


Figure 4.22 Zoom of Initialization Points

4.5.6 Evolution of Pyrite Reactivity

Figures 4.23 to 4.25 show the voltametric responses of the group of pyrites after 4, 10 and 20 weeks of leaching respectively. The differences in reactivities between pyrites were significantly decreased after 4 weeks of leaching. The opposing processes of increased passivation for the initially reactive pyrites (Huckleberry, Louvicourt-1) and loss of galvanic protection for the initially less reactive pyrites (Louvicourt-2 and Tizapa and possibly Zimapan and Brunswick) appear to have effectively homogenized the electrochemical responses of the various pyrites. Individual reactivity differences appeared again after 10 weeks of leaching, developing further after 20 weeks as the characteristics of the pyrite surfaces were likely dominated by the presence of precipitation products and possibly oxidation pits.

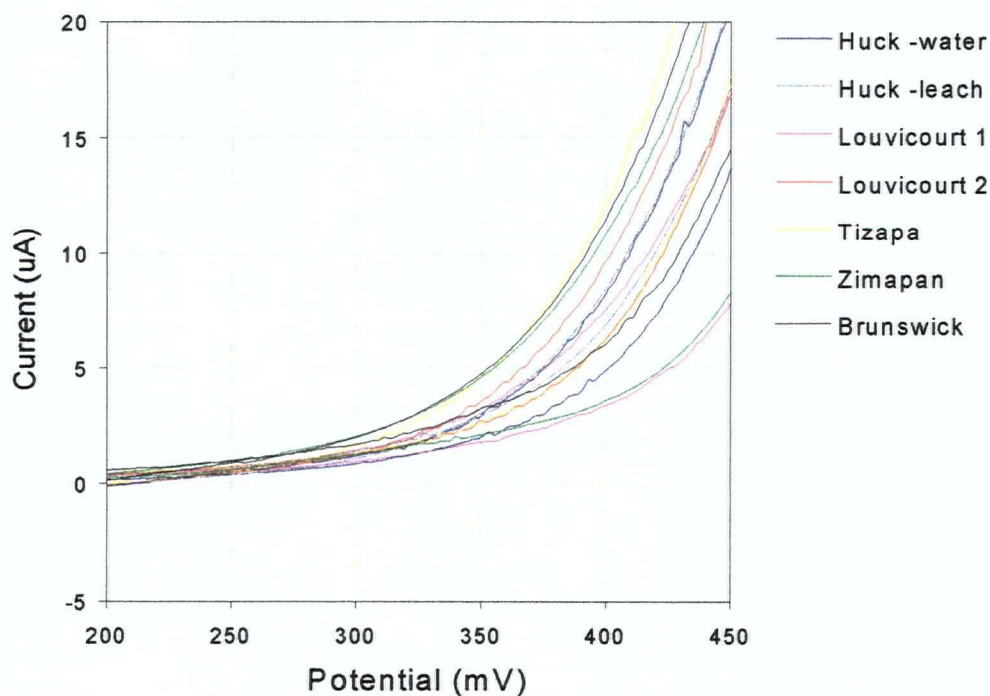


Figure 4.23 All Pyrites, 4-week Leached

Cyclic Voltamperometry – Evolution of Pyrite Reactivities

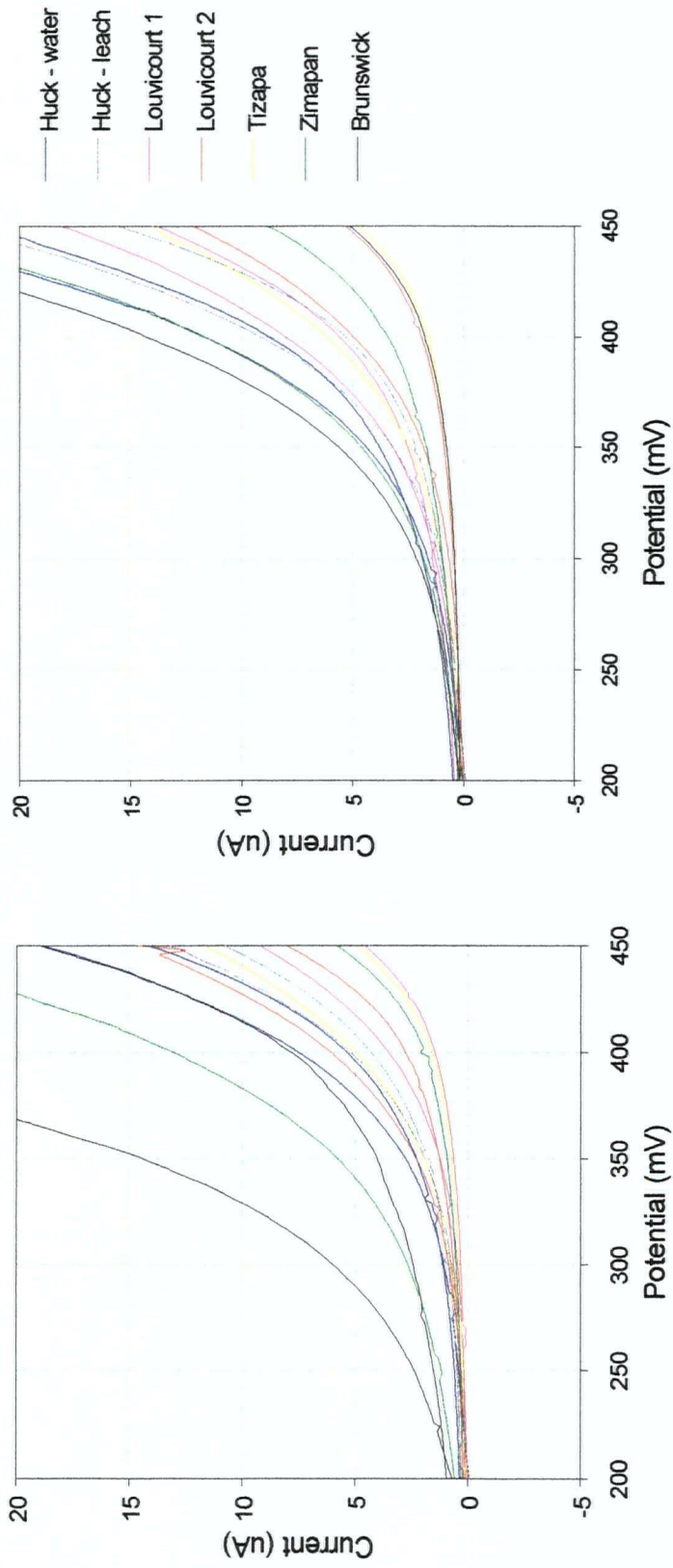


Figure 4.24 All Pyrites, 10-week Leached

Figure 4.25 All Pyrites, 20-week Leached

Table 4.5 shows the relative reactivity of each pyrite at different leaching periods measured at the point of 2.0 μA current release on the voltammograms (on close-up views not presented). Samples exhibiting similar reactivities appear in the same box. Although the reactivity of Huckleberry pyrites continually decreased with advancing leaching cycles, they remained the most reactive of all pyrites after 20 weeks of leaching. Similarly, Tizapa and Louvicourt-2 remained the least reactive. The comparison with Brunswick pyrite reactivity is difficult to establish because of the galena peak effectively hiding the initialization point of pyrite oxidation in the unleached sample and after 4 and 10 weeks of leaching.

This study suggested that the reactivity of the pyrite samples studied depend greatly on the occurrence of mineral impurities and, after some period of leaching, on the composition of the precipitate layer. The latter could be dictated by the various mineral phases being oxidized simultaneously with pyrite.

Table 4.5 Relative Reactivities of Pyrites

	unleached	4 weeks	10 weeks	20 weeks
Increasing reactivity \uparrow	Huckleberry	Huck. Water, Louvicourt-1, Huck. Column	Huck. Water Huck. Column Louvicourt-1	Huck. Water Huck. Column, Louvicourt-1
	Louvicourt-1			
	Louvicourt-2	Louvicourt-2, Zimapan, Tizapa,	Zimapan Tizapa Louvicourt-2	Zimapan Tizapa, Louvicourt-2, Brunswick
	Tizapa			
(Zimapan?) (Brunswick?)	(Brunswick?)	(Brunswick?)		

5 RESULTS – CEMENTED PASTE BACKFILL STUDY

5.1 CHEMICAL ANALYSES OF TAILINGS, BINDER AND PASTE

Chemical analyses of the tailings, paste and slag are presented in Table 5.1. The paste mixture compositions were calculated from the chemical data of Table 5.1 and are presented in Table 5.2. Analyses indicate that Tizapa tailings possess the highest concentrations of sulfide, iron, copper and zinc of all other tailings. They have the second highest concentration of lead and arsenic after Brunswick. Brunswick tailings have a composition similar to that of Tizapa, with high concentrations of sulfide, iron, zinc, lead and arsenic. The maximum pyrite content is estimated at ~70% for both Brunswick and Tizapa tailings, assuming all the iron occurs as pyrite. This estimate is slightly higher than values reported by Brunswick Mining Division Inc. (40 to 65% pyrite) (Noranda Technology Centre, 1998e). The discrepancy probably lies in the 0-5% pyrrhotite content and the iron of the sphalerite not being taken into account in this summary calculation. The Tizapa estimate falls within the values reported by Peñoles (Ybarra, 1998). Tizapa tailings also have the lowest concentration of calcium whereas Brunswick has the highest. FIM and Louvicourt tailings have a similar composition, containing approximately one-third the concentration of sulfide and half the iron than Brunswick or Tizapa, giving a maximum pyrite content of 35% for each tailings. This estimate lies within the Noranda Inc. calculations of 16 to 47% pyrite for Louvicourt. FIM and Louvicourt tailings also have low concentrations of zinc, lead copper and arsenic compared to the other tailings. All tailings have low concentrations of

carbonates, a parameter associated with limestone (CaCO_3) or dolomite ($\text{CaMg}(\text{CO}_3)_2$), suggesting that all tailings have a low acid neutralization potential.

The chemical analyses presented in Table 5.2 indicate that the principal component of OPC is calcium corresponding to the content of tri- and di-calcium silicates (Ca_3SiO_5 and Ca_2SiO_3 respectively) and tri-calcium aluminate ($\text{Ca}_3\text{Al}_2\text{O}_6$), the principal binding agents of OPC. The granulated blast furnace slag used in the Louvicourt formulation has a relatively low iron content and is therefore favourable for use against sulfate rich waters (Kosmatka et al., 1995). The slag is also rich in calcium and silicon, carbonates and magnesium.

Table 5.1 Chemical Analyses of Tailings and Binders Used in Backfill Mixtures

Element	Cement	Slag	Louv.	FIM	Tiz.	Brwk
S _{total} %	1.3	1.1	9.2	10.5	37.4	34.3
S as SO ₄ %	0.2	0.2	1.0	0.2	0.4	3.3
S ²⁻ %	1.1	0.9	8.2	10.3	37.0	31.0
Fe %	1.2	0.3	16.1	16.7	34.4	30.5
Zn %	0.007	0.002	0.11	0.66	2.10	1.08
Pb %	0.003	0.002	0.03	0.07	0.38	1.08
Cu %	0.057	0.022	0.001	0.001	0.180	0.100
Ni %	<0.001	<0.001	<0.001	<0.001	<0.005	0.007
As %	<0.005	<0.005	0.02	0.005	0.31	0.37
Cd %	<0.001	<0.001	0.007	<0.001	<0.001	0.13
SiO ₂ %	18.9	31.7	42.5	34.6	11.2	21.7
CO ₃ %	1.7	7.7	0.6	2.3	2.3	1.6
Al ₂ O ₃ %	4.5	6.9	9.6	5.7	2.7	1.1
Na ₂ O %	0.63	0.09	0.44	0.08	0.07	0.14
CaO %	69.0	44.2	2.8	8.8	0.7	14.3
MgO %	1.4	12.7	6.7	2.0	0.7	4.2
MnO %	0.02	0.74	0.20	1.44	0.09	0.12
K ₂ O %	1.10	0.42	0.02	0.06	0.05	0.11
C %	0.6	0.3	1.3	2.4	0.4	0.2
Sum:	100.3	106.2	89.5	85.3	92.9	110.97

Water (mg/l)	Element
41.8	SO ₄
0.47	Fe
< 0.1	Zn
< 0.1	Pb
< 0.05	Cu
< 0.1	Ni
< 1.0	As
--	Cd
28.2	Si
--	CO ₃
< 0.3	Al
64.8	Na
31.4	Ca
0.77	Mg
< 0.1	Mn
8.7	K
--	C

For all solid samples: Bi <0.001%, Cr <0.02%, Se <0.001%, Te <0.002%
L.O.I. not reported

-- : not analysed

Table 5.2 Final Composition of Paste Samples

Element	Louv.	FIM	Tiz.	Brwk
S _{total} %	8.8	10.2	35.1	32.6
SO ₄ %	1.0	0.2	0.4	3.2
Sulfide %	7.9	10.0	34.7	29.5
Fe %	15.3	16.2	32.3	29.0
Zn %	0.11	0.64	1.97	1.03
Pb %	0.03	0.07	0.36	1.03
Cu %	0.002	0.003	0.17	0.10
Ni %	<0.001	<0.001	<0.005	0.007
As %	0.02	0.005	0.29	0.35
Cd %	<0.001	0.005	<0.001	0.12
SiO ₂ %	41.9	34.1	11.7	21.6
CO ₃ %	0.8	2.3	2.3	1.6
Al ₂ O ₃ %	9.4	5.6	2.8	1.3
Na ₂ O %	0.43	0.10	0.10	0.16
CaO %	4.9	10.6	5.0	17.0
MgO %	6.8	2.0	0.7	4.0
MnO %	0.22	1.40	0.09	0.12
K ₂ O %	0.04	0.09	0.12	0.16
C %	1.3	2.3	0.4	0.2
Sum:	90.2	85.7	93.3	110.44

5.2 ASPECT OF CURED PASTE SAMPLES

The FIM paste samples were very friable and had little cohesion after 14 days of humid curing. Some FIM samples were slightly damaged upon demoulding and partially dissociated or crumbled when first being exposed to water or the $\text{Fe}_2(\text{SO}_4)_3$ solution.

Louvicourt samples were also relatively soft and friable after 14 days of humid curing although more resistant than FIM samples. No dissolution or fracturing was observed upon immersion of the samples.

The cured paste samples of Brunswick and Tizapa were much harder and appeared to have lower porosity than the other two mixtures. Tizapa paste was the densest and hardest of all mixtures. During the curing period, Tizapa samples formed a thin oxidized coating on the paste surface inside the mould (Figure 5.1). The coating penetrated less than 1 mm and was sanded down to expose fresh surfaces to the leaching solutions.

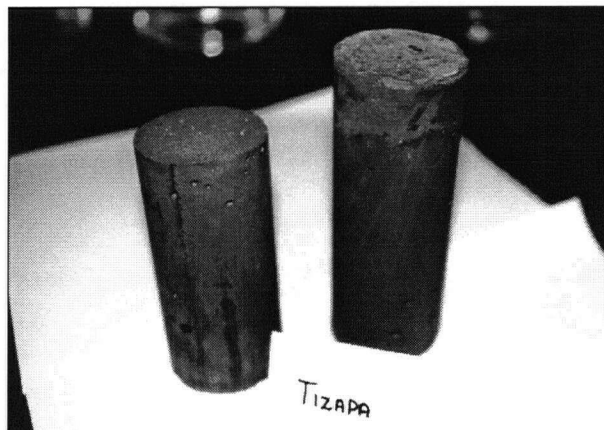


Figure 5.1 Superficial Oxidation of Freshly Cured Tizapa Paste Samples

5.3 WATER ABSORPTION BY THE PASTE

Measurements of water absorption in the puck and cylinder samples after 5 and 20 weeks of leaching are presented in Tables 5.3 a and b respectively. With the exception of the Louvicourt puck sample, the percentage of water absorbed by the pucks and cylinder samples remained relatively unchanged in both the flooded and cycled water environments (Figures 5.2 and 5.3). Tizapa paste had an average water content of 15.7 % after each leaching period, similarly Brunswick paste had a water content around 17.8 %, FIM 22.8% and Louvicourt 23.2 % water. The paste with the lowest water content (Tizapa) corresponding with the mixture having the highest proportion of cement. Following this trend, Brunswick, FIM then Louvicourt had decreasing amounts of cement and increasing water contents.

Equal water contents for samples of similar composition but very different sizes and shapes (such as pucks and cylinders of one particular mixture) suggest that the samples were completely saturated with water and with the ferric sulfate solution. Saturation of the paste is likely achieved within 24 hours after immersion since the cycle-leached samples had similar water contents to the flooded-leached pastes.

Water absorption in the ferric sulfate environment seemed to indicate an increased water content with time for all samples (Figure 5.4). Given that the samples became saturated with water shortly after immersion, the apparent increase in water content is instead a loss of solid mass with leaching time due to dissolution of the sample.

Table 5.3 a Paste Water Content: 5 weeks

	ID	W.wet (g)	W.dry (g)	% H2O	% H2O average
Water - cycled *	TIZAPA # 6 PUCK CYLINDER	26.7 501.5	22.5 428.1	15.9 14.6	15.3
	FIM # 4 PUCK CYLINDER	15.5 409.3	12.0 315.8	22.5 22.8	22.6
	LOUV # 9 PUCK CYLINDER	32.9 400.2	30.9 309.7	6.1 22.6	22.60
	BRWK # 1 PUCK CYLINDER	28.7 480.4	23.5 397.6	18.2 17.2	17.7
	TIZAPA # 5 PUCK CYLINDER	42.3 497.4	35.6 419.5	15.8 15.7	15.8
	FIM # 11 PUCK CYLINDER	31.0 365.8	24.1 280.2	22.3 23.4	22.9
	LOUV # 2 PUCK CYLINDER	52.4 402.4	40.2 310.7	23.2 22.8	23.0
	BRWK # 10 PUCK CYLINDER	40.5 464.6	33.3 383.5	17.6 17.5	17.5
	TIZAPA # 7 PUCK CYLINDER	43.8 511.6	36.6 432.9	16.4 15.4	15.9
	FIM # 8 PUCK CYLINDER	21.5 413.5	16.0 318.9	25.8 22.9	24.3
	LOUV # 4 PUCK CYLINDER	19.2 409.0	14.4 313.4	25.0 23.4	24.2
BRWK # 8 PUCK CYLINDER	38.4 475.5	30.9 390.6	19.5 17.9	18.7	
Fe2(SO4)3 solution					

Table 5.3 b Paste Water Content: 20 weeks

	ID	W.wet (g)	W.dry (g)	% H2O	% H2O average	difference in water absorption
Water - cycled *	TIZAPA # 3 PUCK CYLINDER	52.7 502.8	44.5 426.9	15.5 15.1	15.3	0%
	FIM # 10 PUCK CYLINDER	12.7 382.0	9.8 294.2	23.4 23.0	23.2	2%
	LOUV # 5 PUCK CYLINDER	40.0 373.2	30.8 286.7	23.0 23.2	23.1	2%
	BRWK # 6 PUCK CYLINDER	46.8 467.2	38.5 384.1	17.8 17.8	17.8	0%
	TIZAPA # 4 PUCK CYLINDER	52.9 502.0	44.3 423.6	16.2 15.6	15.9	1%
	FIM # 7 PUCK CYLINDER	33.1 411.0	25.6 316.8	22.6 22.9	22.8	0%
	LOUV # 3 PUCK CYLINDER	56.3 388.1	42.9 297.6	23.8 23.3	23.6	2%
	BRWK # 5 PUCK CYLINDER	54.0 489.2	43.9 404.2	18.7 17.4	18.1	3%
	TIZAPA # 2 PUCK CYLINDER	41.5 496.2	33.5 415.5	19.3 16.3	17.8	12%
	FIM # 3 PUCK CYLINDER	13.6 397.4	9.6 295.9	29.4 25.5	27.4	13%
	LOUV # 8 PUCK CYLINDER	32.6 396.2	24.0 301.5	26.6 23.9	25.3	4%
BRWK # 7 PUCK CYLINDER	48.5 470.4	38.6 380.3	20.4 19.2	19.8	6%	
Fe2(SO4)3 solution						

* Water-cycled measurements taken immediately after the weekly 24 hour immersion period

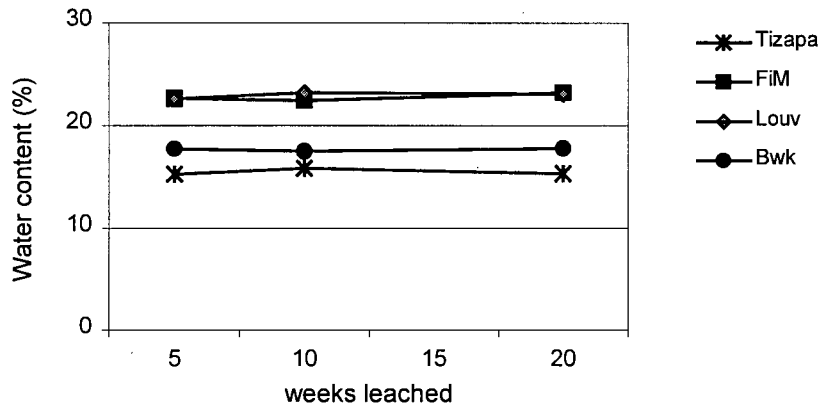


Figure 5.2 Water Absorption in Cyclic-Leaching (water) Environment

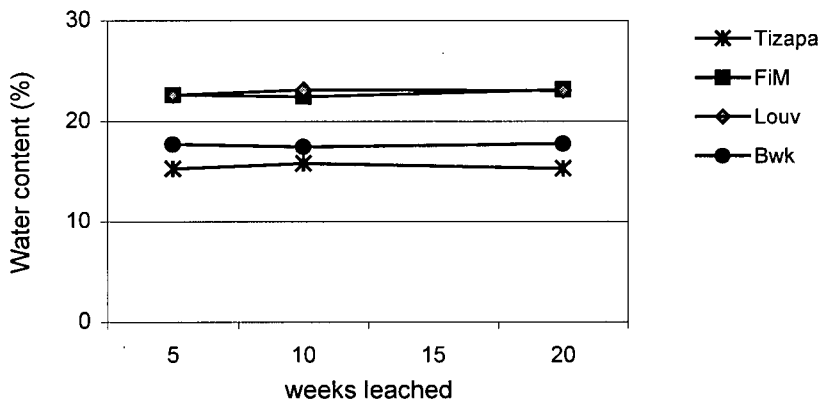


Figure 5.3 Water Absorption in Flooded-Leaching (water) Environment

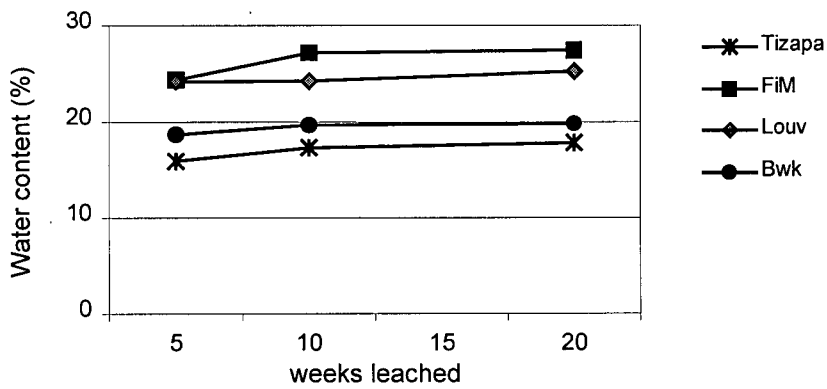


Figure 5.4 Water Absorption in $Fe_2(SO_4)_3$ Solution

5.4 CHEMISTRY OF PASTE LEACHATES

Information on the effect of the different chemical environments on paste was obtained by comparing the chemistry of leachates of the different leaching environments and the solid phase chemistry of the unleached samples. Results indicated that leachate chemistry was controlled more by the characteristics of the leaching environments and the cement content of the paste mixtures than by the mineralogy of the different tailings.

5.4.1 Flooded and Cycled Water-Leached Environments

The chemistry of the flooded-environment and cycled-environment leachates are presented in Appendix II (Tables II-1 and II-2 respectively). Figures 5.5 to 5.32 present graphs of element concentrations with advancing leaching cycles for each water-leached environment. The solid phase concentration of the element or ion appears in the legend box of each graph. Depletion rates were calculated for the elements showing the greatest change with time (calcium, potassium and magnesium) in order to verify the effect of the different leachate volumes extracted from each leaching environment.

Flooded environment pH values remained relatively high (pH 8-9) throughout the 20 weeks of leaching (Figure 5.5), whereas the cycled environment pH reached steady state at pH 6-7, closer to the pH of the distilled water (Figure 5.6). Leachate conductivities were much higher in the early cycles of the flooded environment and reached steady state at a slightly higher level than the leachate of the cycled environment (Figures 5.7 and 5.8). Conductivity measurements are indicative of a greater dissolution of the sample in the

flooded environment compared to the cycled environment. Redox potential measurements are on average higher in the cycled environments than in the flooded environments (Figures 5.9 and 5.10). The higher redox levels in the cycled environment leachate are due to a higher dissolved oxygen concentration resulting from the exposure of air between each cycle.

Trace concentrations of dissolved iron are present in FIM and Louvicourt leachates of both the flooded and cycled environments in the early cycles of leaching (Figures 5.11 and 5.12). The aqueous iron concentrations appear to be unrelated to the iron content of the paste mixtures. The presence of aqueous iron either is from dissolution the tetracalcium aluminoferrite phase of the cement or from the dissolution of pre-existing soluble iron salts originally contained in FIM and Louvicourt tailings.

Zinc concentrations in the flooded environment indicate that zinc is not mobile with the exception of Brunswick in the first 3 cycles of leaching where concentrations of zinc (0.2-0.3 mg/l), slightly above detection limit (0.1 mg/l), are leached out of the paste (Figure 5.13). Higher zinc mobility occurred in the cycled environment throughout the leaching cycles where zinc was mobilized from all pastes (Figure 5.14). Cycled environment zinc concentrations were close to detection limit for Louvicourt and FIM samples, both of which contain the lowest solid phase zinc concentration. Brunswick and Tizapa samples showed higher concentrations of zinc throughout the leaching cycles compared with the flooded environment and a general increase in zinc concentration with leaching time. Leachate zinc concentrations appear to be proportional to solid phase concentrations of zinc and possibly inversely proportional to the cement content of the

samples.

Unlike zinc, lead was not very mobile in either water-leached environment. In the flooded environment, Louvicourt, FIM and Brunswick leachate lead concentrations remained close to or below detection limit throughout the 20 weeks (Figure 5.15). No lead was leached out of the Tizapa samples. Low quantities of lead were leached out from all samples in the early cycles of leaching and out of Louvicourt and Tizapa in the last cycles (Figure 5.16). A direct correlation cannot be made between solid phase lead concentrations and leachate concentrations.

Sulfate concentrations followed a decreasing trend for all samples in both the flooded and cycled water environments (Figures 5.17 and 5.18). pH values were too high to allow for significant sulfide oxidation hence the sulfate in the leachate is most likely derived from the initial sulfate content of the tailings, most probably sulfate salts precipitated from the tailings water upon drying of the tailings. Indeed, sulfate concentrations in the leachate were proportional to the solid phase concentrations of sulfate.

Calcium concentrations also showed a decreasing trend in both the flooded and cycled environments (Figures 5.19 and 5.20). Initial flooded leachate concentrations of calcium were between 682 mg/l (FIM) and 922 mg/l (Brunswick), falling to 185 mg/l and 590 mg/l respectively after 20 weeks of leaching. Louvicourt and Tizapa concentrations fall between those of FIM and Brunswick. The difference in the time series concentration of calcium between both environments resulted from the different leachate sampling protocols. The calcium depletion curves are in fact similar for both environments (Figures 5.21 and 5.22). The flooded environment showed a slightly slower

depletion in the early cycles but quickly reached the values of the cycled environment in the later cycles.

Aqueous concentrations of magnesium, potassium and silicon in both flooded and cycled environments are proportional to the solid phase concentration of each sample for the respective element (Figures 5.23 to 5.32).

In the early cycles of both water-leached environments, Louvicourt leachates had considerably higher concentrations of magnesium than the other samples (Figures 5.23 and 5.24). Magnesium concentrations reached steady state shortly thereafter. Louvicourt concentrations remained slightly higher than the other samples. A correlation can be made between aqueous magnesium concentrations and the slag component of the Louvicourt paste, the latter having the highest solid phase concentration of magnesium of all paste ingredients. It is most probable that the magnesium in the leachate originated from the dissolution of the incompletely cured slag component of the Louvicourt sample. In fact, the granulated blast furnace slag used by Louvicourt requires up to 21 days of curing before participating in cementitious reactions (Dallaire, 1997). The steady state conditions reached after the first cycles of leaching were probably the consequence of a more complete curing of the binder, reducing the availability of magnesium. Depletion profiles of magnesium were similar for all samples in both water-leached environments, with the exception of Tizapa (Figures 5.25 and 5.26). After 20 weeks of leaching, the depletion of magnesium from the Tizapa sample in the cycled environment was double that of the flooded environment. The continued depletion of magnesium from Tizapa may be related to the dissolution of a magnesium mineral (i.e. dolomite: $\text{CaMg}(\text{CO}_3)_2$),

unaffected by the curing of the cement phase.

In the case of potassium, the most important source of that element in the paste is the cement phase (refer to Table 5.2). The highest leachate concentrations of potassium coincide with the Tizapa pastes, characterized by the highest proportion of cement (Figure 5.27 and 5.28). Potassium depletion rates are similar for both water-leached environments for all samples, with the exception of Louvicourt, which had a higher K depletion rate in the flooded environment (Figures 5.29 and 5.30).

Silicon concentrations remained low in both water-leached environments (Figures 5.31 and 5.32). The general stability of silicate minerals in the pH and redox conditions of the leaching cells suggests that silicon is dissolving from the more soluble cement phases such as the tobermorite gel ($\text{Ca}_3\text{Si}_2\text{O}_7 \cdot 3\text{H}_2\text{O}$), the principal binding agent of cement. Continued decomposition of this phase would have serious consequences on the stability of the binder.

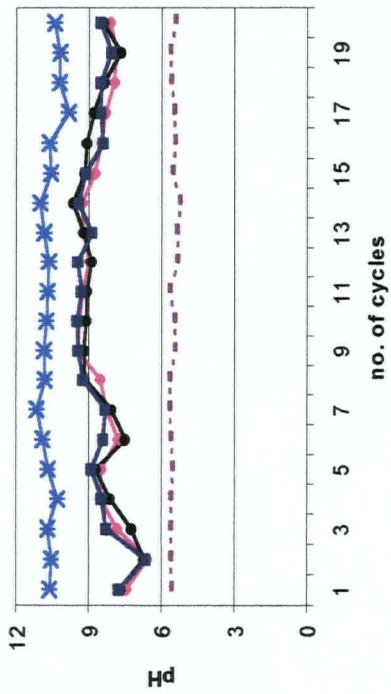


Figure 5.5 Flooded Cells – Leachate pH

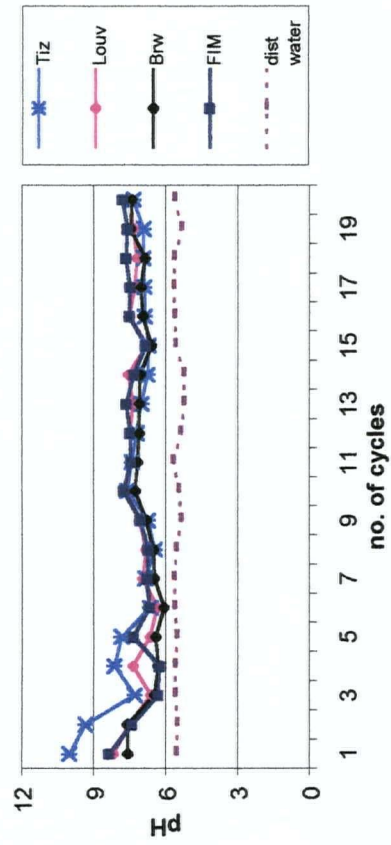


Figure 5.6 Cycled Cells - Leachate pH

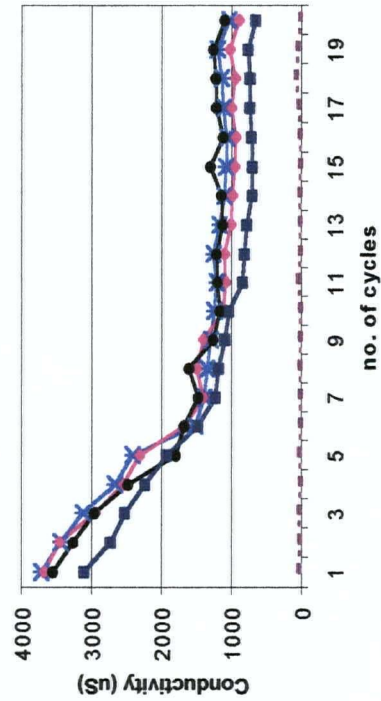


Figure 5.7 Flooded Cells – Conductivity

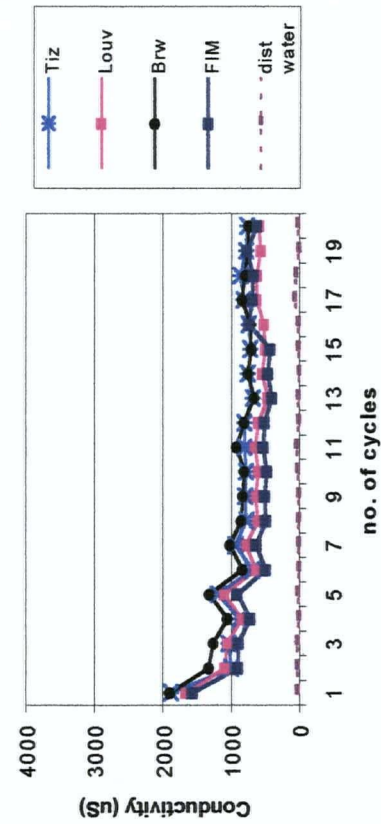


Figure 5.8 Cycled Cells - Conductivity

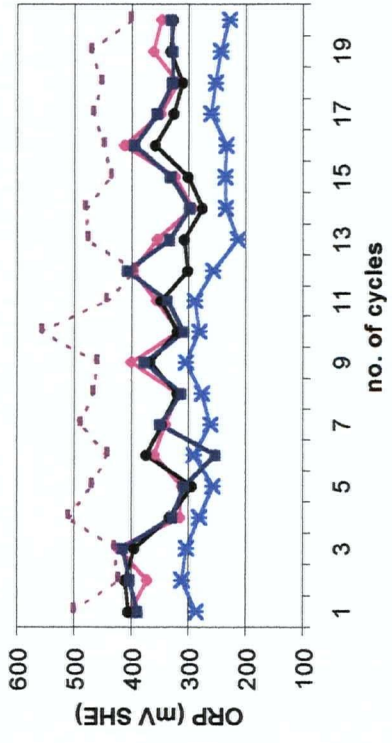


Figure 5.9 Flooded Cells - Redox Potential

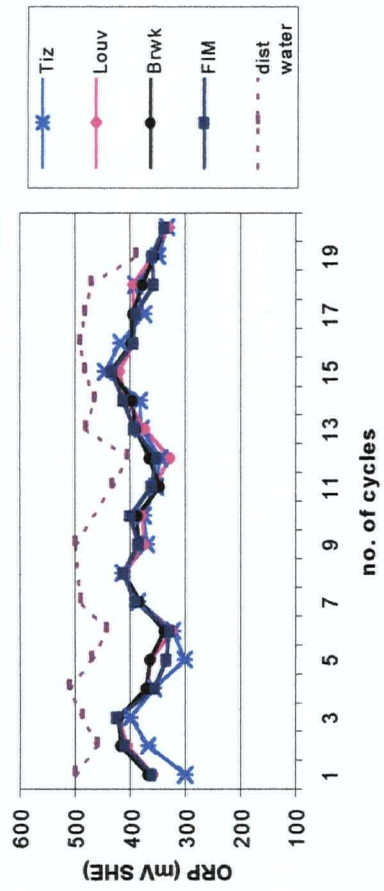


Figure 5.10 Cycled Cells - Redox Potential

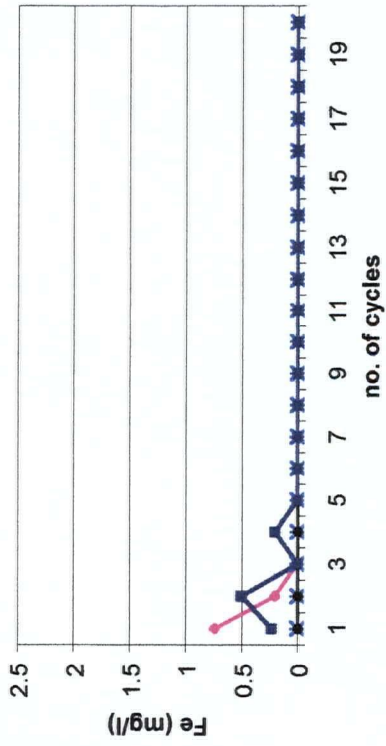


Figure 5.11 Flooded Cells - Dissolved Iron

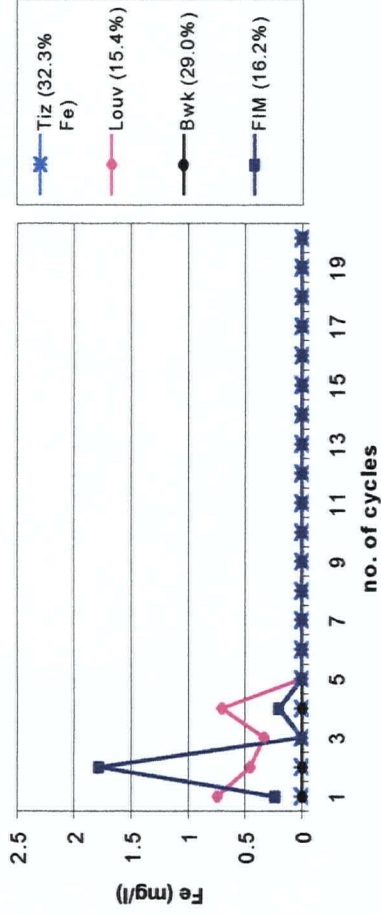


Figure 5.12 Cycled Cells - Dissolved Iron

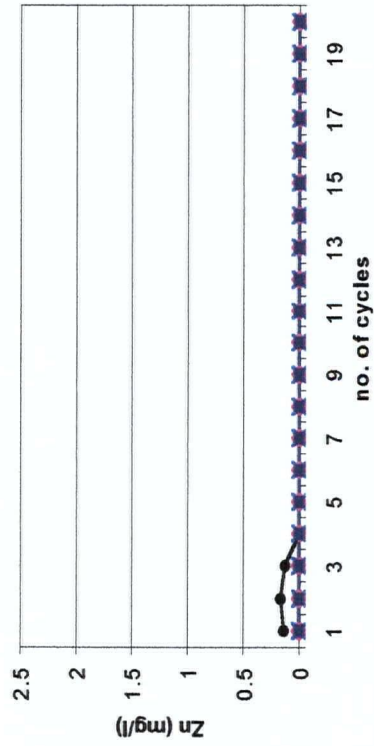


Figure 5.13 Flooded Cells - Dissolved Zinc

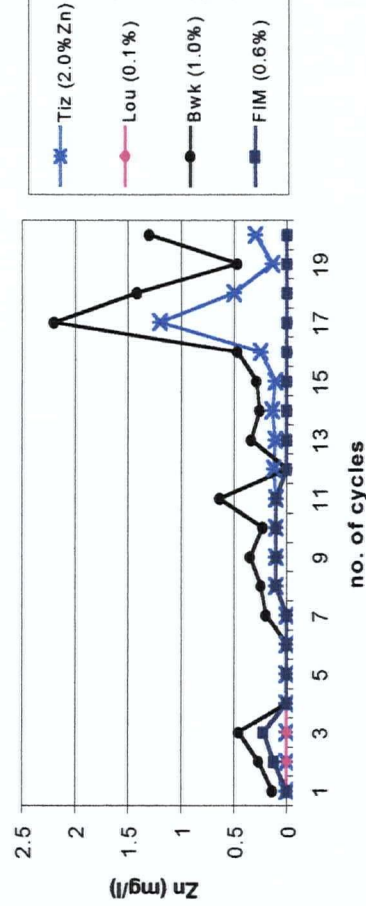


Figure 5.14 Cycled Cells - Dissolved Zinc

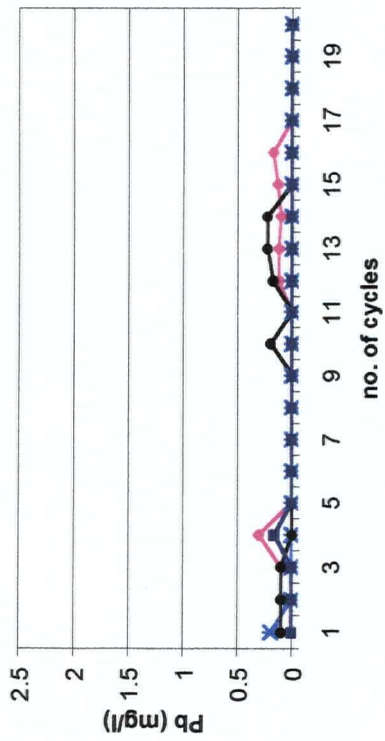


Figure 5.15 Flooded Cells - Dissolved Lead

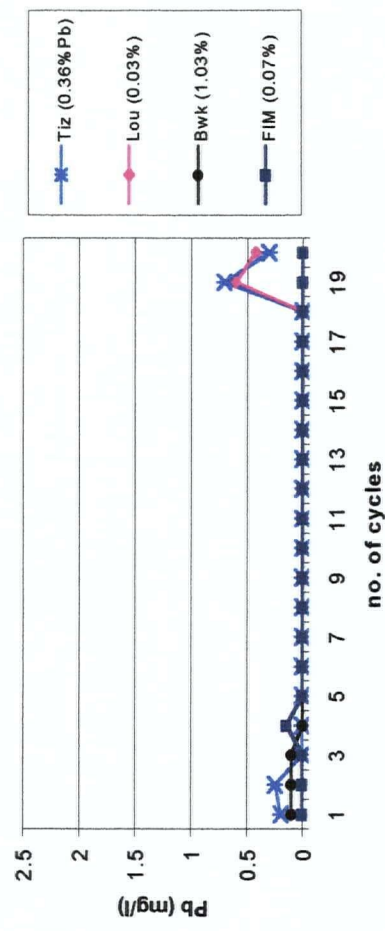


Figure 5.16 Cycled Cells - Dissolved Lead

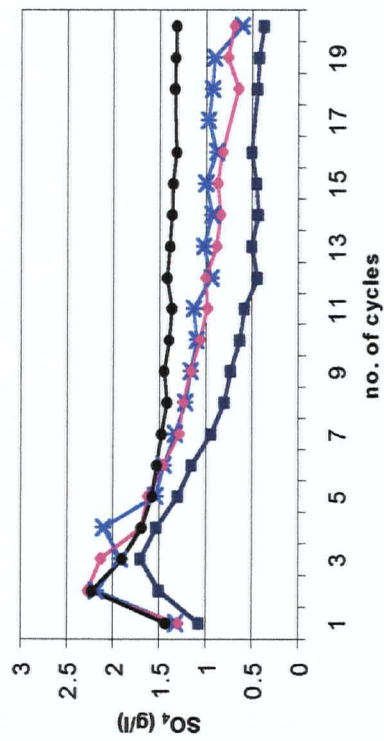


Figure 5.17 Flooded Cells - Sulfate Concentration

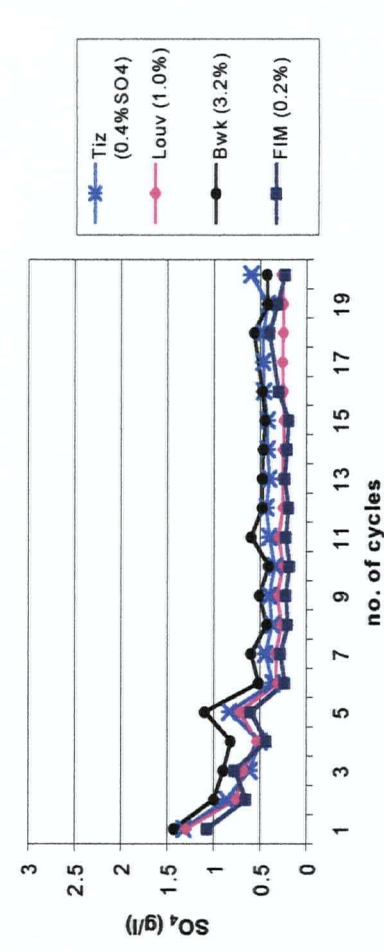


Figure 5.18 Cycled Cells - Sulfate Concentration

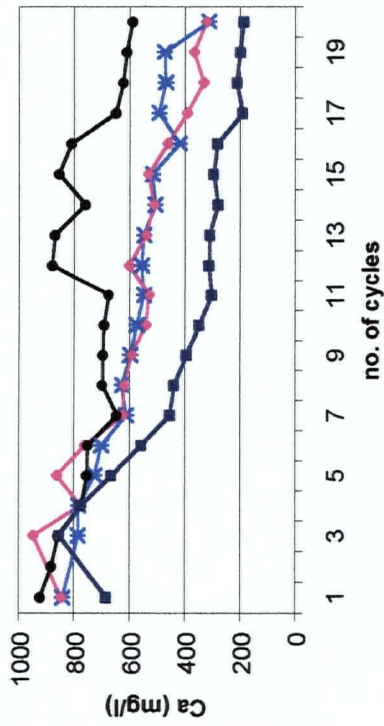


Figure 5.19 Flooded Cells – Calcium Concentration

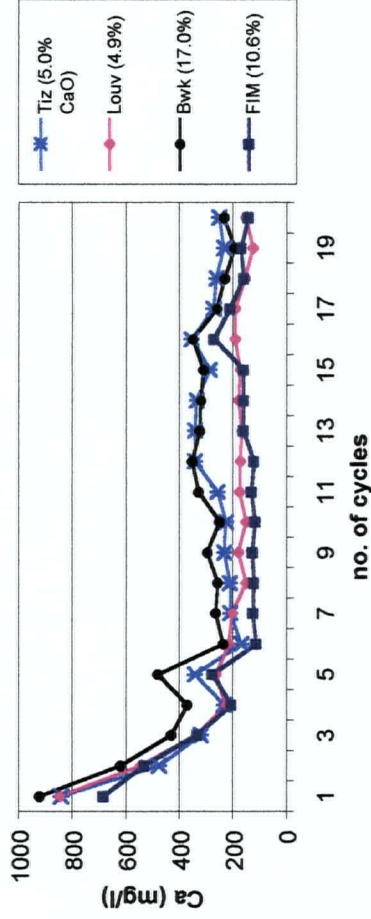


Figure 5.20 Cycled Cells - Calcium Concentration

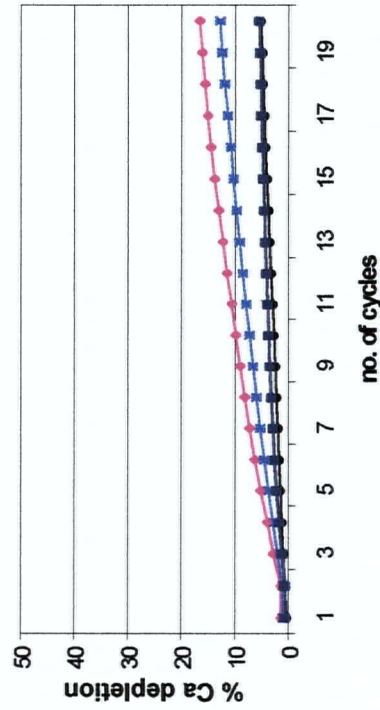


Figure 5.21 Flooded Cells - Calcium depletion rate

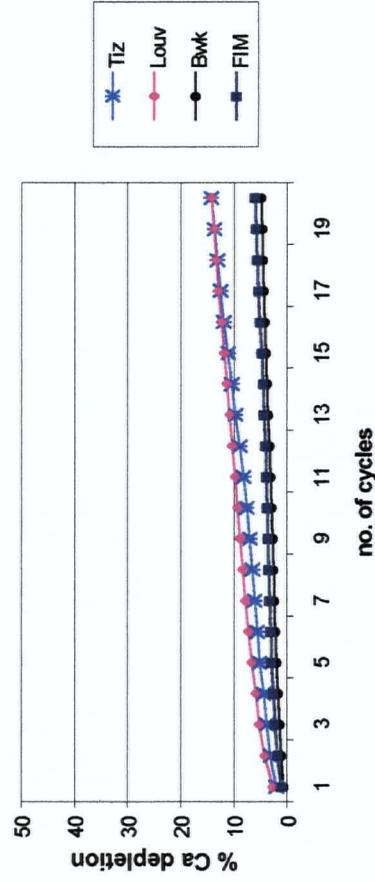


Figure 5.22 Cycled Cells – Calcium depletion rate

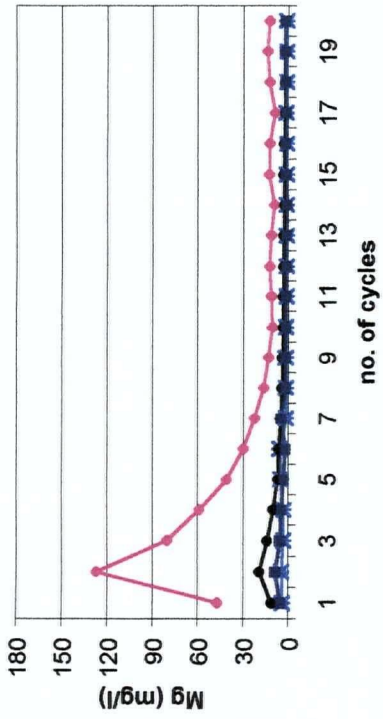


Figure 5.23 Flooded Cells - Magnesium Concentration

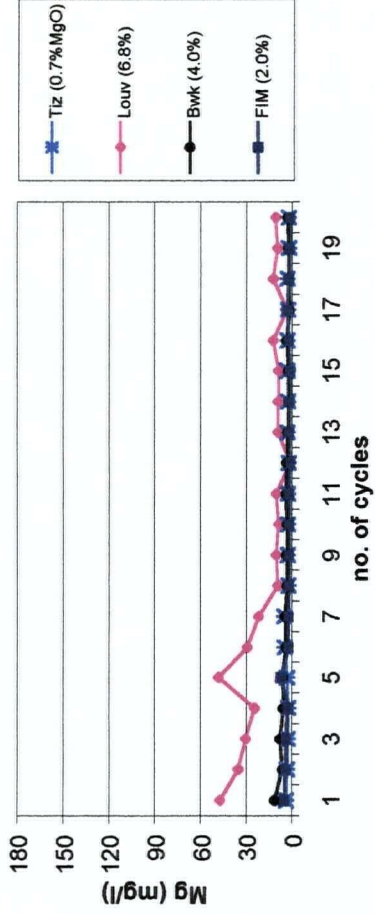


Figure 5.24 Cycled Cells - Magnesium Concentration

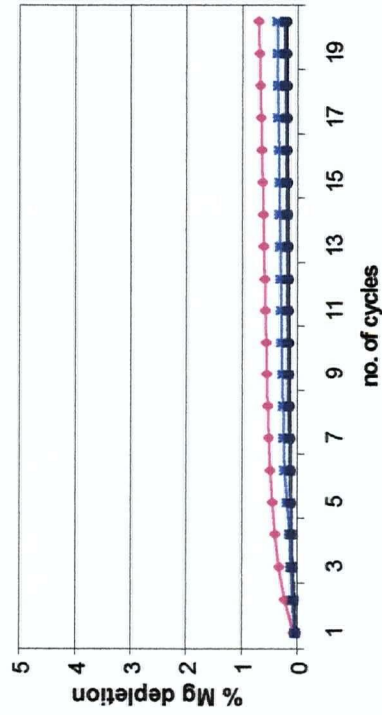


Figure 5.25 Flooded Cells - Magnesium depletion rate

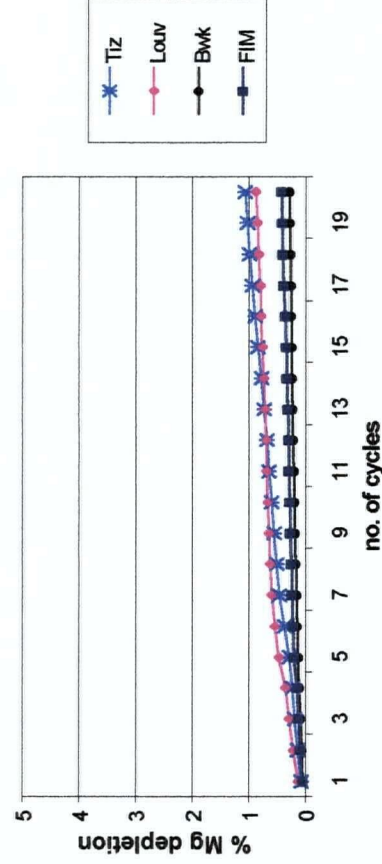


Figure 5.26 Cycled Cells - Magnesium depletion rate

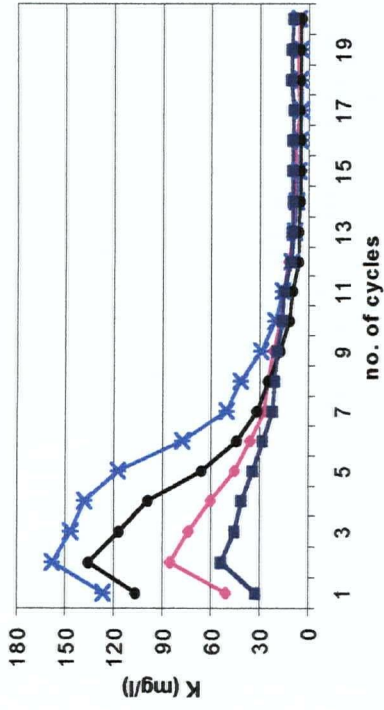


Figure 5.27 Flooded Cells - Potassium Concentration

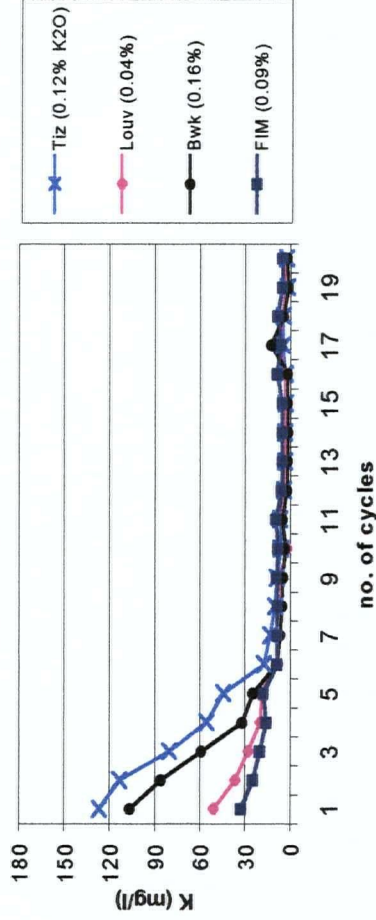


Figure 5.28 Cycled Cells - Potassium Concentration

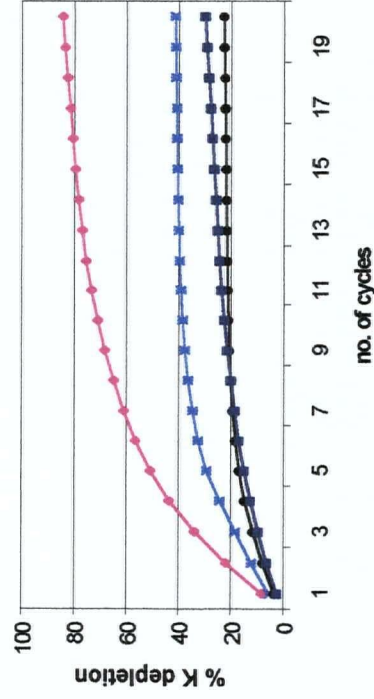


Figure 5.29 Flooded Cells – Potassium Depletion Rate

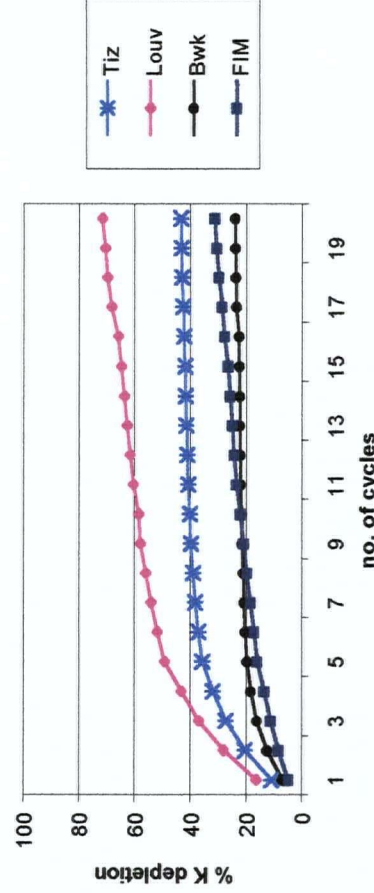


Figure 5.30 Cycled Cells – Potassium Depletion Rate

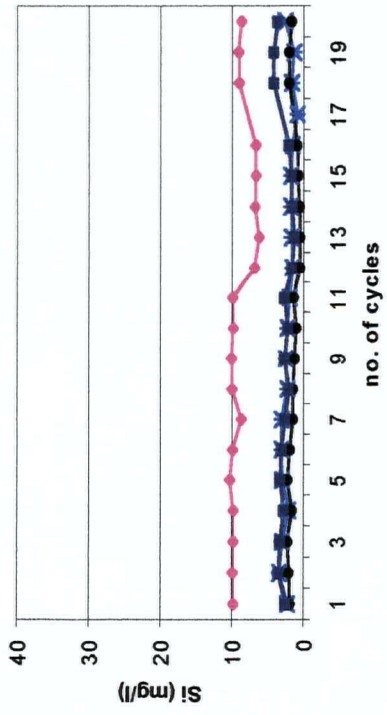


Figure 5.31 Flooded Cells - Silicon Concentration

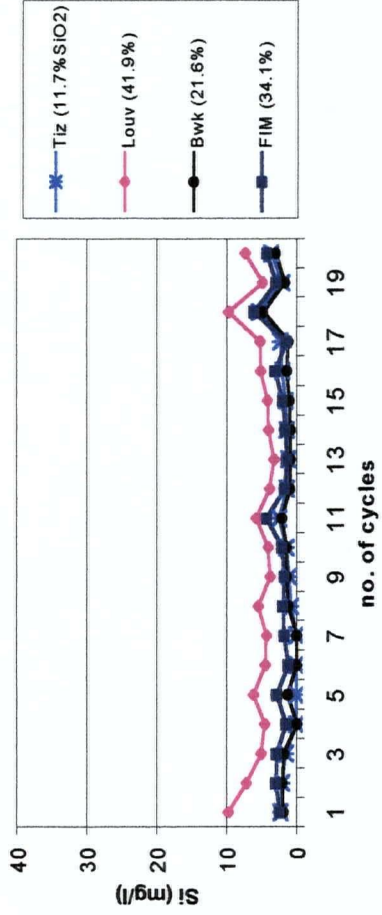


Figure 5.32 Cycled Cells - Silicon Concentration

5.4.2 $\text{Fe}_2(\text{SO}_4)_3$ Solution-Leached Environment

The chemical results of the ferric sulfate leachate solutions are presented in Appendix II (Table II-3). Time series concentration graphs, as well as calculated depletion rates for calcium, potassium and magnesium, are shown in Figures 5.33 to 5.50.

The acidic pH (2.4 – 2.6) of the ferric sulfate solution was almost instantly neutralized when coming in contact with the paste sample (Figure 5.33). In the first leaching cycles, ferric sulfate solutions were buffered to a pH of 6-7 for all samples. After 40 cycles of leaching (20 weeks), Louvicourt, Brunswick and Tizapa solutions were buffered to an average pH of 3.5 whereas FIM leach solution was buffered to a slightly higher average pH of 5. Conductivities of the leachate solutions show a considerable drop in the first four cycles of leaching, stabilizing at a lower level (1500 μS) than that of the ferric sulfate solution (2300 μS) (Figure 5.34). This indicates that the ions are precipitating from the solution upon contact with the samples. The ferric sulfate solution added to the samples bi-weekly has an average redox potential of 620 millivolts SHE. Initial leachate redox values (after 3 to 4 day contact periods with the samples) are around 130 mV, rising to near ferric sulfate solution values in the final cycles (Figure 5.35). Louvicourt, Brunswick and Tizapa leachates had final redox values around 480 mV whereas FIM final redox conditions were around 330 mV. The evolution of the redox values in all leachates again indicates that the ferric sulfate solution is decreasingly altered or buffered by the sample as leaching progresses.

In the initial stages of leaching, dissolved iron concentrations in the leachate were much

lower than those of the ferric sulfate leaching solution. Iron was precipitated out of solution onto the surfaces of the paste samples as a dark orange ferric hydroxide precipitate (Figure 5.36). As leaching progressed, leachate iron concentrations of all samples slowly increased, approaching the values of the ferric sulfate solution (Figure 5.37). This indicates that the ferric hydroxide coating was forming much more slowly.

Unlike the water-leached environments, a considerable amount of zinc was continuously leached out of the Brunswick paste sample, averaging a concentration of 15 mg/l throughout the leaching cycles (Figure 5.38). Zinc was also leached out of the Tizapa sample (average of 4 mg/l), increasing in the last five cycles to about 9 mg/l. Louvicourt and FIM samples released low concentrations of zinc relative to the other samples (below 3 mg/l) but higher than in the water leached environments. The samples with the highest solid phase zinc concentrations (Tizapa and Brunswick) yielded the highest leachate concentration of zinc.

The mobility of lead was slightly higher in the ferric sulfate environment than in the water environments (Figure 5.39). Tizapa and Brunswick leachates had the highest concentration of aqueous lead throughout the leaching cycles, both slowly increasing to an average of 1.6 and 1.2 mg/l respectively in the last 10 cycles. Lead concentrations in the Louvicourt leachate were close to detection limit throughout the leaching cycles whereas FIM showed trace concentrations of lead only in the final cycles. As with zinc, lead concentration in the leachate appears to be proportional to the solid phase concentration.

In the first cycles, sulfate concentrations in the leachate were greater than the leaching

solution sulfate. After the third leaching cycle, leachate concentrations were essentially the same as the ferric sulfate solution. These concentrations were maintained throughout the remaining leaching cycles. This suggests that the sulfate ion of the leaching solution is not participating in cement-altering reactions within the pastes.

Calcium was leached from all samples throughout the test. Relatively high concentrations were leached in the early cycles, decreasing to steady state around the 10th leaching cycle (Figure 5.41). The variation of calcium concentrations between the different samples is much greater in the ferric sulfate environment than in water-leached environments. Louvicourt had the lowest aqueous calcium concentration as well as the lowest solid phase concentration of calcium. FIM and Brunswick had generally the highest leachate concentrations of calcium as well as the highest solid phase concentration. Leachate calcium concentrations are proportional to the solid phase concentration prior to leaching. Ferric sulfate-leached depletion rates of calcium (Figure 5.42) were slightly higher than in the water environments with the exception of FIM for which the depletion rate was double that of the water environments.

As with the water-leached environments, aqueous concentrations of magnesium, potassium and silicon are also related to the solid phase concentration of the element. Aqueous magnesium concentrations were highest in the Louvicourt leachate, which also possessed the highest solid phase concentration (Figure 5.43). In the initial cycles, leachate Mg concentrations were similar to those of the flooded environment. As leaching progressed, however, the Mg concentrations remained high in the ferric sulfate solution. Tizapa, Brunswick and FIM leachate concentrations of Mg were also slightly

higher in the ferric sulfate environment than in the flooded water environment. Depletion rates of Mg were, in fact, much higher in the ferric sulfate environment (Figure 5.44) compared to the water-leached environment.

Potassium concentrations of each leachate followed a trend similar to that of the flooded environment (Figure 5.45). Leachate concentrations of K in the first cycles were similar for both environments. However, the decrease in concentrations occurred more suddenly and earlier in the ferric sulfate environment, falling to near detection limit around the 5th leaching cycle. Depletion rates of K are similar in all three environments, with the exception of Louvicourt for which the depletion rate is lower in the ferric sulfate than in flooded water (Figure 5.46).

Leachate concentrations of silicon were similar to those of the flooded environments in the initial cycles, the highest concentration being that of the Louvicourt leachate (Figure 5.47). Contrary to the water-leach environments, silicon concentrations in the ferric sulfate environment showed a continued increase for all samples. Given the low pH conditions of the leachate, especially in the final cycles, the dissolved silicon in this environment may be leached from silicate minerals as well as the tobermorite phase of the binder.

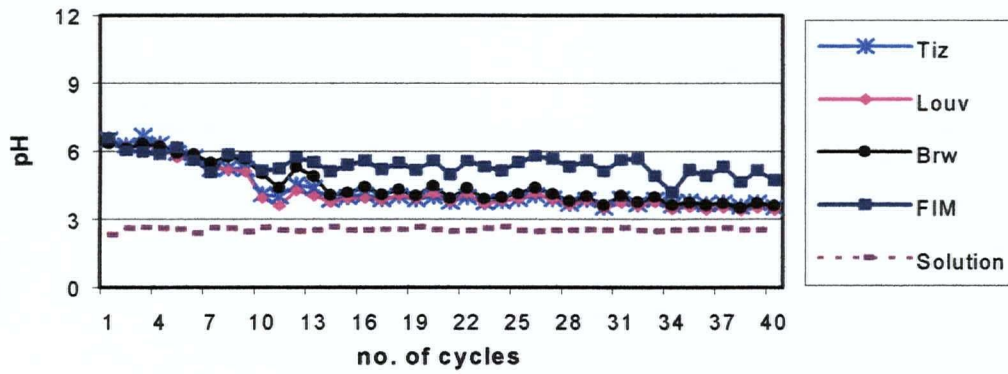


Figure 5.33 $\text{Fe}_2(\text{SO}_4)_3$ Cells - pH

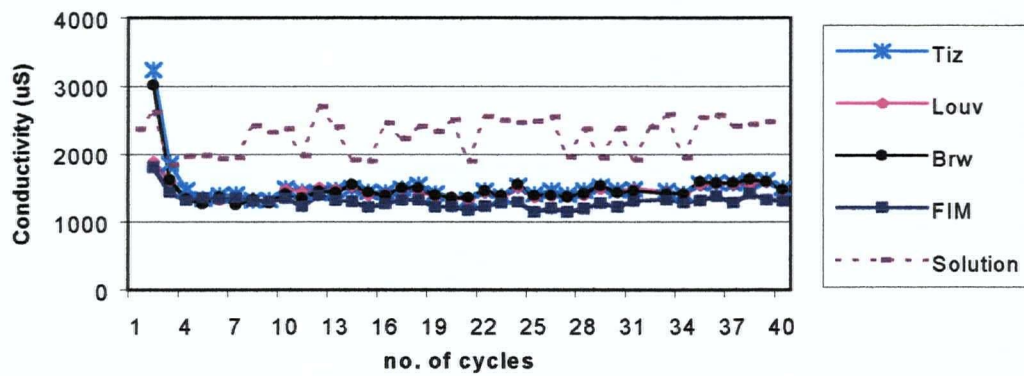


Figure 5.34 $\text{Fe}_2(\text{SO}_4)_3$ Cells - Conductivity

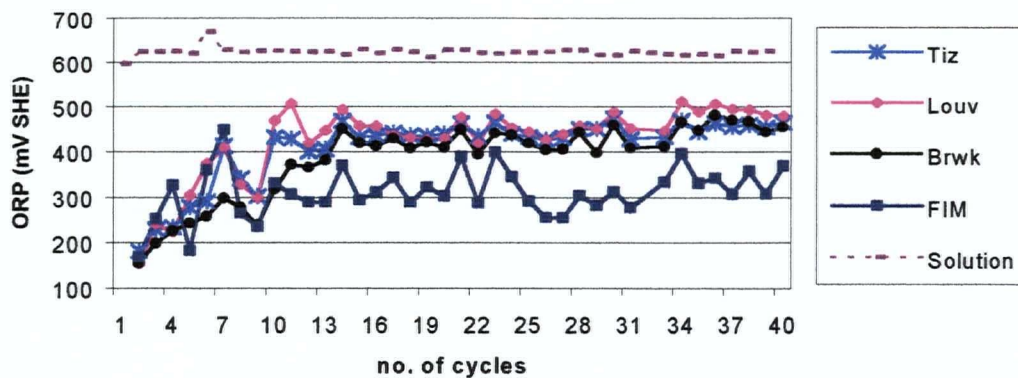


Figure 5.35 $\text{Fe}_2(\text{SO}_4)_3$ Cells - Redox Potential

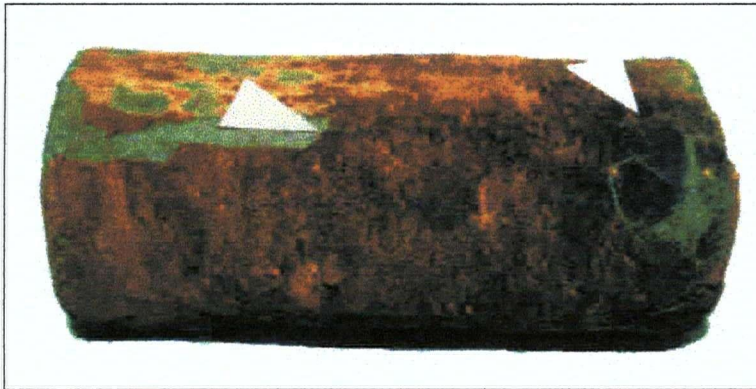


Figure 5.36 Ferric Hydroxide Coating on Paste Sample

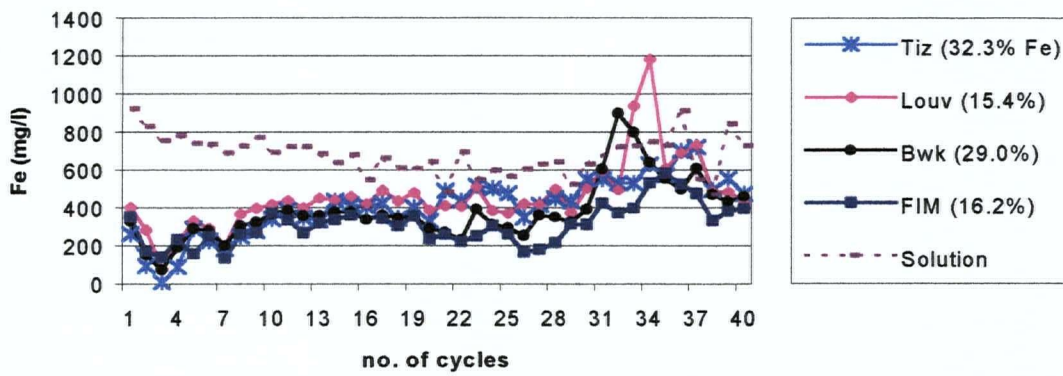


Figure 5.37 $Fe_2(SO_4)_3$ Cells – Dissolved Iron

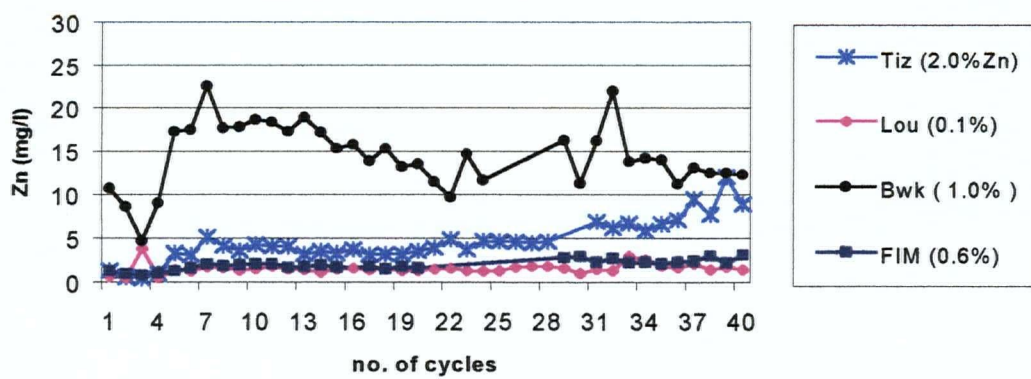


Figure 5.38 $Fe_2(SO_4)_3$ Cells – Dissolved Zinc

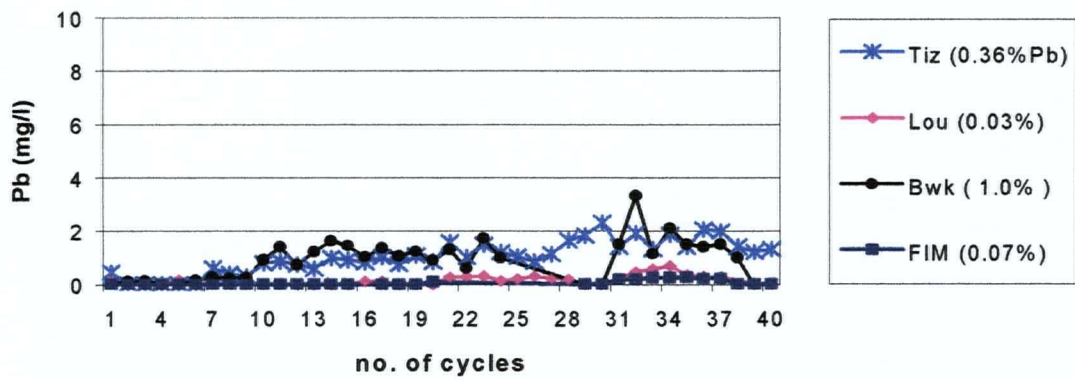


Figure 5.39 $Fe_2(SO_4)_3$ Cells – Dissolved Lead

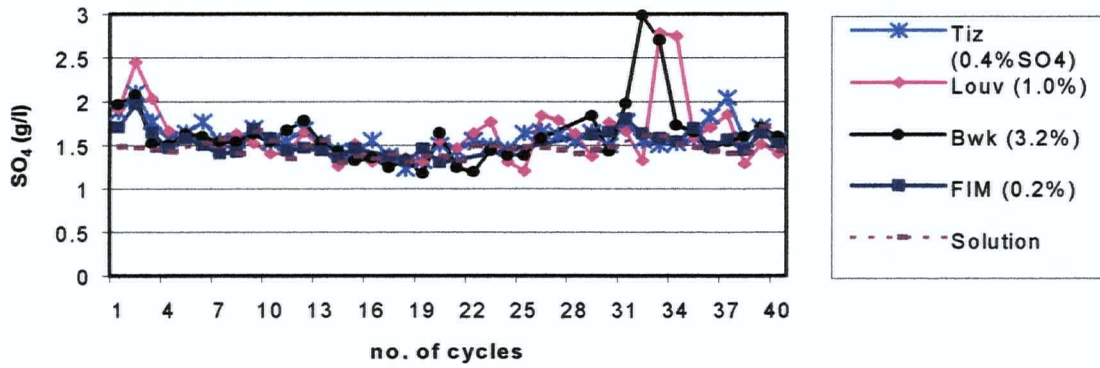


Figure 5.40 $Fe_2(SO_4)_3$ Cells – Sulfate Concentration

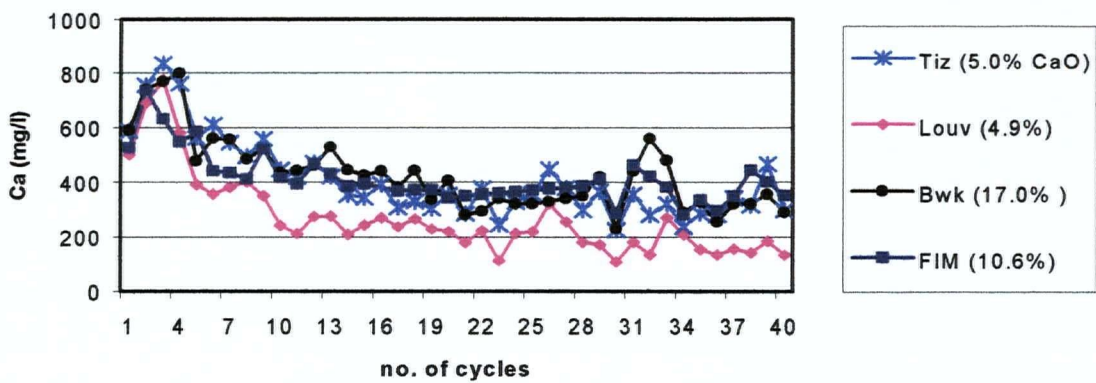


Figure 5.41 $Fe_2(SO_4)_3$ Cells – Calcium Concentration

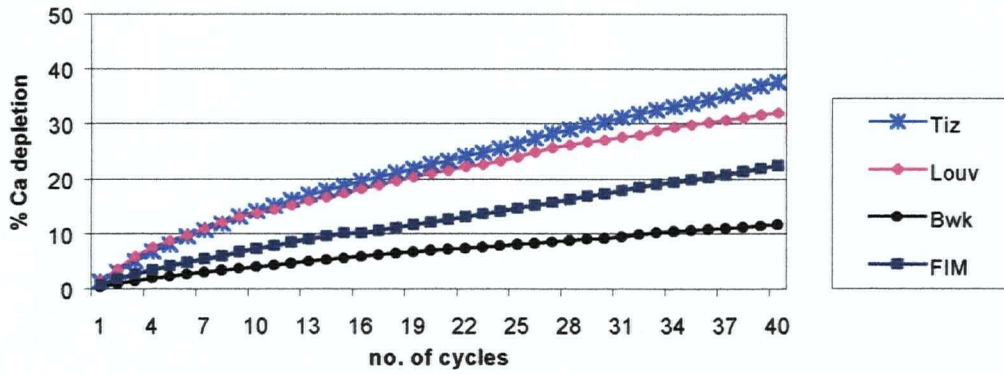


Figure 5.42 Fe₂(SO₄)₃ Cells – Calcium Depletion Rate

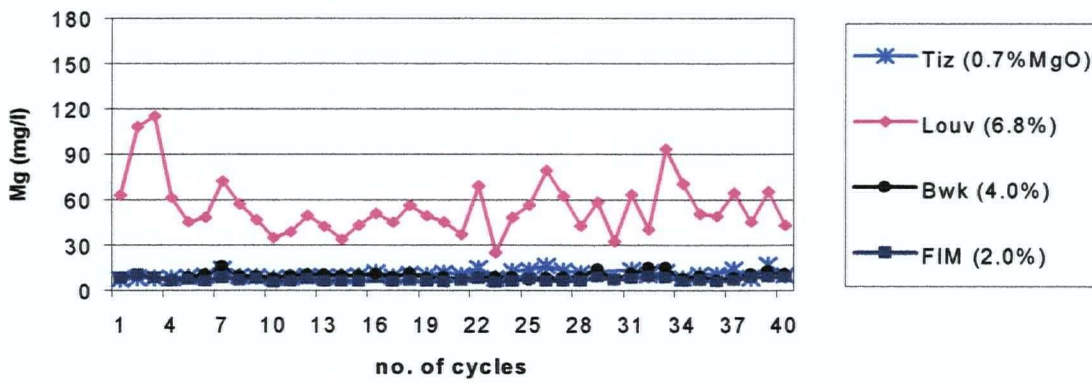


Figure 5.43 Fe₂(SO₄)₃ Cells – Magnesium Concentration

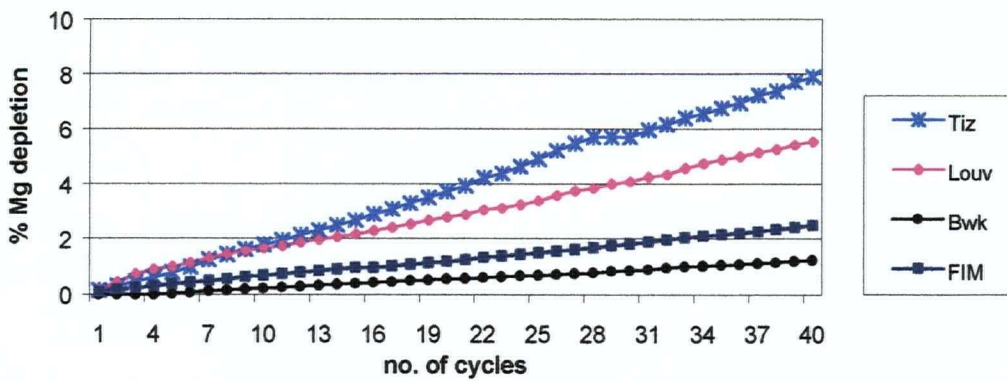


Figure 5.44 Fe₂(SO₄)₃ Cells – Magnesium Depletion Rate

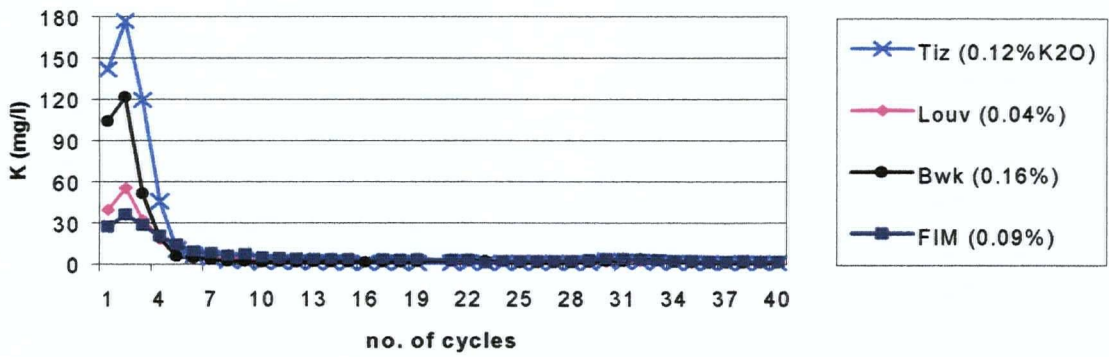


Figure 5.45 Fe₂(SO₄)₃ Leach Cells – Potassium Concentration

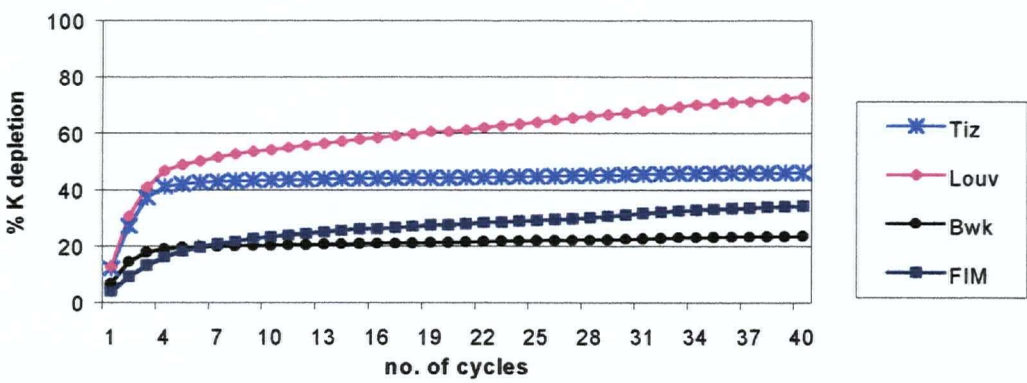


Figure 5.46 Fe₂(SO₄)₃ Leach Cells – Potassium Depletion Rate

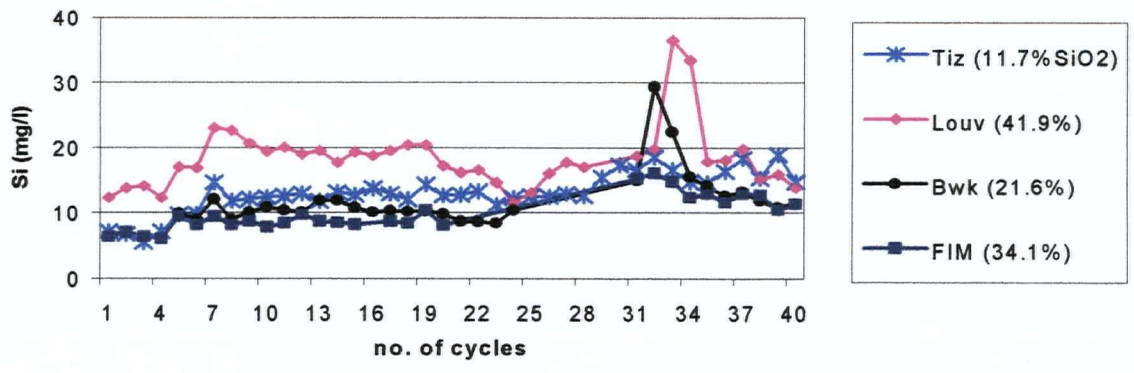


Figure 5.47 Fe₂(SO₄)₃ Leach Cells – Silicon Concentration

5.4.3 Summary of Observations from Leachate Chemistry

The chemistry of the leachate together with the initial concentrations of each element in the paste provide the following information on processes occurring in the first 20 weeks of leaching with water and artificial ARD solution:

Water-leached environments:

- The paste samples provided a high immediate buffering capacity to the leaching water. The buffer was most likely coming from the dissolution of the portlandite phase of the cement (Ca(OH)_2). Higher pH in the flooded environment suggests that portlandite dissolution was more intensive in the flooded environment although calcium depletion rates were similar for both environments. The longer contact time between the leaching solution and the solid sample may have allowed for the precipitation of a secondary calcium phase within the samples, thereby explaining the similarity between calcium depletion rates.
- Conductivity values were indicative of the extent of sample dissolution. Higher conductivities occurred at steady-state conditions in the flooded environments for all samples. This indicates that more intensive dissolution occurred in the flooded environment throughout the leaching cycles because of longer contact times between the samples and the leaching solution.
- The combination of high sulfate concentrations and low concentrations of iron and zinc suggests that sulfate was not the product of sulfide oxidation but rather was leached from a soluble sulfate phase present in the tailings (prior to cement

addition). Considering the high concentrations of sulfate of the tailings water (Table 2.2, Chapter 2), the sulfate in the samples likely originated from a sulfate salt precipitated when the tailings were dried, and redissolved when coming in contact with the leaching solutions.

- Comparison of major ion chemistry (Ca, K, Mg, and Si) in the leachate and in the solid phase of the samples suggests that the binder was actively dissolving. Calcium was most likely leached from the highly soluble portlandite phase of the cement ($\text{Ca}(\text{OH})_2$) (dissociation constant $K_{eq} = 6.3\text{E}22$, Appelo and Postma, 1994; Pakhurst, 1995) whereas silica and potassium were likely dissolved from the tobermorite gel phase. Magnesium, in relative abundance only in the Louvicourt leachate, was likely dissolved from the slag portion of the binder. The decreasing loading of major ions suggests the following: 1) a depletion of the dissolving phases in the outer layers of the paste sample and/or 2) a continued curing of the sample, binding the major ions into more stable, less soluble hydrated cement phases.

Ferric sulfate-leached environment:

- Leachate pH, redox potentials and aqueous iron concentrations evolved towards the values of the ferric sulfate leaching solution with advancing leaching cycles. This suggests that the ferric sulfate solution was decreasingly modified or buffered by the paste with which it came in contact.
- The leaching solution sulfate did not appear to be consumed in secondary, expansive mineral growth reactions in the samples over the 40 cycles of leaching, as the sulfate

concentration of the leaching solution and the leachates remained unchanged throughout the leaching period.

- The relatively high aqueous zinc concentrations in the Brunswick sample suggests either 1) active oxidation of sphalerite that occurred in the outer layers of the paste and/or 2) dissolution of a soluble zinc phase (sulfate, oxide or hydroxide) present in the tailings. The pyrite reactivity study indicated that sphalerite present in the Brunswick pyrite samples was readily oxidized, loading the leachate with dissolved zinc to a much greater extent than the other samples. The pyrite study supports the possibility of active sphalerite oxidation. Pyrite or pyrrhotite oxidation was not verifiable from the leachate data as the leaching solution iron and sulfate concentrations masked any evidence of oxidation of these minerals.
- The presence of lead, albeit in low concentrations, suggest that some dissolution of galena occurred in the Tizapa and Brunswick pastes, both of which contained the largest concentration of lead in the paste prior to leaching.
- Major ion chemistry (Ca, K, Mg, and Si) compared with the solid phase concentrations of the samples suggests that, as in the water-leached environment, binder phases were actively dissolving. Calcium was most likely leached from the portlandite phase (Ca(OH)_2), with the OH^- ions consumed to neutralize the acidic ferric sulfate solution. Higher depletion rates of calcium, potassium and magnesium occurred in the ferric sulfate environment (compared to the water) indicating that the ARD solution was more aggressive than water.

5.5 SOLID PHASE CHEMISTRY OF LEACHED PASTE

Tables 5.4 to 5.7 contain scanned images of the leached paste samples showing concentric altered layers. The sample sections were cut through either pucks (rectangular) or cylinder samples (pie-shaped). The above mentioned tables also contain comparative chemical analyses of each altered layer of the samples. The detailed analytical reports are presented in Appendix III.

The chemistry of each layer is presented as the difference in concentration (in percentage) with respect to the core of the particular sample in the flooded environment. This method of analysis was devised to show only the statistically significant differences in concentrations between the altered layers of a particular backfill mixture, taking into consideration the 5% margin of analytical error reported by the laboratory. The comparative studies are based on the premise that the core of the flooded samples have undergone the least amount of alteration, a hypothesis verified by various leaching studies of cemented mixtures (DeCeukelaire, 1991; Revertegat et al., 1992; Kosmatka et al., 1995; Casanova et al., 1996).

5.5.1 Tizapa

Water-leached environments

Table 5.4 shows a net loss of sulfate and calcium in the outer layers of both water-leached environments compared to the core of the flooded sample. The loss of calcium is greater in the 4 mm outer layer of the cycled sample than in the 0.75 mm outer layer of

the flooded layer. Calcium is most likely depleted from the highly soluble portlandite phase ($\text{Ca}(\text{OH})_2$) of cement and possibly also from some de-calcification of the tobermorite phase ($\text{Ca}_3\text{Si}_2\text{O}_5 \cdot 3\text{H}_2\text{O}$), as reported in other concrete leaching experiments (Revertégat *et al*, 1992; Carde and Francois, 1997). The less depleted concentration of calcium in the flooded paste may indicate the precipitation of a secondary calcium phase in the outer layer.

Sulfide levels are similar in all layers suggesting that sulfide oxidation is not occurring in this layer. The sulfate leached out of the sample therefore came from the dissolution of a soluble sulfate phase already present in the paste, a similar observation extracted from the leachate geochemistry data.

Ferric sulfate-leached environment

Considerable differences in solid phase chemistry were observed between the first and second alteration layers of the sample exposed to the ferric sulfate solution. The outermost layer (layer 1) showed an enriched sulfate concentration but depleted concentrations of total sulfur and sulfide-sulfur, calcium, magnesium, zinc and lead compared to the underlying layer 2 and to core concentrations of the flooded sample. These results indicate that oxidation of sphalerite and dissolution of galena was probably occurring in this area. No information is available to verify the oxidation of the iron sulfides although leachate geochemistry data suggests that it is minimal. Layer 2 was depleted in sulfate and further depleted in calcium and magnesium compared to the layer 1 and the core of the flooded sample. Solid phase concentrations in the 3rd layer had almost all reverted to the values of the core sample in the flooded environment,

with the exception of calcium and magnesium which still remained slightly depleted.

A progressive depletion of cement occurred from the centre of the sample towards the edges. The greater loss of cement in the outer layer exposed to the ferric sulfate leach solution allowed sulfide mineral oxidation to take place.

5.5.2 Brunswick

Water-leached environments

Table 5.5 shows that, like the Tizapa water-leached samples, the outer layers of both water-leached Brunswick samples underwent a net loss of sulfate and calcium, with a more severe depletion occurring in the cycled environment. The dissolved calcium and sulfate likely originated from cement phases (portlandite and tobermorite) and pre-existing sulfate phases respectively, as described for the Tizapa samples. In addition, similar sulfide concentrations and sulfur to metals ratios in all water-leached layers suggest that no sulfide oxidation occurred in any water-leached sample.

Ferric sulfate-leached environment

Sulfate concentrations were significantly depleted only in the 2nd layer of the ferric sulfate-leached paste. Precipitation of a secondary sulfate phase from the leachate solution most likely replaced the lost sulfate due to dissolution of the solid phase, explaining the unchanged sulfate concentrations in the outermost layer of the paste. The depleted sulfate concentrations, unchanged sulfide concentrations and stable sulfur to metal ratios suggest that, like in the Tizapa case, no oxidation occurred in layers 2 and 3

of the ferric sulfate-leached paste. Sulfide mineral oxidation was also unlikely in layer 1 as indicated by the similar sulfide concentrations between layer 1 of the ferric sulfate environment and the core of the flooded paste. Also similar to Tizapa, calcium was progressively less depleted in underlying layers 2 and 3, reflecting the decreasing dissolution of portlandite (and de-calcification of tobermorite) with depth.

5.5.3 Louvicourt

Water leached environments

No alteration layers were evident upon observation of the water-leached samples (Table 5.6). An outer layer of 1 mm was, therefore, arbitrarily chosen and analysed for verification. The thin layers extracted did not provide enough sample to allow for complete elemental analyses. Sulfur species analyses showed depleted sulfate concentrations in the outer layers of both environments with respect to the core of the flooded sample, resulting from the dissolution of pre-existing sulfate phases. The absence of significant changes in sulfide concentrations and in total sulfur to sulfide ratios suggests that no oxidation of sulfide minerals occurred in these layers.

Ferric sulfate-leached environment

Two distinct layers of alteration were observed on this sample. However, only the second layer provided enough material to carry out elemental analyses. Similar to the Tizapa ferric sulfate-leached sample, layer 2 of the Louvicourt sample showed depleted concentrations of sulfate, calcium, magnesium, zinc, copper and lead. Some oxidation of

sphalerite along with dissolution of galena and possibly some soluble copper phases may have occurred in this layer. The similar sulfide concentration with respect to core values does not, however, support the occurrence of significant sulfide mineral oxidation.

5.5.4 Francisco I. Madero

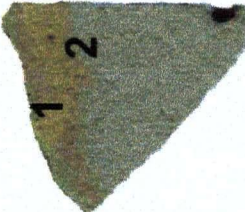
Water leached environments

Table 5.7 shows a net loss of sulfate in layer 1 of both water-leached environments, as well as a net gain in copper in layer 1 of the flooded sample. The elevated copper concentration suggests a mobilisation of copper from an internal area to the edges of the sample where it may have precipitated as a more stable phase. The migration of elements may have been facilitated by the greater porosity and lower binder proportion of the FIM backfill mixture compared to the others.

Ferric sulfate-leached environment

Layer 1 was characterized by depleted concentrations of sulfate, calcium and magnesium and a considerably enriched concentration of iron. As with the other ferric sulfate-leached samples, the depletion of sulfate and major ions may be explained by the dissolution of pre-existing sulfate phases and cement phases in that layer, namely portlandite and perhaps tobermorite. The enriched iron may be explained by a deeper penetration of surficial ferric hydroxide precipitates observed on all samples in this environment because of lower binder content of the FIM paste mixture.

Table 5.4 Tizapa - Description of Leached Paste Sections

		Flooded Environment		Cycled Environment		Fe ₂ (SO ₄) ₃ Environment (flooded)		
Paste								
X-section								
Scales								
Flooded: 1:2								
Cycled: 3:2								
Fe-sol.: 3:2								
Layers		1	Core (of cylinder)	1	2	1	2	3
Layer Thickness		0.75 mm	-	4 mm	2 mm	2 mm	4 mm	2 mm
Color		orange-gray	medium gray	orange	light gray	dark gray	dark orange	light gray
Texture		low porosity, mod. hard	low porosity, very hard	low porosity, mod. soft	low porosity, hard	mod. porosity, friable	mod. porosity, mod. soft	mod. porosity, mod. hard
% conc. difference from core	S _{total}	1	(36 ppm)	1	1	0.9	1	1
	S as SO ₄ ²⁻	0.4	(1.2 ppm)	0.3	0.2	1.2	0.2	1
	S as S ²⁻	1	(35 ppm)	1	1	0.8	1	1
	Ca	0.8	(3.5 ppm)	0.4	0.7	0.1	0.01	0.4
	Mg	1	(0.40 ppm)	1	1	0.6	0.5	0.8
	Al	1	(1.5 ppm)	1	1	1	1	1
	Zn	1	(1.5 ppm)	n.a.	1	1	1	1
	Cu	1	(0.14 ppm)	1	1	1	1	1
Pb	1	(0.31 ppm)	1	1	0.4	1	1	

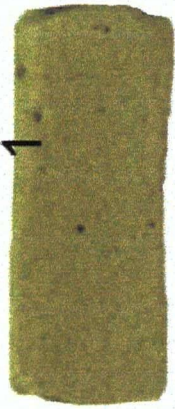
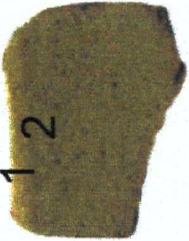
Note: Fe > 25% in all layers of the analysed samples; n.a. not available

Table 5.5 Brunswick - Description of Leached Paste Sections

		Flooded Environment			Cycled Environment			Fe ₂ (SO ₄) ₃ Environment (flooded)		
Paste X-section										
Scale (all): 1:1										
Layers		1	2	Core	1	2	1	2	3	
Layer Thickness		3 mm	~ 3 mm	-	~3 mm	~ 3 mm	1 mm	2 mm	7 mm	
Color		brown-gray	brown-gray	brown-gray	orange-gray	brown-orange	orange-brown	dark gray	brown fading to yellow-gray	
Texture		mod. low porosity, soft	high porosity	high porosity	low porosity, soft	high porosity	very low porosity, fractured	high porosity	high porosity	
% conc. difference from core	S _{total}	1	1	(29 ppm)	1	1	1	1	1	
	S as SO ₄ ²⁻	0.6	0.2	(1.6 ppm)	0.1	0.2	1	0.2	1	
	S as S ²⁻	1	1	(28 ppm)	1	1	1	1	1	
	Ca	0.8	0.8	(3.8 ppm)	0.6			0.2	0.8	
	Mg	1	1	(0.68 ppm)	1			1	1	
	Al	1	1	(1.1 ppm)	1			1	1	
	Zn	1	1	(0.89 ppm)	1			1	1	
	Cu	1	1	(0.08 ppm)	1			1	1	
Pb	1	1	(0.76 ppm)	1			1	1		

Note: Fe > 25% in all layers of the analysed samples.

Table 5.7 Francisco I. Madero - Description of Leached Paste Sections

	Flooded Environment		Cycled Environment	Fe ₂ (SO ₄) ₃ Environment (flooded)
Paste X-section				
Scale (all): 2:1				
Layers	1	Core (of cylinder)	1	1 2
Layer Thickness	1 mm	-	1 mm (arbitrary thickness)	0.8 mm
Color	yellow-gray	beige-gray	beige-gray	orange
Texture	moderate porosity, soft	moderate porosity, soft	moderate porosity, soft	moderate porosity, soft
% concentration difference from core	S _{total}	1	1	1
	S as SO ₄ ²⁻	0.2	0.2	1.9
	S as S ²⁻	1	1	1
	Ca	1	1	0.4
	Mg	1	1	0.8
	Al	1	1	1
	Fe	1	1	1.5
	Zn	1	1	1
	Cu	1.2	1	1
	Pb	1	1	1

5.5.5 Summary of Observations from the Solid Phase Chemistry

Water-leached pastes:

- No significant oxidation of sulfide minerals occurred in any layer of all water-leached samples. Sulfate contained in the paste was readily leached out of the backfill from a pre-existing sulfate phase present in the mixture. In all but the FIM samples, sulfate depletion was more severe in the cycled environment than the flooded environment.
- Calcium was readily leached out from the outermost layers of all samples analysed, in both water-leached environments. Depletion was more severe in the cycled environment for both Tizapa and Brunswick samples. No data were available for Louvicourt. The less depleted amount of calcium in the flooded paste may indicate the precipitation of a secondary calcium phase in the outer layer in that environment. Calcium was likely lost from the dissolution of the cement phases of portlandite ($\text{Ca}(\text{OH})_2$) and possibly from decalcification of tobermorite ($\text{Ca}_3\text{Si}_2\text{O}_5 \cdot 3\text{H}_2\text{O}$). The latter was also reported by Revertégat *et al*, (1992) and Carde and Francois (1997) in similar experiments.
- The maximum thickness of the alteration layers in both water-leached environments was larger for paste mixtures containing the highest percentage of pyrite and largest proportion of binder. Indeed, the maximum thickness of the alteration layer for Louvicourt and FIM pastes was 1 mm in 20 weeks, compared to 6 mm for Tizapa and Brunswick mixtures.

Ferric sulfate-leached pastes:

- Similar or increased sulfate levels on the edges of the samples suggest that one or both of the following were occurring in the samples: 1) penetration and precipitation of sulfate from the solution as the solution came in contact with the pore solution of the paste and/or 2) active oxidation of sulfide minerals (sphalerite and possibly some iron sulfides) producing sulfate and releasing metal ions. Both cases involve the advancement of a ferric sulfate solution front into the paste.
- Greater net losses of calcium and magnesium occurred in the ferric sulfate environment compared to the water-leached environments, indicating a more intensive dissolution of portlandite and perhaps tobermorite (through decalcification). Portlandite, a hydroxide mineral, is considerably more soluble in an acidic environment than in the a near-neutral water-leached environment, the hydroxyl ion being consumed to buffer the acidic solution.
- The alteration layers of samples leached in ferric sulfate solution penetrated deeper than in the water environments. In addition, similar to the water-leached environments, mixtures with higher pyrite and high binder content had deeper penetrating alteration: 8 mm and 10 mm in 20 weeks for Tizapa and Brunswick respectively, compared to 2.75 mm and 1.8 mm for Louvicourt and for FIM pastes.
- In general, as a result of the more intensive dissolution of the binder phases, the readily oxidized sulfide minerals such as sphalerite present in the outermost layers were most likely oxidized by the acidic (unbuffered) ferric sulfate solution. The

oxidation of sulfide minerals did not, however, occur in all samples in that environment. The net loss of lead in the altered layers of some samples indicated that galena was probably dissolved or oxidized from those areas.

5.6 BUFFERING CAPACITY AND ACID-BASE ACCOUNTING

Paste pH measurements and ABA results are presented in Tables 5.8 a to d.

Paste pH can give qualitative information on the immediate buffering capacity or acid production of soil or rocks. In this study, alkaline paste pH suggested the presence of a readily available source of neutralizing minerals and little or no acidity. The paste pH of unleached Louvicourt (8.4), Brunswick (10.3) and Tizapa (11.1) samples were high. These values corresponded to a binder content of 4.5% for Louvicourt (0.9% cement and 3.6 % slag) and to cement contents of 5% for Brunswick and 6.2% for Tizapa respectively. For comparison, the paste pH values of these tailings ranged from 5.0 to 5.8. FIM paste sample had a paste pH of 8.9, a smaller increase from the tailings pH of 7.3. These values reflect the smaller proportion of cement (3%) of the FIM paste mixture. Paste pH values corresponded well to the cement content of the paste mixtures.

5.6.1 Evolution of Acid Producing and Acid Neutralizing Potentials:

As a preliminary step to acid-base accounting (ABA), fizz ratings ranged from no fizz to moderate fizz for both the tailings and unleached paste mixtures of Tizapa, Brunswick and Louvicourt. FIM tailings and unleached paste produced a strong fizz. Ratios of neutralizing potential (NP) to acid production potential (AP) or NPR of all tailings,

unleached pastes and of each altered layer of the 20 week-leached pastes also figure in Tables 5.8 a to d.

All tailings possessed NPR values below 0.5. The addition of cement provided some neutralizing capacity to all the mixtures. However, NPR values all remained below 1, hence a strong potential for acid generation remained. In all cases, the proportion of cement was not sufficient to change the classification of the backfill to a potentially non acid-generating residue.

In all cases, as leaching progressed, AP values remained statistically similar (within the 5 % margin of analytical error) while NP was being depleted. NP depletion was attributed to the dissolution of portlandite, agreeing with the leachate and solid phase chemistry data. In addition, NP depletion was more severe in the cycle-leached environment than in the flooded environment. Resulting NPR values were lower for the outer layers of samples in the cycle-leached environments than in the flooded environments.

Ferric sulfate or artificial ARD solution leaching depleted NP values to a greater extent than water-environments. This agrees with the solid phase chemistry, indicating that the dissolution of portlandite was considerably more significant in the ferric sulfate environment. In fact, negative NP values in the outer layers of the ferric sulfate environment in all cases analysed indicated not only complete depletion of buffering minerals but also the initiation of acidic conditions in those layers of the samples.

Table 5.8a TIZAPA - Paste pH and Acid-Base Accounting Test Results

Sample	Paste pH	Fizz rating	HCl Normality (mol/L)	NaOH Normality (mol/L)	Sample weight (g)	HCl volume (ml)	NaOH volume (ml)	NP kg CaCO ₃ /ton	S _{tot} % SO ₄ % S ²⁻ %	AP kg CaCO ₃ /ton	NP/AP	NP/AP average
Tails	5.2	none	0.14	0.13	2.05	20	16.9	13	37.4 0.40 37.0	1156	0.01	0.01
			0.12	0.10	2.00	20	16.7	16				
Paste	11.1	moderate	0.14	0.13	2.06	40	21.8	62	35.1 0.39 34.8	1086	0.06	0.05
			0.14	0.13	2.02	40	22.5	61			0.06	
			0.12	0.10	2.00	40	26.3	55			0.05	
			0.12	0.10	2.00	40	27.0	53			0.05	
20 wk leach:												
Flooded												
Layer 1		strong	0.11	0.10	1.54	40	17.6	88	36.8 0.49 36.3	1135	0.08	0.08
			0.11	0.10	2.00	40	10.7	85			0.08	
Core												
Cycled												
Layer 1		slight	0.12	0.10	2.00	40	38.3	24	37.2 0.38 36.8	1150	0.02	
Layer 2		strong	0.09	0.10	2.00	60	33.4	56	36.4 0.30 36.1	1128	0.05	0.05
			0.09	0.10	2.00	60	35	52			0.05	
Fe ₂ (SO ₄) ₃												
Layer 1		none	0.09	0.10	2.00	15	21	-18	31.1 1.46 29.6	926	0	
Layer 2		none	0.09	0.10	2.00	20	19.9	-3	40.0 0.22 39.8	1244	0	0
			0.09	0.10	2.00	15	16.05	-5			0	
Layer 3		slight	0.09	0.10	2.00	40	35.8	3	36.3 1.23 35.1	1096	0.003	0
			0.09	0.10	2.00	40	36.2	2			0.003	
			0.09	0.10	2.00	40	36.8	1			0.003	
Core		mod-strong							35.8 1.28 34.5	1079		

Table 5.8b BRUNSWICK - Paste pH and Acid-Base Accounting Test Results

Sample	Paste pH	Fizz rating	HCl Normality (mol/L)	NaOH Sample weight (g)	HCl volume (ml)	NaOH volume (ml)	NP kg CaCO ₃ / ton	S _{tot} % SO ₄ % S ²⁻ %	AP kg CaCO ₃ / ton	NP/AP	NP/AP average		
Tails	5.9	moderate	0.70	0.66	2.01	30	24.6	34.3	3.32	31.0	968	0.12	0.21
			0.70	0.66	2.03	30	24.6					0.30	
Paste	10.4	moderate	0.70	0.66	2.05	30	26.1	32.6	3.16	29.5	921	0.10	0.10
20 wk leach:													
Flooded													
Layer 1		moderate	0.12	0.10	2.00	40	22.4	30.2	0.85	29.3	916	0.07	
Layer 2		moderate	0.09	0.10	2.00	80	49.6	29.6	0.28	29.1	909	0.07	0.07
			0.09	0.10	2.00	75	44.7					0.07	
Core			0.09	0.10	2.00	75	44.3	30.5	1.52	28.4	887		0.07
Cycled													
Layer 1		moderate	0.12	0.10	2.00	40	29.0	29.3	0.16	29.0	906	0.05	0.05
			0.09	0.10	2.00	40	20.0					0.05	
Layer 2		moderate	0.09	0.10	0.48	15	7.3	29.0	0.34	28.6	894	0.08	
Fe ₂ (SO ₄) ₃													
Layer 1		none	0.09	0.10	2.00	15	18.2	27.3	1.34	25.7	803	0	0
			0.09	0.10	1.92	12	14.9					0	
Layer 2		none	0.09	0.10	2.00	20	16.1	30.6	0.31	30.0	938	0.01	0.01
			0.09	0.10	2.00	25	20.2					0.01	
Layer 3		moderate	0.09	0.10	2.00	40	21.7	29.1	1.37	27.8	869	0.04	0.04
			0.09	0.10	2.00	50	31.5					0.04	
			0.09	0.10	2.00	50	32.7					0.04	

Table 5.8c LOUVICOURT - Paste pH and Acid-Base Accounting Test Results

Sample	Paste pH	Fizz rating	HCl Normality (mol/L)	NaOH Sample weight (g)	HCl volume (ml)	NaOH volume (ml)	NP kg CaCO ₃ ton	S _{tot} % SO ₄ % S ²⁻ %	AP kg CaCO ₃ ton	NP/AP	NP/AP average
Tails	5.0	none	0.14	2.01	30	17.2	45	9.19 1.00 8.9	278.1	0.16	0.15
			0.12	2.00	20	8.6	38			0.14	
Paste	8.4	slight	0.14	2.00	60	37.0	83	8.83 0.96 8.5	265.9	0.31	0.27
			0.14	2.06	40	18.6	73			0.27	
			0.12	2.00	40	23.0	63			0.24	
20 wk leach:											
Flooded											
Layer 1		slight	0.12	2.00	40	23.5	60	9.23 0.56 8.7	271	0.22	0.22
Cycled											
Layer 1		none	0.12	2.00	40	29.5	45	8.89 0.30 8.6	268	0.17	0.17
Fe ₂ (SO ₄) ₃											
Layer 1		none	0.09	1.36	10	13	-14	insufficient sample			
Layer 2		none	0.09	1.96	15	14.4	-2	9.79 0.23 9.6	299	-0.01	-0.01
Layer 3			0.09	1.55	10	9.3	-1	insufficient sample			

Table 5.8d FRANCISCO I. MADERO - Paste pH and Acid-Base Accounting Test Results

Sample	Paste pH	Fizz rating	HCl Normality (mol/L)	NaOH Sample weight (g)	HCl volume (ml)	NaOH volume (ml)	NP kg CaCO ₃ (ton)	S _{tot} % SO ₄ % S ²⁻ %	AP kg CaCO ₃ (ton)	NP/AP	NP/AP average
Tails	7.3	strong	0.12	2.00	80	42.5	134	10.5 0.20 10.3	322	0.42	0.41
			0.12	2.00	80	43.5	131				
Paste	8.9	strong	0.12	2.00	80	36.5	149	10.2 0.20 10.0	313	0.47	0.47
			0.12	2.00	80	37	147				
20 wk leach:											
Flooded Layer 1		strong	0.11	2.00	80	33.1	141	8.2 0.06 8.1	254	0.55	0.55
Cycled Layer 1		strong	0.11	2.00	80	36.0	134	8.2 0.07 8.1	253	0.53	0.53
			0.09	2.00	80	21.5	132			0.52	0.52
			0.09	2.00	90	31.0	132			0.52	0.52
Fe ₂ (SO ₄) ₃ Layer 1		none		insufficient sample			-	8.7 0.58 8.1	253	-	-
Core		strong						8.3 0.31 8.0	250	-	-

5.7 SCANNING ELECTRON MICROSCOPE (SEM) OBSERVATIONS

The sections shown in Tables 5.4 to 5.7 discussed earlier, were observed under SEM to identify the mineralogical changes that occurred as leaching progressed. The layer identification system and thicknesses described in these tables was used to guide the SEM observations. Energy dispersive x-ray analyses (EDX) were carried out on many different mineral surfaces. The fragility of the surfaces did not allow the sections to be polished flat since they would easily crumble. All EDX analyses reported in this section are therefore qualitative and used in conjunction with SEM micrographs to identify the general composition of mineral phases. Plates 5.1 to 5.8 show the typical morphology and qualitative composition (EDX scans) of tobermorite, portlandite, gypsum and ettringite encountered in this study.

5.7.1 Tizapa

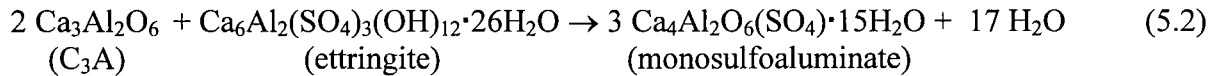
The Tizapa paste contained the largest proportion of cement (6.2%) making possible the observation of many distinct phases of hydrated cement. Tizapa samples displayed the greatest differences in cement mineralogy between the altered layers.

i) Flooded Water Environment

Layer 1: 0 – 0.8 mm

An extensive layer of densely packed euhedral portlandite crystals covered the surface of the sample (Plate 5.9). Portlandite was also abundant down to a depth of 0.8 to 1 mm,

exhausted (in the first hours of hydration) and the ettringite proceeds to react with the excess C₃A to produce monosulfoaluminate (Ca₄Al₂O₆(SO₄)·15H₂O; a wavy, leaf-like morphology - not observed in this sample) according to:



Monosulfoaluminate forms away from the C₃A surface, leaving the mineral surface free to continue to hydrate, consuming excess portlandite and providing some additional strength to the mixture (see reaction (3) in Table 1.1, Chapter 1). In this case, however, sulfate continues to be present in the pore water in equilibrium with the primary ettringite, preventing further hydration of C₃A and consumption of portlandite. Both factors impede the normal development of strength.

ii) Cycled Water Environment

Layer 1: 0 – 4 mm

The outer layer of the cycle-leached sample was characterized by poorly developed tobermorite gel in the exterior portion of the layer (Plate 5.15), only partially covering tailings grains. Ettringite needles and abundant gypsum were also visible in the upper portion of this layer (Plate 5.16 and 5.17). In the deeper portion (>2mm), the cement phases were well developed and distributed. Plate 5.18 suggests that the cement phase was not very strong as many tailings grains were removed during the sample preparation process, leaving empty grain-shaped cavities.

Core: > 4 mm

As with the flooded core, this area of the cycle-leached paste was characterised by abundant ettringite covering phases of tobermorite and unhydrated C₃A (Plate 5.19). Tobermorite cover was generally extensive and well developed (Plate 5.20).

iii) Ferric Sulfate Environment

Layer 1: 0 - 2 mm

This layer of the ferric sulfate-leached sample was generally porous with sparse hydrated cement phases (Plate 5.21). Most pyrite grains (as well as other tailings grains) showed only traces of cement cover (Plate 5.22). Some isolated areas did have well-developed tobermorite (Plate 5.23). Oölitic masses of iron sulfate were exclusive to this layer (Plates 5.24 and 5.25). This phase could either have been precipitated directly from the ferric sulfate solution in contact with the pore water of the sample or could have precipitated following sulfide mineral oxidation in that area.

Layer 2: 2 – 6 mm

The hydrated cement cover was more uniform and better developed in this layer, offering better protective cover to all grains such as pyrite (Plate 5.26). Under SEM, the presence of amorphous hydrated cement cover masked the presence of amorphous iron phases such as hydrated iron oxide or iron oxyhydroxide. The rust colour of this layer suggests, however, the presence of these phases.

Layer 3: 6 – 8 mm

This was an apparent transition zone between layer 2 and the core of the sample, where the mineralogy was similar to that of the core of the flooded sample.

5.7.2 Brunswick

i) Flooded Water-Leached Environment

Layer 1: 0 – 3 mm

Similar to the Tizapa sample, portlandite was also present in abundance in this layer, along with fairly well developed tobermorite covering the tailings grains (Plates 5.27 and 5.28). The cement appeared to be less resistant than in deeper layers as empty grain cavities were observed (Plate 5.29). The cavities were, however, less numerous than in the ferric sulfate-leached sample.

Layer 2: 3 – 6 mm

This layer possessed well-developed and abundant tobermorite covering the tailings particles (Plate 5.30). No portlandite was visible. An acicular phase, most likely ettringite, was also observed from this depth down to the core of the sample.

ii) Cycled Water-Leached Environment

Layer 1: 0 – 3 mm

Tobermorite appeared to be well developed, covering the tailings grains fairly well (Plate 5.31). The paste was porous but did not show any empty grain cavities (Plate 5.32). No gypsum or acicular ettringite were observed at any depth in this sample.

Layer 2: 3 – 6 mm

No obvious mineralogical differences were observed under SEM between this layer and Layer 1.

iii) Ferric Sulfate-Leached Environment

Layer 1: 0 – 1 mm

Macroscopically, this layer showed an outer rim of iron oxyhydroxide precipitated from the leaching solution (refer to Figure 5.36). Under SEM, a 0.5 mm crust was visible with vertical fractures extending 1.5 to 2 mm down (Plate 5.34). Many grain cavities were visible suggesting that the strength of the hydrated cement was relatively poor (Plates 5.34 and 5.35). Acicular minerals were also present in this area but were too small to obtain a reliable EDX identification (Plate 5.36). The morphology of the phase suggested ettringite.

Layer 2: 1 – 3 mm

The hydrated cement phases appeared to be more resistant at this depth, showing a smoother sample surface with less grain cavities (Plate 5.37). Masses of oölitic iron sulfate phases were abundant in this layer, possibly a type of jarosite (Plate 5.38). Similar to the Tizapa sample, this iron sulfate phase either was precipitated directly from the ferric sulfate solution in contact with the pore water of the paste or was a product of sulfide mineral oxidation in the area. Euhedral gypsum crystals were encountered inside sample pores (Plate 5.39). No ettringite needles were identified in this layer.

Layer 3: 3 – 10 mm

Macroscopically, a gradient in colour was visible from 3mm to 10 mm and a very pale line marked the 10mm depth. This fine layer was not noticeable under SEM and layer 3 appeared as a transition zone between layer 2 and the core of the sample. In the upper and middle portion of layer 3, cement binder strength appeared to be greater (Plate 5.40), the topographic lows were related to the porosity of the paste rather than to empty grain cavities. Tailings grains were also better covered by cement (Plate 5.41). No ettringite needles or gypsum was positively identified in this layer.

5.7.3 Louvicourt

The high slag proportion of the Louvicourt paste gave the binder a different aspect from the OPC binder used in the other mixtures. The hydrated slag was identified by its morphology and occurrence, appearing as both masses of subangular crystals (Plate 5.42)

and delicate, semi-dendritic crystals covering the tailings grains (Plate 5.43). Both morphologies are typical of well-hydrated slag (Taylor, 1997). The composition of the tobermorite developed from slag is slightly different from that from Portland cement, generally having a lower concentration of Ca but higher Al and Mg. Plate 5.44 presents a typical EDX spectrograph of slag tobermorite (from the flooded paste). Plate 5.45 shows the general aspect of the paste.

i) Flooded Water-Leached Environment

Layer 1: 0 – 1 mm

Contrary to Brunswick and Tizapa pastes, no portlandite was observed in any area of the flooded paste sample. Tobermorite was well developed, covering the tailings grain to a greater extent the previous two samples in the same area. The tobermorite content was slightly lower in some areas of the outer layer (Plate 5.46) compared to deeper areas where tobermorite was more abundant and evenly distributed (Plate 5.47). No ettringite, monosulfoaluminate or gypsum was identified in any area of the flooded paste.

ii) Cycled Water-Leached Environment

Layer 1: 0 – 1 mm

A greater depletion of tobermorite was observed down to 500 μ m from the surface (Plate 5.48) compared to the flooded environment. Binder cover of tailings grains in this area was still greater than Tizapa and Brunswick at that depth (Plate 5.49). Below 500 μ m, tobermorite abundance and distribution was similar to that of the flooded paste (Plate

5.50).

Secondary gypsum growth occurred in the deeper portion of the paste (Plate 5.51) which could have been a source of internal stress within the sample. No gypsum was found closer to the surface. No portlandite, ettringite or monosulfo-aluminate was identified in any area of the cycled sample.

A vertical fracture traversing the height of puck was observed under SEM (not visible to the naked eye) (Plate 5.52). Dendritic and platy crystal forms of Tobermorite were observed lining the fracture walls (Plate 5.53) indicating that the fracture was formed during leaching rather than during later-stage sample preparation. Secondary fracturing reveals the occurrence of internal stress after only 20 weeks of leaching in water.

iii) Ferric Sulfate-Leached Environment

Layer 1: 0 – 0.75 mm

Tobermorite in the outermost layer was most depleted in the ferric sulfate environment (Plate 5.54), however, not so much as in samples containing OPC binder in a similar environment. Its morphology was slightly altered compared to deeper areas, the masses were more rounded and amorphous (Plate 5.55), possibly resulting from an altered chemistry due to leaching of some elements, as described by Taylor (1997). Tobermorite content and increased again at 1 mm (Plate 5.56), regaining its more typical morphology.

A partly separated crust was present on the surface of the puck, visible under SEM (Plate 5.57). No obvious secondary minerals were observed on the walls of the fracture

suggesting that fracturing may have occurred during sample preparation. The constant thickness of the fracture indicates, however, that it developed along an existing plane of weakness.

Layer 2: 1 – 3 mm

Like in Tizapa and Brunswick, some iron sulfate precipitates were observed in this layer. The morphology of these precipitates differed from the other samples. They occurred as larger botryoidal masses (20 μm – Plate 5.58) rather than the loosely bound oölitic masses occurring in Brunswick and Tizapa. EDX analysis suggests that these precipitates may be a form of jarosite (Plate 5.59) or some other hydrated iron sulfate phase. No portlandite, gypsum or monosulfoaluminate phases were identified in this sample at any depth. Long, rectangular-shaped crystals (Plate 5.60) were analysed but the EDX spectrogram was not sufficiently precise to provide a definite identification. The morphology was similar to that of ettringite. Tobermorite gel was well developed (Plate 5.61) although slightly less abundant than deeper towards the core of the sample.

Below 3mm depth, tobermorite was abundant, well developed and well distributed, similar to that encountered in the core of the flooded sample. No gypsum or monosulfoaluminate were observed although the rectangular ettringite-shaped crystals were still present.

5.7.4 Francisco I. Madero

FIM samples contained the lowest proportion of cement (3%) of all paste mixtures.

Macroscopically, neither the flooded nor the cycled water-leached environments displayed visible alteration layers after 20 weeks of leaching. SEM observations revealed few differences between superficial layers and the cores of the samples.

i) Flooded Water-Leached Environment

Layer 1: 0 – 1 mm

The outer layer of the flooded paste showed a good distribution of well-developed tobermorite (Plate 5.62), similar to Brunswick tobermorite distribution although FIM contains 60% of the cement content. No portlandite or ettringite were identified in this layer or deeper.

Core: > 1 mm

A gradual decline in tobermorite content and degree of development was visible between ~750 μm and 1mm, below which the tobermorite appeared as fibrous and scattered, incompletely covering the tailings grains (Plate 5.63). This morphology is suggested in the literature to be typical of decalcified tobermorite (Taylor, 1997). These phases were, unfortunately, too scattered and thin to provide reliable EDX analyses to measure the calcium to silicon ratio.

ii) Cycled Water-Leached Environment

Layer 1: 0 – 1 mm

Tobermorite was moderately well developed but less abundant than in the flooded

sample. The cement phases in the outer layer appeared as masses of small individual crystals ($<1\mu\text{m}$ size) gathered in bunches rather than intergrown (Plate 5.64). This morphology was encountered throughout the cycled sample and was distinct from the morphology encountered in any other mixture, where it appeared as amorphous masses. These cement phases could not be accurately identified, as the crystals were too small and not sufficiently abundant to obtain reliable EDX analyses. No secondary minerals such as portlandite, ettringite or gypsum were observed at any depth in this sample.

iii) Ferric Sulfate-Leached Environment

Layer 1: 0 – 1 mm

Plates 5.65 and 5.66 show the porous but homogeneous aspect of the outer edge of the sample. The small proportion of cement in the mixture appeared evenly distributed, showing better tailings grain cover than Tizapa in a similar environment (Plate 5.67). Wavy, leaf-like minerals, most likely monosulfoaluminate, were discernible deeper, at 1.8 mm (Plates 5.68). Acicular ettringite could not be positively identified in this area or anywhere in the sample. The presence of monosulfoaluminate over ettringite suggests that relatively low concentrations of aqueous Ca^{2+} and SO_4^{2-} ions were present in the pore solution in the area – see reaction (5.2). This may be a consequence of the low sulfate levels present in the FIM tailings, the lowest of all the samples. Cement cover of tailings (pyrite) grains appeared to be slightly improved at 4 mm depth compared to the surface (Plate 5.69).

Identification of Hydrated Cement Minerals

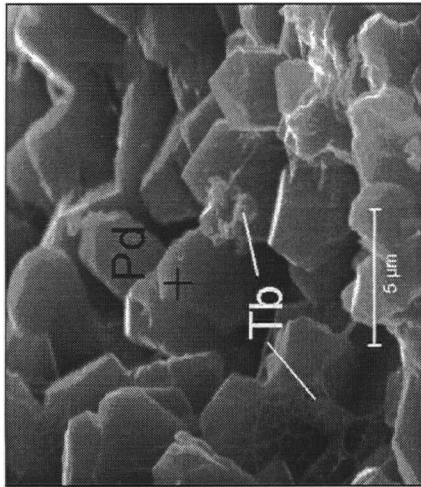


Plate 5.1 Portlandite (Pd) crystals

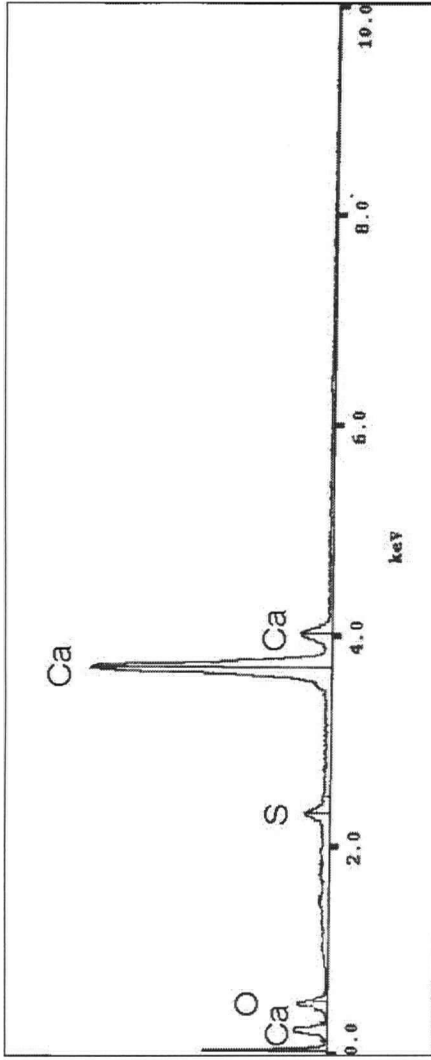


Plate 5.2 Typical EDX of portlandite

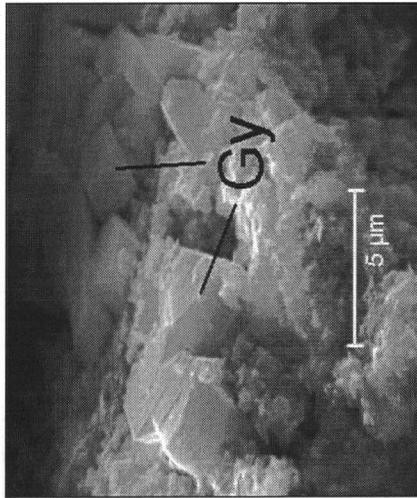


Plate 5.3 Secondary gypsum (Gy) crystals

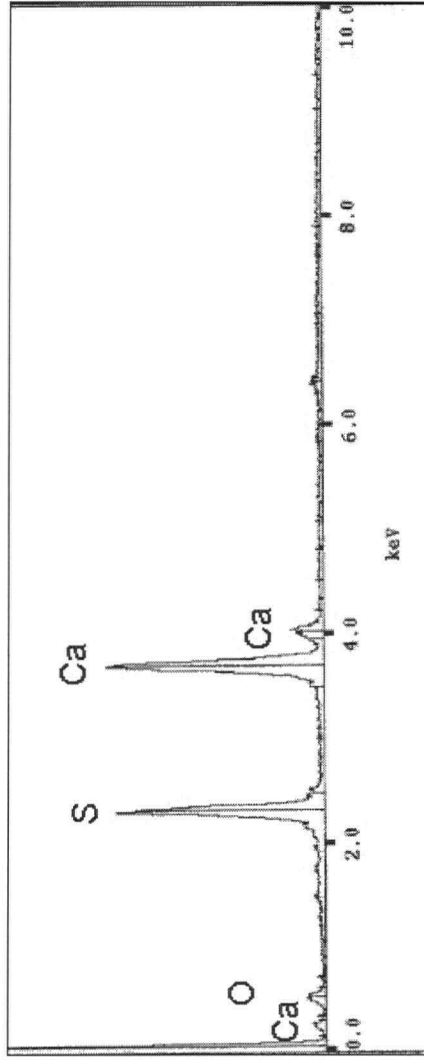


Plate 5.4 Typical EDX of gypsum

Identification of Hydrated Cement Minerals

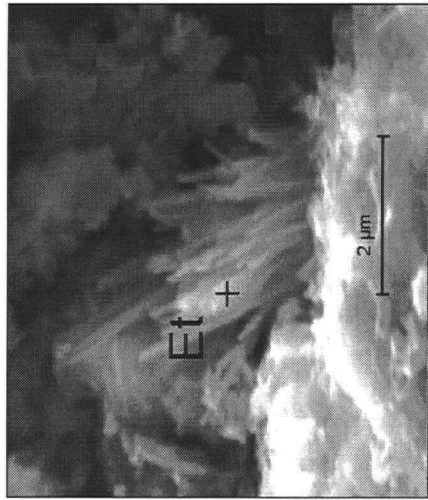


Plate 5.5 Acicular ettringite (Et)

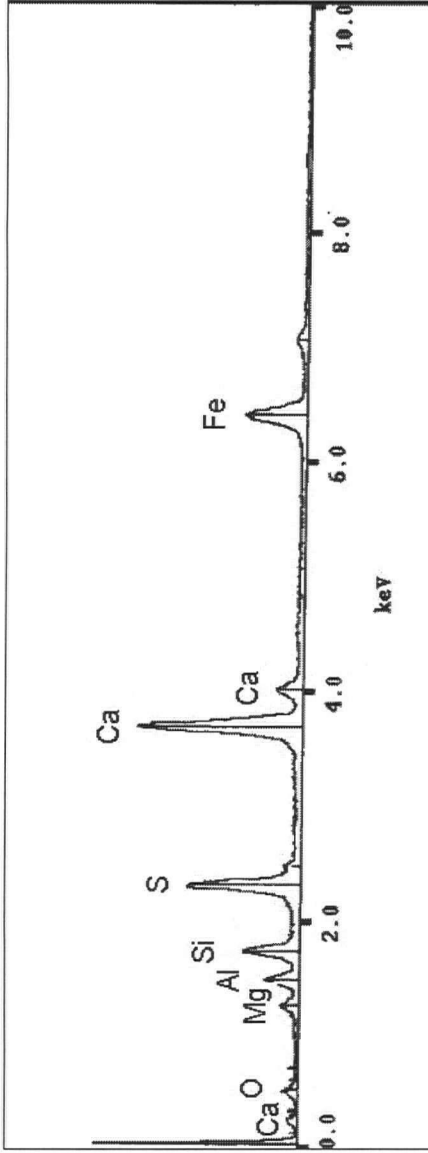


Plate 5.6 Typical EDX of ettringite

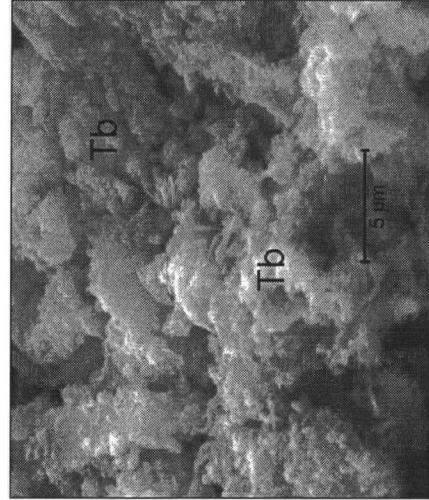


Plate 5.7 Amorphous tobermorite

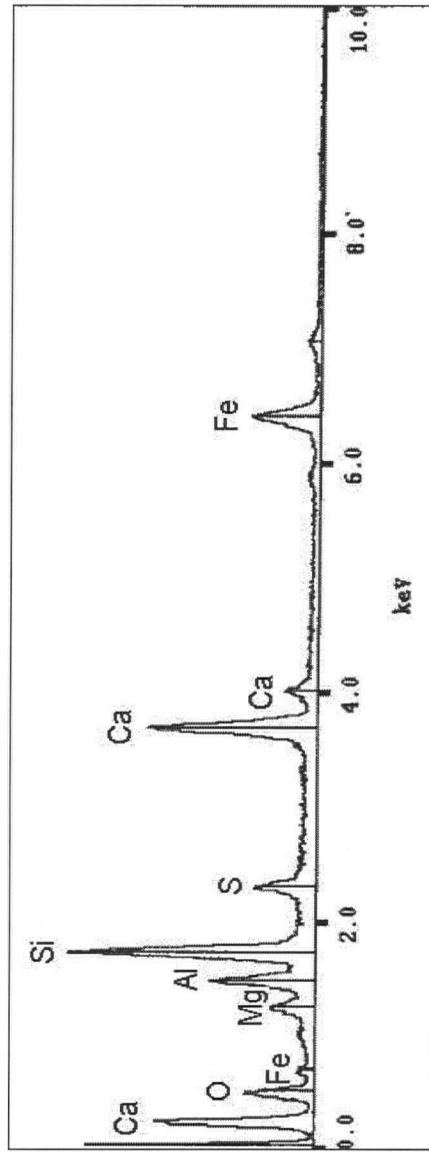


Plate 5.8 Typical EDX of amorphous tobermorite (C-H-S gel)

Tizapa – Flooded-Leached Paste Samples

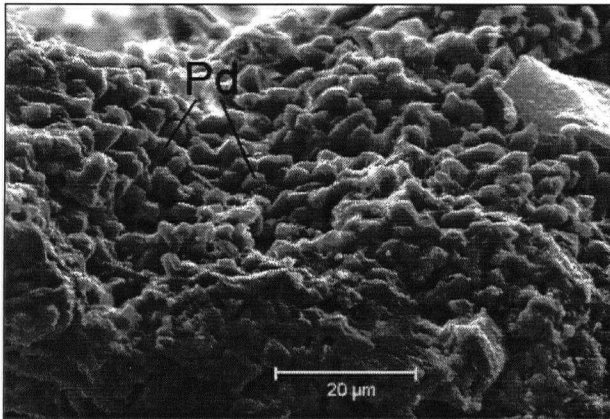


Plate 5.9 Portlandite cover on sample surface

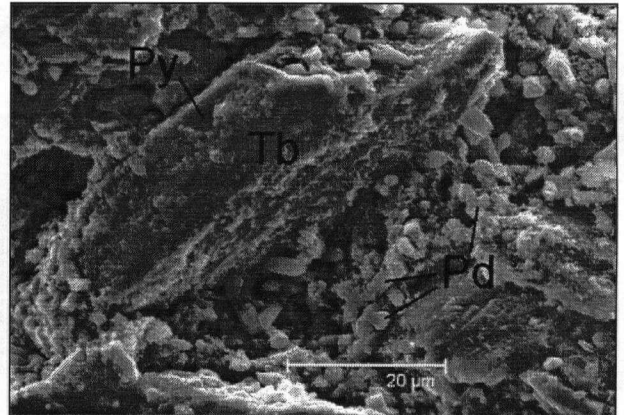


Plate 5.10 Bottom of layer 1

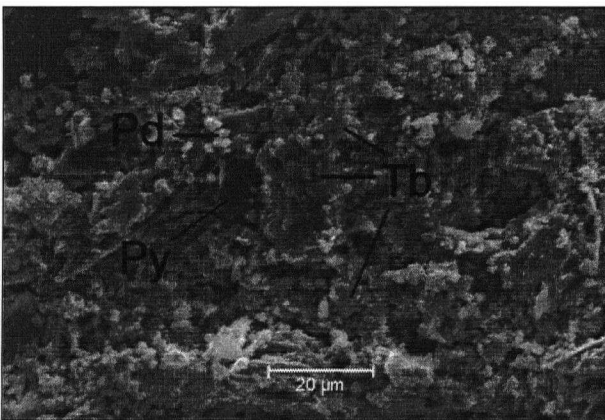


Plate 5.11 Bottom of layer 1

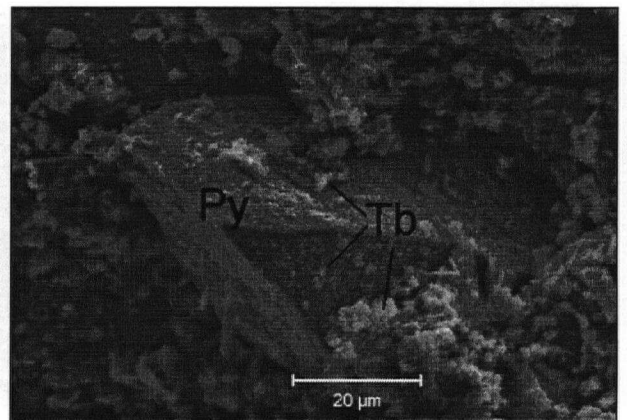


Plate 5.12 Poorly developed Tb, below layer 1

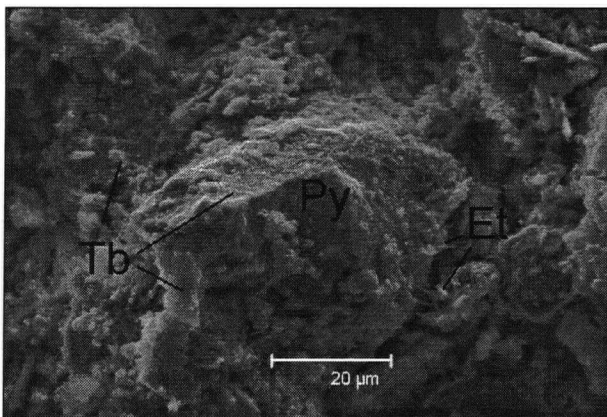


Plate 5.13 Core of sample

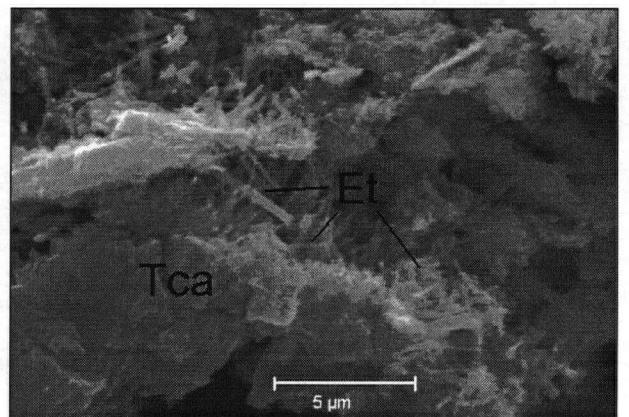


Plate 5.14 Primary ettringite on incompletely hydrated cement grain (Tca), core of sample

Pd = portlandite; Tb = tobermorite gel (amorphous); Py = pyrite; + = area of EDX analysis

Tizapa – Cycle-leach Paste Samples

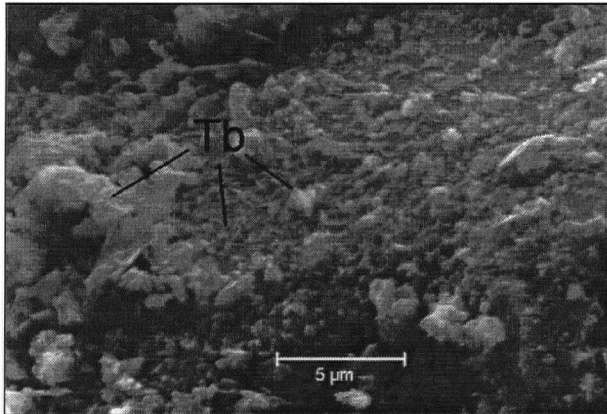


Plate 5.15 Poorly developed Tb, layer 1

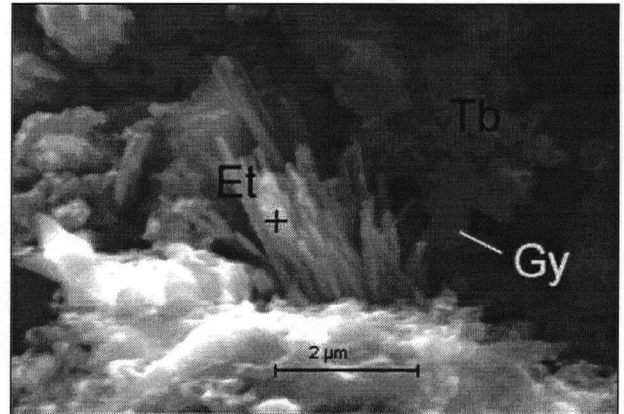


Plate 5.16 Ettringite, upper layer 1

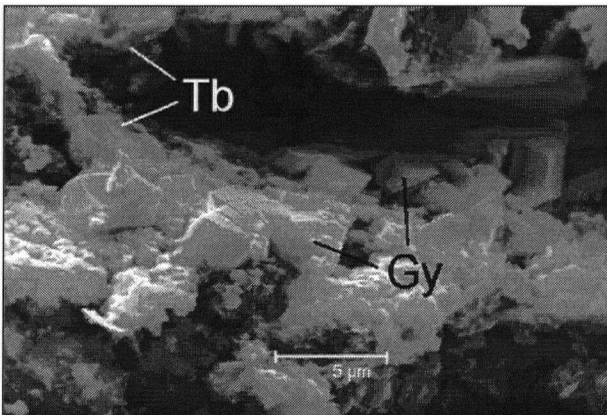


Plate 5.17 Secondary gypsum, upper layer 1

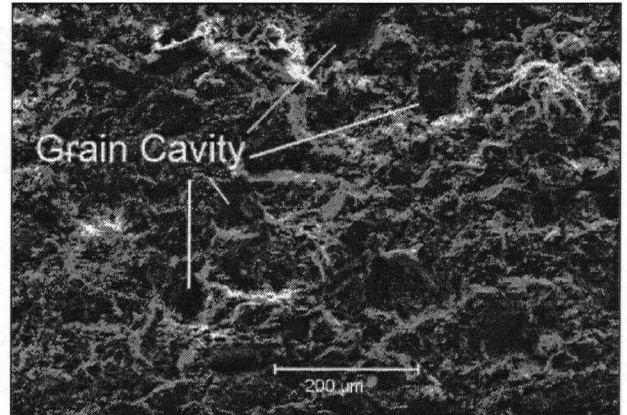


Plate 5.18 General paste aspect, layer 1

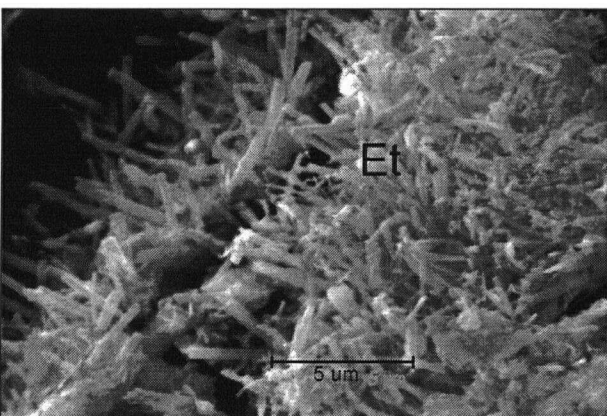


Plate 5.19 Ettringite in core of sample

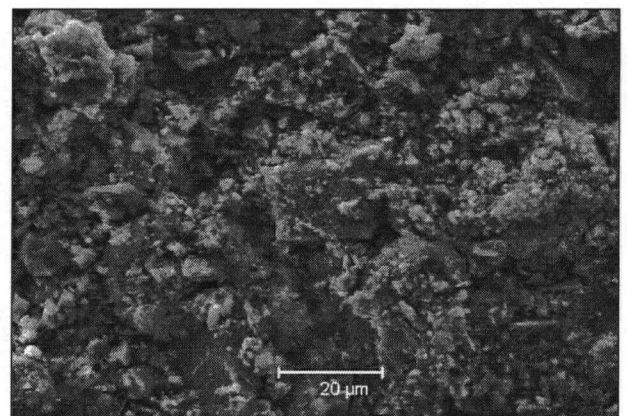


Plate 5.20 Good tobermorite development at core of sample

Et = ettringite; Tca = tricalcium aluminate (unhydrated cement grain); Gy = gypsum

Tizapa – $\text{Fe}_2(\text{SO}_4)_3$ Solution-leached Paste Samples

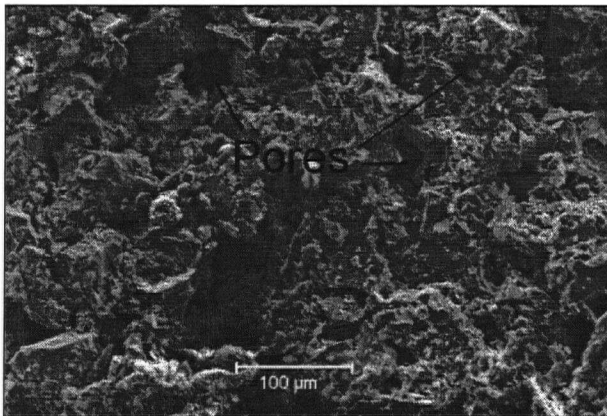


Plate 5.21 Porous layer 1

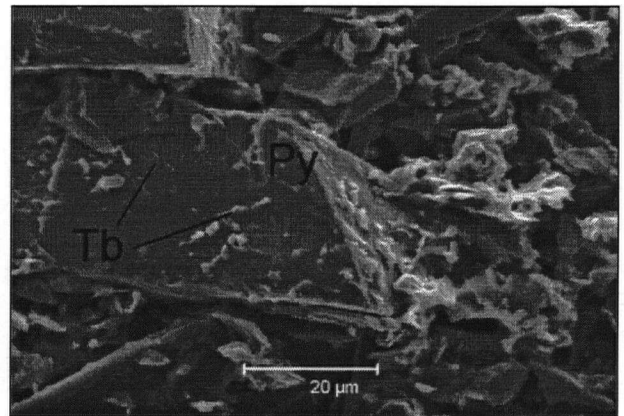


Plate 5.22 Depleted tobermorite, layer 1

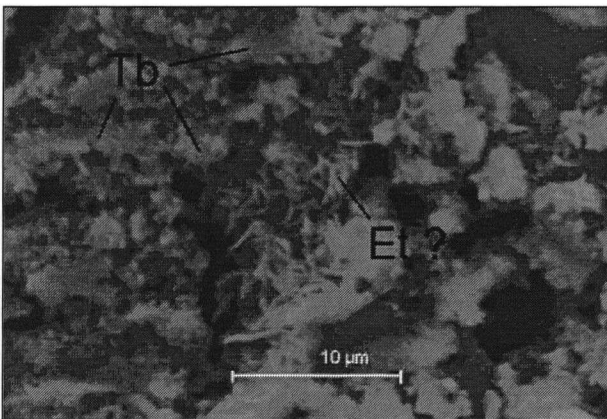


Plate 5.23 Area of good tobermorite, layer 1

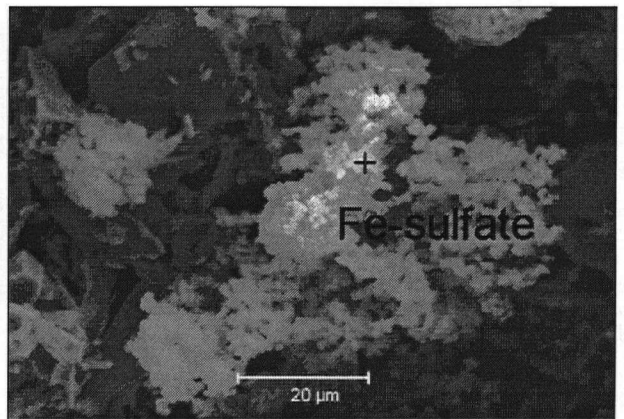


Plate 5.24 Layer 1, iron sulfate precipitate

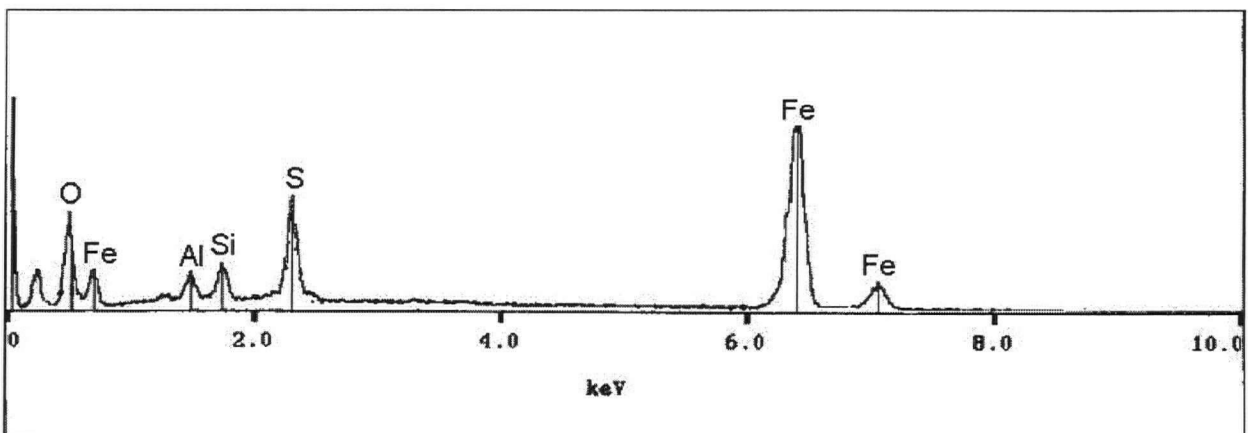


Plate 5.25 EDX of iron sulfate precipitate

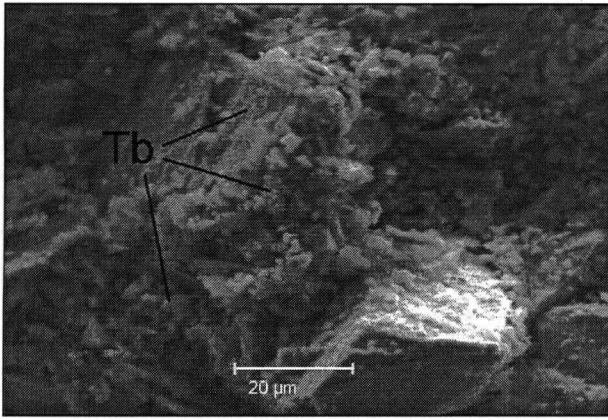


Plate 5.26 Good tobermorite cover, layer 2

Brunswick – Flooded-leach Paste Samples

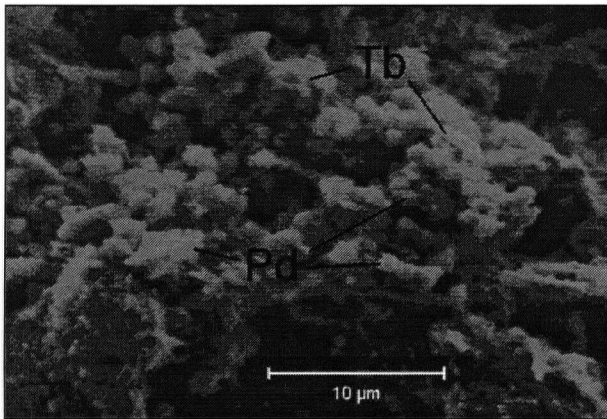


Plate 5.27 Layer 1

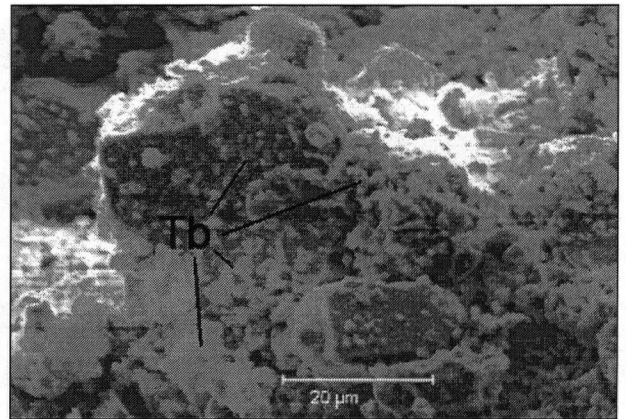


Plate 5.28 Layer 1

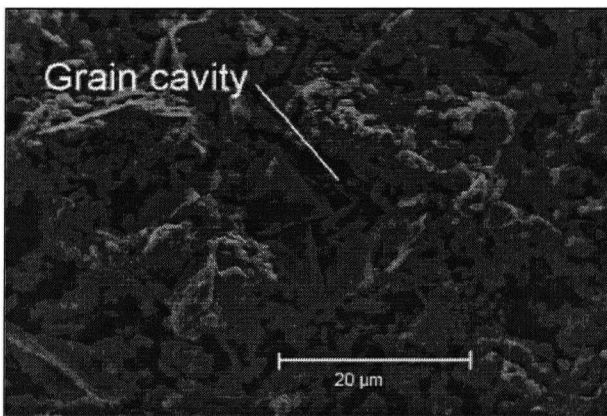


Plate 5.29 Less resistant tobermorite, layer 1

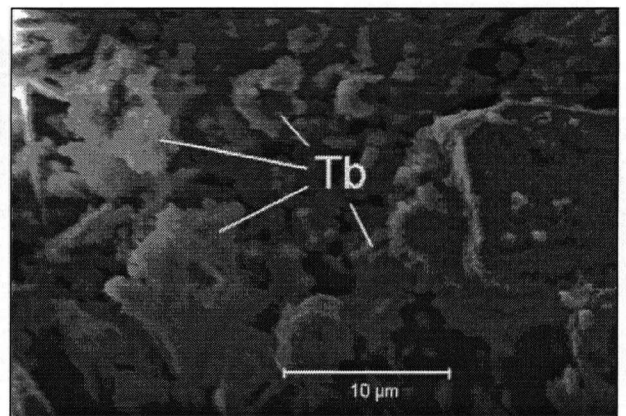


Plate 5.30 Abundant tobermorite, layer 2

Brunswick – Cycle-leach Paste Samples

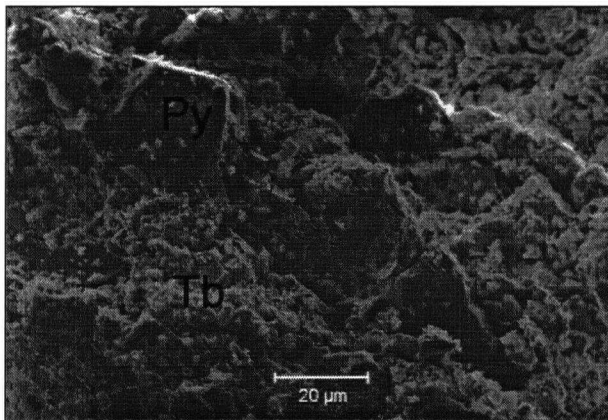


Plate 5.31 Good tobermorite cover, layer 1

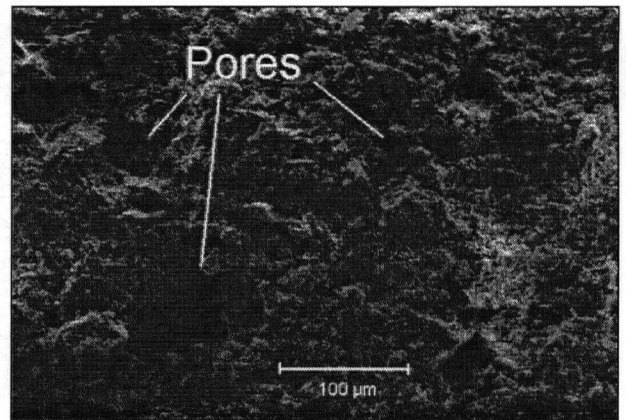


Plate 5.32 General aspect of paste, layer 1

Brunswick – $\text{Fe}_2(\text{SO}_4)_3$ Solution-leach Paste Samples

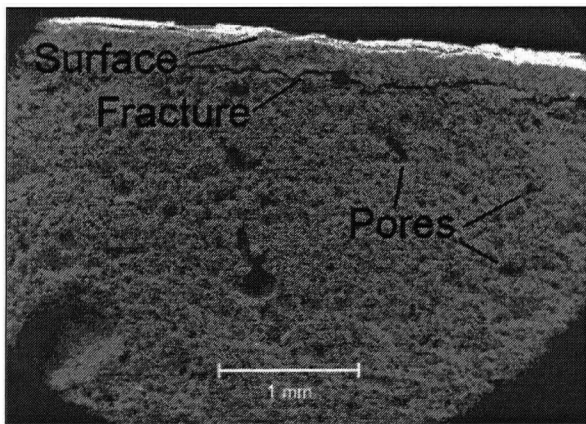


Plate 5.33 Paste surface

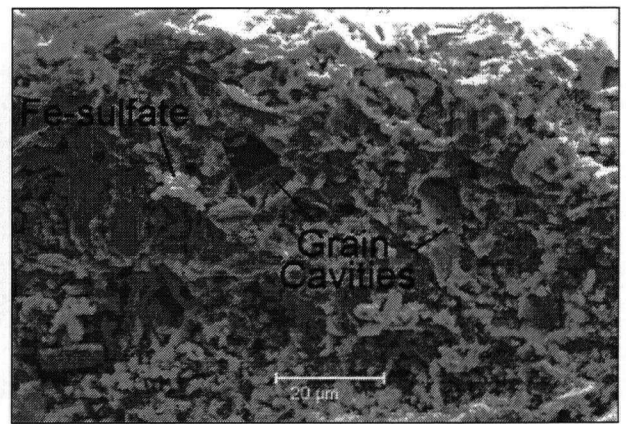


Plate 5.34 General aspect of paste, layer 1

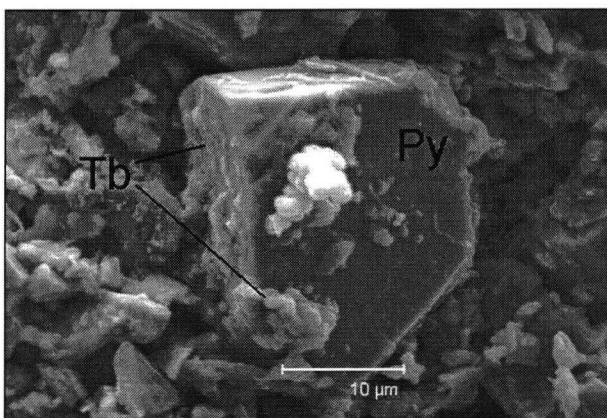


Plate 5.35 Poor tobermorite cover, layer 1

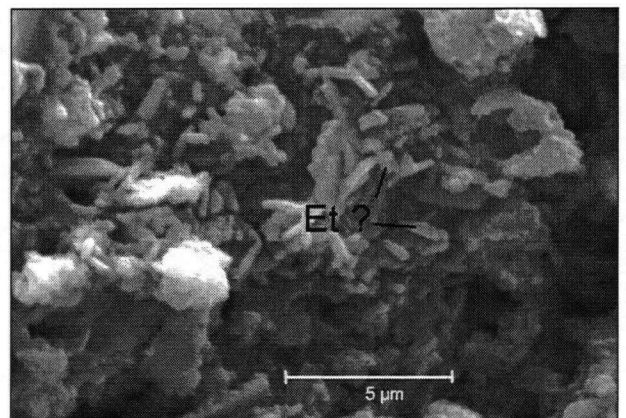


Plate 5.36 Possible 2^{ry} ettringite, layer 1

Brunswick – $\text{Fe}_2(\text{SO}_4)_3$ Solution-leached Paste Samples

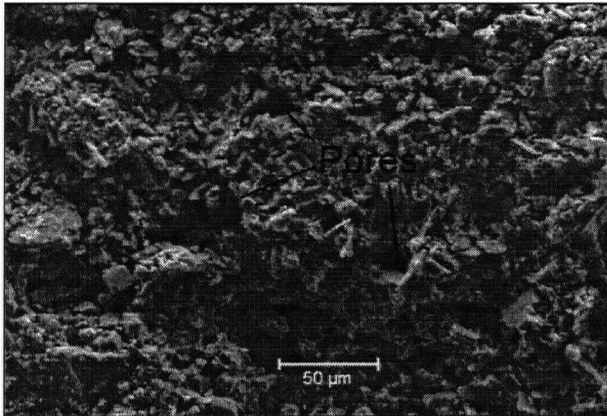


Plate 5.37 General aspect of paste, layer 2

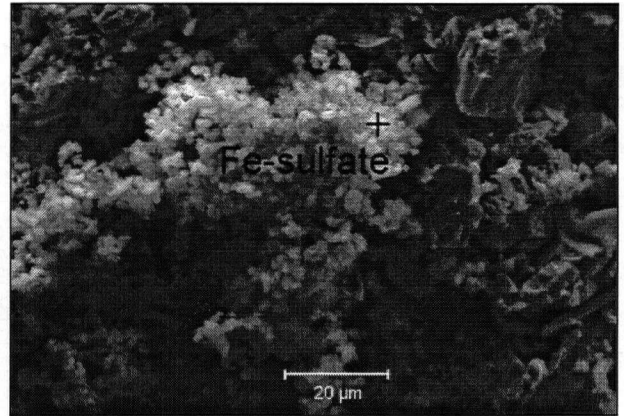


Plate 5.38 Fe-sulfate precipitate, layer 2

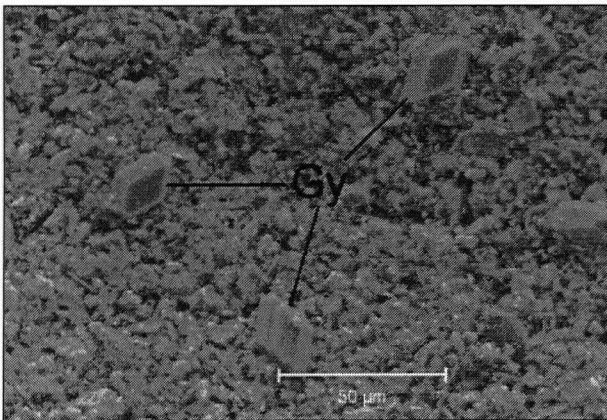


Plate 5.39 Inside large pore, layer 2

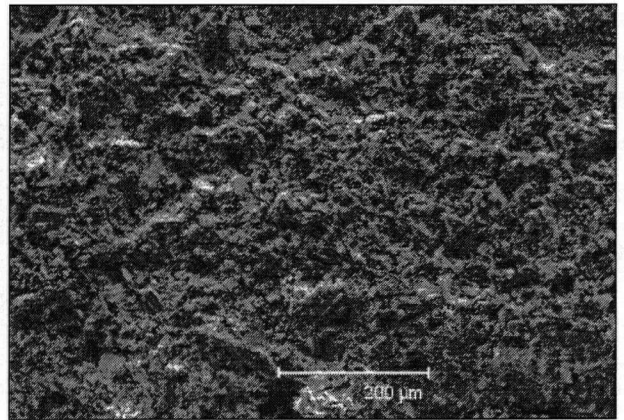


Plate 5.40 General aspect of paste, layer 3

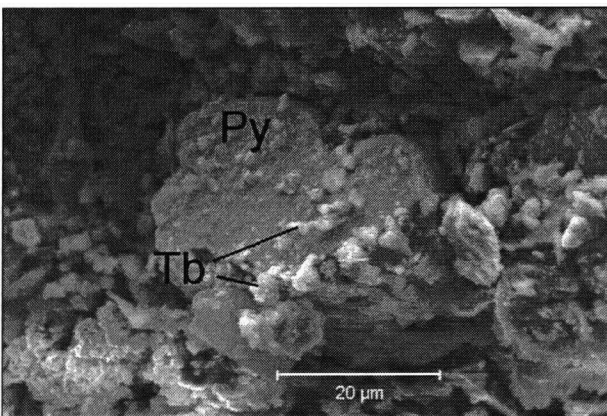


Plate 5.41 Layer 3

Louvicourt – Aspects of Hydrated Slag-OPC binder

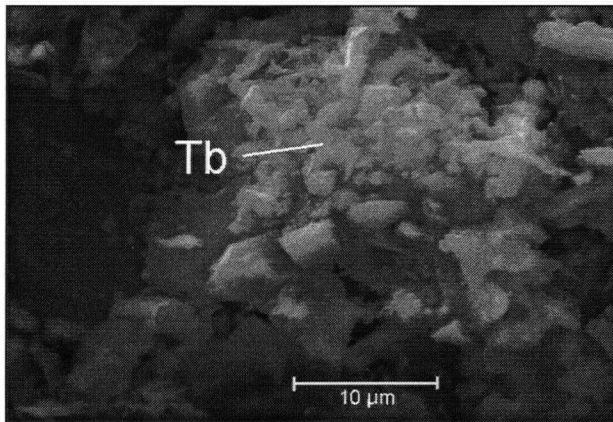


Plate 5.42 Massive tobermorite

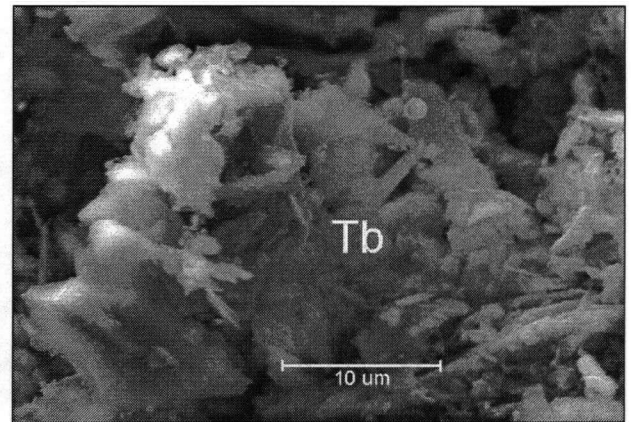


Plate 5.43 Dendritic tobermorite

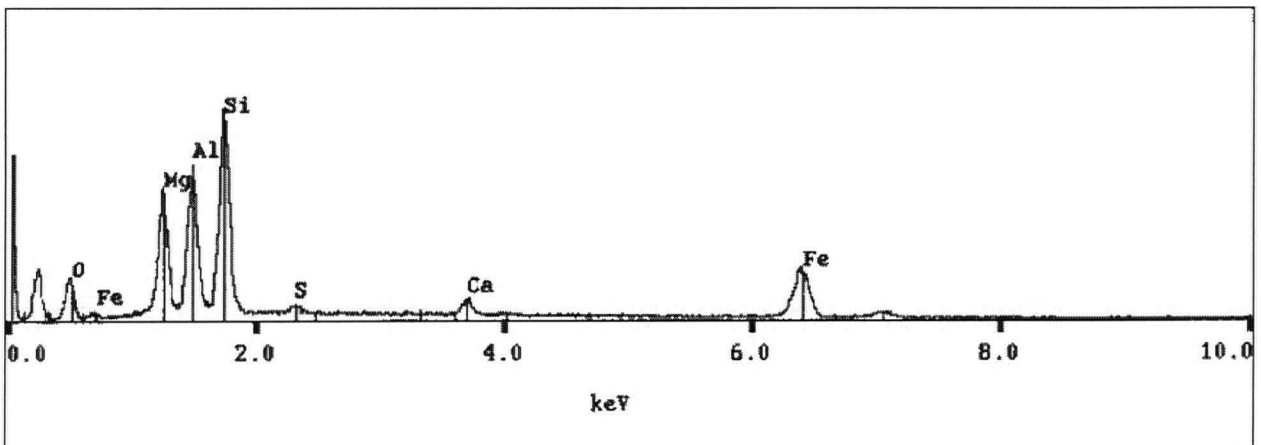


Plate 5.44 EDX of tobermorite developed from slag

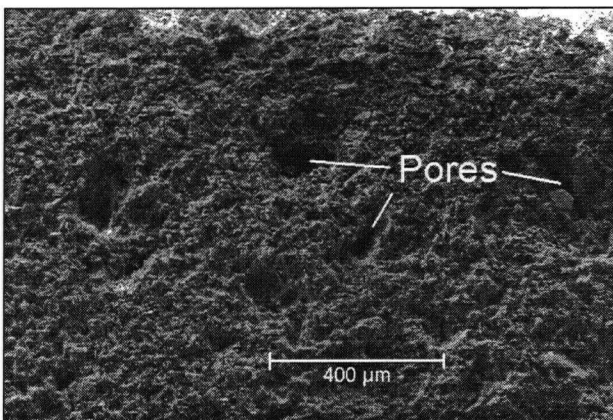


Plate 5.45 General aspect of paste mixture

Louvicourt – Flooded-leached Paste Samples

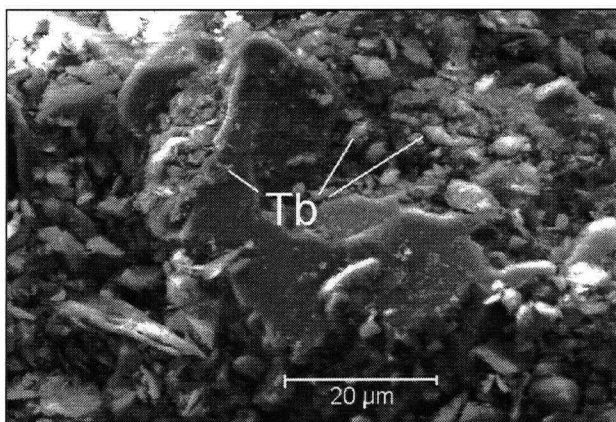


Plate 5.46 Less tobermorite in upper layer 1

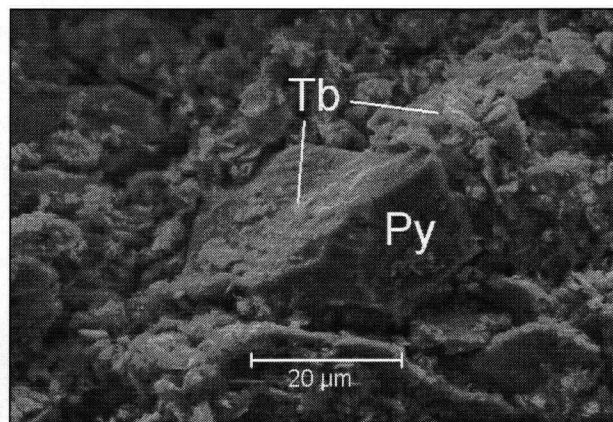


Plate 5.47 More abundant tobermorite in lower layer 1

Louvicourt – Cycle-leached Paste Samples

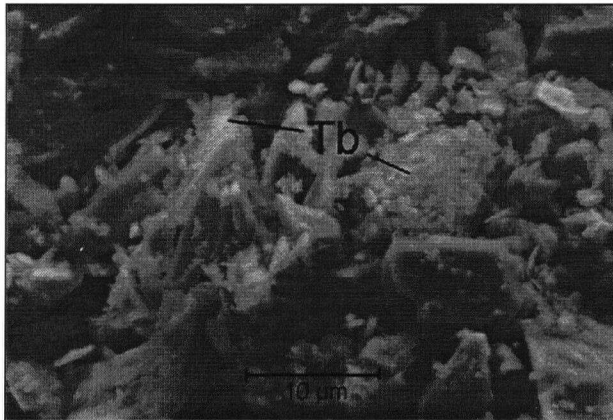


Plate 5.48 Poorly developed Tb, upper layer 1

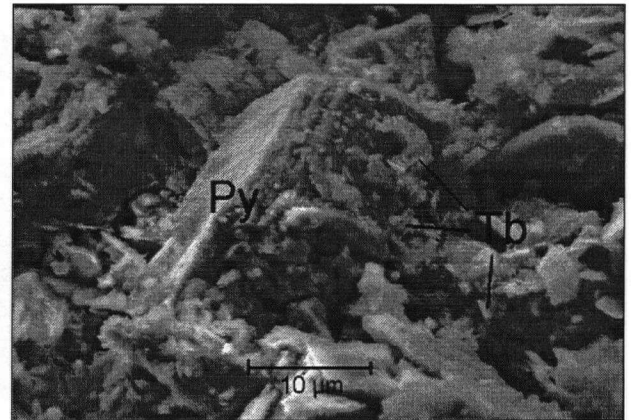


Plate 5.49 Upper layer 1

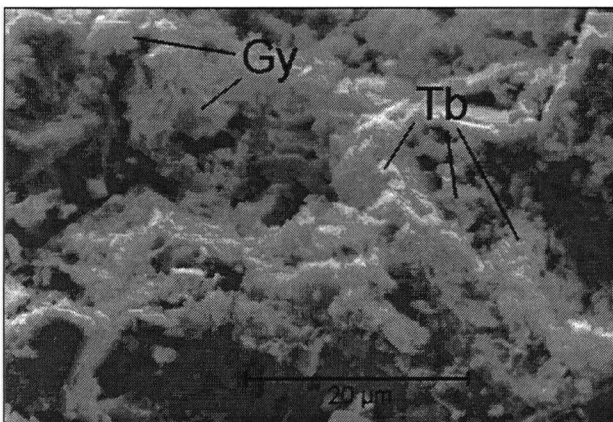


Plate 5.50 More developed Tb, lower layer 1

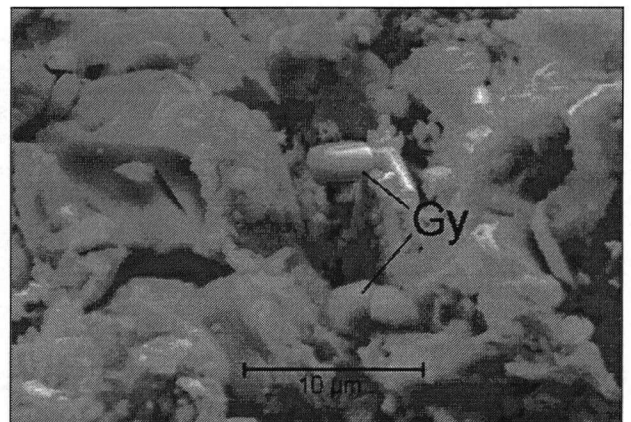


Plate 5.51 Secondary gypsum, lower layer 1

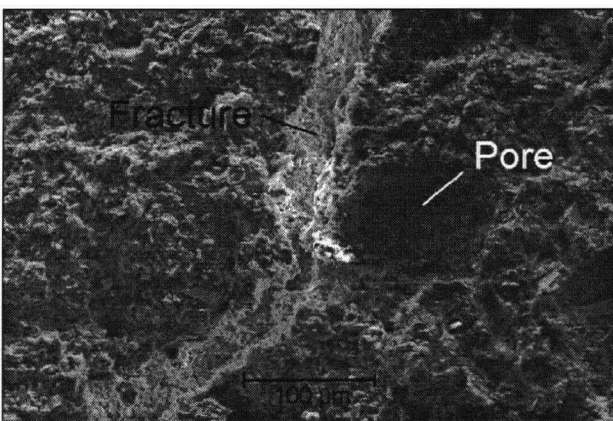


Plate 5.52 Tobermorite-lined fracture in paste

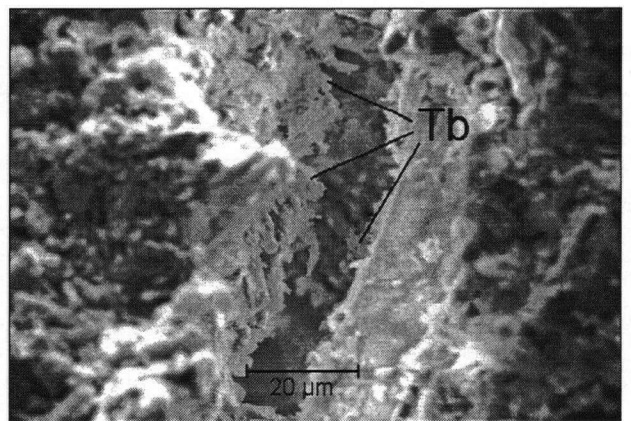


Plate 5.53 Close-up view of tobermorite

Louvicourt – Fe₂(SO₄)₃ Solution-leached Paste Samples

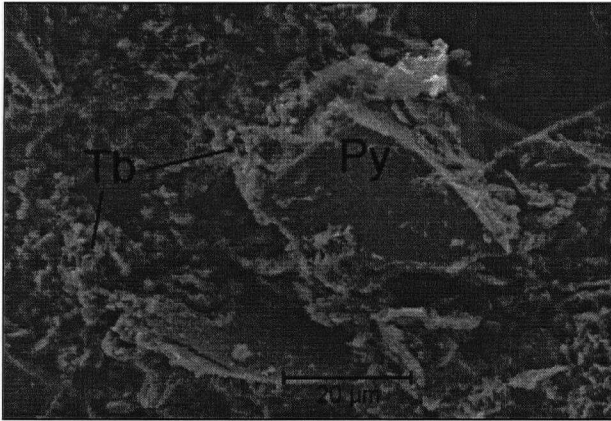


Plate 5.54 Depleted tobermorite, layer 1

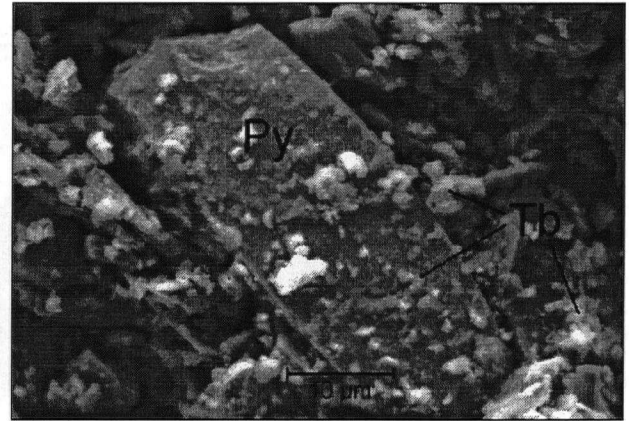


Plate 5.55 Masses of tobermorite at upper layer 1

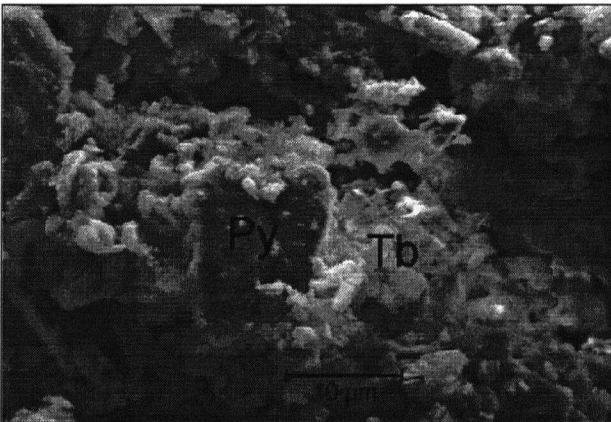


Plate 5.56 Increased Tb content, below layer 1

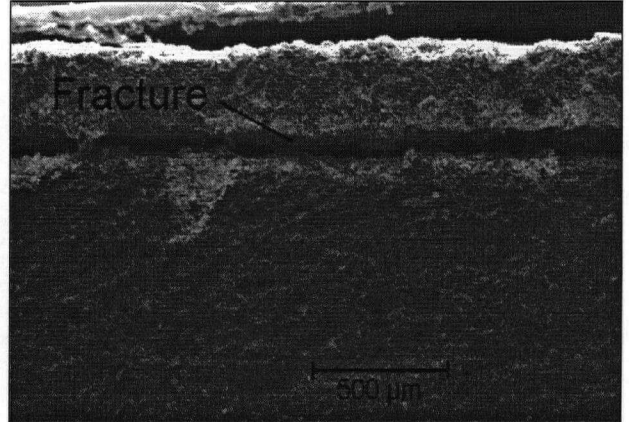


Plate 5.57 Fracture developed possibly along existing plane of weakness

Louvicourt – Fe₂(SO₄)₃ Solution-leached Paste Samples

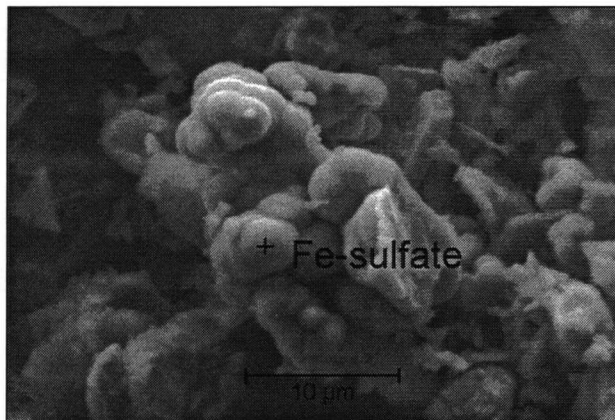


Plate 5.58 botryoidal mass of iron sulfate precipitate

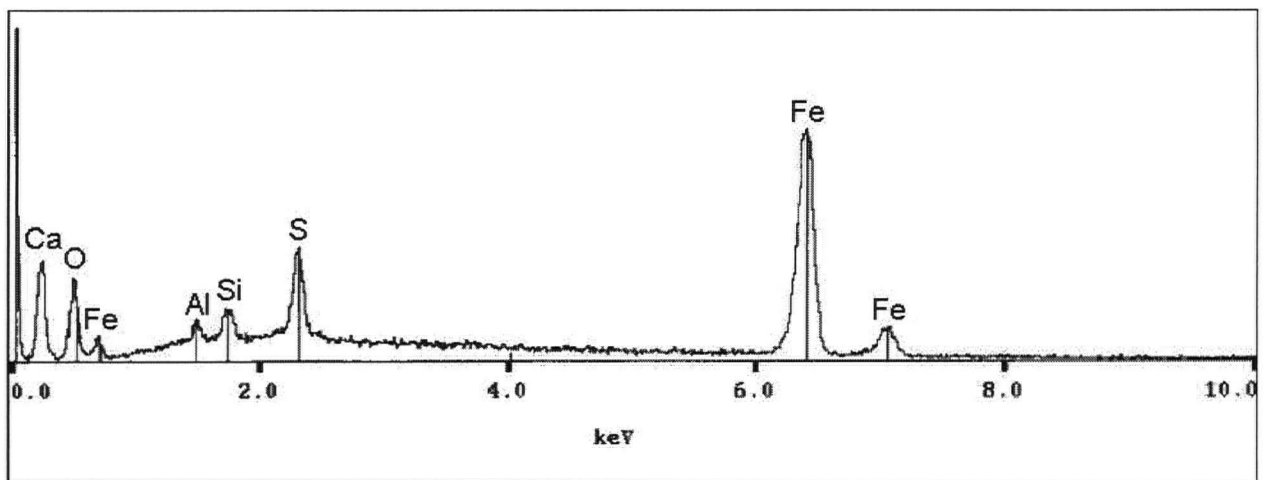


Plate 5.59 EDX of iron sulfate precipitate (type of jarosite?)

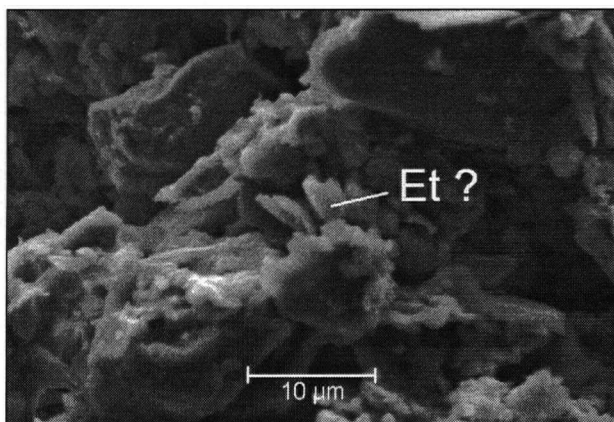


Plate 5.60 Possibly ettringite, layer 2

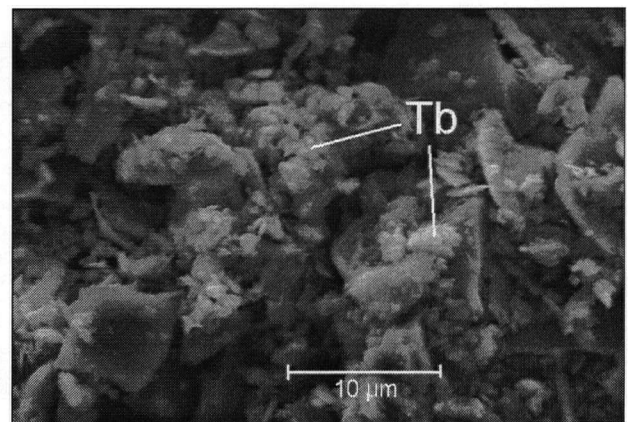


Plate 5.61 Well developed tobermorite, lower layer 2

Francisco I. Madero – Flooded-leached Paste Samples

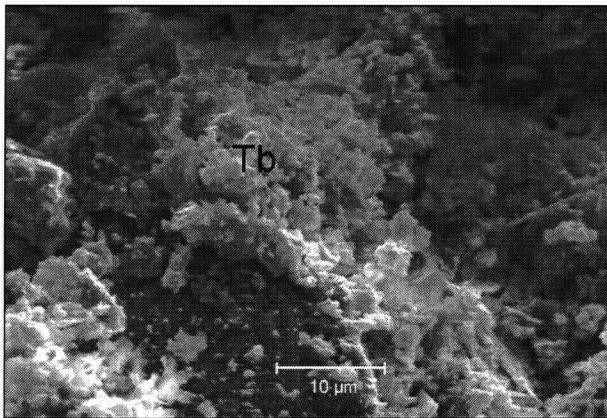


Plate 5.62 Layer 1, flooded sample

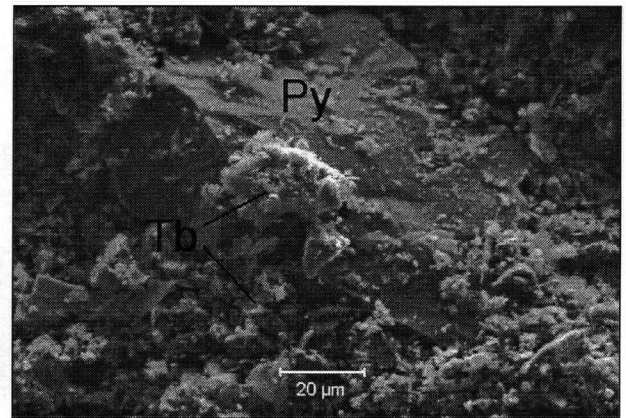


Plate 5.63 Core of flooded sample

Francisco I. Madero – Cycle-leached Paste Samples

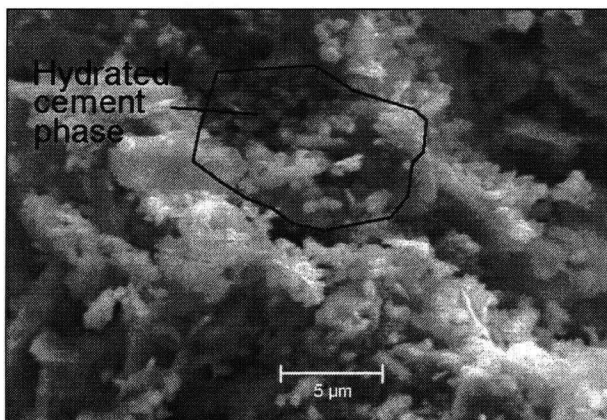


Plate 5.64 Layer 1, hydrated cement phase (may be Et, Pd, Tb and/or Gy)

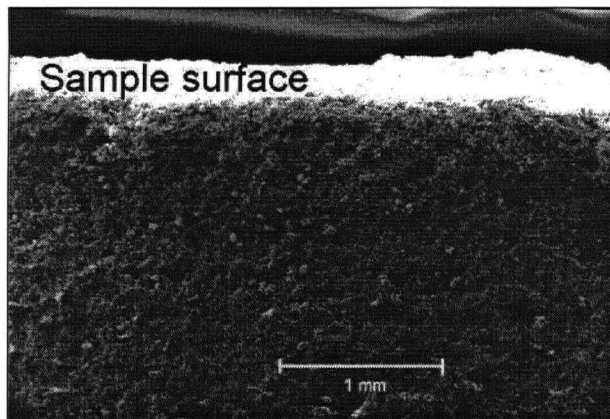


Plate 5.65 General aspect of paste

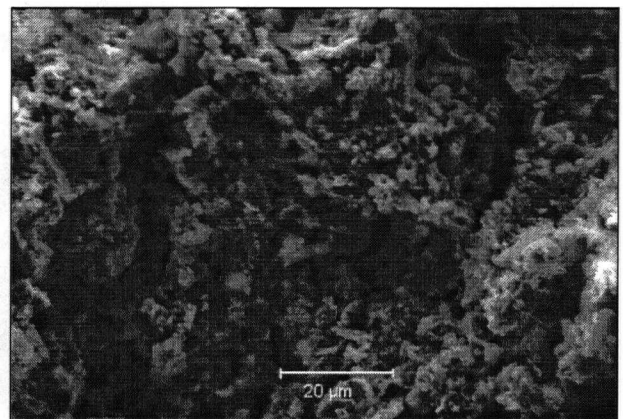


Plate 5.66 Good development of tobermorite, layer 1

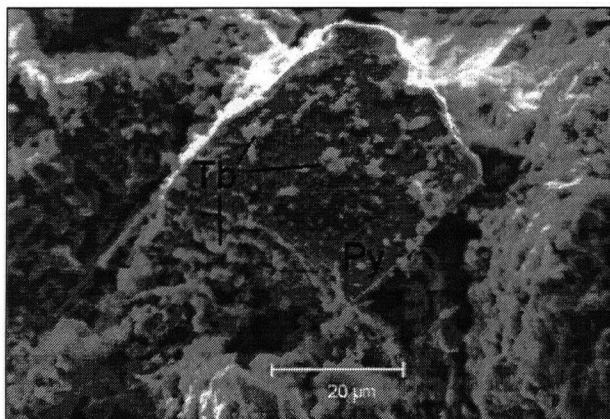


Plate 5.67 Layer 1

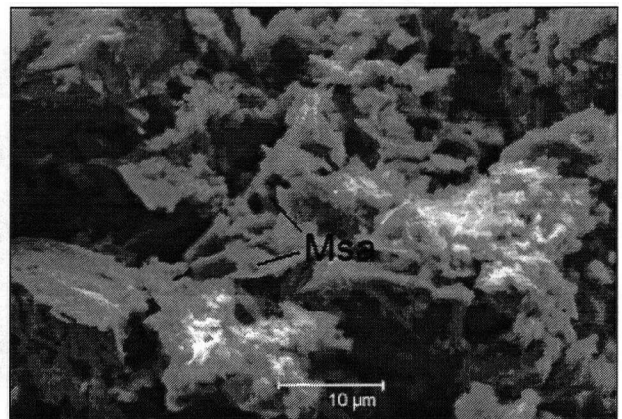


Plate 5.68 Monosulfoaluminate (?), below layer 1

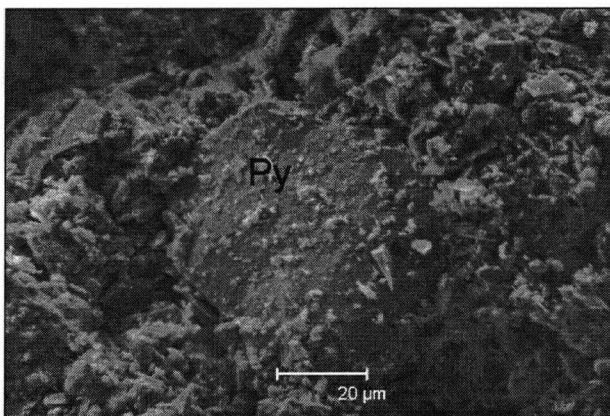


Plate 5.69 Core of sample

Msa = monosulfoaluminate

5.7.5 Summary of Observations from Scanning Electron Microscopy

Distinct secondary precipitates were observed between mixtures containing only OPC binder and the Louvicourt mixture containing 80% slag in its binder. In general, the tobermorite developed from the slag-cement was observed to be more resistant to leaching in all environments.

Flooded Water Environment:

- In OPC binder mixtures, Euhedral portlandite crystals were present in relative abundance in the outer edges of flooded water-leached samples exclusively. The abundance of portlandite appeared to be proportional to the cement content of the sample. The longer contact time between the water and the sample in the flooded environment most likely allowed for the pore water to become supersaturated with calcium hydroxide and re-precipitate this phase. These observations agree with the solid phase and leachate chemistry data.
- Tobermorite, the main binding agent of cement, was present in smaller amounts in the outer edges of the samples compared to the cores. The amount of depletion was much less in the slag-cement Louvicourt mixture. In all cases and all depths, the tobermorite that was present was evenly distributed and well developed.
- Ettringite was easily discernible in the core of samples that contained the largest amount of OPC binder (Tizapa and Brunswick). This suggests that dissolved Ca^{2+} and SO_4^{2-} were abundant in the pore solution in the core of these samples but were

leached out on the edges. The concentration gradient would drive a gradual and continued depletion of these ions from deeper areas within the paste.

- No secondary, expansive minerals such as ettringite, gypsum or monosulfoaluminate were observed in the slag-cement binder mixture. This attests to the increased resistance to water-leaching and sulfate attack of this binder mixture.

Cycled water environment:

- No portlandite was found in the outer edges of any cycle-leached sample. Supersaturation of portlandite was most likely inhibited in the cycled environment as OH⁻ ions were consumed to neutralize the leaching solution, and Ca²⁺ was dissolved and flushed out of the system before equilibrium could be reached.
- No portlandite was observed in the slag-binder mixture as expected, as slag generally generates little portlandite upon hydration, another feature of sulfate resistance (Taylor, 1997).
- Tobermorite was depleted in the outer edges of the cycled water-leached pastes relative to the sample cores, the extent of which appears to be greater than in the flooded environments for both the OPC and slag-cement binder mixtures.
- Presence or greater abundance of grain-shaped voids in the outer edges of the OPC binder pastes suggests a decreased cement binding strength in these areas relative to the core. The loss in binding strength may be caused by the lower amount of cement and/or by a degradation (i.e. decalcification) of the cement phase in this area relative

to the core.

- Although tobermorite was depleted in the outer layer of the slag-cement mixture, no apparent loss of binder strength or empty grain cavities were observed.
- Secondary, euhedral gypsum crystals were observed in the outer layers of the Tizapa sample along with acicular ettringite. Secondary gypsum was also observed in the Louvicourt paste below 4 mm depth. These minerals indicate that a source of internal stress created by the pressure of crystal growth is present within the backfill.

Ferric sulfate environment:

- Tobermorite was depleted in the outer edges of the ferric sulfate-leached pastes, to a similar extent than in the cycled environments, for mixtures of both binder types. The level of depletion was much lower in the Louvicourt sample than in the others.
- Oölitic or botryoidal masses of iron sulfate precipitates (possibly jarosite) were encountered in the 2nd layer of alteration for all paste mixtures. This location may indicate the penetration front of the ferric sulfate leach solution at the interface with the high pH pore solution of the samples.
- Phases of ettringite, monosulfoaluminate and/or gypsum were present at various depths in the ferric sulfate-leached samples, indicating that dissolved Ca^{2+} and SO_4^{2-} ions were present in sufficient quantity in the pore solution. These ions were therefore not completely depleted from the pore solution in any area of the ferric sulfate-leached samples.

5.8 COMPRESSIVE STRENGTH MEASUREMENTS

Unconfined compressive strength (ucs) measurements were carried out on unleached paste samples and on the 5, 10 and 20-week leached samples of all 3 environments. The results shown on Figures 5.48 through 5.51 should be interpreted in a qualitative manner since only one sample was tested per environment, per leaching period.

Ucs requirements by each respective mine were achieved for all paste mixtures and surpassed for the Tizapa mixture (Table 5.9). Brunswick, Louvicourt and FIM ucs appeared to remain constant as leaching progresses, regardless of the leaching environment. A small decrease in ucs was observed in the Tizapa paste in all environments as leaching progressed. This loss may not be statistically significant.

Alteration of the cement phases upon leaching was not only expected, from the literature review, but was also observed under SEM. The layers where alteration occurred were probably too thin after 20 weeks of leaching to influence the compressive strength of the entire sample.

Unconfined compressive strength of any material is a function of the surface area of the sample subjected to compression according to the formula:

$$f = \frac{F}{A} \quad (5.3)$$

where F is the force applied to the sample by the compressor, in kg, (multiplied by gravity) and A is the area of the sample in contact with the piston. Postulating that the loss of cementing material seen under SEM resulted in a loss of strength in the oxidized layers, then the unaltered core of the samples should possess higher strength than the unleached samples. Although no measurements were made to verify this, it is possible that the cores of the leached samples gained strength over the leaching period because of the longer curing time of the samples in an aqueous environment. This would suggest that uniaxial compressive strength may not constitute an appropriate measuring tool to characterize the strength of weathered backfill samples.

Table 5.9 Unconfined Compressive Strength of Paste Samples (MPa units)

	Tizapa		Louvicourt		Brunswick		FIM	
	Flooded	Cycled Fe-soln	Flooded	Cycled Fe-soln	Flooded	Cycled Fe-soln	Flooded	Cycled Fe-soln
Requirement	2.0 - 3.5		0.7 (14 days)		0.5 - 1.0		0.5	
Unleached	4.3		0.7		1.4		0.03	
5 weeks	2.4	2.4	0.7	0.8	1.0	1.2	0.4	0.3
10 weeks	3.4	3.1	0.9	0.8	1.0	1.0	0.1	0.3
20 weeks	3.8	3.5	0.7	0.5	1.3	1.1	0.2	0.3

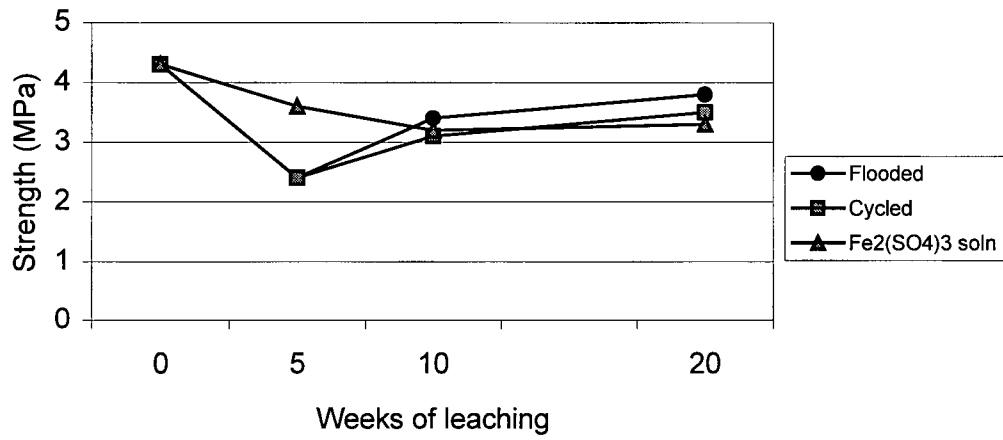


Figure 5.48 Tizapa Paste - UCS with Leaching Time

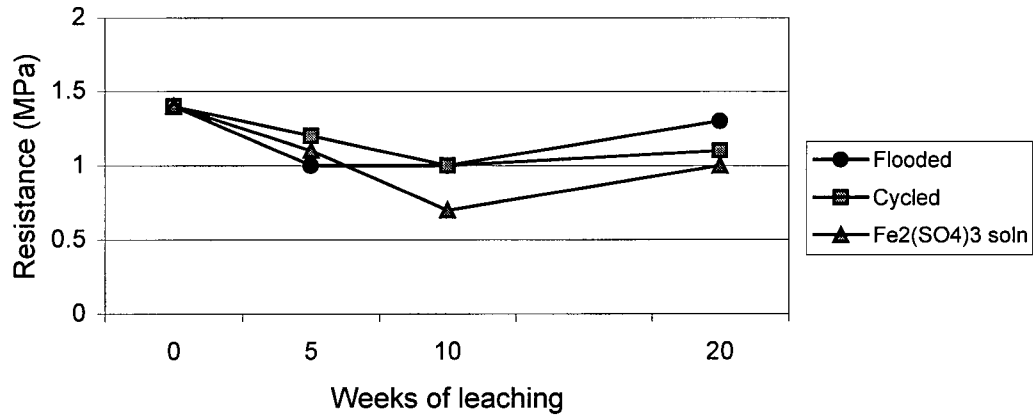


Figure 5.49 Brunswick Paste - UCS with Leaching Time

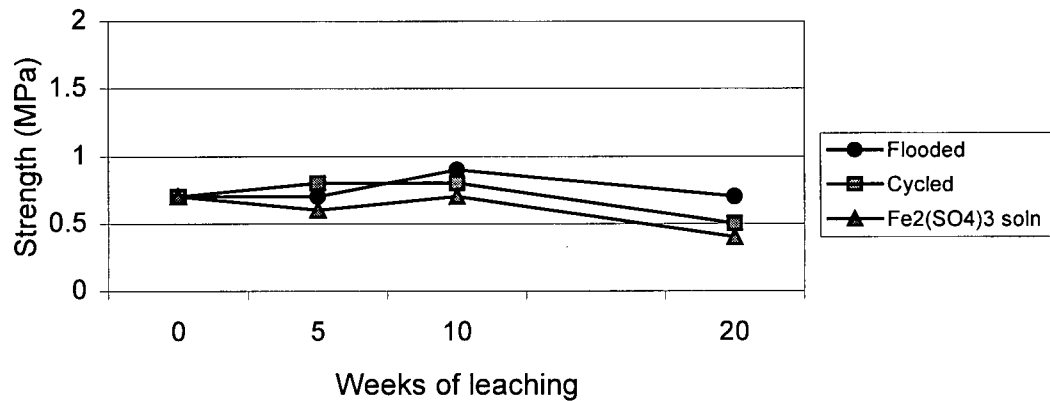


Figure 5.50 Louvicourt Paste - UCS with Leaching Time

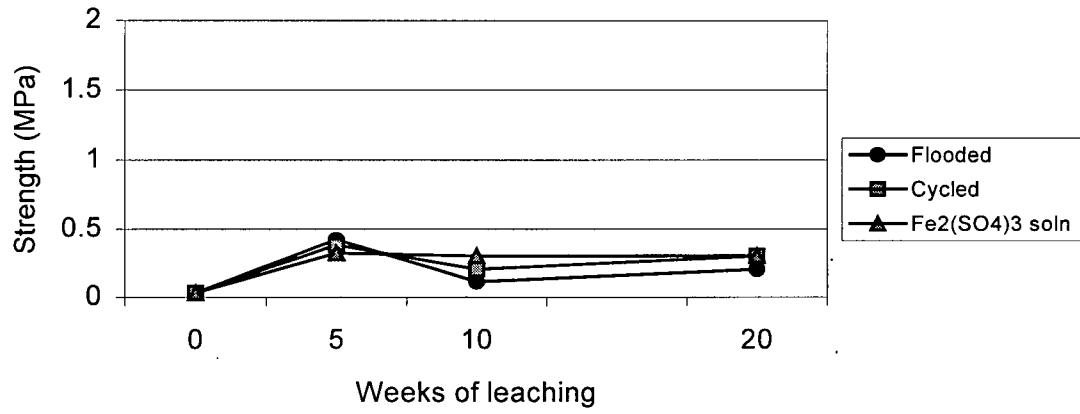


Figure 5.51 Francisco I. Madero Paste - UCS with Leaching Time

6 DISCUSSION

6.1 PYRITE REACTIVITY STUDY

The mineral surface characterisation technique of cyclic voltamperometry provided a measure of the combined effects of the different mineral characteristics on the reactivity of pyrite, such as chemistry, crystal morphology, stoichiometry and presence of other sulfide phases associated with pyrite (termed mineral impurities). This method of analysis established that, initially, Huckleberry pyrite was the most reactive of all samples studied, most likely due to its relatively low concentration of separate sulfide phases. Conversely, Louvicourt-2 and Tizapa pyrites were the least reactive because of the considerable amount of galena and sphalerite texturally associated with pyrite in the samples. This study suggested that the presence of these mineral phases in the pyritic samples effectively decreased the reactivity of pyrite to a greater extent than either stoichiometric proportions of Fe:S, chemical impurities in the crystal lattice, crystallinity or morphology of pyrite crystals could have increased the reactivity of pyrite.

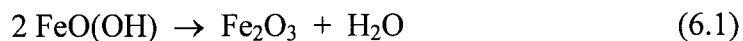
The following sections discuss the effects of the various mineral characteristics observed in this study, on the reactivity of pyrites.

6.1.1 Effect of Precipitate Coatings on the Passivation of Pyrite: Huckleberry and Louvicourt-1 Samples

Higher dissolved iron and sulfate concentrations in the leachate supported the voltamperometric data suggesting that the unleached Huckleberry pyrite was the most

reactive of all samples analyzed. The relatively high reactivity of Huckleberry pyrites may, in part, be caused by the greater amount of fine size particles in the sample. Grain size is not believed to be the only cause of Huckleberry reactivity since the finer grain size Brunswick sample possessed the lowest reactivity after 20 weeks of leaching. As leaching progressed, however, both water and waste rock solution-leached Huckleberry pyrites were rapidly oxidized and became less reactive.

The amount of iron oxyhydroxide precipitates on pyrite surfaces that were visible under SEM formed a very discontinuous layer even after 20 weeks of leaching. These precipitates alone may not account for the decreasing reactivity exhibited in the voltamperometric study. The visible precipitates may be however, local accumulations of a more extensive FeOOH precipitates and/or polysulfide layers not visible under SEM. Mineral coatings of FeOOH on oxidized pyrite were observed by many researchers. Nicholson and others (1990) measured a continuous α -Fe₂O₃ (maghemite) precipitate layer on pyrite of an average of 0.6 μ m thickness after 400 days of leaching. In that study, the chemistry of the precipitate layer was believed to be a dehydrated form of γ -FeOOH (lepidocrocite) transformed by the high vacuum of the auger electron spectroscopy (AES) instrument, according to:



The presence of such thin oxidation rims on pyrite were also documented by Alpers and others (1994) and Jambor (1994). Many other researchers also documented the formation of iron oxide, iron oxyhydroxide, and/or sulfur, sulfoxianion or polysulfide layers on the

pyrite surface following electrode oxidation, all of which effectively decreased the leachability (or reactivity) of the underlying pyrite (Peters, 1984; Buckley *et al.*, 1988; Ahmed, 1991; Zhu *et al.*, 1992; Ahmed and Giziewicz, 1992). In addition, Moses and Herman (1991) proposed that accumulation of Fe^{2+} on pyrite surfaces in early stages of leaching effectively decreased the rate of pyrite oxidation and that FeOOH deposits on the pyrite surfaces in slowly-stirred, long-term leaching experiments were the cause of decrease pyrite oxidation rates.

Although no specific information is available on the composition of the oxidized layers observed by SEM on pyrite grains in many samples, literature indicates that thin FeOOH , sulfur or polysulfide layers could be responsible for the increasingly efficient passivation of Huckleberry pyrites or any of the other pyrites studied.

Louvicourt-1 and -2 samples came from the same mineral deposit but exhibited large differences in their chemical and stoichiometric composition as well as in their oxidation behaviour. The unleached Louvicourt-1 pyrite sample showed a similar voltamperometric response to the Huckleberry sample and, likewise, a similar evolution of reactivity with increasing leaching-time. The more abundant, amorphous iron precipitates covering the surfaces of Louvicourt-1 pyrites did not appear however, to result in a greater loss of reactivity. It is probable that sulfur or polysulfide layers could have been more instrumental in passivating the pyrite surfaces than the apparently discontinuous iron oxyhydroxide precipitate coatings.

6.1.2 Effect of Stoichiometry on Pyrite Reactivity: Louvicourt-1 and Louvicourt-2 Samples

Pyrite stoichiometry was not found a determinant factor in the reactivity of pyrite compared to the presence of sphalerite. The relative depletion of iron in the Louvicourt-1 pyrite structure consisted of an acceptor defect that should have theoretically protected the pyrite from oxidation (Shuey, 1975; Kwong, 1993) compared to Louvicourt-2 pyrite having a S:Fe ratio of exactly 2.0. Similarly, although arsenic contents were similar for both Louvicourt samples, SEM observations showed that Louvicourt-1 arsenic was mainly contained in separate arsenopyrite phases whereas Louvicourt-2 arsenic principally occurred as lattice impurities within pyrite. The presence of arsenic impurities in the crystal lattice of pyrite creates a donor defect, which should theoretically promote the oxidation of Louvicourt-2 pyrite (Shuey, 1975; Kwong, 1993). Voltamperometric analyses of the unleached Louvicourt pyrites indicated, however, that Louvicourt-2 pyrite was the less reactive one. The presence of arsenic may have influenced the way in which the Louvicourt-2 pyrite sample oxidized, as a greater density of oxidation pits were visible on Louvicourt-2 pyrites compared to Louvicourt-1 after 10 and 20 weeks of leaching.

In summary, for all the pyrites studied, the effects of iron to sulfur ratios and the presence of arsenic impurities in the pyrite crystal lattice were overcome by an opposing, more determinant factor on the reactivity of pyrite. This factor is believed to be the presence of sphalerite and galena impurities in the pyrite samples, which offered galvanic protection to pyrite.

6.1.3 Effect of Mineral Impurities on Pyrite Reactivity

6.1.3.1 Galvanic Protection by Sphalerite: Louvicourt-2 and Tizapa Samples

Tizapa and Louvicourt-2 pyrite samples possessed similar mineralogies and showed a similar evolution of pyrite reactivity. Both were characterized by an initial gain in reactivity after 4 weeks of leaching, followed by a decreasing reactivity. This study suggests that during the leaching period, sphalerite grains in contact with pyrite acted as an anode and were preferentially oxidized over pyrite. The cathodic reaction could involve the reduction of oxygen, as described by Murr and Metha (1983):

Anodic reaction: sphalerite oxidation



Cathodic reaction: reduction of water



Kwong and Lawrence (1994) also proposed that the formation of galvanic couples affected the reactivity of pyrite to a greater extent than mineralogical defects, stoichiometric imbalances, grain size, crystallographic orientation or bacterial activity. Results of both this and the Kwong and Lawrence studies are supported by the research of Metha and Murr (1983) who measured the contribution of galvanic interaction on the reactivity of pyrite in an acidic solution of 1M H₂SO₄. They proposed that galvanic interactions were responsible for the cathodic protection of a sulfide mineral with higher rest potential (pyrite) in contact with a mineral of lower rest potential (sphalerite,

chalcopyrite) which acts as the anode and oxidized preferentially.

The gain of reactivity in both Louvicourt-2 and Tizapa samples coincided with higher concentrations of zinc in both sample leachates, following reaction 6.2. SEM observations showed that in both samples, when sphalerite and pyrite occurred on the same grain, sphalerite phases were extensively corroded compared to pyrite phases. Pyrite generally possessed smooth surfaces and sharp grain edges in the 4th and 10th weeks for Tizapa and Louvicourt-2 respectively.

The subsequent passivation of pyrite coincided with the decline in leachate zinc concentrations, occurring around the 5th week (10th cycle) for Tizapa and the 10th week (20th cycle) for Louvicourt-2. Indeed, in later leaching cycles SEM observations showed sphalerite grains becoming precipitate-covered and corroded, suggesting that sphalerite could also have been passivated and were no longer available to oxidize and offer galvanic protection to pyrite. Sphalerite passivation may be caused by a covering of the surface by elemental sulfur shown in reaction 6.2. Increases in the intensity of pyrite pitting were observed in the 10th week for Tizapa and 20th week for Louvicourt-2, suggesting a more intensive oxidation of pyrite following the decreased oxidation of sphalerite. The increasing supply of partly oxidized sulfur and dissolved iron to the leachate could then have promoted the formation of iron oxyhydroxide and/or sulfur-polysulfide coatings on all grains, effectively decreasing pyrite reactivity. A decrease in the reactivity of pyrite was indeed observed electrochemically in the 10th and 20th week of leaching in the Tizapa and Louvicourt-2 samples respectively.

The absence of sphalerite in the Louvicourt-1 sample probably enabled

that pyrite surface to oxidize from the first leaching cycle onward, allowing for an earlier production of a passivating layer. Voltamperometric studies indicated that Louvicourt-1 pyrite was more reactive prior to leaching but was passivated at an early stage.

6.1.3.2 Effect of the Presence of Galena: Zimapan and Brunswick Samples

The presence of galena was detected on the Zimapan and Brunswick voltamograms by the occurrence of a characteristic peak around 0 mV. In that way, a concentration of galena as low as 1.5 % was electrochemically detected in the Zimapan pyrite sample. A more intense peak was observed in the Brunswick sample that contained a higher galena content (9%). The amplitude of peaks attributed to galena appeared to be proportional to the galena content of the sample.

The fact that galena is highly susceptible to oxidation is well documented in the literature (Metha and Murr, 1983; Nicholson, 1994; Alpers et al., 1994; Jambor, 1994; Blowes et al., 1995). In this study, galena was also found to oxidize rapidly: only traces of galena were present in the Brunswick sample after 10 weeks of leaching. Galena was replaced with anglesite (PbSO_4) either by direct replacement (i.e. in Tizapa where anglesite is found covering skeletal galena) or by precipitation from solution (i.e. in Brunswick and Zimapan where anglesite is dispersed throughout the sample). The low solubility of anglesite (Table 6.1) explains why dissolved lead readily precipitated as lead sulfate in the sample effectively scavenging the dissolved lead from the leachate solutions. Unlike lead, dissolved zinc does not tend to precipitate as a secondary zinc hydroxide or sulfate but tends to remain in the leachate solution. In the case of Brunswick, it is possible that

the leachate solution was oversaturated with respect to anglesite due to the large amount of galena being oxidized.

Table 6.1 Dissociation Constants for Secondary Minerals of Zn and Pb

Zinc Secondary Minerals	Dissociation Constant (log K) ¹	Lead Secondary Minerals	Dissociation Constant (log K) ¹
ZnSO ₄	3.0	PbSO ₄	-7.8
Zn ₂ (OH) ₂ SO ₄	7.5	Pb ₃ O ₂ SO ₄	10.4
Zn ₄ (OH) ₆ SO ₄	28.4	Pb ₄ O ₃ SO ₄	22.1
Zn(OH) ₂	11.5	Pb(OH) ₂	8.2

¹(Parkhurst, 1995: PhreeqC database updated 1996)

6.1.4 The Huckleberry Problem

The potentially acid generating Huckleberry pyrite was found the most reactive of all pyrites tested. This classification may be due in part by the larger fine grain proportion of the sample, increasing the surface area of the sample and possibly increasing the oxidation rate of pyrite (McKibben and Barnes, 1986; Kwong 1993). This is not necessarily the principal cause of the Huckleberry's high reactivity, however, since the Brunswick sample, which had a higher proportion of fines, exhibited the lowest reactivity (following the disappearance of galena in the sample). An important factor remains that the reactivity of Huckleberry pyrite declined from the 4th week onward. Although Huckleberry remained the most reactive pyrite sample throughout the 20-week leaching period, the waste rock solution-leached pyrite showed the greatest loss of reactivity (0.07 volts) after Zimapan (0.1 volts). The reactive nature of these pyrite samples was progressively overcome by the precipitate coatings, which are believed to have caused the reactivity decrease.

The slight gain in reactivity observed in the 20th week of leaching in the solution-leached Huckleberry pyrites as well as in Tizapa and Louvicourt-2 samples, however, suggested that surface properties of the pyrite (or its precipitate cover) continually evolved during leaching, affecting the reactivity of pyrite. Evolution of surface properties may include changes in precipitate chemistry or morphology, bacteriological alteration of grain surfaces, or many other factors. The electrochemically observed changes in reactivity could be paralleled with the constantly evolving chemistry of mineral waste solids and leachates, making predictions difficult to establish with an acceptable degree of certainty.

6.2 CHEMICAL STABILITY OF PASTE MIXTURES

6.2.1 Effect of Cementing Tailings Waste

Binder (Portland cement and slag-cement mixtures) does provide some buffering capacity to the tailings. The small proportion of binder added to the reactive tailings studied (less than 6% in this study) is, however, far from sufficient to neutralise all the potential acidity of the tailings studied which had NPR values below 0.1. NPR values of all the backfill mixtures studied remained well below 1 after cement addition, remaining potentially acid generating like the tailings that make up the backfill.

Paste pH measurements suggest that both binders (OPC and slag-OPC) contain readily dissolved buffering minerals that provide efficient, early-stage buffering capacity to the backfill. ABA analyses as a function of leaching time indicated that binder NP is readily consumed in the early stages of contact with water or ARD solution. Depletion is observed to be more severe in ARD solution for all cases studied. As a result, even if

cementing material was added initially in sufficient quantity to raise the NPR of the backfill to environmentally safe levels (i.e. $NPR > 3$), the NP may be depleted in this environment at a very early stage, leaving the tailings unprotected.

In most cemented backfilling operations, the backfill is exposed to the environment almost immediately after placement. This study suggests that exposure of the backfill to an aqueous leaching environment prior to being properly cured will promote the loss of binder material, which, in the cases studied, accounted for the majority of backfill buffering capacity. This could potentially be accentuated where slag-cement binders are used, as slag is typically slower to react (hydrate and cure) than OPC. The loss of material was further accelerated in ARD solution. Fully cured backfill could, however, show a different response to leaching. Conversely, if the backfill is not exposed to any leaching solution, for example in a dry area of the mine, the cement content should be conserved until the mixture is properly cured.

In the case of Tizapa paste backfill which contained the highest proportion of cement and the highest proportion of sulfide minerals in the tailings, surficial oxidation of the samples began to occur within the 14-day curing period. This suggests that the sulfide portion of the waste was not sufficiently covered or protected by binder to prevent its oxidation in air. Paste containing such high proportions of reactive sulfides would likely require complete submergence in water at an early stage to prevent oxidation of the sulfide portion of the tailings. Such a material may not be suitable for storage above ground, or underground above the water table, where it could be exposed to air and humidity for extended periods of time.

6.2.2 Cemented Backfill Alteration with Leaching

In 20 weeks of leaching, differences in alteration were more influenced by the leaching environment and binder content (OPC and slag-cement) of the paste mixtures than by tailings composition. Binder content was found to be the most important factor affecting leachate water quality. Calcium, potassium, silicon and magnesium loadings in the leachates were found to be directly proportional to the solid phase concentration of these elements in the paste mixture, in turn, proportional to the binder content of the mixture.

6.2.2.1 Water-Leached Environments

The leachate and solid phase geochemistry along with ABA analyses, indicated that calcium concentrations in the leachate came principally from the dissolution of the portlandite phase ($\text{Ca}(\text{OH})_2$) of cement, where OH^- ions were consumed to buffer the pH of the leaching solution. This agrees with previous investigations on the effect of water leaching of cemented mixtures (Adenot and Buil, 1992; Revertegat, 1992; Benzaazoua, 1997). EDX microanalyses under SEM were not sufficiently precise (due to uneven sample surfaces) to measure a quantifiable decalcification of the tobermorite, as expected from the literature review. The modified morphology of the exposed tobermorite observed in altered regions, however, was similar to the morphological descriptions of Ca-depleted tobermorite by Adenot and Buil (1992), Carde and François (1997) and Taylor (1997). They have found that in situations of severe leaching, tobermorite generated from both OPC and slag-OPC binder lost its volume and took the shape of dehydrated gel-like (silica-rich) filaments, losing binding strength in the process.

The Tizapa and Brunswick mixtures containing the highest percentage of pyrite and largest proportion of binder showed deeper penetrating alteration layers compared to the Louvicourt and FIM mixtures. The tobermorite developed from the slag binder in the Louvicourt paste was considerably less depleted than OPC tobermorite in all environments and showed generally fewer expansive minerals after 20 weeks of leaching. This indicates that the slag-cement binder of Louvicourt offered increased resistance to water leaching as well as to sulfate attack compared to OPC-binder backfills.

Flooded vs Cyclic Water-Leached Environments

Portlandite supersaturation was achieved in the flooded environment for both the Tizapa and Brunswick samples, which contained the highest proportion of binder. Masses of euhedral portlandite lined the outer edge of the samples and were observed to 1 mm and 3 mm depths respectively after 20 weeks of leaching. No portlandite was observed in the Louvicourt or FIM pastes.

Penetration of the leachate solution and the resulting concentration gradients of calcium and hydroxyl ions between the sample pore solution and the leachate drove the dissolution of portlandite and the diffusion of these ions out of the sample. The chemical conditions at the sample edge may have induced the precipitation of secondary minerals at that location. The same can be suspected to have occurred for all soluble backfill components. Supersaturation conditions must occur in the leachate solution before the secondary mineral may nucleate and grow. Longer contact times between the solution and the paste, such as in the flooded environment simulated in this study, facilitate the

achievement of supersaturated conditions and precipitation of secondary minerals such as gypsum or portlandite.

SEM observations showed, however, that no expansive ettringite or gypsum was present after 20 weeks of leaching in the flooded environment in either Tizapa or Brunswick samples. Instead, secondary gypsum and ettringite were encountered in the outer edges of the cycled environment samples. It is clear then that in the case of cemented tailings backfill, the occurrence of secondary minerals is a solubility-controlled process.

Table 6.2 presents the ranges of solubility constants (K_{ps}), associated solubilities in water (in mg/l) and equilibrium constants (K_{eq}) of the secondary minerals encountered in concrete mixture. Lime, calcite and salt (halite) are also shown for comparison.

Mineral solubility can be evaluated using the solubility product constant (K_{sp}) in instances where dissolution of the mineral *in pure water* is not affected by water pH.

Given any dissolving mineral 'AB':



K_{sp} is evaluated from the activities of species (activity of a solid = 1) according to:

$$K_{sp} = [A]^y \times [B]^z \quad (6.3)$$

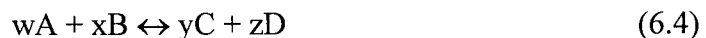
**Table 6.2 Solubility Products and Dissociation Constants of Secondary Minerals
Derived from Hydrated Portland Cement and Other Reference Minerals**

Mineral and Dissociation Reaction	Solubility Product (Ksp or moles/l at 25°C)	Solubility (in water at 25°C) *	Dissociation Constant (Keq at 25°C)
Portlandite: $\text{Ca}(\text{OH})_2$ $+ \text{H}^+ \rightarrow \text{Ca}^{2+} + 2 \text{H}_2\text{O}$	(1) 5.5×10^{-6} (2) 3.2×10^{-5}	depends on pH for pH < 10.7	(5,6) 6.3×10^{22}
Ettringite: $\text{Ca}_6\text{Al}_2(\text{SO}_4)_3(\text{OH})_{12} \cdot 26\text{H}_2\text{O}$ $\rightarrow 6\text{Ca}^{2+} + 2\text{Al}^{3+} + 3\text{SO}_4^{2-} +$ $12 \text{OH}^- + 26\text{H}_2\text{O}$	(3) 1.23×10^{-45} (4) 10^{-112}	depends on pH for pH < 11	not available
Gypsum: $\text{CaSO}_4 \cdot 2\text{H}_2\text{O}$ $\rightarrow \text{Ca}^{2+} + \text{SO}_4^{2-} + 2\text{H}_2\text{O}$	(5) 9×10^{-6} (8) 2.5×10^{-5}	(5) 520 mg/l (7) 2100 mg/l	(1) 3.2×10^{-5}
Calcite: CaCO_3 $\rightarrow \text{Ca}^{2+} + \text{CO}_3^{2-}$	(1) 2.8×10^{-9} (8) 4.5×10^{-9}	(1) 3 mg/l (8) 4 mg/l	(5) 3.1×10^{-9}
Lime: CaO $+ \text{H}_2\text{O} \rightarrow \text{Ca}^{2+} + 2 \text{OH}^-$			(6) 6.3×10^{32}
Halite (salt): NaCl $\rightarrow \text{Na}^+ + \text{Cl}^-$	(7) 3.4×10^1	(7) 360 000 mg/l	(6) 3.4×10^1

* Solubility calculated from Ksp values unless stated otherwise; (1) Brown and Lemay, 1977; (2) Duchesne and Reardon, 1995; (3) Myneni et. al., 1998; (4) Warren and Reardon, 1994; (5) Appelo and Postma, 1994; (6) Pakhurst, 1995 (Phreeqc database updated 1996); (7) Freeze and Cherry, 1979 (Ksp values calculated from solubilities); (8) Fetter, 1993

For minerals affected by pH, such as some oxides and hydroxides, mineral solubility is better represented by the equilibrium constant (Keq). Keq is determined from the law of mass action, which states that the rate of chemical reaction is proportional to the activity of the participating substances (including water):

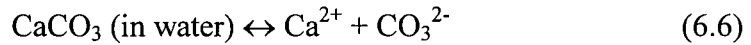
Given any two substances:



Keq is evaluated from the activity of species (activity of solids and H₂O = 1) according to:

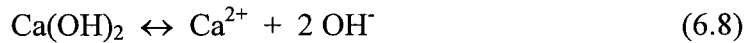
$$\text{Keq} = \frac{[\text{C}]^y \times [\text{D}]^z}{[\text{A}]^w \times [\text{B}]^x} \quad (6.5)$$

In minerals such as calcite, the relationship between K_{sp} and Keq is explained by:



$$\text{Keq} = \text{K}_{\text{sp}} = [\text{Ca}^{2+}] \times [\text{CO}_3^{2-}] \cong 3.2 \times 10^{-9} \quad (6.7)$$

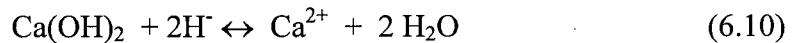
However for portlandite, K_{sp} and Keq differ because of the dependence of portlandite on the pH of water. The simple dissolution of portlandite follows:



And therefore:

$$\text{K}_{\text{sp}} = [\text{Ca}^{2+}] \times [\text{OH}^-] \cong 1.9 \times 10^{-5} \quad (6.9)$$

Whereas the solubility of portlandite is expressed as:



$$\text{Keq} = \frac{[\text{Ca}^{2+}]}{[\text{H}^+]^2} = 6.3 \times 10^{22} \quad (6.11)$$

Equation 6.11 shows that solution pH is inversely proportional to portlandite solubility, explaining why portlandite dissolves more readily in a low pH ARD solution.

Portlandite has the same solubility range as gypsum but the above showed that

portlandite is much less stable in neutral or acidic pH conditions than gypsum or ettringite. In these conditions, portlandite will readily dissolve and saturate the pore water with calcium. In the cases of Tizapa and Brunswick backfill (highest proportions of cement), secondary portlandite was found in the outer sample edges of the flooded environment only, whereas secondary gypsum was found in the outer edges of the samples in the cycled environment only. One possible explanation for these occurrences is that the pore solution of both water-leached environments becomes supersaturated with portlandite within 24 hours, hence precipitating this phase in the outer edges of the samples. With increasing leaching time, the secondary portlandite redissolves in response to the declining concentration of calcium in the pore solution as other more stable mineral phases continue to dissolve and supply other elements (i.e. Al) necessary for ettringite or gypsum to become supersaturated, nucleate and precipitate out of solution.

This study suggests that in a flooded environment, where hydraulic conductivity of the saturated material is low and the backfill mixtures contain relatively high proportions of Portland cement, secondary expansive minerals may form. Consequently, in addition to the dissolution and loss of binder components and eventually loss of binder strength, expansive minerals will create internal stresses accelerating the disintegration of the backfill.

In cyclic leaching environments where the backfill is exposed to a leaching agent for short periods, the leachate contact time may not be sufficient to precipitate secondary, expansive ettringite and gypsum. Instead, the leachate acts as an ion sink, driving

dissolution and depletion of the binder components, especially the very unstable portlandite, and flushing them out before supersaturation and precipitation of expansive mineral phases can occur. Solid phase geochemistry showed that calcium and sulfate were more effectively depleted on the edges of the samples in the cycled environments compared to flooded environment. Cyclic leaching resulted in an accelerated loss of binder material and, in the case of OPC-binder, a loss of tobermorite integrity in the periphery of the samples as indicated by the more abundant grain cavities and greater depletion of major ions in the outer layers of the cycled samples. The extent of tobermorite depletion was lower in the slag-cement binder mixture of Louvicourt pastes.

SEM observations and solid phase geochemistry of the altered layers of all samples, indicate that backfill leaching is a surface phenomenon characterized by alteration layers widening inwards with increasing leaching time. The data obtained in this relatively short term leaching study does not, however, provide information on the long-term rate of advancement of the leaching front, whether the leaching front would continue to progress or eventually cease its advancement. In all water-leached cases, the augmented porosity resulting from binder dissolution, combined with the precipitation of expansive secondary minerals suggests that advancement will likely continue to proceed as porosity is augmented with time and the leachate can more easily penetrate the backfill.

Effect of low binder content

The absence of portlandite, gypsum or ettringite in the FIM and, to some extent, in the Louvicourt samples, is likely related to both the small proportion of hydrated Portland cement available to be dissolved and to the generally higher porosity of these samples.

High sample porosity will facilitate contact between solute and solvent and the diffusion of dissolved elements out of the sample making supersaturation more difficult to achieve. In addition, if the initial concentration of portlandite to be dissolved is small, pore solution supersaturation may not be attained. This is especially true in the case of slag-mixed binders where the hydration reaction and formation of tobermorite consumes portlandite (Taylor, 1997; Kosmatka et al., 1995). In this case, supersaturation of high calcium phases (such as ettringite) is more difficult to achieve without a readily available source of dissolved calcium. Gypsum supersaturation can occur, however, as was observed in the deeper areas of the cyclic-leached pastes. This, in time, will create internal pressure within the backfill. Wide-spread secondary gypsum growth would be responsible for internal breakdown and loss of strength of the backfill.

6.2.3 Ferric Sulfate or Artificial ARD Environments

Pore water in concrete has a stable pH ~12, the stability pH of portlandite. The artificial ARD solution pH of 2.4-2.5 used in this experiment is considerably more conducive to portlandite dissolution than water. Decreased pore solution pH accelerates the dissolution of portlandite whose hydroxide ions are consumed to buffer the solution pH. This was demonstrated in these experiments by the leachate geochemistry data, where pH was buffered on contact with the pastes in the early cycles of leaching. The ABA tests also attested to the high, early dissolution of portlandite whereby NP depletion was considerably more severe and deeper penetrating in the ARD-leached pastes than in the water-leached pastes for both OPC and slag-OPC binder mixtures. Alteration layers of the ferric sulfate-leached pastes were almost double in thickness to those of the water-

leached pastes. Indeed, ARD-leached pastes had a measurable loss of mass in 20 weeks of leaching, contrary to the water-leached pastes.

SEM observations of the altered layers of OPC binder backfills showed important losses of tobermorite volume as well as more pronounced changes in tobermorite morphology (likely from the decalcification of tobermorite) and apparent strength losses (increased grain cavities viewed with SEM) in the altered layers compared to the water-leached samples. Tobermorite loss was slightly lower in the slag-OPC binder (Louvicourt) pastes, but still higher than in water-leached environments. The limited UCS tests carried out on all samples did not show, however, any strength loss with time. This is probably due to the relative thin rim of alteration compared to the diameter of the entire sample.

All ARD-leached paste samples were covered by surficial iron hydroxide precipitates. They also possessed similar amorphous, oölitic or botryoidal iron sulfate precipitates, possibly jarosite, in the second alteration layer (2nd from edge). It remains unclear, however, whether these minerals were precipitated directly from the ferric sulfate solution or precipitated as a product of the oxidation of iron sulfide in these areas. Both cases imply the penetration of an acidic ferric sulfate solution front into the paste. The sulfide minerals would have been oxidized in the acidic environment whereas metal sulfates and hydroxides would have been precipitating on the pore solution side of the front where pH and ionic strength could allow the precipitation of these minerals. In any case, it is possible that continued growth of both or either of these precipitates (iron hydroxide and/or iron sulfate) eventually passivates the surface of samples.

The evolution of leachate pH, redox potentials and aqueous iron concentrations

towards the values of the leaching solution support the suggestion that the samples were passivating as leaching progressed. It is unclear whether the depressed reactivity of the paste was a consequence of precipitate coatings from the ARD-solution (ferric hydroxide precipitates visible on all ARD-leached pastes), or if it was due to an exhaustion of soluble buffering minerals in the area actively leached. In the latter case, loading rates of paste constituents to the leachate would be proportional to the infiltration rate of the solution into the backfill. Regardless of the processes responsible for the apparent passivation of the paste, the implication is that paste backfill exposed to ARD will eventually lose its ability to buffer the drainage, following which the acidic, metal-loaded mine drainage coming in contact with the backfill would be free to flow unaltered around the backfill to the surrounding groundwater or surface water.

Another aspect of the eventual passivation of the paste is that the aggressive sulfate solution would eventually be prevented from penetrating the backfill and degrade the hydrated cement phases of the mixture. In any case, the unchanging sulfate levels in the leachates suggest that the sulfate in the leaching solution may not actively participate in cement altering reactions in the first 20 weeks of leaching. All data suggest that in 20 weeks of leaching, external sulfate plays a minimal role in cement-altering reactions when tailings already contain high concentrations of sulfate.

The presence of relatively high aqueous zinc concentrations in the Brunswick sample, combined with the results of the pyrite reactivity study, support the possibility of active sulfide mineral oxidation in the outer layers of the paste. Absence of dissolved iron in the leachate indicate one of two possibilities: 1) no oxidation of iron sulfide minerals

(pyrite, pyrrhotite), or more likely 2) oxidation of iron sulfides followed by precipitation of iron sulfate within the backfill. The pyrite reactivity study suggests that pyrite may get passivated at an early stage. Verification of the latter would require further investigation.

7 CONCLUSIONS

The following conclusions are made based on the results of this study:

7.1 PYRITE REACTIVITY STUDY

- Results of the electrochemical study supported by chemical, mineralogical and leachate chemistry data, suggested that the presence of non-pyrite sulfide mineral impurities, in contact with pyrite was the most important parameter affecting pyrite reactivity in initial leaching cycles. In more advanced stages of leaching, electrochemical analyses together with SEM observations suggested that precipitate coatings, either visible FeOOH coatings or angstrom thick sulfur or polysulfide layers not visible under SEM, played a dominant role in the reactivity of pyrites, effectively decreasing pyrite reactivity as leaching progressed.
- The presence of sphalerite was believed to form a galvanic couple with pyrite until sphalerite itself became unreactive because of precipitate coatings on its surface. Once the availability of sphalerite became limited, pyrite became free to oxidize and develop a precipitate coating, which proceeded to decrease its reactivity.
- The extent of galvanic protection offered by sphalerite was proportional to the sphalerite content of the sample. Lower concentrations of sphalerite in Louvicourt-2 is believed to have offered either less efficient or shorter time of galvanic protection compared to the Brunswick sample. Higher leachate concentrations of iron and

increased pitting of the Louvicourt-2 pyrite suggested that this sample oxidized to a greater extent than the Brunswick pyrite.

- Leachate concentrations of zinc were proportional to the sphalerite content of unleached pyrite samples. The high solubility of zinc sulfate and zinc hydroxide explains why no zinc precipitates were found in any of the leached samples.
- The presence of galena in pyrite samples was signalled by a current release at around 0 mvolts, lower than the potential at which pyrite oxidized in that environment. The intensity of the voltametric peak appeared to be proportional to the concentration of galena in the sample. Contrary to zinc, leachate lead concentrations remained low throughout the leaching period by precipitating out as anglesite (PbSO_4). It is possible that the precipitation of secondary anglesite could have indirectly provided pyrite grains some resistance to oxidation by reducing the surface area of pyrite available to oxidize.
- After the 20-week leaching period, all pyrites had decreased reactivities with respect to its unleached reactivity regardless of the presence of mineral impurities. In many cases, however, a slight regain of reactivity observed in the 20th week of leaching may indicate that surface precipitates were modified, no longer providing increasing levels of passivation. This study does not provide information as to the resistance of the passivating layers to changing conditions in the leachate. This factor commands caution in the long-term extrapolation of the effectiveness of passivation layers.

7.1.1 Huckleberry Pyrite

The potentially acid generating Huckleberry pyrite was found to be the most reactive of all samples studied. However, the reactivity of Huckleberry pyrites began to decrease within 4 weeks of leaching, progressively overcoming its reactive nature. Reactivity loss was slightly greater in the waste rock (low-grade ore)-leached sample, possibly because of the greater amount of ions in solution available to for precipitate coatings. The potentially reactive pyrite present in the low grade ore for which were carried out 3-year kinetic tests may also have been reactive but surfaces of the pyrites probably passivated from early cycles onward by the ionically charged leachate solution to which it was exposed. Post leaching mineralogical analyses should have been carried out to characterize the surfaces of these pyrites.

7.1.2 Application of this Study to Field Investigations

As pyrite is never the only sulfide mineral in a deposit or in mineral wastes, this study has shown that, at the scale of the study, occurrence of mineral impurities was the most determinant factor of the reactivity of pyrite, above crystal morphology or stoichiometric imbalances. Optical and electronic microscopy in conjunction with point source chemical analyses permitted to distinguish between solid solutions and separate mineral phases. The mode of occurrence of impurities present with pyrite dictates the ability of that mineral phase to oxidize and provide galvanic protection. If a sphalerite grain has a very small contact area with a pyrite grain or is separated by a micron size phase of a different mineral, galvanic protection could be diminished or ineffective.

Some pyrite grains that were not in contact with mineral impurities, for example in the Tizapa and Zimapan samples, oxidized to a similar extent than pyrite grains in the Huckleberry or Louvicourt-1 samples. This indicates how the intrinsic mineralogical heterogeneity of a given geologic deposits or mineral waste pile make predicting ARD generation tentative at best. Although detailed stoichiometry and mineralogy can give indications as to the expected reactivity of a mineral, these characteristics may not be the dominant factors affecting the water quality and/or overall reactivity of a waste rock pile or tailings pond. Megascopic features such as pile or pond construction, hydrology or other site conditions also influence the possible generation of ARD from a given mineral waste as observed by many researchers (Kwong, 1991; Ritchie, 1994; Schafer et al., 1994; Woyshner and St-Arnaud, 1994; Otwinowski, 1997). It is therefore imperative that representative mineralogical samples and megascopic characteristics, such as (but not limited to) multiple grain size fractions that could include sulfide mineral pockets, be included in the make up of rock samples used in kinetic tests in order to make more accurate ARD predictions.

At a fundamental level of understanding the reactivity of pyrite, however, the electrochemical characterisation technique of cyclic voltamperometry on carbon paste electrodes used in this study was an effective tool to demonstrate how the various mineralogical characteristics work together to influence the overall reactivity of pyrite. Cyclic voltamperometry was found to effectively measure the ability of pyrite to oxidize under the conditions of the kinetic tests carried out in this study. This type of analyses can be revealing in situations where kinetic test results are inconclusive, such as in the

case of Huckleberry. The high degree of expertise involved in interpreting the results of an electrochemical study, however, can be an obstacle to the widespread use of this technique as an ARD predictive tool.

7.2 CEMENTED PASTE BACKFILL LEACHING STUDY

- The small proportion of binder added to reactive tailings in this study was insufficient to rise NPR ratios above 1 or change the status of potentially acid generating tailings to non-acid generating backfill. The addition of cement to reactive tailings does not necessarily constitute an effective prevention against generation of ARD from reactive tailings.
- Some backfill mixtures that contain a high concentration of reactive pyritic tailings used as the principal aggregate (such as Tizapa backfill) may oxidize in air. This type of backfill would likely require complete submergence in water at an early stage to prevent oxidation of the tailings. Such a material would not be suitable for storage above ground or underground above the water table, where it could be exposed to air and humidity for extended periods of time.
- The hydrated portland cement phases of backfill readily dissolve in water. The extent and rapidity of depletion is generally more pronounced in a low pH solution (i.e. ARD). The small addition of neutralisation potential provided by the cement is depleted at an early stage in the external layers of the samples, leaving the tailings in these areas exposed to the environment. In 20 weeks of leaching, differences in alteration were in general more pronounced between the different leaching

environments than between the different tailings mineralogy making up the backfill mixtures. Binder content (cement or cement/slag) of the paste mixtures was found to be the most important factor affecting the release of major ions to the leachate in all environments.

- Backfill leaching is a surface phenomenon characterized by alteration layers widening towards the core of the sample with increasing leaching time. The same would be suspected to occur in underground mine workings filled with cemented backfill. The backfill would start to deteriorate at the contact with the host rock, with the depth of penetration of the alteration zone increasing with time. The current short-term leaching study does not provide, however, information on the long-term rate of advancement of the alteration zones, whether it would remain constant or eventually cease its advancement. It can be postulated from the experimental data, however, that in water-leached environments, the augmented porosity and precipitation of expansive minerals will encourage leachate penetration into the backfill. Hence in these environments, the rate of advancement of the alteration zone would probably not slow down.
- This study indicated that in ARD-leached environments, the backfill material become passivated with time. The passivation mechanism remains unclear, however, either due to an increasing thickness of ARD-solution precipitates onto the backfill or due to the formation of self-sealing iron precipitates resulting from sulfide oxidation in the outer layers of the backfill. In either case, the consequence is a decreased capacity of the backfill to neutralize incoming ARD solution generated within the host rock. In

time, the acidic and metal-loaded mine drainage could flow unaltered around the backfill to the surrounding groundwater or surface water. This study suggests that cemented tailings may not constitute, in the moderate to long-term, an effective buffering material to neutralize ARD generated within the mine or untreated ARD effluent.

- Some oxidation of sphalerite and galena occurred in the ARD and cyclic leaching environment but not in the flooded water-leached environment. Oxidation of pyrite and pyrrhotite may have occurred in the ARD or cyclic environments but would have reprecipitated within the backfill matrix. The reactivity of iron sulfides within backfill would require specific investigation.
- The apparent loss in strength that was observed under SEM for some ARD and water-leached pastes was not manifested in the ucs tests of the leached samples. These results may not be statistically significant as only one sample per category was tested. Conversely, they could indicate that the thin alteration layer is not sufficiently significant to alter the strength of the entire sample measured by the apparatus. The study methodology was not designed to measure the strength of different areas within the sample. Knowledge of the peripheral strength would be very useful (i.e. periphery of backfilled stopes) as this area is exposed to blasting when mining next to the backfill. Lower peripheral strength of the backfill may cause higher than expected dilution of the ore. Ouellet *et al.* (1998) have pointed out that this was a particular problem at the Louvicourt mine with a previous backfill formulation.

- This study showed a definite alteration of the backfill when subjected to water or ARD leaching solution, resulting in some apparent losses in strength of the backfill in the altered layers. Thicknesses of the alteration zones, however, ranged from less than 1mm to 10mm in 20 weeks, with the thicker alteration zones associated with the sulfide-rich tailings in ARD-leach solutions. It is necessary to place these results into the context of a mine setting where field rates of alteration can be higher or lower, depending on the local groundwater regime and annual precipitation on the site. The possible impacts of leaching paste backfill depend on the purpose for which the backfill is used. For example, a highly pyritic cemented backfill may not suit the purpose of a buffering plug meant to neutralize pre-existing acidic drainage within the mine. The same backfill could, however, effectively serve the purpose of ground support if placed in an isolated stope and promptly submerged in a non-ARD environment or if placed in a dry area.
- This study highlights the importance of carrying out leaching studies on cemented paste backfill mixtures in order to evaluate its stability under the conditions to which it will be exposed.

8 RECOMMENDATIONS

8.1 PYRITE REACTIVITY STUDY

Electrochemical studies of minerals should be considered where static test results are inconclusive as to the potential acid generation of a mineral waste. These studies could be realized during kinetic tests, for one or a number of sulfide minerals of concern to a particular mine site. The test set-up could consist, for example, of retrievable pockets of the sulfide mineral of concern placed into the column of rock sample being kinetically tested or placed as an appendage, similar to the Huckleberry solution-leached set-up of this study. The evolution of sulfide mineral reactivity could, in this way, be verified periodically along with the resistance of passivation coatings.

The following recommendations should be followed to facilitate interpretation and enhance the understanding of sulfide mineral leaching tests:

1. In order to facilitate the observation of precipitate products and the evolution of grain surfaces, the pyrite samples should be washed in an ultrasound bath to remove the small mineral particles electrostatically stuck to pyrite surfaces. This would not only yield particle-free pyrite surface but also provide a uniform grain size sample from which could be calculated oxidation rates per surface area of pyrite.
2. Further analyses of the precipitate products should be carried out to define the composition of the precipitates and test the resistance of the passivation layer. This

would involve:

- Detailed cathodic electrochemical analyses of the leached grains to verify the relative resistance of the grain coatings with advancing leaching cycles, increasing the cathodic current sweep to -1.5 volts.
 - Detailed quantitative mineral analyses of the precipitation products or grain surfaces. This would require making resin-mounted polished sections of leached samples and analyzing the grain edges by using either point source chemical analyses (EDX, WDX or EAS) or image analyses under SEM.
3. Additional information should be obtained on the effect of oxidation pits on the reactivity of pyrite. Cyclic voltamperometry could be performed on unleached and pitted grains of the same sample, previously acid-washed to remove the precipitate coatings.

8.2 PASTE BACKFILL STUDY

The following recommendations could facilitate future backfill leaching studies and help to resolve issues pending from this study.

1. Longer-term leaching studies would be useful for the following:
 - To obtain information on the progression of the leaching rate of the backfill with advancing leaching times and determine if the rates will increase, decrease or will remain the same as leaching progresses.

- To obtain thicker leaching zones, which would facilitate separation of the different layers and to provide a greater amount of sample to carry out multiple analyses of solid phase geochemistry, acid-base accounting or any other analyses. Bigger sample dimensions would also help in this respect, keeping sample diameter = $\frac{1}{2}$ height specification for the UCS test.
- To provide the opportunity to observe under microscope and document the oxidation of sulfide minerals.
- Larger sample sizes would be necessary in longer-term tests to keep a relatively unleached core for comparison purposes and for the determination of the rate of penetration of the alteration zone, making sure that the alteration zone will not fully penetrate the sample.
- Control samples should be prepared and stored for the duration of the tests in a lime solution at pH 12. Both the leached samples and the control samples could then be chemically analyzed and physically tested to compare the effects of leaching.
- The following analyses should be carried out as they provide very useful information as to the geochemical changes occurring within the pastes: evolution of ABA parameters in the altered layers compared to the control sample and to the core of the flooded sample; elemental analyses of the leachate, the solid phase of the altered layers, of the control sample and of the core of each leached sample. Analytical parameters should include the following: Ca, Al, Mg, K, Si, CO_3^{2-} , Fe, Zn, Cu, Pb, trace elements (depending on the mineralogy of the tailings, i.e. As, Hg, Sb, Cd) as

well as pH, conductivity and redox potentials of the leachate solutions and the sulfide speciation (S_{total} , SO_4^{2-} , S^{2-}) of the solid phase samples.

2. Preparation of the samples for analyses:
 - A polished section of the altered paste could be prepared by using ultra low viscosity resin that would be deeply penetrating. Such samples would allow quantitative EDX analyses necessary to more easily identify the various hydrated binder phases and possibly the presence of oxidation rims on sulfide minerals. These samples should be prepared in addition to the flat unpolished sections that permit the observation of 3-dimensional crystal morphologies useful for mineral identification.
3. Carry out leaching analyses of 3-month cured samples in parallel with 14-day cured samples (or earlier if necessary) to verify the effects of advanced curing on the leachability of the hydrated cement in the backfill.
4. Carry out multiple (minimum 3) leaching cells of the same samples in order to perform multiple ucs analyses, for statistical significance. This could be organized as one large cell containing 3 samples, to ensure that all are subjected to similar conditions.
5. Carry out instrumented compression tests to measure differences in strengths of the different alteration zones in the leached backfill samples.
6. With respect to excessive dilution of ore when blasting next to backfilled areas: measure the effect of blasting vibrations on partially cured and fully cured backfill to

verify its effect on the development of strength of the backfill.

7. Because of the likelihood of backfill dissolution once in place in a wet environment, it is recommended that CPB be subjected to similar scrutiny and attention as other mining wastes such as tailings and waste rock, especially in environmentally sensitive areas (i.e. above ground) or when reactive tailings are used in the backfill.

REFERENCES

- Adenot F. and Buil M., 1992: *Modelling of the Corrosion of the Cement Paste by Deionized Water*, Cement and Concrete Research, vol.22, nos. 2-3: 489-496.
- Ahmed S.M. and Giziewicz E., 1992: *Electrochemical Studies of Iron Sulfides in Relation to their Atmospheric Oxidation and Prevention of Acid Drainage; Part-II*, in: Proceedings of the International Symposium on Electrochemistry in Mineral and Metal Processing: 372-389.
- Ahmed S.M., 1991: *Electrochemical and Surface Chemical Methods for the Prevention of the Atmospheric Oxidation of Sulphide Tailings*, in: Second International Conference on the Abatement of Acidic Drainage, Montreal, Quebec, September 1991, Conference Proceedings: 305-319.
- Alpers C.N., et al., 1994: *Secondary Minerals and Acid Mine Water Chemistry*, in: Short Course Handbook on Environmental Geochemistry of Sulfide Mine-Wastes, Jambor and Blowes Editors: 245-270.
- Archibald J. and Chew J., 1998: *Brunswick Paste Fill Optimization Study, Monthly Report #1*, unpublished report to Noranda Mining and Exploration Inc., Brunswick Mining Division, March 1998, 11 pages.
- ASTM Standard C 192-90a, 1990: *Standard Practice for Making and Curing Concrete Test Specimens in the Laboratory*, Annual Book of ASTM Standards, vol. 04.02.: 119-121.
- ASTM Standard C 470-87, 1987: *Standard Specification for Molds for Forming Concrete Test Cylinders Vertically*, Annual Book of ASTM Standards, vol. 04.02.: 246-249.
- Akoz F., et al., 1995: *Effects of Sodium Sulfate Concentration on the Sulfate Resistance of Mortars with and without Silica Fume*, Cement and Concrete Research, vol. 25, no. 6: 1360-1368.
- Appelo C.A.J. and Postma D., 1994: *Geochemistry, Groundwater and Pollution*, Balkema publishers, 536 pages.
- Benzaazoua M., 1997: *Etude chimique, minéralogique et microstructurale du remblai à 4.5% liant de la mine Louvicourt*, Confidential Report by the Unité de Recherche et de Service en Technologie Minérale (URSTM), August 1997, 11 pages.
- Bethune K.J. et al., 1997: *Acid Mine Drainage: Comparison of Laboratory Testing to Mine Site Conditions*, in: Fourth International Conference on Acid Rock Drainage, Vancouver, B.C., May 1997, vol.1: 305-318.

- Bigham J.M., 1994: *Mineralogy of Ochre Deposits Formed by Sulfide Oxidation*, in: Short Course Handbook on Environmental Geochemistry of Sulfide Mine-Wastes, Jambor and Blowes Editors: 103-132.
- Blowes D. W. et al., 1995: *Microbiological, Chemical and Mineralogical Characterization of the Kidd Creek Mine Tailings Impoundment, Timmins Area, Ontario*, Geomicrobiology Journal, vol. 13: 13-31.
- Brown A.D. and Jurinak J.J., 1989: *Mechanism of Pyrite Oxidation in Aqueous Mixtures*, Journal of Environmental Quality, vol. 18: 545-550.
- Brown T.L. and Lemay H.E., 1977: *Chemistry the Central Science*, 3rd edition, Prentice-Hall, 893 pages.
- Buckley A.N., et al., 1988: *Studies of the Surface Oxidation of Pyrite and Pyrrhotite Using X-Ray Photoelectron Spectroscopy and Linear Potential Sweep Voltammetry*, in: Proceedings of the International Symposium on Electrochemistry in Mineral and Metal Processing: 234-246.
- Carde C. and Francois R., 1997: *Effect of the Leaching of Calcium Hydroxide from Cement Paste on Mechanical and Physical Properties*, Cement and Concrete Research, vol. 27, no. 4: 539-550.
- Casanova I. et al., 1996: *Aggregate Expansivity Due to Sulfide Oxidation – 1. Reaction System and Rate Model*, Cement and Concrete Research, vol. 26, no. 7: 993-998.
- Cincilla W.A. et al., 1997: *Application of Paste Technology to Surface Disposal of Mineral Wastes*, in "Tailings and Mine Waste '97": 343-356.
- Dahlstrom D.A., 1997: *Disposal of Fine Tailings in the Underground Mine*, in "Tailings and Mine Waste '97": 327-334.
- Dallaire B., Personal communication, November 13, 1997.
- DeCeukelaire L., 1991: *Concrete Surface Deterioration Due to the Expansion by the Formation of Jarosite*, Cement and Concrete Research, vol. 21, no. 4: 563-574.
- Djuric M. et al., 1996: *Sulfate corrosion of Portland Cement – Pure and Blended with 30% of Fly Ash*, Cement and Concrete Research, vol. 26, no. 9: 1295-1300.
- Domville S.J., et al., 1994: *Weathering Behaviour of Mine Tailings and Waste Rock: A Surface Investigation*, in: Third International Conference on the Abatement of Acidic Drainage, Pittsburgh, Pennsylvania, April 1994: 167-176.
- Doyle F.M. and Mirza A.H., 1996: *Electrochemical Oxidation of Pyrite Samples with Known Composition and Electric Properties* in: Proceedings of the 4th International Symposium on Electrochemistry in Mineral and Metal Processing, vol.96-6, Woods, Doyle and Richardson Editors: 203-241.

- Duchesne J., and Reardon E.J., 1995: *Measurement and Prediction of Portlandite Solubility in Alkali Solutions*, Cement and Concrete Research, vol. 25, no.5: 1043-1053.
- Eidså, G. et al., 1997: *Pyrite Oxidation Measured by Oxygen Consumption and Carbon Dioxide Production in Laboratory Respirometer Tests*, in: Fourth International Conference on Acid Rock Drainage, Vancouver, B.C., May 1997, vol.1: 319-331.
- Fetter W.C., 1993: *Contaminant Hydrogeology*, Macmillan, 458 pages.
- Free M.L. et al., 1993: *A Comparison of Leaching by Attached and Nonattached Bacteria of a Pyrite/Arsenopyrite gold-ore concentrate*, Biohydrometallurgical Technologies, vol. 1, Proceedings of the 1993 International Biohydrometallurgy Symposium, Torma, Wey and Lakshmanan Editors: 459 - 468.
- Freeze A., Cherry J., 1979: *Groundwater*, Prentice-Hall, 604 pages.
- Fu, Y. et al., 1995: *A Kinetic Study of Delayed Ettringite Formation in Hydrated Portland Cement Paste*, Cement and Concrete Research, vol. 25 no. 1: 63-70.
- Gay F. and Constantiner D., 1998: *Additives for Improving Paste Backfill Mixes*, in Tailings and Mine Waste '98 Conference Proceedings, Fort Collins, Colorado, January 1998: 159-166.
- Gifford P.M. and Gillott, J.E., 1997: *Behaviour of mortar and concrete made with activated blast furnace slag cement*, Canadian Journal of Civil Engineering, vol. 24: 237-249.
- Goldhaber M.B., 1983: *Experimental Study of Metastable Sulfur Oxianion Formation During Pyrite Oxidation at pH 6-9 and 30°C*, American Journal of Science, vol. 283: 193-217.
- Herrera M.H. et al, 1989: *The Kinetics of Sulfur Oxidation by *Thiobacillus ferrooxidans**, in: Biohydrometallurgy 1989, International Symposium Proceedings, Salley, Cready and Wichlacz Editors; 415-421.
- Hopkins P.H. and Beaudry M.S., 1989: *An Evaluation of Binder Alternatives for Hydraulic Mill Tailings*, in Innovations in Mining Backfill Technology, Hassani et al. Editors: 447-452.
- Idorn G.M., 1992: *Expansive Mechanisms in Concrete*, Cement and Concrete Research, vol. 22, no.6: 1039-1046.
- Irassar E.F., et al., 1996: *Sulfate Attack on Concrete with Mineral Admixtures*, Cement and Concrete Research, vol. 26, no.1: 113-123.

- Jambor J.L., 1994: *Mineralogy of Sulfide-rich Tailings and Their Oxidation Products*, in: Short Course Handbook on Environmental Geochemistry of Sulfide Mine-Wastes, Jambor and Blowes Editors: 59-102.
- Kosmatka S.H., et al., 1995: *Design and Control of Concrete Mixtures*, Canadian Portland Cement Association, 6th edition, 221 pages.
- Kwong Y.T.J., and Lawrence J.R., 1994: *Mineralogical Controls of Sulfide Oxidation*, National Hydrology Research Institute (NHRI) Contribution no. 94010, 87 pages.
- Kwong Y.T.J., 1993: *Prediction and Prevention of Acid Rock Drainage from a Geological and Mineralogical Perspective*, MEND Report no. 1.32.1, 47 pages.
- Kwong Y.T.J., 1991: *Acid Generation in Waste Rock as Exemplified by the Mount Wauington Minesite, British Columbia, Canada*, Conference Proceedings of the 2nd International Conference on the Abatement of Acidic Drainage, Montreal, Quebec, September 1991: 175-190.
- Lamos A.W. and Clark I.H., 1989: *The Influence of Material Composition and Sample Geometry on the Strength of Cemented Backfill*, in Innovations in Mining Backfill Technology, Hassani Scoble and Yu Editors: 89-94.
- Landriault D. et al., 1998: *Paste Technology for Underground Backfill and Surface Tailings Disposal Applications*, Short Course Notes prepared by Golder Paste Technology Ltd., January 25, 1998.
- Lawrence R.L. and Wang Y., 1997: *Determination of Neutralization Potential in the Prediction of Acid Rock Drainage*, in: Fourth International Conference on Acid Rock Drainage, Vancouver, B.C., May 1997, vol.1: 449-464.
- Lawrence R.L., 1997: *Kinetic Tests on Huckleberry Low-Grade Ore, Waste Rock and Tailings, Summary Progress Report*, unpublished consultation report prepared for Huckleberry Mines Ltd., by Lawrence Consulting Ltd, April 1997, 7 pages.
- Lázaro et al., 1995: *The Use of Carbon Paste Electrodes with Non-Conducting Binder for the Study of Minerals: Chalcopyrite*, Hydrometallurgy, vol. 38: 277-287.
- Levens, R.L. and Boldt, C.M.K., 1994: *Mine Waste Sandfill*, Mining Environmental Management, vol. 2, no. 4: 16-20.
- Li J. et al., 1992: *Application of Mixed Potential Theory in Hydrometallurgy*, Hydrometallurgy, vol.29: 47-90.
- Lord E.R.F. and Liu Y., 1998: *Depositional and Geotechnical Characteristics of Paste Produced from Oil Sands Tailings*, in "Tailings and Mine Waste '98" Conference Proceedings, Fort Collins Colorado, January 1998: 147-157

- Lowson R.T., 1982: *Aqueous Oxidation of Pyrite by Molecular Oxygen*, Chemical Reviews, vol. 82, no. 5: 461-497.
- Luff W.M. et al., 1992: *Evidence for a Feeder Pipe and Associated Alteration at the Brunswick No.12 Massive-Sulfide Deposit*, Exploration and Mining Geology, vol.1, no.2: 167-185.
- Lundgren D.G. and Silver M., 1980: *Ore Leaching by Bacteria*, Annual Reviews in Microbiology, vol 34: 263-283.
- Mangat P.S. and Khatib, J.M., 1995: *Influence of fly ash, silica fume, and slag on sulfate resistance of concrete*, ACI materials Journal, vol. 92, no.5: 542-552.
- McKibben M.A. and Barnes H.L., 1986: *Oxidation of Pyrite in Low Temperature Acidic Solutions: Rate Laws and Surface Textures*, Geochimica et Cosmochimica Acta, vol. 50: 1509-1520.
- Metha A.P. and Murr L.E., 1983: *Fundamental Studies of the Contribution of Galvanic Interaction to Acid-Bacterial Leaching of Mixed Metal Sulfides*, Hydrometallurgy, vol.9: 235-256.
- Moerman A., 1997: files sent to Valérie Bertrand via electronic mail, October 1997.
- Moses C.O. et al., 1987: *Aqueous Pyrite Oxidation by Dissolve Oxygen and by Ferric Iron*, Geochimica et Cosmochimica Acta, vol. 51: 1561-1571.
- Moses C.O. and Herman J.S., 1991: *Pyrite Oxidation at Circumneutral pH*, Geochimica et Cosmochimica Acta, vol.55: 471-482.
- Mustin C., 1992: *Approche physico-chimique et modélisation de l'oxydation bactérienne de la pyrite par Thiobacillus ferrooxidans: Rôle déterminant de la phase minérale*. Doctoral Thesis, Université de Nancy, Nancy, France: 222 pages.
- Myneni S.C.B. et al., 1998: *Ettringite Solubility and Geochemistry of the $\text{Ca}(\text{OH})_2\text{-Al}_2(\text{SO}_4)_3\text{-H}_2\text{O}$ System at 1 atm Pressure and 298K*, Chemical Geology, vol. 148: 1-19.
- Nicholson R.V., 1994: *Iron-sulfide Oxidation Mechanisms: Laboratory Studies*, in: Short Course Handbook on Environmental Geochemistry of Sulfide Mine-Wastes, Jambor and Blowes Editors: 163-183.
- Nicholson R.V. et al., 1990: *Pyrite Oxidation in Carbonate-buffered Solution: 2. Rate Control by Oxide Coatings*, Geochimica et Cosmochimica Acta, vol. 54: 395-402.
- Nicholson R.V. et al., 1988: *Pyrite Oxidation in Carbonate-buffered Solution: 1. Experimental Kinetics*, Geochimica et Cosmochimica Acta, vol. 52: 1077-1085.

- Noranda Technology Centre, 1998a: *BMD Paste Backfill Chemical and Physical Stability Project - Progress report #1*, unpublished internal report prepared for Brunswick Mining Division, Noranda Inc., January 1998, 6 pages.
- Noranda Technology Centre, 1998b: *BMD Paste Backfill Chemical and Physical Stability Project - Progress report #2*, unpublished internal report prepared for Brunswick Mining Division, Noranda Inc., February 1998, 37 pages.
- Noranda Technology Centre, 1998c: *BMD Paste Backfill Chemical and Physical Stability Project - Progress report #3*, unpublished internal report prepared for Brunswick Mining Division, Noranda Inc., March 1998, 16 pages.
- Noranda Technology Centre, 1998d: *BMD Paste Backfill Chemical and Physical Stability Project - Progress report #4*, unpublished internal report prepared for Brunswick Mining Division, Noranda Inc., April 1998, 36 pages.
- Noranda Technology Centre, 1998e: *Benchmarking of BMD Tailings Against Louvicourt Tailings*, unpublished internal report prepared for Brunswick Mining Division, Noranda Inc., April 1998, 19 pages.
- Otwinowski M., 1997: *Meso-Scale Characterization of the Geochemical and Physical Processes Responsible for Acid rock Drainage*, in: 4th International Conference on Acid Rock Drainage, Vancouver, B.C., May 1997, vol.2: 569-585.
- Ouellet J. et al., 1998: *Mechanical, Mineralogical and Chemical Characterization of a Paste Backfill*, in: Tailings and Mine Waste '98 Conference Proceedings, Fort Collins Colorado, January 1998: 139-146.
- Pakhurst D.L., 1995: PHREEQC computer program for geochemical calculations, U.S. Geological Survey, Water-Resources Investigations Report no. 954227, 134 pages.
- Peters E., 1984: *Electrochemical Mechanisms for Decomposing Sulfide Minerals*, in: Proceedings of the International Symposium on Electrochemistry in Mineral and Metal Processing, Richardson, Srinivasan and Woods Editors: 343-361.
- Price W.A. et al., 1997: *Guidelines for the Prediction of Acid Rock Drainage and Metal Leaching for Mines in British Columbia: Part II. Recommended Procedures for Static and Kinetic Testing*, in: 4th International Conference on Acid Rock Drainage, Vancouver, B.C., May 1997, vol.1: 15-30.
- Revertegat E. et al., 1992: *Effect of pH on the Durability of Cement Pastes*, Cement and Concrete Research, vol. 22, no. 2-3: 259-272.
- Ritchie A.I.M., 1994: *Sulfide Oxidation Mechanisms: Controls and Rates of Oxygen Transport*, in: Short Course Handbook on Environmental Geochemistry of Sulfide Mine-Wastes, Jambor and Blowes Editors: 201-245.

- Schafer W.M. et al., 1994: *Monitoring Gaseous and Liquid Flux in Sulfide Waste Rock*, in: 3rd International Conference on the Abatement of Acidic Drainage, Pittsburgh, Pennsylvania, April 1994: 410-418.
- Singer P.C. and Stumm W., 1970: *Acidic Mine Drainage: The Rate-Determining Step*, Science, vol. 167: 1121-1123.
- Shayan A., 1988: *Deterioration of a Concrete Surface Due to the Oxidation of Pyrite Contained in Pyritic Aggregates*, Cement and Concrete Research, vol. 18, no. 5: 723-730.
- Steffen, Robertson and Kirsten Ltd., 1989: *Draft Acid Rock Drainage Technical Guide*, vol. 1, BCAMD Task Force Report no.5.10.
- Taylor H.F.W., 1997: *Cement chemistry*, Thomas Telford editors, 459 pages.
- Torii K et al., 1995: *Sulfate Resistance of High Fly Ash Content Concrete*, Cement and Concrete Research, vol. 25, no. 4: 759-768.
- Udd J.E., 1989: *Backfill Research in Canadian Mines*, in "Innovations in Mining Backfill Technology", Hassani, Scoble and Yu Editors: 3-13.
- Vernet C., 1994: *Introduction to Portland Cement Chemistry*, in "Applications of NMR Spectroscopy to Cement Science", Colombet and Grimmer Editors: 29-53.
- Wadsworth M.E. et al., 1993: *Electrochemistry of Pyrite*, in: Hydrometallurgy; Fundamentals, Technology and Innovations, Proceedings of the 4th International Symposium on Hydrometallurgy, Hiskey and Warren Editors, Salt Lake City, Utah, August 1993: (Chapter 5) 85-99.
- Warren C.J. and Reardon E.J., 1994: *The Solubility of Ettringite at 25 deg. C*, Cement and Concrete Research, vol. 24, no. 8: 1515-1524.
- Williams D.J., 1997: *Effectiveness of Co-disposing Coal Washery Wastes*, in: Tailings and Mine Waste '98 Conference Proceedings, Fort Collins Colorado, January 1998: 335-341.
- Woysner M.R. and St-Arnaud L., 1994: *Hydrogeological Evaluation and Water Balance of a Thickened Tailings Deposit Near Timmins, ON, Canada*, in: 3rd International Conference on the Abatement of Acidic Drainage, Pittsburgh, Pennsylvania, April 1994: 198-207.
- Ybarra, R.R., 1998: *Predicción de la Generación de Drenajes Acidos en una Presa de Jales con Altos Contenidos de Pirita*. M.Sc. Thesis, Faculty of Chemical Sciences, Universidad Autónoma de San Luis Potosí (Mexico).

Zhu X., et al., 1992: *Transpassive Oxidation of Pyrite*, in: Proceedings of the International Symposium on Electrochemistry in Mineral and Metal Processing, Woods y Richardson Editors: 391-409.

APPENDIX I - ANALYTICAL RESULTS: PYRITE LEACHATE

Table I-1 (cont'd) Pyrite - Leachate Chemistry

Cycle	Pyrite Leach Solution																				
	Pb (mg/l)							Zn (mg/l)							As (mg/l)						
	Hk-l	Hk-w	Lou1	Lou2	Tiz	Zim	Brw	Hk-l	Hk-w	Lou1	Lou2	Tiz	Zim	Brw	Hk-l	Hk-w	Lou1	Lou2	Tiz	Zim	Brw
1	0.5	0.4	6.1	4.9	6.8	19	61	0.3	1.6	2.8	22	18	28	240	<1	<1	<1	<1	<1	<1	<1
2	1.4	1.4	5.1	4.3	7.4	5.9	73	2.3	0.4	8.3	47	42	94	366	<1	<1	<1	<1	<1	<1	<1
3	1.0	1.1	5.0	3.8	5.8	5.5	87	0.5	0.2	7.7	53	48	75	320	<1	<1	<1	<1	<1	<1	<1
4	0.7						92	0.1	0.1	2.5	33	8.4	51	174	<1	<1	<1	<1	<1	<1	<1
5							92	0.1	0.2	4.1	39	9.2	68	177	<1	<1	<1	<1	<1	<1	<1
6							71	0.3	0.1	3.2	40	17	59	180	<1	<1	<1	<1	<1	<1	<1
7							46	0.1	0.6	2.0	31	10	43	188	<1	<1	<1	<1	<1	<1	<1
8							49	0.1	0.4	3.0	42	12	52	225	<1	<1	<1	<1	<1	<1	<1
9		0.2	3.0	2.2	5.4	8.0	37	0.2	<0.	2.1	36	9.0	36	273	<1	<1	<1	<1	1.1	3.4	<1
10	0.4	0.4	3.3	1.3	5.2	6.0	27	0.2	0.1	2.0	33	6.5	32	261	<1	<1	<1	<1	<1	2.7	<1
11	0.3	<0.1	4.3	2.3	7.2	17	21	0.1	<0.	0.8	18	2.7	15	295	<1	<1	<1	<1	1.0	4.4	<1
12	0.1	0.2	4.2	1.7	6.6	13		0.1	<0.	0.4	9	1.6	7	222	<1	<1	<1	<1	1.0	3.2	<1
13	0.5	0.3	4.1	2.0	6.8	10		0.3	1.2	0.7	14	2.2	10	239	<1	<1	<1	<1	<1	3.7	<1
14	0.3	0.3	2.3	1.4	7.9	11	9.5	<0.1	0.9	1.7	28	3.4	11	183	<1	<1	<1	<1	<1	4.1	<1
15	0.5	0.8	3.3	1.8	6.5	14	9.9	<0.1	0.5	1.2	15	2.7	8.8	176	<1	<1	<1	<1	1.4	4.6	<1
16	0.5	0.5	3.4	1.8	6.1	13	6.5	0.2	0.1	1.0	22	3.2	9.5	154	<1	<1	<1	<1	1.4	4.1	<1
17	0.4	0.5	3.7	1.0	6.0	13	7.0	0.3	<0.	0.8	16	1.9	6.1	149	<1	<1	<1	<1	1.5	4.2	<1
18	0.9	0.2	2.8	0.8	6.3	12	8.4	0.2	<0.	1.2	19	2.1	7.3	145	<1	<1	<1	<1	1.4	3.4	<1
19	1.6	1.7	2.4	1.5	5.9	13	9.4	0.1	0.1	1.1	22	2.4		135	<1	<1	<1	<1	1.3	3.6	<1
20	0.3	3.1	2.3	0.5	6.0	10	8.3	0.2	0.1	0.9	16	2.1	6.6	133	<1	<1	<1	<1	1.6	3.4	<1
21	0.6	0.6	2.6	0.6	7.6	11	7.4	0.3	0.1	1.1	18	2.4	6.4	131	<1	<1	<1	<1	1.6	3.4	<1
22	0.2	2.7	2.6	0.5	6.5	14	5.1	0.1	0.3	0.5	8.4	1.5		151	<1	<1	<1	<1	1.6	4.1	<1
23	0.2	0.5	2.6	0.7	7.8		5.4	<0.1	0.1	0.8	9.5	2.2		146	<1	<1	<1	<1	1.7		<1
24	0.1	0.3	2.5	0.6	6.6	13	7.3	<0.1	<0.	0.5	7.2	1.9	3.6	147	<1	<1	<1	<1	<1	5.7	<1
25	0.2	0.3	2.8	0.5	6.8	11	6.9	0.1	0.2	0.6	7.1	1.6	3.3	187	<1	<1	<1	<1	<1	4.6	<1
26	0.1	0.6	1.8	0.2	7.2	5.7	4.2		0.2	0.5	4	1	1.4	201	<1	<1	<1	<1	1.1	1.5	<1
27	0.2	0.6	1.3	0.2	5.5	6.4	4.1	0.3	0.3	0.5	5.3	1.2	1	248	<1	<1	<1	<1	<1	2.1	<1
28	0.4	0.4	1.8	0.5	3.9	2.0	4.4	0.4	0.2	0.5	3.8	1.3	0.7	213	<1	<1	<1	<1	<1	3	<1
29	0.1	1.1	1.3	0.3	6.3	5.9	3.7	0.2	0.3	0.8	4.6	1	1.5	246	<1	<1	<1	<1	1	2.8	<1
30	0.2	0.3	1.4	0.3	6.7	8.1		0.3	0.1	0.6	4.8	1.1	1.4		<1	<1	<1	<1	<1	3	
31	0.1	0.5	1.7	0.4	7.1	7.9	2.8	0.1	0.3	0.5	4	1.2	1.1	100	<1	<1	<1	<1	<1	2.6	<1
32	0.4	1.2					5.5	0.2	0.8	0.1					<1	<1	<1	<1	<1		<1
33	0.3	0.3					6.7	0.4	0.1		4.4	1.1			<1	<1	<1	<1	<1		<1
34	0.3	0.5	0.4	1.1	5.4	1.9	6.2	0.6	0.1	0.5	0.2	1.3	1.1		<1	<1	<1	<1	<1	1.7	<1
35	0.2	0.2	0.8	0.3	7.3	7.2	7.2	0.2	0	0.5	5	1.1	1		<1	<1	<1	<1	<1	2.1	<1
36	0.3	0.3	0.6	<0.1	7.2	6.6	9.9	0.2	0	0.7	3.2	0.8	0.9	65	<1	<1	<1	<1	<1	2.3	<1
37	0.2	0.4	0.7	0.1	7.0	6.1	6.7	0.3	0.2	0.8	4.1	1.4	1.5	62	<1	<1	<1	<1	<1	2.7	<1
38	0.2	0.3	0.8	0.2	6.1	4.6	5.0	0.2	0.3	0.7	3.9	1.2	2	57	<1	<1	<1	<1	<1	2.5	
39	0.6	0.5	0.5	0.2	5.6	3.3	5.6	0.6	0.2	0.4	3.3	1.2	1	27	<1	<1	<1	<1	<1	2.1	
40	0.4	0.59	<0.1	<0.1	6.5	3.3		0.7	0.4	0.4	2.8	1	0.8		<1	<1	<1	<1	<1	1.8	

Table I-1 (cont'd) Pyrite Leachate Chemistry

Cycle	Pyrite Leach Solution																				
	Fe total (mg/l)							SO4 (g/l)							Cu (mg/l)						
	Hk-l	Hk-w	Lou1	Lou2	Tiz	Zim	Brw	Hk-l	Hk-w	Lou1	Lou2	Tiz	Zim	Brw	Hk-l	Hk-w	Lou1	Lou2	Tiz	Zim	Brw
1	388	679	80	85	86	27	8.0	1.0	1.3	0.3	0.3	0.2	0.1	0.1	<0.1	0.2	0.1	0.4	0.2	0.2	<0.1
2	848	764	80	97	64	118	0.5	1.7	1.9	0.3	0.4	1.7	0.3	0.2	<0.1	<0.1	2.0	<0.1	16	<0.1	<0.1
3	738	818	69	108	61	97	0.3	2.4	1.9	0.4	0.3	0.2	0.3	0.2	<0.1	<0.1	1.1	<0.1	22	0.3	<0.1
4	475	427	44	66	45	86	0.2	0.9				0.1	0.2	0.1	<0.1	0.1	0.4	0.1	0.4	0.3	<0.1
5	345	448	70	75	46	68	0.3	1.1				0.2	0.3	0.1	0.1	0.0	0.9	0.1	6.6	0.4	<0.1
6	419	364	47	66	38	53	0.3	0.9				0.1	0.2	0.1	0.0	0.0	0.5	0.0	4.2	0.3	<0.1
7	340	286	39	58	35	45	0.2	0.7			0.2	0.1	0.2	0.1	0.1	0.1	0.4	0.1	4.4	0.3	<0.1
8	273	336	49	64	43	45	0.2	0.8			0.2	0.1	0.2	0.2	0.0	0.0	0.1	0.1	8.4	0.3	<0.1
9	302	280	48	57	47	40	0.2	0.5	0.1	0.2	0.2	0.2	0.1	0.1	0.1	<0.1	0.4	<0.1	3.6	0.3	<0.1
10	246	304	50	52	45	34	0.2	0.3	0.9	0.3		0.2	0.2	0.5	<0.1	<0.1	0.4	<0.1	3.4	0.3	<0.1
11	247	173	33	35	30	27	0.2	0.8	0.4	0.2		0.2	0.2	0.5	<0.1	<0.1	0.2	<0.1	1.9	0.2	<0.1
12	146	122	17	21	19	15		0.9	0.4	0.2		0.1	0.1	0.1	<0.1	<0.1	0.2	<0.1	1.6	0.2	0.2
13	80	156	23	26	24	19		0.4	0.4	0.3		0.2	0.2	0.2	<0.1	0.1	0.3	<0.1	1.4	0.2	<0.1
14	128	287	41	51	33	20		0.4	0.6	0.2		0.2	0.2	0.2	<0.1	0.1	0.4	<0.1	2.1	0.2	<0.1
15	256	203	35	40	37	21		0.5	0.5	0.3		0.4	0.2	0.1	0.1	<0.1	0.3	<0.1	1.6	0.2	0.2
16	152	181	34	36	39	17		0.1	0.5	0.5	0.1	0.1	0.0	0.1	<0.1	0.12	0.4	<0.1	2.2	<0.1	<0.1
17	129	160	35	30	29	14		0.2	0.1	0.2	0.1	0.1	0.0	0.2	<0.1	<0.1	0.4	<0.1	1.7	<0.1	<0.1
18	125	180	46	28	28	14		0.3	0.5	0.4	0.1	0.1	0.1	0.1	<0.1	<0.1	0.5	<0.1	1.5	0.3	<0.1
19	139	161	42	31	31	13		0.3	0.6	0.2	0.2	0.2	0.3	0.2	<0.1	<0.1	0.4	<0.1	1.9	0.2	<0.1
20	142	163	41	24	33	14		0.5	0.4	0.1			0.1	0.6	0.11	<0.1	0.2	<0.1	1.6	0.2	<0.1
21	112	156	47	21	33	13		0.4							<0.1	<0.1	0.3	<0.1	1.9	0.3	<0.1
22	106	123	28	14	26	12									<0.1	<0.1	<0.1	<0.1	1.0	0.2	0.1
23	75	139	46	17	28	11	0.5								0.00	<0.1	0.2	<0.1	1.4		<0.1
24	91	89	26	12		12	0.7		<0.1	0.2		0.2	0.1	0.2	0.00	0.15	0.2	0.1	1.6	<0.1	<0.1
25	60	99	28	12		9	1.1	0.3			0.1			0.4	0.14	0.18	0.2	0.2	1.4	<0.1	0.2
26		73	15	8	30	2	2.1	0.3	0.3	0.0	0.1	0.1			0.00	0.13	0.2	0.1	0.8	<0.1	0.4
27		85	17	8		3	7.9	0.3	0.3	0.1	0.1	0.1	0.1	0.2	0.17	0.14	0.2	0.1	1.0	<0.1	0.1
28	70	58	15	6		<0.1	16		0.3			0.1	0.1	0.5	0.17	0.1	0.1	<0.1	0.9	<0.1	0.3
29	47	67	20	8		3	31	0.1	0.3				0.1	0.5	0.14	0.11	0.1	0.1	0.8	<0.1	0.5
30	47	69	19	9	12	3		0.2	0.3			0.1	0.1		0.12	0.13	0.2	0.1	0.9	0.1	
31		73	20	11	15	3	53	0.6	0.2	0.1				0.5	0.13	<0.1	0.1	0.8	0.1	<0.1	
32	46	103					57	0.3						0.5	0.00	0.28	0.1	0.1	1.1	0.1	1.5
33	68	98					55							0.4	0.13	0.15	0.2	0.1	0.9	0.1	2.4
34	71	87	15	11	17	2	66		0.3	<0.1	<0.1	0.1	0.1	0.4	0.12	0.16	<0.1	<0.1	1.3	<0.1	4.2
35	58	82	21	12	19	3	82	0.2	0.2	0.1	<0.1	0.1	0.1	0.5	0.10	0.12	<0.1	<0.1	1.0	<0.1	6.4
36	60	67	16	10	15	3	76	0.2	0.2	<0.1	<0.1	0.1	0.1		0.00	<0.1	<0.1	<0.1	0.7	<0.1	4.3
37	60	88	21	13	16	3	89	0.2	0.2	<0.1	0.1	0.2	0.1	0.3	0.00	0.11	0.1	<0.1	1.1	<0.1	4.5
38	67	73	22	12	15	4	127	0.2	0.2	<0.1	<0.1	0.1	0.1		0.11	<0.1	0.1	<0.1	1.0	<0.1	
39	64	72	19	10	13	3	110		0.2	0.1	0.1	0.2	0.1		0.13	0.11	<0.1	<0.1	0.8	<0.1	
40	52.8	61.1	16	10	11	1.9		0.2	0.2	<0.1	<0.1	0.1	0.1		<0.1	0.14	0.1	<0.1	<0.1	0.1	

Table I-1 (cont'd) Pyrite Leachate Chemistry

Cycle	Pyrite Leach Solution																					
	conductivity (uS)							pH							Redox potential (mV)							
	Hk-l	Hk-w	Lou	Lou	Tiz	Zim	Brw	Hk-l	Hk-w	Lou1	Lou2	Tiz	Zim	Brw	Hk-l	Hk-w	Lou1	Lou2	Tiz	Zim	Brwk	
1		1954	508	548			947		3.8	4.3	4.5	4.1	4.8	5.0								208
2		1751	2900	576	676	524	581	647	3.1	2.7	3.6	3.9	3.5	4.7	5.2							194
3		3900	2860	424	573	490	487	609	2.4	2.4	3.4	3.6	3.3	3.9	5.1							245
4		2440	1909	344	444	418	519	529	2.4	2.6	3.5	3.8	3.4	4.0	5.1							204
5		1744	2490	367	439	409	524	541	2.6	2.4	3.5	3.8	3.3	3.6	4.9							276
6		2460	2360	405	450	413	515	511	2.4	2.4	3.4	3.8	3.4	3.4	5.0							219
7		2430	1697	322	391	409	476	538	2.5	2.6	3.6	3.9	3.3	3.4	5.0							289
8		1820	2400	385	470	443	478	573	2.5	2.4	3.4	3.6	3.2	3.3	4.9							155
9		2420	1917	402	430	481	466	668	2.3	2.5	3.4	3.7	3.2	3.4	5.0							256
10		1908	2160	381	361	444	369	196	2.6	2.5	3.4	4.4	3.2	3.5	5.1							196
11		1945	1296	299	277	380	304	665	2.5	2.6	3.4	3.7	3.2	3.3	5.0							220
12		1412	972	195	207	243	174	687	2.6	2.9	3.8	5.6	3.7	3.7	5.1		332	301	131	295	286	268
13		899	1111	227	256	307	227	629	3.0	2.6	3.4	3.5	3.2	3.4	5.4	334	320	309	291	322	315	228
14		1119	1391	358	396	411	260	473	2.6	2.7	3.4	3.7	3.2	3.4	5.4	329	331	310	292	324	308	139
15		1440	1088	320	328	403	261	487	2.7	2.8	3.3	3.6	3.1	3.4	5.3	332	315	305	280	315	304	143
16		1123	1378	296	701	410	236	478	2.9	2.6	3.4	3.6	3.1	3.4	5.5	317	335	311	290	327	298	140
17		1207	1190	329	281	390	247	473	2.6	2.6	3.3	3.6	3.1	3.4	5.4	331	329	311	297	343	320	173
18		1167	1374	418	275	365	242	423	2.7	2.6	3.3	3.7	3.2	3.4	5.4	333	326	317	288	314	310	237
19		1251	1301	417	292	434	243	445	2.7	2.6	3.3	3.6	3.2	3.5	5.4	334	335	317	295	329	319	231
20		1365	1230	335	245	366	220	410	2.7	2.5	3.2	3.6	3.1	3.3	5.3	340	335	308	279	327	330	251
21		1042	1379	435	244	425	225	434	2.7	2.6	3.3	3.7	3.1	3.4	5.5	333	329	315	292	325	318	149
22		1124	883	269	159	323	305	503	2.8	2.8	3.4	3.8	3.2	3.5	5.8	331	320	291	283	307	305	196
23		757	1336	416	182	567	179	485	2.9	2.7	3.3	3.7	3.2	3.5	5.2	315	323	311	284	307	299	178
24		950	950	262	173	372	147	429	2.8	2.8	3.4	3.8	3.2	3.7	5.4	323	326	303	284	318	301	
25		818	1087	301	160	313	129	517	2.9	2.8	3.5	4.0	3.3	3.9	5.4	319	325	304	274	307	269	233
26		944	695	142	110	197	135	603	2.9	3.0	4.1	3.6	3.6	3.3	5.1	325	309	242	135	241	144	209
27		674	829	196	136	222	101	683	3.3	2.8	3.5	3.8	3.3	4.1	5.0	311	323	270	240	277	236	197
28		526	798	212	120	270	400	655	3.2	2.9	3.7	4.1	3.5	4.2	4.7	302	279	299	257	305	145	204
29		231	684	223	154	240	130	666	3.9	3.1	3.7	4.2	3.6	4.0	5.3	273	286	285	261	288	255	153
30		588	679	189	124	195	69	654	3.3	3.1	3.9	4.2	3.6	4.4	5.2	302	281	242	217	267	218	
31		629	720	244	130	198	75	874	3.2	3	3.7	4.2	3.7	5.0	4.1	270	318	292	276	302	241	257
32		653	837	241	157	246	77	731	3.2	2.9	3.6	3.8	3.5	5.5	4.1	303	320	286	263	286	184	257
33		748	797	222	146	256	67	720	3	2.9	3.7	4.0	3.5	4.6	3.7	293	316	288	252	288	194	266
34		754	736	166	128	221	82	783	3.1	3.1	4.1	4.5	3.8	5.6	3.5	317	319	256	213	277	128	241
35		701	701	231	141	243	63	830	3.1	3	3.7	4.0	3.6	4.5	3.5	324	318	293	271	300	220	273
36		712	580	152	110	194	68	739	3.1	3.1	3.8	4.1	3.5	4.4	3.3	324						308
37		654	685	180	119	226	55	771	3.1	3.1	3.8	4.3	3.6	4.6	3.2		319	284	240	302	223	310
38		697	635	190	118	196	69	802	3.1	3.1	3.7	4.1	3.6	4.5	3.2	322	311	281	242	289	216	312
39		691	619	158	99	160	55	721	3.1	3	3.9	4.3	3.7	5.3	3.2	306	312	240	224	273	175	317
40		575	453	128	91	153	47	795	3.3	3.2	4.0	4.2	3.7	4.7	3.2	309	306	230	221	279	190	315

Table I-1 Pyrite Leachate Chemistry

Days	Date	Cycle	Column Leach soln											Distilled water			
			con (uS)	pH	vol (ml)	edo (mV)	Fetot (mg/l)	SO4 (g/l)	Cu (mg/l)	Zn (mg/l)	Ca (mg/l)	Mg (mg/l)	Na (mg/l)	K (mg/l)	pH	cond (uS)	Redox (mV)
0	07-Nov-97	1			233		0.31	0.11	<0.1	<0.1	31	3.6	26	9.5	5.4		
3	10-Nov-97	2		6.7	228		0.10	0.10	<0.1	<0.1	30	1.7	24	9.0	5.6	2.1	
6	14-Nov-97	3	340	5.5	245		0.42	0.12	<0.1	<0.1	26	1.5	22	8.5	5.3	1.6	
10	18-Nov-97	4	221	7.8	213		0.10	0.01	<0.1	<0.1	23	1.3	20	7.4	5.5		
14	21-Nov-97	5	288	6.8	212										5.6	19	
17	24-Nov-97	6	277	6.2	225		0.04	0.12	<0.1	<0.1	28	1.9	20	9.2	5.6	1.8	
20	27-Nov-97	7	258	6.4	205		0.01	0.08	<0.1	<0.1	28	1.8	18	7.3	5.5	4.6	
23	01-Dec-97	8	238	6.2	202		0.00	0.09	<0.1	<0.1	29	1.6	15	6.5	5.6	2.6	
27	04-Dec-97	9	240	6.2	203		0.23		<0.1	<0.1	26	1.5	16	7.0	5.5	10	
30	08-Dec-97	10	247	6.3	217		<0.1	0.25	<0.1	1.7	39	1.8	15	7.2	5.6	16	
34	12-Dec-97	11	235	6.4	206		<0.1	0.80	<0.1	<0.1	38	1.7	15	7.4	5.5	28	269
38	15-Dec-97	12	188	6.6	202		<0.1	0.25	<0.1	<0.1	40	2.0	14	7.3	5.4	21	128
41	18-Dec-97	13	163	6.6	202	90	<0.1	0.18	<0.1	<0.1	31	1.5	10	4.8	5.4	26	232
44	29-Dec-97	14	157	6.6	195	209	<0.1	0.08	<0.1	<0.1	30	1.4	12	6.0	5.5	27	248
55	05-Jan-98	15	295	5.9	205	231	<0.1	0.10	<0.1	<0.1	51	2.5	13	7.3	5.5	17	256
62	08-Jan-98	16	287	6.1	210	122	<0.1	0.14	<0.1	<0.1	56	2.7	14	8.4	5.5	8.3	178
65	12-Jan-98	17	181	6.3	194	137	<0.1	0.11	<0.1	<0.1	45	2.3	12	6.5	5.4	7.3	269
69	15-Jan-98	18	219	6.1	204	174	<0.1	0.11	<0.1	<0.1	83	7.8	14	6.6	5.6	9.2	144
72	19-Jan-98	19	169	6.4	198	161	<0.1	0.09	<0.1	<0.1	35	2.1	13	7.0	5.4	9.4	271
76	23-Jan-98	20	170	5.7	200	231	<0.1	0.25	<0.1	<0.1	36	1.7	10	5.5	5.4	10	134
80	26-Jan-98	21	151	6.2	200	159	<0.1	0.05	<0.1	<0.1	36	2.0	11	5.9	5.5	4.5	217
83	29-Jan-98	22	154	6.4	205	157	<0.1	0.10	<0.1	<0.1	70	6.6	10	5.3	5.7	8.7	183
86	02-Feb-98	23	138	6.1	197	180	<0.1	0.07	<0.1	<0.1	28	1.3	10	4.9	5.5	6.1	248
90	06-Feb-98	24	163	5.7	181	165	<0.1	0.08	<0.1	<0.1	62	6.0	11	5.1	5.3	4.6	265
94	09-Feb-98	25	163	5.7	181	165	<0.1	0.07	<0.1	<0.1	33	1.94	11	5.1	5.5	6.4	250
97	12-Feb-98	26	147	5.7	185	217	<0.1	0.06	<0.1	<0.1	41	1.86	10	6.06	5.5	6.4	250
104	16-Feb-98	27	143	6.0	184	148	<0.1	0.07	<0.1	<0.1	32	2.0	9.6	7.12	5.6	9.3	272
107	19-Feb-98	28	143	5.9	171	167	<0.1	0.07	<0.1	<0.1	27	1.73	9.6	5.81	5.6	9.5	184
111	23-Feb-98	29	130	6.4	226	193	<0.1	0.06	<0.1	<0.1	29	1.82	11	6.36	5.5	18	213
111	26-Feb-98	30	163	6.3	205	157	<0.1	0.08	<0.1	<0.1	31	1.89	11	6.8	5.6	39	232
114	02-Mar-98	31	152	6.1	191	203	<0.1	0.07	<0.1	<0.1	35	1.73	10	6.76	5.3	6.9	221
118	05-Mar-98	32	166	6.0	190	206	<0.1	0.07	<0.1	<0.1	53	2.15	10	6.89	5.3	5.8	241
121	09-Mar-98	33	160	5.9	204	123	<0.1	0.06	<0.1	<0.1	41	1.21	9.2	6.2	5.6	5.4	250
125	12-Mar-98	34	170	5.8	214	171	<0.1	0.06	<0.1	<0.1	35	1.44	8.9	5.8	5.5	8.8	247
128	16-Mar-98	35	165	6.2	192	164	<0.1	0.06	<0.1	<0.1	28	1.5	9.5	5.64	5.6	48	163
132	20-Mar-98	36	166	5.8	168	161	<0.1	0.10	<0.1	<0.1	31	1.3	10	6.5	5.4	4.1	211
136	25-Mar-98	37	168	5.8	190	160	<0.1	0.07	<0.1	<0.1	33	1.8	9.1	6.2	5.3	16	234
141	27-Mar-98	38	169	6.1	187	204	<0.1	0.05	<0.1	<0.1	36	2.1	9.3	6.53	5.2	3.4	263
143	30-Mar-98	39	165	6.2	187	198	<0.1	0.07	<0.1	<0.1	38	2.2	9	6.36	5.6	14	204
146	02-Apr-98	40	166	6.2	185	142	<0.1	0.07	<0.1	<0.1	39	2.25	8.7	6.41	5.6	14	173

Note: empty spaces = no data available

APPENDIX II - ANALYTICAL RESULTS: PASTE BACKFILL LEACHATE

Table II-1 Paste Leachate Chemistry - Flooded Water Cells

ay	Date	ycl	Distilled water data				Paste leach water								Redox potential			
			batch	cond	pH	redox	conductivity (uS)				pH				(mV SHE)			
							(uS)	(mV)	Tiz	Louv	Brw	FIM	Tiz	Louv	Brw	FIM	Tiz	Lou
4	16-Dec-97	1	1	28	5.5	499	3710	3670	3550	3100	11	7.4	7.7	7.8	286	400	405	388
7	18-Dec-97	2	2	17	5.6	422	3440	3450	3260	2720	11	6.6	6.7	6.7	311	371	410	402
18	30-Dec-97	3	3	33	5.6	429	3120	2940	2960	2520	11	7.8	7.2	8.3	303	422	395	414
25	06-Jan-98	4	4	6.1	5.6	509	2660	2540	2480	2230	10	8.5	8.1	8.5	280	314	333	328
32	13-Jan-98	5	5	18	5.5	469	2410	2310	1798	1920	11	8.5	8.7	8.9	257	311	295	307
40	21-Jan-98	6	6	5.8	5.58	442	1519	1668	1678	1475	11	7.8	7.5	8.4	290	359	374	252
46	27-Jan-98	7	7	6.3	5.61	488	1384	1403	1477	1225	11	8.3	8.1	8.3	261	340	347	349
54	04-Feb-98	8	8	16	5.61	466	1346	1496	1610	1185	11	8.5	9.2	9.2	276	318	320	313
61	11-Feb-98	9	9	3.3	5.4	459	1295	1398	1261	1091	11	9.4	9.2	9.4	304	400	368	376
68	18-Feb-98	10	10	5.5	5.4	555	1242	1111	1167	1031	11	9.4	9.1	9.5	280	316	321	308
75	25-Feb-98	11	11	39	5.6	443	1212	1082	1201	838	11	9.3	9.1	9.3	288	356	350	337
82	04-Mar-98	12	12	6.1	5.3	393	1256	1097	1218	811	11	9.0	8.9	9.5	257	396	302	407
89	11-Mar-98	13	13	7.8	5.3	475	1169	1005	1127	777	11	9.2	9.2	8.9	213	354	308	333
96	18-Mar-98	14	14	15	5.2	479	1101	982	1149	701	11	9.3	9.7	9.4	234	294	276	298
103	25-Mar-98	15	15	6.5	5.5	434	1080	952	1305	699	11	8.7	9.2	9.1	236	324	301	332
108	30-Mar-98	16	16	14	5.4	447	1067	937	1120	715	11	8.5	9.1	8.4	233	412	359	394
117	08-Apr-98	17	17	30.7	5.5	466	1113	1003	1221	737	9.8	8.3	8.8	8.5	260	349	326	354
124	15-Apr-98	18	18	65	5.6	452	1140	947	1228	732	10	7.9	8.4	8.5	252	319	312	329
131	22-Apr-98	19	19	47	5.6	469	1200	1026	1260	761	10	7.9	7.7	8.1	243	361	332	327
138	29-Apr-98	20	20	10.5	5.4	400	1033	890	1104	656	10	8.1	8.4	8.5	228	347	327	330

ay	Date	ycle	Fe total (mg/l)				Cu (mg/l)				Zn (mg/l)				Pb (mg/l)			
			Tiz	Louv	Brw	FIM	Tiz	Louv	Brw	FIM	Tiz	Louv	Brw	FIM	Tiz	Lou	Brw	FIM
4	16-Dec-97	1	<0.1	0.74	<0.1	0.23	<0.1	<0.1	<0.1	<0.1	<0.1	<0.1	0.14	<0.1	0.2	0.1	0.1	<0.1
7	18-Dec-97	2	<0.1	0.20	<0.1	0.5	<0.1	<0.1	<0.1	<0.1	<0.1	<0.1	0.17	<0.1	<0.1	0.1	0.1	<0.1
18	30-Dec-97	3	<0.1	<0.1	<0.1	<0.1	<0.1	<0.1	<0.1	<0.1	<0.1	<0.1	0.13	<0.1	<0.1	0.1	0.1	<0.1
25	06-Jan-98	4	<0.1	<0.1	<0.1	0.20	<0.1	<0.1	<0.1	<0.1	<0.1	<0.1	<0.1	<0.1	<0.1	0.3	<0.1	0.2
32	13-Jan-98	5	<0.1	<0.1	<0.1	<0.1	<0.1	<0.1	<0.1	<0.1	<0.1	<0.1	<0.1	<0.1	<0.1	<0.1	<0.1	<0.1
40	21-Jan-98	6	<0.1	<0.1	<0.1	<0.1	<0.1	<0.1	<0.1	<0.1	<0.1	<0.1	<0.1	<0.1	<0.1	<0.1	<0.1	<0.1
46	27-Jan-98	7	<0.1	<0.1	<0.1	<0.1	<0.1	<0.1	<0.1	<0.1	<0.1	<0.1	<0.1	<0.1	<0.1	<0.1	<0.1	<0.1
54	04-Feb-98	8	<0.1	<0.1	<0.1	<0.1	<0.1	<0.1	<0.1	<0.1	<0.1	<0.1	<0.1	<0.1	<0.1	<0.1	<0.1	<0.1
61	11-Feb-98	9	<0.1	<0.1	<0.1	<0.1	<0.1	<0.1	<0.1	<0.1	<0.1	<0.1	<0.1	<0.1	<0.1	<0.1	<0.1	<0.1
68	18-Feb-98	10	<0.1	<0.1	<0.1	<0.1	<0.1	<0.1	<0.1	<0.1	<0.1	<0.1	<0.1	<0.1	<0.1	<0.1	0.2	<0.1
75	25-Feb-98	11	<0.1	<0.1	<0.1	<0.1	<0.1	<0.1	<0.1	<0.1	<0.1	<0.1	<0.1	<0.1	<0.1	<0.1	<0.1	<0.1
82	04-Mar-98	12	<0.1	<0.1	<0.1	<0.1	<0.1	<0.1	<0.1	<0.1	<0.1	<0.1	<0.1	<0.1	0.1	0.2	<0.1	<0.1
89	11-Mar-98	13	<0.1	<0.1	<0.1	<0.1	<0.1	<0.1	<0.1	<0.1	<0.1	<0.1	<0.1	<0.1	0.1	0.2	<0.1	<0.1
96	18-Mar-98	14	<0.1	<0.1	<0.1	<0.1	<0.1	<0.1	<0.1	<0.1	<0.1	<0.1	<0.1	<0.1	0.1	0.2	<0.1	<0.1
103	25-Mar-98	15	<0.1	<0.1	<0.1	<0.1	<0.1	<0.1	<0.1	<0.1	<0.1	<0.1	<0.1	<0.1	0.1	<0.1	<0.1	<0.1
108	30-Mar-98	16	<0.1	<0.1	<0.1	<0.1	<0.1	<0.1	<0.1	<0.1	<0.1	<0.1	<0.1	<0.1	0.2	<0.1	<0.1	<0.1
117	08-Apr-98	17	<0.1	<0.1	<0.1	<0.1	<0.1	<0.1	<0.1	<0.1	<0.1	<0.1	<0.1	<0.1	<0.1	<0.1	<0.1	<0.1
124	15-Apr-98	18	<0.1	<0.1	<0.1	<0.1	<0.1	<0.1	<0.1	<0.1	<0.1	<0.1	<0.1	<0.1	<0.1	<0.1	<0.1	<0.1
131	22-Apr-98	19	<0.1	<0.1	<0.1	<0.1	<0.1	<0.1	<0.1	<0.1	<0.1	<0.1	<0.1	<0.1	<0.1	<0.1	<0.1	<0.1
138	29-Apr-98	20	<0.1	<0.1	<0.1	<0.1	<0.1	<0.1	<0.1	<0.1	<0.1	<0.1	<0.1	<0.1	<0.1	<0.1	<0.1	<0.1

Note: distilled water batch 1 put into cells Dec 12th '97, cycle 1 chemical data taken on Dec.16th '97

Table II-1 (cont'd) Paste Leachate Chemistry - Flooded Water Cells

ay	Date	ycle	SO ₄ (mg/l)				Ca (mg/l)				Mg (mg/l)				K (mg/l)			
			Tiz	Louv	Brw	FIM	Tiz	Louv	Brw	FIM	Tiz	Louv	Brw	FIM	Tiz	Lou	Brw	FIM
4	16-Dec-97	1	1.3	1.3	1.4	1.1	840	845	922	682	3.6	47	11	4.8	127	51	107	32
7	18-Dec-97	2	2.2	2.3	2.2	1.5			883		4.0	127	19	8.3	158	85	136	53
18	30-Dec-97	3	1.9	2.1	1.9	1.7	784	945	857	852	2.8	80	14	5.0	146	74	117	45
25	06-Jan-98	4	2.1	1.7	1.7	1.5	782	776	773	774	2.7	59	10	4.5	138	60	99	41
32	13-Jan-98	5	1.5	1.6	1.6	1.3	725	860	755	664	4.7	41	7.0	2.8	117	45	66	34
40	21-Jan-98	6	1.5	1.5	1.5	1.2	700	760	751	556	5.5	30	6.4	2.0	78	36	44	28
46	27-Jan-98	7	1.3	1.3	1.5	0.9	610	622	646	452	1.3	22	5.0	4.5	50	27	32	22
54	04-Feb-98	8	1.2	1.2	1.4	0.8	626	617	699	437	1.2	16	4.4	1.9	41	25	25	20
61	11-Feb-98	9	1.2	1.2	1.5	0.7	595	591	697	392	1.4	13	4.1	1.9	29	21	17	19
68	18-Feb-98	10	1.1	1.1	1.4	0.6	572	538	692	347	1.2	10	3.6	1.7	20	17	12	16
75	25-Feb-98	11	1.1	1.0	1.4	0.6	547	526	675	301	1.2	11	3.6	1.5	16	15	10	15
82	04-Mar-98	12	0.9	1.0	1.4	0.4	554	600	880	310	0.9	12	3.2	1.0	10	12	6.0	10
89	11-Mar-98	13	1.0	0.9	1.4	0.5	546	540	870	308	1.0	11	3.2	1.0	8.3	9.2	6.2	10
96	18-Mar-98	14	0.9	0.8	1.4	0.4	504	510	760	278	1.0	9.0	2.7	0.8	7.2	8.2	5.1	9.3
103	25-Mar-98	15	1.0	0.9	1.4	0.5	515	530	855	294	0.9	13	3.2	1.5	5.7	7.9	4.8	10
108	30-Mar-98	16	0.9	0.8	1.3	0.5	417	460	810	280	0.7	12	3.0	1.7	4.8	7.1	4.7	10
117	08-Apr-98	17	1.0				492	390	650	190	1.3	8.4	2.4	1.3	4.1	5.0	5.3	9.0
124	15-Apr-98	18	0.9	0.7	1.3	0.4	467	330	623	209	0.7	12	2.4	1.8	4.6	6.5	5.0	11
131	22-Apr-98	19	0.9	0.8	1.3	0.4	472	365	610	198	0.6	14	2.3	1.9	4.4	6.0	5.1	10
138	29-Apr-98	20	0.6	0.7	1.3	0.4	312	320	590	185	0.8	12	2.0	1.6	5.5	5.2	4.3	9.1

ay	Date	ycle	Si (mg/l)				Al (mg/l)				As (mg/l)			
			Tiz	Louv	Brw	FIM	Tiz	Louv	Brw	FIM	Tiz	Louv	Brw	FIM
4	16-Dec-97	1	2.2	9.7	1.9	2.4	< 0.30	< 0.30	< 0.30	< 0.30	< 1.0	< 1.0	< 1.0	< 1.0
7	18-Dec-97	2	3.3	9.8	2.0	3.4	< 0.30	< 0.30	< 0.30	< 0.30	< 1.0	< 1.0	< 1.0	< 1.0
18	30-Dec-97	3	2.9	9.7	2.2	3.2	< 0.30	< 0.30	< 0.30	< 0.30	< 1.0	< 1.0	< 1.0	< 1.0
25	06-Jan-98	4	2.0	9.7	1.6	2.7	< 0.30	< 0.30	< 0.30	< 0.30	< 1.0	< 1.0	< 1.0	< 1.0
32	13-Jan-98	5	2.9	10	2.2	3.2				< 1.0	< 1.0	< 1.0	< 1.0	
40	21-Jan-98	6	3.0	9.8	1.9	3.0				< 1.0	< 1.0	< 1.0	< 1.0	
46	27-Jan-98	7	3.0	8.6	1.5	2.5				< 1.0	< 1.0	< 1.0	< 1.0	
54	04-Feb-98	8	2.2	9.9	1.5	2.0	< 0.3	< 0.3	< 0.3	< 0.3	< 1.0	< 1.0	< 1.0	< 1.0
61	11-Feb-98	9	2.4	10	1.2	2.6	< 0.3	< 0.3	< 0.3	< 0.3	< 1.0	< 1.0	< 1.0	< 1.0
68	18-Feb-98	10	2.2	9.7	1.0	2.1	< 0.3	< 0.3	< 0.3	< 0.3	< 1.0	< 1.0	< 1.0	< 1.0
75	25-Feb-98	11	1.9	9.8	1.4	2.6	< 0.3	< 0.3	< 0.3	< 0.3	< 1.0	< 1.0	< 1.0	< 1.0
82	04-Mar-98	12	1.5	6.8	0.5	1.6	0.32	< 0.3	< 0.3	< 0.3	< 1.0	< 1.0	< 1.0	< 1.0
89	11-Mar-98	13	1.6	6.1	0.5	1.3	0.32	< 0.3	< 0.3	< 0.3	< 1.0	< 1.0	< 1.0	< 1.0
96	18-Mar-98	14	1.7	6.7	0.5	1.5	0.34	< 0.3	< 0.3	< 0.3	< 1.0	< 1.0	< 1.0	< 1.0
103	25-Mar-98	15	1.7	6.6	0.8	1.6	0.33	< 0.3	< 0.3	< 0.3	< 1.0	< 1.0	< 1.0	< 1.0
108	30-Mar-98	16	1.5	6.6	0.9	2.0	0.63	< 0.3	< 0.3	< 0.3	< 1.0	< 1.0	< 1.0	< 1.0
117	08-Apr-98	17	0.8				< 0.3	< 0.3	< 0.3	< 0.3	< 1.0	< 1.0	< 1.0	< 1.0
124	15-Apr-98	18	1.6	8.9	2.0	4.1	< 0.3	< 0.3	< 0.3	< 0.3	< 1.0	< 1.0	< 1.0	< 1.0
131	22-Apr-98	19	1.3	9.0	2.0	4.1	< 0.3	< 0.3	< 0.3	< 0.3	< 1.0	< 1.0	< 1.0	< 1.0
138	29-Apr-98	20	2.5	8.6	1.7	3.6	< 0.3	< 0.3	< 0.3	< 0.3	< 1.0	< 1.0	< 1.0	< 1.0

Note: distilled water batch 1 put into cells Dec 12th '97, cycle 1 chemical data taken on Dec.16th '97

Table II-2 Paste Leachate Chemistry - Cycled Water Cells

Day	Date	Cycle	Distilled water data				Paste leach water								Redox potential			
			batc	cond	pH	edox	conductivity (uS)				pH				(mV SHE)			
				(uS)	(mV)	Tiz	Louv	Brw	FIM	Tiz	Louv	Brw	FIM	Tiz	Louv	Brw	FIM	
1	12-Dec-97	1	1	27.5	5.5	499	1880	1660	1902	1565	10	8.2	7.6	8.4	300	358	368	361
6	18-Dec-97	2	2	28.8	5.5	359	1000	1090	1330	900	9.3	7.5	7.6	7.4	367	405	417	411
12	30-Dec-97	3	3	26.8	5.6	485	1038	1054	1268	892	7.3	6.6	6.5	6.3	399	420	421	423
20	07-Jan-98	4	4	6.09	5.6	509	885	846	1060	724	8.1	7.3	6.3	6.3	356	367	371	356
28	15-Jan-98	5	5	17.7	5.5	469	1192	1104	1322	906	7.8	6.6	6.4	7.3	300	362	364	334
34	21-Jan-98	6	6	5.83	5.58	442	692	639	842	495	6.6	6.3	6.1	6.7	321	323	338	329
41	28-Jan-98	7	7	6.3	5.61	488	935	775	1025	633	6.8	6.9	6.5	6.8	385	390	383	390
48	04-Feb-98	8	8	4.5	5.52		778	609	860	491	6.4	6.8	6.5	6.7	413	409	412	412
50	11-Feb-98	9	9	4.0	5.32	498	795	635	838	504	6.7	7.1	6.8	7.1	369	374	385	385
57	18-Feb-98	10	10	17.9	5.42		779	601	813	476	7.6	7.7	7.3	7.7	375	378	388	400
64	25-Feb-98	11	11	34.9	5.64	432	803	647	928	528	7.4	7.5	7.2	7.4	352	356	347	361
71	04-Mar-98	12	12	6.57	5.34	404	810	596	818	509	7.2	7.5	7.1	7.5	345	328	365	352
78	11-Mar-98	13	13	14.9	5.2	479	684	459	669	400	7.0	7.4	7.1	7.6	379	373	390	392
84	18-Mar-98	14	14	2.0	5.2	464	758	540	758	459	6.7	7.6	7.1	7.3	381	405	396	412
90	24-Mar-98	15	15	8.8	5.55	481	721	496	708	432	6.7	6.8	6.6	6.8	445	419	434	433
99	30-Mar-98	16	16	15	5.59	490	745	520	724	745	6.9	7.5	7.0	7.5	418	393	398	394
107	08-Apr-98	17	17	55	5.62	411	820	625	847	693	6.9	7.3	7.0	7.5	374	393	396	390
113	16-Apr-98	18	18	48	5.6	470	863	623	801	676	6.9	7.2	6.9	7.7	390	395	378	357
120	22-Apr-98	19	19	4.62	5.3	389	785	567	765	773	6.9	7.3	7.5	7.6	348	358	357	360
138	29-Apr-98	20	20	18	5.59		767	592	749	628	7.3	7.4	7.4	7.8	332	329	338	338

Day	Date	Cycle	Fe total (mg/l)				Cu (mg/l)				Zn (mg/l)				Pb (mg/l)			
			Tiz	Louv	Brw	FIM	Tiz	Louv	Brw	FIM	Tiz	Louv	Brw	FIM	Tiz	Louv	Brw	FIM
1	12-Dec-97	1	<0.1	0.74	<0.1	0.23	<0.1	<0.1	<0.1	<0.1	<0.1	<0.1	0.1	<0.1	0.2	0.1	0.1	<0.1
6	18-Dec-97	2	<0.1	0.5	<0.1	1.78	<0.1	<0.1	<0.1	<0.1	<0.1	<0.1	0.3	0.1	0.2	0.1	0.1	<0.1
12	30-Dec-97	3	<0.1	0.3	<0.1	<0.1	<0.1	<0.1	<0.1	<0.1	<0.1	<0.1	0.5	0.2	<0.1	0.1	0.1	<0.1
20	07-Jan-98	4	<0.1	0.7	<0.1	0.2	<0.1	<0.1	<0.1	<0.1	<0.1	<0.1	<0.1	<0.1	<0.1	<0.1	<0.1	0.1
28	15-Jan-98	5	<0.1	<0.1	<0.1	<0.1	<0.1	<0.1	<0.1	<0.1	<0.1	<0.1	<0.1	<0.1	<0.1	<0.1	<0.1	<0.1
34	21-Jan-98	6	<0.1	<0.1	<0.1	<0.1	<0.1	<0.1	<0.1	<0.1	<0.1	<0.1	<0.1	<0.1	<0.1	<0.1	<0.1	<0.1
41	28-Jan-98	7	<0.1	<0.1	<0.1	<0.1	<0.1	<0.1	<0.1	<0.1	<0.1	<0.1	0.2	<0.1	<0.1	<0.1	<0.1	<0.1
48	04-Feb-98	8	<0.1	<0.1	<0.1	<0.1	<0.1	<0.1	<0.1	<0.1	<0.1	<0.1	0.3	0.1	<0.1	<0.1	<0.1	<0.1
50	11-Feb-98	9	<0.1	<0.1	<0.1	<0.1	<0.1	0.1	0.1	<0.1	0.1	0.1	0.4	0.1	<0.1	<0.1	<0.1	<0.1
57	18-Feb-98	10	<0.1	<0.1	<0.1	<0.1	<0.1	0.1	0.1	<0.1	0.1	0.1	0.2	0.1	<0.1	<0.1	<0.1	<0.1
64	25-Feb-98	11	<0.1	<0.1	<0.1	<0.1	<0.1	0.1	0.1	<0.1	0.1	0.1	0.6	0.1	<0.1	<0.1	<0.1	<0.1
71	04-Mar-98	12	<0.1	<0.1	<0.1	<0.1	<0.1	<0.1	<0.1	<0.1	0.12	<0.1	<0.1	<0.1	<0.1	<0.1	<0.1	<0.1
78	11-Mar-98	13	<0.1	<0.1	<0.1	<0.1	<0.1	<0.1	<0.1	<0.1	0.11	<0.1	0.3	<0.1	<0.1	<0.1	<0.1	<0.1
84	18-Mar-98	14	<0.1	<0.1	<0.1	<0.1	<0.1	<0.1	<0.1	<0.1	0.14	<0.1	0.3	<0.1	<0.1	<0.1	<0.1	<0.1
90	24-Mar-98	15	<0.1	<0.1	<0.1	<0.1	<0.1	<0.1	<0.1	<0.1	0.11	<0.1	0.3	<0.1	<0.1	<0.1	<0.1	<0.1
99	30-Mar-98	16	<0.1	<0.1	<0.1	<0.1	<0.1	<0.1	<0.1	<0.1	0.3	<0.1	0.5	<0.1	<0.1	<0.1	<0.1	<0.1
107	08-Apr-98	17	<0.1	<0.1	<0.1	<0.1	<0.1	<0.1	<0.1	<0.1	1.2	<0.1	2.2	<0.1	<0.1	<0.1	<0.1	<0.1
113	16-Apr-98	18	<0.1	<0.1	<0.1	<0.1	<0.1	<0.1	<0.1	<0.1	0.5	<0.1	1.4	<0.1	<0.1	<0.1	<0.1	<0.1
120	22-Apr-98	19	<0.1	<0.1	<0.1	<0.1	<0.1	<0.1	<0.1	<0.1	0.14	<0.1	0.5	<0.1	0.7	0.6	<0.1	<0.1
138	29-Apr-98	20	<0.1	<0.1	<0.1	<0.1	<0.1	<0.1	<0.1	<0.1	0.3	<0.1	1.3	<0.1	0.3	0.42	<0.1	<0.1

Note: distilled water put into cells for 24 hours prior to leachate analysis

Table II-2 (cont'd)

Paste Leachate Chemistry - Cycled Water Cells

Day	Date	Cycle	SO ₄ (mg/l)				Ca (mg/l)				Mg (mg/l)				K (mg/l)			
			Tiz	Louv	Brw	FIM	Tiz	Louv	Brw	FIM	Tiz	Louv	Brw	FIM	Tiz	Louv	Brw	FIM
1	12-Dec-97	1	1.3	1.3	1.4	1.1	840	845	922	682	3.6	47	11	4.8	127	51	107	32
6	18-Dec-97	2	0.9	0.8	1.0	0.7	475	543	621	530	3.0	35	6.3	4.0	113	36	86	25
12	30-Dec-97	3	0.6	0.7	0.9	0.8	318	333	431	332	2.6	30	7.8	3.8	80	27	59	20
20	07-Jan-98	4	0.5	0.5	0.8	0.4	232	225	370	204	2.0	24	5.6	2.6	55	19	32	16
28	15-Jan-98	5	0.8	0.7	1.1	0.6	340	261	481	276	3.0	48	6.0	6.8	44	19	25	17
34	21-Jan-98	6	0.4	0.3	0.5	0.2	167	214	238	111	4.5	29	4.0	2.0	17	8.2	9.0	8.5
41	28-Jan-98	7	0.4	0.3	0.6	0.3	208	200	265	123	4.8	22	4.7	2.0	13	6.7	6.7	8.6
48	04-Feb-98	8	0.4	0.3	0.4	0.2	210	148	257	120	2.2	8.8	3.3	1.6	10	5.9	5.5	8.4
50	11-Feb-98	9	0.4	0.3	0.5	0.2	230	178	296	125	2.4	10	3.9	1.7	8.6	6.1	4.9	8.9
57	18-Feb-98	10	0.3	0.3	0.4	0.2	225	150	250	116	2.3	8.3	3.4	1.6	5.9	1.9	3.5	7.9
64	25-Feb-98	11	0.4	0.3	0.6	0.2	255	174	329	129	2.3	10	4.1	1.8	6.3	5.9	5.3	9.1
71	04-Mar-98	12	0.4	0.3	0.5	0.2	340	170	353	120	2.1	1.1	3.8	1.0	4.1	3.7	2.2	5.7
78	11-Mar-98	13	0.4	0.3	0.5	0.2	340	164	325	160	2.8	9.0	2.9	1.9	3.5	3.0	1.9	5.0
84	18-Mar-98	14	0.4	0.3	0.5	0.2	335	178	320	158	2.3	9.0	2.2	1.5	3.3	3.2	1.8	5.1
90	24-Mar-98	15	0.4	0.2	0.5	0.2	285	170	310	160	3.0	8.7	2.5	1.3	3.0	3.2	1.9	5.1
99	30-Mar-98	16	0.5	0.3	0.5	0.3	354	190	350	270	2.8	12	3.6	2.1	3.0	3.6	2.0	8.6
107	08-Apr-98	17	0.5	0.3			271	190	260	210	2.4	3.1	1.7	3.0	5.0	7.4	13	6.4
113	16-Apr-98	18	0.5	0.3	0.6	0.4	260	152	232	158	2.7	12	2.0	1.8	4.4	4.8	4.7	8.1
120	22-Apr-98	19	0.4	0.3	0.4	0.3	233	124	195	168	1.8	9.2	2.3	1.4	1.7	2.4	1.4	5.2
138	29-Apr-98	20	0.6	0.3	0.4	0.2	249	150	233	142	2.0	11	3.2	1.3	2.4	3.3	2.4	5.0

Day	Date	Cycle	Si (mg/l)				Al (mg/l)				As (mg/l)			
			Tiz	Louv	Brw	FIM	Tiz	Louv	Brw	FIM	Tiz	Louv	Brw	FIM
1	12-Dec-97	1	2.2	9.7	1.9	2.4	<0.3	<0.3	<0.3	<0.3	<1.0	<1.0	<1.0	<1.0
6	18-Dec-97	2	2.0	7.1	2.0	2.9	<0.3	<0.3	<0.3	<0.3	<1.0	<1.0	<1.0	<1.0
12	30-Dec-97	3	1.5	5.0	1.8	2.8	<0.3	<0.3	<0.3	<0.3	<1.0	<1.0	<1.0	<1.0
20	07-Jan-98	4	<0.5	4.5	<0.5	1.4	<0.3	<0.3	<0.3	<0.3	<1.0	<1.0	<1.0	<1.0
28	15-Jan-98	5	<0.5	6.1	1.3	2.8	<0.3	<0.3	<0.3	<0.3	<1.0	<1.0	<1.0	<1.0
34	21-Jan-98	6	<0.5	4.4	<0.5	1.1	<0.3	<0.3	<0.3	<0.3	<1.0	<1.0	<1.0	<1.0
41	28-Jan-98	7	<0.5	4.2	<0.5	1.7	<0.3	<0.3	<0.3	<0.3	<1.0	<1.0	<1.0	<1.0
48	04-Feb-98	8	0.8	5.4	1.2	1.9	<0.3	0.5	<0.3	<0.3	<1.0	<1.0	<1.0	<1.0
50	11-Feb-98	9	1.0	3.7	1.4	1.7	<0.3	0.3	<0.3	<0.3	<1.0	<1.0	<1.0	<1.0
57	18-Feb-98	10	1.4	4.0	1.4	2.0	<0.3	<0.3	<0.3	<0.3	<1.0	<1.0	<1.0	<1.0
64	25-Feb-98	11	2.5	5.7	2.1	4.2	<0.3	<0.3	<0.3	<0.3	<1.0	<1.0	<1.0	<1.0
71	04-Mar-98	12	1.4	3.8	1.0	1.6	<0.3	<0.3	<0.3	<0.3	<1.0	<1.0	<1.0	<1.0
78	11-Mar-98	13	1.2	3.2	0.9	1.3	<0.3	<0.3	<0.3	<0.3	<1.0	<1.0	<1.0	<1.0
84	18-Mar-98	14	1.4	4.0	0.9	1.6	<0.3	<0.3	<0.3	<0.3	<1.0	<1.0	<1.0	<1.0
90	24-Mar-98	15	1.6	4.1	1.0	1.9	<0.3	<0.3	<0.3	<0.3	<1.0	<1.0	<1.0	<1.0
99	30-Mar-98	16	2.0	5.1	1.4	3.0	<0.3	<0.3	<0.3	<0.3	<1.0	<1.0	<1.0	<1.0
107	08-Apr-98	17	2.3	5.2	1.2	1.4	<0.3	<0.3	<0.3	<0.3	<1.0	<1.0	<1.0	<1.0
113	16-Apr-98	18	5.3	9.7	4.8	6.0	<0.3	<0.3	<0.3	<0.3	<1.0	<1.0	<1.0	<1.0
120	22-Apr-98	19	2.0	4.8	1.7	2.9	<0.3	<0.3	<0.3	<0.3	<1.0	<1.0	<1.0	<1.0
138	29-Apr-98	20	3.6	7.3	3.0	4.2	<0.3	<0.3	<0.3	<0.3	<1.0	<1.0	<1.0	<1.0

Table II-3 Paste Leachate Chemistry - Fe₂(SO₄)₃ Solution Cells

Day	Date	Cycle	Fe ₂ (SO ₄) ₃ Solution					Paste leach solution								Redox potential				
			batc no.	cond (uS)	pH (mV)	OR (mg/l)	Fe to SO ₄ (g/l)	conductivity (uS)				pH				(mV SHE)				
								Tiz	Louv	Brw	FIM	Tiz	Lou	Brw	FIM	Tiz	Lou	Brw	FIM	
0.5	12-Dec-97	1	1	2735	2.9	587	920	1.5					6.5	6.4	6.3	6.6				
6	17-Dec-97	2	2	2360	2.3	596	826	1.5	3240	1890	3020	1800	6.2	6.2	6.1	6.0	181	154	155	169
18	29-Dec-97	3	3	2610	2.6	623	754	1.4	1855	1605	1623	1432	6.7	6.2	6.3	6.0	228	239	199	252
25	05-Jan-98	4	4	1836	2.6	624	780	1.4	1472	1362	1339	1315	6.3	6.3	6.2	5.9	234	223	226	327
28	08-Jan-98	5	5	1967	2.6	625	740		1338	1311	1268	1350	5.9	5.7	5.9	6.1	278	304	243	182
32	12-Jan-98	6	6	1977	2.6	620	734	1.5	1391	1328	1363	1337	5.7	5.6	5.9	5.6	290	374	258	360
35	15-Jan-98	7	7	1929	2.4	669	689	1.6	1407	1335	1258	1350	5.2	5.3	5.5	5.1	412	409	298	449
39	19-Jan-98	8	8	1942	2.6	629	726	1.4	1318	1314	1331	1307	5.3	5.2	5.7	5.8	341	329	278	265
43	23-Jan-98	9	9	2420	2.6	623	772	1.7	1320	1298	1275	1298	5.2	5.1	5.6	5.7	302	299	239	235
46	26-Jan-98	10	10	2320	2.5	626	692	1.6	1496	1488	1418	1351	4.1	3.9	5.0	5.1	433	470	317	331
49	29-Jan-98	11	11	2370	2.6	626	723	1.3	1448	1453	1349	1232	4.0	3.6	4.4	5.2	428	508	372	306
53	02-Feb-98	12	12	1979	2.5	624	723	1.5	1424	1512	1448	1399	4.5	4.3	5.3	5.7	400	419	365	289
57	06-Feb-98	13	13	2700	2.5	623	687	1.6	1474	1487	1434	1316	4.4	4.0	4.9	5.5	405	447	381	289
60	09-Feb-98	14	14	2400	2.5	625	638	1.3	1502	1517	1552	1304	3.9	3.8	4.1	5.1	469	495	451	370
63	12-Feb-98	15	15	1911	2.7	617	679	1.4	1447	1397	1439	1219	4.0	3.9	4.2	5.4	433	459	420	294
67	16-Feb-98	16	16	1894	2.5	630	548	1.3	1439	1420	1390	1272	4.1	3.9	4.4	5.6	435	457	412	311
70	19-Feb-98	17	17	2460	2.5	621	665	1.4	1494	1490	1504	1320	3.9	3.9	4.1	5.2	443	439	430	344
74	23-Feb-98	18	18	2230	2.6	630	611	1.3	1556	1460	1503	1328	4.0	4.0	4.3	5.5	436	432	408	289
77	26-Feb-98	19	19	2410	2.6	624	609	1.4	1426	1380	1400	1225	3.9	3.9	4.0	5.2	435	428	421	322
81	02-Mar-98	20	20	2330	2.7	612	645	1.4		1375	1354	1232	4.0	4.1	4.5	5.6	440	431	409	302
84	05-Mar-98	21	21	2510	2.5	628	483	1.3	1325	1320	1361	1169	3.8	3.8	3.9	5.0	463	477	450	389
88	09-Mar-98	22	22	1896	2.5	628	695	1.5	1462	1431	1457	1233	4.0	4.1	4.4	5.6	434	419	394	287
91	12-Mar-98	23	23	2550	2.5	621	550	1.5	1374	1353	1387	1280	3.7	3.7	3.9	5.3	466	484	442	399
95	16-Mar-98	24	24	2500	2.6	619	598	1.5	1536	1503	1555	1290	3.8	3.8	4.0	5.1	439	452	437	345
99	20-Mar-98	25	25	2460	2.7	622	564	1.5	1407	1355	1391	1143	3.9	3.9	4.1	5.5	433	444	419	291
103	24-Mar-98	26	26	2480	2.5	621	604	1.5	1466	1377	1395	1199	4.1	4.1	4.4	5.8	426	427	404	255
109	30-Mar-98	27	27	2540	2.5	623	630	1.4	1396	1364	1375	1143	3.9	3.9	4.1	5.6	430	439	405	254
112	02-Apr-98	28	28	1951	2.5	627	641	1.4	1458	1390	1420	1188	3.7	3.6	3.8	5.3	450	457	444	304
116	06-Apr-98	29	29	2360	2.5	627	520	1.4	1523	1479	1535	1272	3.8	3.8	4.0	5.6	450	451	398	281
118	08-Apr-98	30	30	1934	2.5	616	630	1.5	1465	1438	1429	1216	3.5	3.5	3.6	5.1	473	488	460	312
123	13-Apr-98	31	31	2370	2.5	615			1478	1489	1461	1302	3.9	3.7	4.0	5.6	428	451	408	277
126	16-Apr-98	32	32	1901	2.6	624	721	1.6					3.7	3.6	3.8	5.6				
130	20-Apr-98	33	33	2390	2.5	621	725	1.6	1454	1434	1418	1320	3.9	3.7	4.0	4.9	432	445	411	333
133	23-Apr-98	34	34	2580	2.5	617	745	1.5	1405	1399	1417	1275	3.6	3.4	3.6	4.2	469	512	466	395
137	27-Apr-98	35	35	1937	2.5	615	727	1.5	1564	1539	1596	1310	3.8	3.5	3.7	5.2	443	489	448	330
140	30-Apr-98	36	36	2530	2.5	617	910	1.4	1584	1565	1576	1374	3.6	3.4	3.6	4.9	462	506	482	342
144	04-May-98	37	37	2570	2.5	614	550	1.4	1565	1542	1583	1280	3.7	3.5	3.7	5.3	455	494	470	306
147	07-May-98	38	38	2410	2.6	625	470	1.4	1608	1543	1636	1411	3.6	3.4	3.5	4.6	459	493	467	357
151	11-May-98	39	39	2430	2.5	622	840	1.7	1615	1587	1596	1320	3.7	3.5	3.7	5.1	454	481	444	307
154	14-May-98	40	40	2470	2.5	624	725	1.4	1493	1466	1479	1305	3.5	3.4	3.6	4.7	465	479	455	369

Notes:

Empty spaces denote unavailable results

ORP: Oxidation-reduction (redox) potential (SHE)

Table II-3 (cont'd) Paste Leachate Chemistry - Fe₂(SO₄)₃ Solution Cells

Day	Date	Cycle	Fe total (mg/l)				Cu (mg/l)				Zn (mg/l)				Pb (mg/l)			
			Tiz	Louv	Brw	FIM	Tiz	Lou	Brw	FIM	Tiz	Louv	Brw	FIM	Tiz	Lou	Brw	FIM
0.5	12-Dec-97	1	260	400	328	348	<0.1	0.1	<0.1	<0.1	1.3	0.6	11	1.3	0.5	0.1	<0.1	<0.1
6	17-Dec-97	2	94	280	154	169	<0.1	0.1	<0.1	<0.1	0.6	0.4	8.6	1.0	<0.1	<0.1	0.1	<0.1
18	29-Dec-97	3	73	75	74	138	<0.1	0.1	<0.1	<0.1	0.4	3.8	4.7	0.8	<0.1	<0.1	0.2	<0.1
25	05-Jan-98	4	88	216	190	230	<0.1	0.2	<0.1	<0.1	0.9	0.5	9.1	1.1	<0.1	<0.1	<0.1	<0.1
28	08-Jan-98	5	290	329	290	155	0.6	0.5	0.4	0.4	3.3	1.4	17	1.3	<0.1	0.2	<0.1	<0.1
32	12-Jan-98	6	224	290	279	249	0.6	0.5	0.3	0.4	3.1	1.2	18	1.6	<0.1	0.2	0.2	<0.1
35	15-Jan-98	7	183	201	201	134	0.6	0.7	0.3	0.4	5.2	1.8	23	2.1	0.6	0.2	0.3	<0.1
39	19-Jan-98	8	248	368	304	261	0.6	0.3	0.4	0.4	4.2	1.7	18	1.8	0.4	0.2	0.2	<0.1
43	23-Jan-98	9	278	397	323	271	0.3	0.4	0.3	0.3	3.6	1.3	18	2.0	0.3	<0.1	0.3	<0.1
46	26-Jan-98	10	340	417	366	371	0.5	0.4	0.4	0.5	4.3	1.5	19	2.1	0.8	<0.1	0.9	<0.1
49	29-Jan-98	11	388	438	388	335	0.4	0.9	0.3	0.4	4.1	1.8	18	2.1	0.9	<0.1	1.4	<0.1
53	02-Feb-98	12	346	399	357	267	0.4	0.4	0.5	0.6	4.1	1.5	17	1.7	0.8	<0.1	0.7	<0.1
57	06-Feb-98	13	333	451	357	321	<0.1	0.1	0.2	<0.1	3.2	1.4	19	1.8	0.6	<0.1	1.2	<0.1
60	09-Feb-98	14	438	443	379	339	0.2	0.1	0.1	<0.1	3.6	1.2	17	2.0	1.0	<0.1	1.6	<0.1
63	12-Feb-98	15	417	459	378	361	0.1	0.3	0.1	<0.1	3.3	1.5	15	1.7	0.9	<0.1	1.4	<0.1
67	16-Feb-98	16	406	421	336		0.1	0.3	0.1		3.8	1.6	16		0.8	0.1	1.0	
70	19-Feb-98	17	424	492	359	343	0.1	0.3	0.1	<0.1	3.2	1.4	14	1.8	1.0	0.1	1.4	<0.1
74	23-Feb-98	18	343	436	345	304	<0.1	0.2	0.1	<0.1	3.2	1.5	15	1.5	0.8	<0.1	1.1	<0.1
77	26-Feb-98	19	402	479	355	356	<0.1	0.2	0.1	<0.1	3.2	1.4	13	1.8	1.1	<0.1	1.2	<0.1
81	02-Mar-98	20	329	387	290	236	0.2	0.2	0.2	0.2	3.6	1.3	14	1.7	0.9	<0.1	0.9	0.1
84	05-Mar-98	21	490	411	270	260	0.1	0.1	0.2	0.2	4.0	1.5	12		1.6	0.3	1.3	
88	09-Mar-98	22	438	407	230	221	0.1	0.1	0.2	0.2	5.0	1.6	9.7		1.0	0.3	0.6	
91	12-Mar-98	23	518	510	393	250	0.2	0.1	0.3	0.4	3.8	1.3	15		1.5	0.3	1.7	
95	16-Mar-98	24	502	384	310	305	0.1	0.3	0.2	0.2	4.7	1.3	12		1.2	0.1	1.0	
99	20-Mar-98	25	476	370	295	260	<0.1	0.1	0.2	0.2	4.7	1.3			1.0	0.2		
103	24-Mar-98	26	348	420	254	166	<0.1	0.2	0.1	0.3	4.7	1.7			0.9	0.3		
109	30-Mar-98	27	416	417	360	180	<0.1	0.2	0.2	0.4	4.5	1.8			1.1	0.2		
112	02-Apr-98	28	448	497	350	215	<0.1	0.2	0.2	0.3	4.7	1.8			1.6	0.2		
116	06-Apr-98	29	433	370	325	312	<0.1	0.1	0.2	0.2		1.6	16	2.8	1.8	<0.1	<0.1	<0.1
118	08-Apr-98	30	549	502	390	310	<0.1	0.3	0.2	0.1		1.0	11	2.9	2.3	<0.1	<0.1	<0.1
123	13-Apr-98	31	552	594	605	423	0.3	0.1	0.3	0.5	6.9	1.4	16	2.3	1.4	0.2	1.5	0.2
126	16-Apr-98	32	530	494	900	370	0.3	0.2	0.7	0.4	6.2	1.3	22	2.7	1.9	0.5	3.3	0.2
130	20-Apr-98	33	530	935	800	395	0.2	0.3	0.7	0.4	6.7	3.0	14	2.2	1.3	0.6	1.2	0.2
133	23-Apr-98	34	630	1180	640	530	0.0	0.3	0.4	0.3	5.9	2.5	14	2.3	1.9	0.7	2.1	0.2
137	27-Apr-98	35	570	605	554	580	0.2	0.2	0.4	0.2	6.6	1.8	14	2.1	1.4	0.3	1.5	0.2
140	30-Apr-98	36	700	690	498	520	0.2	0.3	0.3	0.1	7.1	1.6	11	2.3	2.1	0.3	1.4	0.2
144	04-May-98	37	720	730	610	474	0.1	0.3	0.3	<0.1	9.5	2.1	13	2.4	2.0	0.3	1.5	0.2
147	07-May-98	38	490	485	470	330	<0.1	0.1	<0.1	<0.1	7.7	1.4	13	3.0	1.4		1.0	<0.1
151	11-May-98	39	555	480	433	380	<0.1	0.1	<0.1	<0.1	12	1.7	13	2.2	1.2	<0.1	<0.1	<0.1
154	14-May-98	40	472	430	460	393	<0.1	0.1	<0.1	<0.1	8.9	1.4	12	3.1	1.3	<0.1	<0.1	<0.1

Table II-3 (cont'd)

Paste Leachate Chemistry - Fe₂(SO₄)₃ Solution Cells

Days	Date	Cycle	SO ₄ (mg/l)				Ca (mg/l)				Mg (mg/l)				K (mg/l)			
			Tiz	Louv	Brw	FIM	Tiz	Louv	Brw	FIM	Tiz	Louv	Brw	FIM	Tiz	Louv	Brw	FIM
0.5	12-Dec-97	1	1.9	1.9	2.0	1.7	586	498	590	525	7.1	63	8.0	142	39.3	104	27	
6	17-Dec-97	2	2.1	2.5	2.1	2.0	756	691	742	736	8.0	108	10	177	55.3	122	36	
18	29-Dec-97	3	1.8	2.0	1.5	1.6	835	773	770	631	8.0	115	8.3	120	32	51	28	
25	05-Jan-98	4	1.6	1.7	1.5	1.5	761	581	800	546	8.0	61	6.4	46	18.2	20	20	
28	08-Jan-98	5	1.6	1.6	1.6	1.6	562	390	477	583	8.8	45	8.9	7.5	11	6.3	5.8	14
32	12-Jan-98	6	1.8	1.6	1.6	1.5	611	355	561	440	9.7	48	11	6.3	6.3	4.3	4.4	9.2
35	15-Jan-98	7	1.6	1.5	1.5	1.4	543	381	557	433	14	72	16	8.5	4.4	4.0	3.6	8.0
39	19-Jan-98	8	1.6	1.6	1.5	1.4	494	401	484	411	9.3	57	9.7	7.0	2.6	3.7	2.1	6.2
43	23-Jan-98	9	1.7	1.5	1.6	1.7	559	350	522	522	9.2	47	9.6	8.0	2.4	3.0	2.1	7.0
46	26-Jan-98	10	1.5	1.4	1.5	1.6	446	241	435	416	8.3	35	8.3	5.5	1.4	1.9	1.5	4.8
49	29-Jan-98	11	1.6	1.4	1.7	1.4	419	211	443	394	8.7	39	9.8	6.4	1.5	2.3	1.8	4.3
53	02-Feb-98	12	1.7	1.7	1.8	1.5	472	275	461	466	9.7	50	11	7.6	1.3	2.4	1.5	3.9
57	06-Feb-98	13	1.5	1.5	1.5	1.4	420	277	529	429	9.0	42	11	6.5	1.4	2.4	1.9	3.7
60	09-Feb-98	14	1.4	1.3	1.4	1.4	353	209	444	385	9.4	34	9.7	6.4	1.0	1.9	1.4	3.8
63	12-Feb-98	15	1.4	1.5	1.3	1.5	344	244	427	395	9.9	43	9.9	6.4	1.0	2.6	1.5	3.7
67	16-Feb-98	16	1.6	1.3	1.4		393	271	442		12	51	11		1.0	1.9	1.4	
70	19-Feb-98	17	1.4	1.3	1.2	1.4	307	237	381	367	9.3	45	8.6	6.2	0.9	2.1	1.5	3.6
74	23-Feb-98	18	1.2	1.4	1.3	1.3	330	266	443	372	11	56	11	6.7	0.9	2.1	1.5	3.0
77	26-Feb-98	19	1.3	1.3	1.2	1.5	305	229	337	372	10	49	8.4	6.4	1.0	2.2	1.8	3.4
81	02-Mar-98	20	1.5	1.6	1.6	1.3	356	220	407	343	12	45	9.0	5.9				
84	05-Mar-98	21	1.4	1.5	1.2		285	180	280		10	37	7.0		1.2	2.1	2.6	3.0
88	09-Mar-98	22	1.6	1.6	1.2		377	222	294		15	69	8.6		1.2	2.4	3.1	3.0
91	12-Mar-98	23	1.5	1.8	1.4		244	113	340		8.2	25	9.0		1.0	1.8	2.4	1.0
95	16-Mar-98	24	1.5	1.3	1.4		328	213	320		13	48	8.8		1.0	2.1	2.2	2.0
99	20-Mar-98	25	1.6	1.2	1.4		357	218			14	56			0.9	1.8	1.0	2.0
103	24-Mar-98	26	1.7	1.8	1.6		447	320			16	79			0.9	2.5	1.0	2.0
109	30-Mar-98	27	1.6	1.8			379	254			13	62			0.8	2.0	1.0	2.0
112	02-Apr-98	28	1.6	1.6			297	180			11	42			0.8	1.7	1.0	2.0
116	06-Apr-98	29	1.7	1.4	1.8	1.6	364	169	420	410		58	14	9.0	0.8	2.0	1.4	2.9
118	08-Apr-98	30	1.5	1.8	1.4	1.7	225	107	230	285		32	7.3	7.0	2.5	1.7	2.4	3.8
123	13-Apr-98	31	1.8	1.7	2.0	1.8	355	180	440	460	13	63	11	7.8	1.6	2.2	2.4	3.5
126	16-Apr-98	32	1.6	1.3	3.0	1.6	279	134	560	420	10	40	15	9.6	1.7	2.2	3.8	3.2
130	20-Apr-98	33	1.5	2.8	2.7	1.6	320	270	480	380	12	93	15	8.6	1.2	2.7	2.8	2.9
133	23-Apr-98	34	1.5	2.7	1.7	1.5	236	207	290	280	7.9	70	7.9	6.1	1.0	2.1	1.5	2.0
137	27-Apr-98	35	1.6	1.6	1.7	1.7	284	152	327	333	11	50	9.5	7.0	0.8	1.2	1.3	2.1
140	30-Apr-98	36	1.8	1.7	1.5	1.5	280	133	255	294	10	49	6.6	5.8	0.5	1.2	1.0	1.6
144	04-May-98	37	2.0	1.9	1.5	1.6	340	154	320	348	14	64	8.6	6.7	0.6	1.1	0.9	1.7
147	07-May-98	38	1.6	1.3	1.6	1.4	314	140	321	443	8.0	45	11	9.0	0.5	1.6	1.2	2.0
151	11-May-98	39	1.7	1.5	1.7	1.6	466	183	355	400	17	65	13	9.0	0.6	2.0	0.9	1.6
154	14-May-98	40	1.6	1.4	1.6	1.5	296	132	290	350	10	43	11	9.0	0.5	1.7	0.9	1.8

Table II-3 (cont'd) Paste Leachate Chemistry - Fe₂(SO₄)₃ Solution Cells

Days	Date	Cycle	Si (mg/l)				Al (mg/l)				As (mg/l)			
			Tiz	Louv	Brw	FIM	Tiz	Louv	Brw	FIM	Tiz	Louv	Brw	FIM
0.5	12-Dec-97	1	7.0	12		6.2	<0.3	<0.3	<0.3	<0.3	<1	<1	<1	<1
6	17-Dec-97	2	6.6	14		6.9	<0.3	<0.3	<0.3	<0.3	<1	<1	<1	<1
18	29-Dec-97	3	5.4	14		6.2	<0.3	<0.3	<0.3	<0.3	<1	<1	<1	<1
25	05-Jan-98	4	7.0	12		5.9	<0.3	<0.3	<0.3	<0.3	<1	<1	<1	<1
28	08-Jan-98	5	9.6	17	9.8	9.4	<0.5	<0.5	<0.5	2.7	<1	<1	<1	<1
32	12-Jan-98	6	9.7	17	8.9	8.0	<0.5	<0.5	<0.5	0.7	<1	<1	<1	<1
35	15-Jan-98	7	15	23	12	9.3	1.2	1.82	<0.5	<0.5	<1	<1	<1	<1
39	19-Jan-98	8	12	23	8.9	8.0	0.6	<0.5	<0.5	<0.5	<1	<1	<1	<1
43	23-Jan-98	9	12	21	10	8.6	<0.5	<0.5	<0.5	<0.5	<1	<1	<1	<1
46	26-Jan-98	10	12	19	11	7.7	0.6	1.63	<0.5	<0.5	<1	<1	<1	<1
49	29-Jan-98	11	13	20	10	8.3	0.8	<0.5	<0.5	<0.5	<1	<1	<1	<1
53	02-Feb-98	12	13	19	10	9.6	0.7	1.1	<0.5	<0.5	<1	<1	<1	<1
57	06-Feb-98	13	12	20	12	8.6	0.7	1.5	0.9	<0.3	<1	<1	<1	<1
60	09-Feb-98	14	13	18	12	8.4	1.4	2.3	0.9	<0.3	<1	<1	<1	<1
63	12-Feb-98	15	13	19	11	8.1	1.0	2.0	0.8	<0.3	<1	<1	<1	<1
67	16-Feb-98	16	14	19	10		1.4	2.5	0.9		<1	<1	<1	<1
70	19-Feb-98	17	13	20	10	8.6	1.0	1.7	1.0	0.5	<1	<1	<1	<1
74	23-Feb-98	18	12	20	10	8.3	1.1	1.7	0.8	0.6	<1	<1	<1	<1
77	26-Feb-98	19	14	20	10	10	<0.3	1.6	0.8	<0.3	<1	<1	<1	<1
81	02-Mar-98	20	13	17	9.7	8.0	<0.3	<0.3	<0.3	<0.3	<1	<1	<1	<1
84	05-Mar-98	21	13	16	8.6		1.8	1.6	0.5	1.0	<1	<1	<1	<1
88	09-Mar-98	22	13	17	8.5		1.2	0.9	0.7	<0.3	<1	<1	<1	1
91	12-Mar-98	23	11	15	8.3		2.3	2.1	1.2	1.0	<1	<1	<1	1
95	16-Mar-98	24	12	12	10		1.7	1.3	0.7	1.0	<1	1.2	<1	<1
99	20-Mar-98	25	12	13			1.1	0.8	1.0	<0.3	<1	1.0	2.0	<1
103	24-Mar-98	26	12	16			0.5	0.7	<0.3	<0.3	<1	1.4	<1	<1
109	30-Mar-98	27	13	18			0.7	0.9	<0.3	<0.3	<1	1.3	2.0	<1
112	02-Apr-98	28	12	17			1.7	1.4	1.0	<0.3	<1	<1	1	<1
116	06-Apr-98	29	15				<0.3	<0.3	<0.3	<0.3	<1	<1	<1	<1
118	08-Apr-98	30	17				<0.3	<0.3	<0.3	<0.3	<1	<1	<1	<1
123	13-Apr-98	31	17	19	15	15	1.1	1.1	1.0	<0.3	<1	<1	<1	<1
126	16-Apr-98	32	19	20	29	16	1.6	1.3	2.1	<0.3	<1	<1	<1	<1
130	20-Apr-98	33	17	36	22	15	1.3	2.1	1.5	0.3	<1	<1	<1	<1
133	23-Apr-98	34	15	33	16	12	2.3	1.4	2.1	1.6	<1	<1	<1	<1
137	27-Apr-98	35	15	18	14	13	1.4	2.1	1.4	1.0	<1	<1	<1	<1
140	30-Apr-98	36	16	18	13	12	2.0	2.4	1.3	0.9	<1	<1	<1	<1
144	04-May-98	37	18	20	13	13	1.8	2.0	1.1	0.5	<1	<1	<1	<1
147	07-May-98	38	15	15	12	13	1.8	2.0	1.4	0.4	<1	<1	<1	<1
151	11-May-98	39	19	16	11	10	2.1	1.5	0.9	<0.3	<1	<1	<1	<1
154	14-May-98	40	15	14	11	11	2.0	1.7	1.3	0.7	<1	<1	<1	<1

APPENDIX III - ANALYTICAL RESULTS: PASTE BACKFILL SOLID PHASE



Chemex Labs Ltd.

Analytical Chemists * Geochemists * Registered Assayers
 212 Brooksbank Ave., North Vancouver
 British Columbia, Canada V7J 2C1
 PHONE: 604-984-0221 FAX: 604-984-0218

To: UNIVERSITY OF BRITISH COLUMBIA
 DEPARTMENT OF MINING AND MINERAL PROCESS ENG.
 517 - 6350 STORES ROAD
 VANCOUVER, BC
 V6T 1Z4

A9824966

Comments: ATTN: VALERIE BERTRAND

CERTIFICATE A9824966

(LRO) - UNIVERSITY OF BRITISH COLUMBIA

Project: 11-R-51236
 P.O. #:

Samples submitted to our lab in Vancouver, BC.
 This report was printed on 4-AUG-98.

SAMPLE PREPARATION

CHEMEX CODE	NUMBER SAMPLES	DESCRIPTION
225	13	Run as received
285	13	ICP - HF digestion charge

ANALYTICAL PROCEDURES					
CHEMEX CODE	NUMBER SAMPLES	DESCRIPTION	METHOD	DETECTION LIMIT	UPPER LIMIT
578	13	Ag ppm: 24 element, rock & core	AAS	0.2	100.0
573	13	Al %: 24 element, rock & core	ICP-AES	0.01	25.0
565	13	Ba ppm: 24 element, rock & core	ICP-AES	10	10000
575	13	Be ppm: 24 element, rock & core	ICP-AES	0.5	1000
561	13	Bi ppm: 24 element, rock & core	ICP-AES	2	10000
576	13	Ca %: 24 element, rock & core	ICP-AES	0.01	25.0
562	13	Cd ppm: 24 element, rock & core	ICP-AES	0.5	500
563	13	Co ppm: 24 element, rock & core	ICP-AES	1	10000
569	13	Cr ppm: 24 element, rock & core	ICP-AES	1	10000
577	13	Cu ppm: 24 element, rock & core	ICP-AES	1	10000
566	13	Fe %: 24 element, rock & core	ICP-AES	0.01	25.0
584	13	K %: 24 element, rock & core	ICP-AES	0.01	10.00
570	13	Mg %: 24 element, rock & core	ICP-AES	0.01	15.00
568	13	Mn ppm: 24 element, rock & core	ICP-AES	5	10000
554	13	Mo ppm: 24 element, rock & core	ICP-AES	1	10000
583	13	Na %: 24 element, rock & core	ICP-AES	0.01	10.00
564	13	Ni ppm: 24 element, rock & core	ICP-AES	1	10000
559	13	P ppm: 24 element, rock & core	ICP-AES	10	10000
560	13	Pb ppm: 24 element, rock & core	AAS	2	10000
582	13	Sr ppm: 24 element, rock & core	ICP-AES	1	10000
579	13	Ti %: 24 element, rock & core	ICP-AES	0.01	10.00
572	13	V ppm: 24 element, rock & core	ICP-AES	1	10000
556	13	W ppm: 24 element, rock & core	ICP-AES	10	10000
558	13	Zn ppm: 24 element, rock & core	ICP-AES	2	10000
367	13	C %: Leco furnace	LECO-IR DETECTOR	0.01	100.0
1381	13	C %: Inorganic	LECO-GASOMETRIC	0.05	100.0
439	13	T.O.C. %: C(Total) - CO2	CALCULATION	0.01	100.0
1066	13	Sulfide S %: Total S - Sulfate S	CALCULATION	0.01	100.00
1379	13	Sulfate S %: Dilute HCl leach	GRAVIMETRIC	0.01	100.00
1380	13	S %: Leco furnace	LECO-IR DETECTOR	0.01	100.0
379	13	S %: HNO3-bromide digestion	GRAVIMETRIC	0.01	100.00



Chemex Labs Ltd.

Analytical Chemists * Geochemists * Registered Assayers
212 Brooksbank Ave., North Vancouver
British Columbia, Canada V7J 2C1
PHONE: 604-984-0221 FAX: 604-984-0218

To: UNIVERSITY OF BRITISH COLUMBIA
DEPARTMENT OF MINING AND MINERAL PROCESS ENG.
517 - 6350 STORES ROAD
VANCOUVER, BC
V6T 1Z4

A9825771

Comments: ATTN: VALERIE BERTRAND

CERTIFICATE **A9825771**

(LRO) - UNIVERSITY OF BRITISH COLUMBIA

Project: 11-R-51236
P.O.#:

Samples submitted to our lab in Vancouver, BC.
This report was printed on 26-JUL-98.

SAMPLE PREPARATION

CHEMEX CODE	NUMBER SAMPLES	DESCRIPTION
244	6	Pulp; prev. prepared at Chemex

ANALYTICAL PROCEDURES

CHEMEX CODE	NUMBER SAMPLES	DESCRIPTION	METHOD	DETECTION LIMIT	UPPER LIMIT
316	6	Zn %: Conc. Nitric-HCL dig'n	AAS	0.01	100.0